Shedding light on the link between the actin cytoskeleton and stress response in *Saccharomyces cerevisiae*

A thesis submitted in partial fulfillment of the requirements
for the degree of Doctor of Philosophy
in Biochemistry

Massey University, Auckland
New Zealand

Martina Dautel
March 2012

Abstract

Understanding how eukaryotic cells adapt to stress remains a fundamental question in biology. One important stress which affects all cells is amino acid (AA) starvation. Upon perception of AA starvation the Gcn2 protein binds an effector protein complex consisting of Gcn1 and Gcn20. Subsequently, Gcn2 becomes activated and phosphorylates the eukaryotic translation initiation factor 2. This leads to a reduced global protein synthesis and simultaneously to an increased translation of Gcn4, a transcriptional activator of genes necessary for overcoming stress. This signaling pathway is called general amino acid control (GAAC) in yeast. Failing to activate this signaling cascade impairs the starvation response and cellular growth.

Yih1 inhibits Gcn2 by competing with Gcn2 for Gcn1 binding, consequently leading to an impaired stress response. However, Yih1 is not a general inhibitor of Gcn2 but only impedes Gcn2 activation upon release from the cytoskeleton protein actin. Our understanding of the role of actin in Gcn2 signaling and Yih1 itself is limited. Also, the circumstances under which Yih1 is released from actin are unknown. Thus, the scope of this study is to elucidate the link between the actin cytoskeleton and stress response. To achieve this goal, actin mutants were screened for an impaired ability to overcome starvation. Out of 24 mutant strains five exhibited an impaired stress response as indicated by sensitivity to AA analogues, which could be reverted upon Gcn4 induction, and sensitivity to AA imbalance. One of this actin mutations has been proposed to affect the GAAC via an impaired Yih1-actin binding. Another mutation appears to weaken the actin-eEF1A interaction therefore promoting eEF1A mediated Gcn2 inhibition. For the remaining 3 actin mutations the mechanism might be at the transcriptional or translational level. These findings show that actin mutations do affect the GAAC at multiple levels. In addition, the cyclin dependent kinase Cdc28 has been identified as a novel interaction partner of Yih1 and it has been speculated that a link between Yih1 and bud emergence might exist.

The results from this study achieved to shed light on the link between Yih1, the GAAC and the actin cytoskeleton. Yih1 has been placed in the midst of highly regulated and diverse cellular processes, which emphasizes the interconnection that exist between cellular pathways and the likely importance of Yih1 in the cell.

For my family

Acknowledgements

Although my name is printed on the cover of this thesis, this study would not have been possible without the support of a myriad of people. Words are not enough to express my gratitude for their love, support, encouragement and patience over the past few years.

First of all, I want to thank my supervisors Dr. Evelyn Sattlegger, Dr. Jeremy Hyams and Dr. Andrew Sutherland-Smith for taking me on. Thanks Evelyn for giving me the opportunity to pursue my PhD studies in your group and your financial support of my research. I would like to thank Jerry and Andrew for their advice regarding my work.

I would like to acknowledge the funding bodies that made this project possible. My research was funded by grants provided by the Health Research Council of New Zealand, the Maurice & Phyllis Paykel trust and the Massey University Research Fund. In addition, I would like to thank Massey University for my doctoral scholarship and the Institute of Natural Sciences, Massey University for four month of financial support. I must also thank the Institute of Molecular BioSciences for a travel grant and the Albany Student Association for their financial support of my studies.

Thank you Dr. A. Adams for generating the collection of actin mutant strains. I would not have been able to do this study without these strains.

I would like to extend a warm thank you to Dr. Beatriz Castilho for the Yih1 antibodies and Dr. David Botstein for the actin antibodies, which I used during my research. Without these antibodies this study would not have been possible.

I also would like to thank Prof. Dr. Amberg for his collaboration on the yeast-2-hybrid screen.

I want to thank Mr. Gilson for developing the Repetman pipette and the multi-channel pipette. You saved me from suffering from a tennis thumb.

I would like to thank my interns Viviane, Chrissy, Anna, the lab technician Htin and the students Kirsty and Hee Jun for their helping hands with the screens.

I would like to thank Dr. Jyothsna Visweswaraiah, Dr. Andrew Cridge, Su Jung Lee, Dr. Chris Rodley, Dr. Elmira Mohandesan, Dr. Gabrielle Beans Picón, Dr. Katie Hartnup, Ralph Grand, Rashmi Ramesh, Michael Bolech, Renuka Shanmungam and Mack Saraswat for their support in the lab during the years. I would also like to acknowledge Dr. Jyothsna Visweswaraiah, Dr. Andrew Cridge, Dr. Matthew Woods and Dr. Lutz Gehlen for helpful scientific discussions of my work. I addition, I would like to thank the past and present members of the Sattlegger group for their support in the lab.

A special thanks goes to the amazing Jarod Young, who always had some spare chemicals, glassware or equipment I could borrow.

I am unbelievably grateful to Dr. Andrew Cridge, Dr. Matthew Woods, Dr. Gabrielle Beans Picón, Dr. Lutz Gehlen and Dr. Justin O'Sullivan for tirelessly reading through my thesis and offering me critical discussions of my research and writing.

Many thanks go to my friends Jyothsna, Elmira, Gabby, Lutz, Saumya, Jarod, Katie, Chris, Andrew, Ralph, Rashmi, Mack and Mat for their friendship and support over the years. You guys made this lab a fantastic place to work in and kept me sane throughout writing this thesis. Also, I want to thank the past and present members of building 11, who made working in the lab such a pleasant experience.

I am highly indebted to my family. Without their unconditional love, endless support and encouragement I would not be where I am now.

Last but not least, a great thanks goes to Christian, whose love has guided me through this stressful time. Thanks for tolerating me through my thesis writing and for always being there for me. Thanks for all your support and for pushing me to use Latex for writing this thesis. I am looking forward to our future together.

Contents

List of Figures

List of Tables

List of Abbreviations

In addition to the chemical symbols from the periodic table of elements and the système international d'unités (SI), the following abbreviations are used:

+/-	highly charged region
3AT	3-Aminotriazole
$3AT^S$	sensitivity to 3-Aminotriazole
AA	amino acid
AA $imbalance^S$	sensitivity to amino acid imbalance
ABC	ATP-binding cassette
APS	ammonium persulfate
ATP	adenosine triphosphate
bp	base pair
BSA	bovine serum albumin
BiFC	bimolecular fluorescence complementation
cak	cdk activating kinase
cdk2	cyclin dependent kinase 2
CIP	calf intestinal phosphatase
DMSO	dimethylsulfoxide
DNA	deoxyribonucleic acid
dNTP	deoxyribonucleotide triphosphate
DTT	dithiothreitol
EDTA	ethylenediamine tetra acetic acid
eEF1A	eukaryotic elongation factor 1A
eIF2	eukaryotic initiation factor 2
eIF2α-P	eukaryotic initiation factor 2 phosphorylated at subunit α
F-actin	filamentous actin
GAAC	general amino acid control

G-actin	globular actin
Gcn	general control non-derepressible
$Gcn4^C$	Gcn4 constitutively expressed
GDP	guanosine diphosphate
GI	Gcn2 and IMPACT
GST	glutathione S- transferase
GTP	guanosine triphosphate
HA	hemagglutinin
HEPES	4-(2-hydroxyethyl)-1-piperazineethanesulfonic acid
His-RS	histidyl-tRNA synthetase
HRI	heme-regulated inhibitor kinase
IMPACT	imprinted and ancient
IPTG	isopropyl-β-D-thiogalactopyranoside
kDa	kilo dalton
LB	luria-bertani
LiOAc	lithium acetate
Ni-NTA	nickel-nitrilo triacetic acid
OD	optical density
OPNG	o-nitrophenyl-beta-β-galactosidase
ORF	open reading frame
p	plasmid
PAGE	polyacrylamide gel electrophoresis
PCR	polymerase chain reaction
PEG	polyethylene glycol
PERK	PKR-like endoplasmatic reticulum kinase
PKR	protein kinase RNA
PMSF	phenylmethanesulphonyl fluoride
PVDF	polyvinylidine difluoride
RNase	ribonuclease
RWD	RING finger proteins, WD-repeat-containing proteins, yeast DEAD-like helicases
SD	synthetic dropout
SDS	sodium dodecyl sulfate
SM	sulfometuron methyl
SM^S	sensitivity to sulfometuron methyl
$tRNA_i^{Met}$	Methionyl-tRNA
Tris	tris(hydroxymethyl)aminomethane
TAE	tris-acetate EDTA
TBS	tris-buffered saline
TBS-T	TBS-Tween
TC	ternary complex
TE	Tris EDTA

TEMED	N,N,N',N'-Tetramethylethylenediamine
uORF	upstream open reading frame
v/v	volume/ volume
WCE	whole cell extract
w/v	weight/ volume
Yih1	yeast impact homolog
YPD	yeast extract peptone dextrose
YPG	Yeast extract peptone glycerol

1 Introduction

Change is part of life - no matter if multicellular or unicellular organisms are concerned. An environmental change forces the organism to react to this stress in order to survive and flourish. In all organisms multiple intricate cellular regulatory pathways are in place to mitigate stress and assist the organism to survive. One of such regulatory pathway is called general amino acid control (GAAC), which enables the organism to overcome amino acid starvation. Despite the fact that in the last few decades stunning progress has been made in deciphering this signaling pathway, the GAAC pathway is still not completely understood.

1.1 The general amino acid control pathway

Yeast cells recognize and process nutritional stress signals inside the cell by activation of the GAAC pathway [19, 111, 136]. As a result global translation is reduced. Since the process of translation consumes a notable amount of energy (estimated as up to 50% of the cellular energy, depending on the or-

ganism [49]), this results in a considerable saving of energy. The decrease in protein synthesis also prevents the production of proteins that could interfere with the cellular stress response. In parallel to this stress-induced attenuation of global translation, selective translation of proteins that are required for cell survival under stress occurs. The molecular mechanism underlying this signaling pathway is described below.

1.1.1 Translation control by phosphorylation of the eukaryotic translation initiation factor 2

The general GAAC pathway enables yeast cells to rapidly respond to nutritional deprivation including amino acid (AA) starvation or amino acid imbalance [89]. The stress response is almost instantaneous, as the gene expression is regulated at a translational level rather than at a transcriptional level. Considering the time required for synthesis and processing of *de novo* mRNA in eukaryotes, regulation of expression of pre-existing mRNA by a controlled translational is more efficient for mitigating stress [49].

The translational control occurs by inhibiting protein synthesis at the initiation stage by reversibly phosphorylating the eukaryotic translation initiation factor 2 (eIF2) at a conserved serine residue (Ser-51 in *Saccharomyces cerevisiae*) [13, 21, 43]. eIF2 is a heterotrimeric protein consisting of three subunits (α, β, γ). The conserved serine residue is located in the α subunit of the initiation factor. eIF2 is part of the key regulatory mechanism for regulating protein synthesis in eukaryotes [78]. In the early steps of translation initiation (summarized in figure 1.1), eIF2 binds to the initiator tRNA ($tRNA_i^{Met}$) in a GTP-dependent manner and forms the ternary complex (TC). This complex is essential for translation initiation as it binds to the 40S ribosomal subunit to form the 43S pre-initiation complex [46]. After binding to the 5' end of the mRNA the 43S complex scans the mRNA in a 5' $\rightarrow$ 3' direction for the start codon AUG [66]. When reaching the start codon the GTP associated with the TC is hydrolyzed and is released in an inactive eIF2-GDP bound form. To be able to participate in another round of initiation eIF2-GDP is recycled to eIF2-GTP by the guanidine nucleotide exchange factor eIF2B [63, 46].

When eIF2α is phosphorylated (eIF2α-P) it is transformed from the substrate of eIF2B into its inhibitor [93], which results in a reduced exchange rate of GDP to GTP on eIF2. Subsequently, the level of ternary complex is decreased leading to reduced global protein synthesis. Since the cellular level of eIF2 molecules is approximately two fold higher than eIF2B [32], a small fraction of phosphorylated eIF2 will have a notable effect on the TC levels and hence on translation initiation [49].

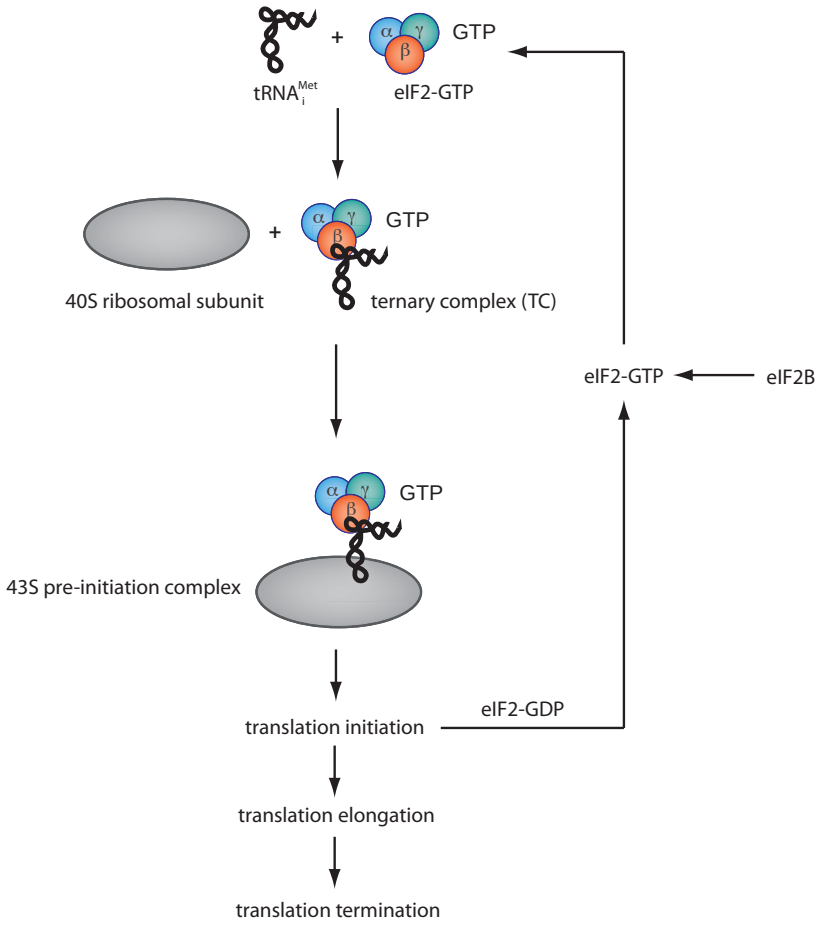

Figure 1.1: Schematic representation of eukaryotic translation initiation involving binding of tRNA$_i^{Met}$ to eIF2-GTP to form the ternary complex. Subsequently, this complex binds the 40S ribosomal subunit to form the 43S pre-initiation complex. Upon translation initiation, eIF2 is released in a GDP bound form and is recycled by eIF2B to eIF2-GTP to take part in another round of translation initiation.

1.1.2 Selectively increased translation mediated by the transcription activator Gcn4

While the general protein synthesis is downregulated by eIF2α-P, the translation of the mRNA of the transcriptional activator Gcn4 is upregulated. The translation of Gcn4 leads to the upregulation of about 10% of the genes in the yeast genome, including genes coding for AA and vitamin biosynthesis, peroxisomal components and AA transporters [48]. This upregulation consequently leads to an increased cellular level of AA which assists the cells in overcoming starvation. The mechanism underlying the augmented expression of Gcn4 mRNA is outlined below.

The leader sequence of *GCN4* mRNA contains a 590 base pair untranslated region with four small upstream open reading frames (uORF) called uORF1, 2, 3, 4 respectively [78]. The scanning pre-initiation complexes recognize the start codon of uORF1 and translation is initiated. Approximately 50% of the ribosomes do not dissociate from the mRNA after translating uORF1. Instead they remain attached to the mRNA and resume scanning as a 40S subunit without a TC. Under non-starvation conditions when the concentration of TC complexes is high the 40S subunit quickly rebinds a TC and is able to re-initiate translation at the next start codon. Most complexes re-initiate at uORF2, 3, or 4. However, in contrast to the translation of uORF1 at the end of these uORF's, the ribosome dissociates from the mRNA leaving *GCN4* untranslated.

Under starvation conditions the amount of TC is decreased due to the phosphorylation of eIF2α. Therefore the majority of the 40S subunits scanning downstream of uORF1 have not rebound a TC when reaching uORF2, 3 or 4 and are unable to re-initiate translation. These subunits therefore continue scanning downstream of the uORF's. Since there is a long stretch of RNA between uORF4 and the start codon of *GCN4* the chance that the 40S subunit acquires a TC and re-initiates translation at *GCN4* is greater. Therefore under starvation conditions the translation of *GCN4* is augmented (see figure 1.2).

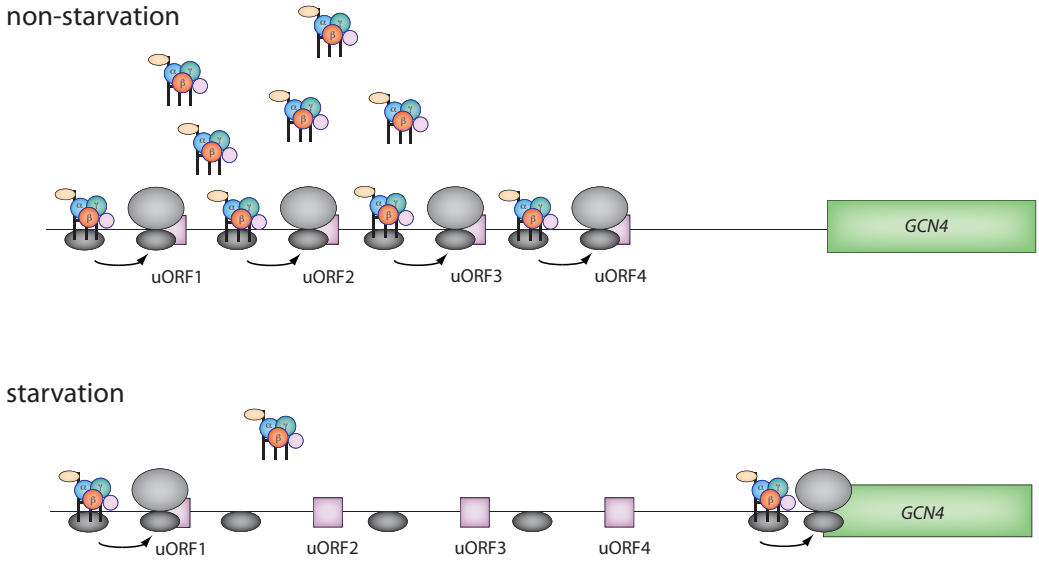

Figure 1.2: Schematic representation of *GCN4* expression under non-starvation (top panel) and starvation (bottom panel) conditions. The leader sequence of *GCN4* mRNA contains four small upstream open reading frames (uORF). The scanning pre-initiation complexes recognize the start codon of uORF1 and translation is initiated. 50% of the ribosomes do not dissociate from the mRNA after translating uORF1. They remain attached to the mRNA and resume scanning as a 40S subunit without a TC. Under non-starvation conditions when the concentration of TC complexes is high the 40S subunit quickly rebinds a TC and is able to re-initiate translation at the next start codon. Most complexes re-initiate at uORF2, 3, or 4. However, in contrast to the translation of uORF1 at the end of these uORF's, the ribosome dissociates from the mRNA leaving *GCN4* untranslated. Under starvation conditions the amount of TC is decreased due to the phosphorylation of eIF2α. Therefore the majority of the 40S subunits scanning downstream of uORF1 have not rebound a TC when reaching uORF2, 3 or 4 and are unable to re-initiate translation. These subunits therefore continue scanning downstream of the uORF's and the chance that the 40S subunit acquires a TC and re-initiates translation at the *GCN4* start codon is greater. Therefore under starvation conditions the translation of *GCN4* is augmented.

1.2 eIF2α protein kinases in mammals

A family of four different protein kinases capable of phosphorylating eIF2α have been identified in mammals. These kinases are homologous in their kinase domains. However, their effector domains are unique and respond to different stress stimuli [49]. The heme-regulated inhibitor kinase (HRI) is

activated by hemin deprivation in erythroid tissue, oxidative shock or heat shock [13], whereas double-stranded RNA produced at viral infection is the stimuli for the protein kinase RNA (PKR) [15]. When there are unfolded proteins in the endoplasmatic reticulum the PKR-like endoplasmatic reticulum kinase (PERK) also called PEK is activated [43, 113]. A protein called general control non-derepressible 2 (Gcn2) is activated by AA deprivation [6, 105, 117], UV irradiation [20, 56] and RNA viruses [7] (see figure 1.3).

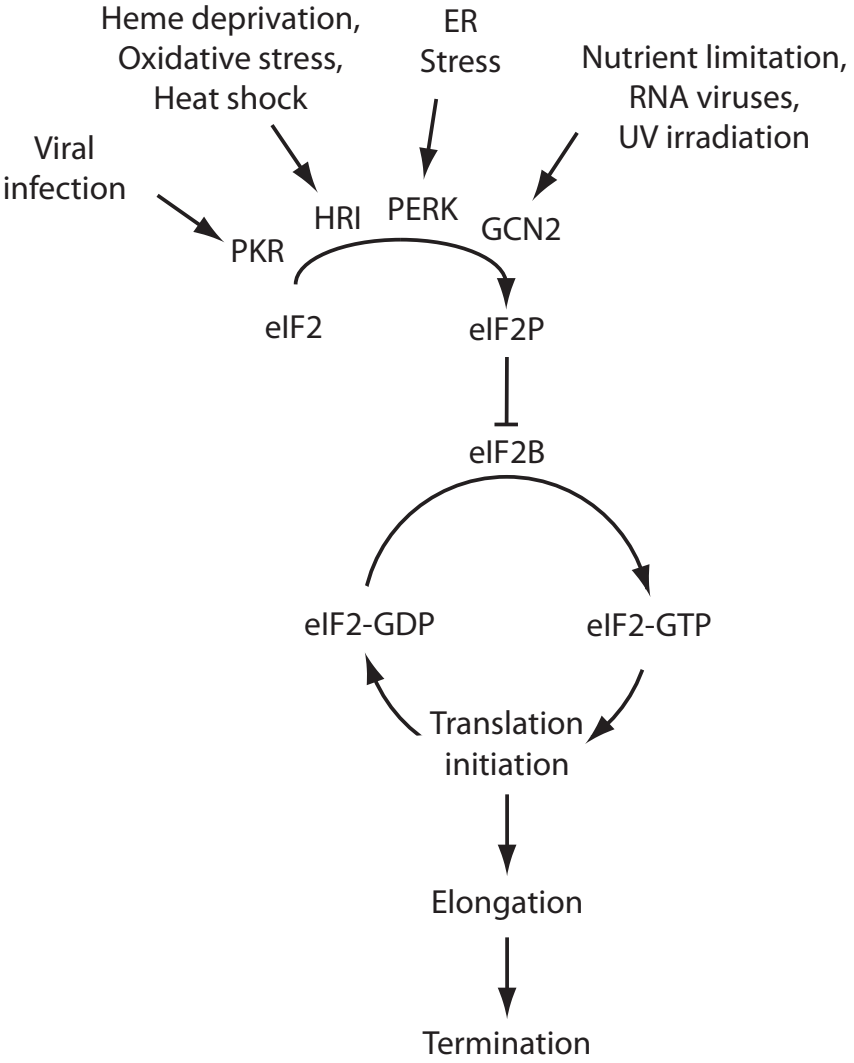

Figure 1.3: Schematic representation of eIF2α protein kinases in mammals and their specific stimuli.

1.3 The eIF2α kinase Gcn2

In contrast to four different eIF2α kinases in mammals, *Saccharomyces cerevisiae* contains only one eIF2α protein kinase, namely Gcn2. The signaling pathway governing Gcn2 is conserved throughout the eukaryotic kingdom. By phosphorylating the α subunit of eIF2 in Ser51 under starvation conditions, this protein kinase inhibits the general protein biosynthesis while specific stress related genes are upregulated.

Under non-starvation conditions Gcn2 is present as an inactive dimer in the cell with no kinase activity [104]. In AA starved cells deacylated tRNAs accumulate, which is the signal for AA starvation, and hereby activate Gcn2. The uncharged tRNAs bind to a regulatory domain in Gcn2 called HisRS-like domain [24] that resembles Histidyl-tRNA Synthetase [129]. So far, all forms of deacylated tRNAs investigated can bind the HisRS-like domain of Gcn2 [24]. The interaction of the deacylated tRNA with the HisRS-like domain has been shown to induce a conformational change in Gcn2 which is necessary for its activation [24]. In yeast, it has been shown that the C-terminal segment binds the ribosomes which is critical for Gcn2 function in the cell [105, 137]. In addition, this domain contains the main dimerisation determinants [104]. N-terminal to the kinase domain lies the Pseudo Kinase (Ψ PK) domain of unknown function that resembles a truncated kinase domain. A highly charged region (+/-) of unknown function is situated N-terminally to the Ψ PK domain . The N-terminal domain of Gcn2 is highly conserved and binds the Gcn1-20 effector protein complex [31] (see figure 1.4).

1.4 The Gcn2 activator protein Gcn1

For function, Gcn2 has to bind to uncharged tRNA, the ribosome and its effector protein Gcn1. Gcn1 is a large 296 kDa protein, which bears a homologous region to translation elongation factor 3 [76]. Together with the ATP-binding cassette protein Gcn20 it forms the Gcn1-Gcn20 regulatory complex for Gcn2 [76].

Under non-starvation conditions, yeast *GCN1* has been shown to be

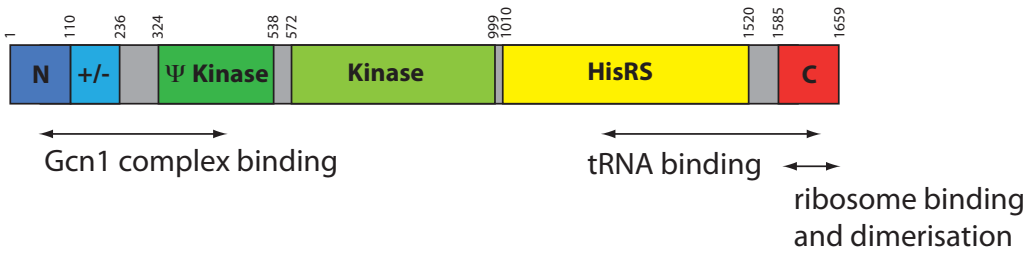

Figure 1.4: Schematic presentation of functional domains in the protein kinase Gcn2. The different domains of Gcn2 are represented in various colors. The N-terminal domain (dark blue) and a highly charged region (+/-, blue) bind the effector protein Gcn1. The pseudo kinase domain (Ψ kinase, green) has homology to a truncated kinase domain and is non-functional as a kinase. The HisRS domain (yellow) is involved in binding uncharged tRNAs. The C- terminal domain (orange) of Gcn2 is known to bind the ribosome, participates in tRNA binding and is responsible for dimerisation of Gcn2 [48].

non-essential. However, it is required for wild-type growth when cells are starved for AA. Deletion of *GCN1* abolished eIF2α phosphorylation by Gcn2 completely under starvation conditions and subsequently translation of *GCN4* [76]. *GCN20* has also been shown to be essential under starvation conditions. However, deletion of *GCN20* only reduces the phosphorylation of eIF2α by Gcn2 but does not abolish the GAAC response [125].

Gcn1 and Gcn20 are neither required for the expression of *GCN2* [76, 125] nor for *in vitro* kinase activity of Gcn2 [76, 125] since in these experiments active Gcn2 was purified from a *GCN1* deletion strain. This suggests that Gcn1 and Gcn20 are required for transmission of the starvation signal to Gcn2 *in vivo*. This hypothesis is supported by the observation that Gcn1 binds Gcn20 and forms a protein complex [125] that then binds Gcn2 at the N-terminal domain [31]. As described earlier, the interaction of the Gcn1-Gcn20 complex with Gcn2 is essential for Gcn2 function *in vivo* [31]. Interestingly, the N-terminal fragment of *Drosophila* Gcn2 has been shown to interact with *S. cerevisiae* Gcn1 [31] leading to the conclusion that the Gcn2-Gcn1 interaction is evolutionary conserved and with it the mechanism of responding to nutrient starvation in eukaryotes.

The N-terminal domain of Gcn2 binds to Gcn1 both *in vitro* and *in vivo* [31]. As this domain can be found in Gcn2 as well as in a mammalian protein

called IMPACT, this domain was called the GI domain [70]. This region is now called the RWD domain from its presence in RING finger proteins, WD-repeat-containing proteins and yeast DEAD-like helicases [23].

In vitro Gcn1 binds to the N-terminus of Gcn2 via a domain comprising AA 2052-2428 located at the C-terminus [109]. This interaction between Gcn1 and Gcn2 is dependent on a single amino acid Arg 2259 since a mutation of this residue abolished Gcn2 binding both *in vivo* and *in vitro*. This Gcn1-Gcn2 interaction has also been shown to be essential for Gcn2 function *in vivo* [109].

1.5 The Gcn2 negative regulator protein Yih1

In contrast to the positive Gcn2 regulator Gcn1, a protein called yeast impact homolog (Yih1) has been shown to be a negative regulator of Gcn2 in yeast. [110, 108, 70].

Yih1 is approximately 29 kDa in size and has been identified as the functional homolog of the mouse protein IMPACT (Imprinted and ancient) [97]. IMPACT is highly abundant in neuronal cells in the brain [97, 9, 41]. The homology of Yih1 and IMPACT is based on several facts. First, overexpression of IMPACT lowers the level of phosphorylated eIF2α as described for Yih1 [110]. Secondly, IMPACT co-precipitates with Gcn1 in an *in vivo* interaction assay as does Yih1 [110, 108]. The C-terminal domain of both Yih1 and IMPACT has homology to the N-terminal half of the YigZ family of prokaryotic proteins of unknown function. Since similar regions are found in bacteria, archaea and eukaryots this region was entitled as the "ancient domain" [41]. Adjacent to the ancient domain, a flexible and highly unstructured linker region has been identified by structure-based sequence comparison [108]. Like Gcn2 and IMPACT, Yih1 contains an RWD domain (formerly known as GI domain) located in its N-terminal half (see figure 1.5) [70].

As mentioned earlier, Yih1 is a negative regulator of Gcn2 in yeast [110, 70]. Yih1 interacts with Gcn1 *in vivo* as determined by yeast-2-hybrid experiments [70] and co-precipitation assays [110], and *in vitro* as shown by *in vitro* interaction assays using purified proteins [69, 110, 108]. Recently,

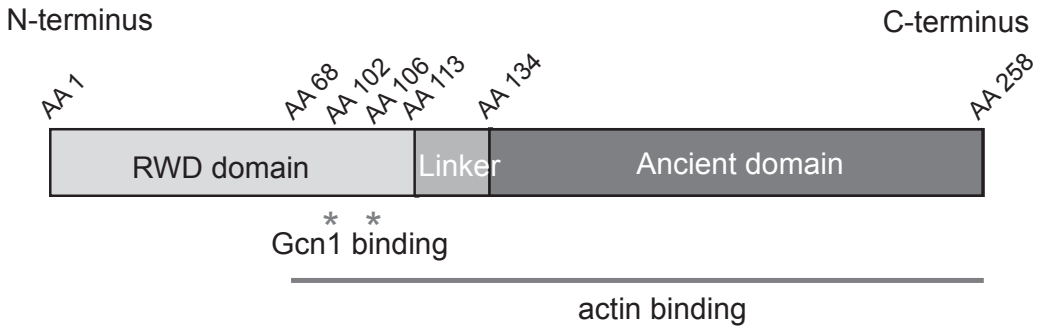

Figure 1.5: Schematic presentation of functional domains in Yih1. The Yih1 protein contains three distinct functional domains. The RWD is present at the N-terminus (light grey) and contains the Gcn1 binding sites, adjacent to it lies a unstructured linker region (medium grey), followed by the ancient domain (dark grey) located at the C-terminus of the protein. Actin binds to a region ranging from amino acids 68-258.

AA Asp-102 and Glu-106 in the RWD domain of Yih1 have been shown to be responsible for Gcn1 binding *in vivo* [108]. A single AA Arg-2259 in the C-terminal region of Gcn1 has been identified as being essential for Yih1 binding *in vitro* and *in vivo* [110, 108]. This Arg-2259 mutation in Gcn1 has also previously been found to abolish interaction with Gcn2 and to inhibit Gcn2 activation under starvation conditions. In addition, overexpression of Yih1 almost halves the Gcn1-Gcn2 complex formation as measured by a immuno-precipitation assay using Gcn1 specific antibodies [110]. From these observations, the hypothesis was formulated that Yih1 competes with Gcn2 for Gcn1 binding and thereby inhibits Gcn2 activation. The fact that overexpressed Yih1 only co-precipitated with Gcn1 and not with Gcn2 supported this idea. Inactivation of Gcn2 function by excess Yih1 in the cell has been demonstrated by impaired growth under AA deprivation conditions [70, 110]. Overexpression of Gcn2 suppressed this slow growth defect indicating competition for Gcn1 binding [110]. In addition, overexpression of Yih1 has been demonstrated to reduce the level of eIF2α phosphorylation by 40% under starvation and 90% under non-starvation conditions indicating that, in fact, the Gcn2 kinase activity is impaired [110]. Taken together these findings point to a potential role of Yih1 as a negative regulator of Gcn2 function by competing with Gcn2 for Gcn1 binding.

However, Yih1 does not seem to be a general inhibitor of Gcn2. Deletion of *YIH1* does not render Gcn2 constitutively active under starvation conditions as indicated by wild type like growth of a *yih1*Δ strain in a growth assay. In addition, deletion of *YIH1* does not alter the level of eIF2α phosphorylation in a *yih1*Δ strain in comparison to a wild type strain [110].

Monomeric globular actin (G-actin) has been identified as a binding partner of Yih1 *in vivo* [110]. G-actin co-precipitated with Yih1 expressed at a native level in a 1:1 complex as confirmed by mass spectrometry and western blot analysis using antibodies against actin [110]. No Gcn1 could be detected in this complex indicating that the Yih1-actin interaction is independent of Gcn1 *in vivo* [110, 108]. In support of this idea, *in vitro* studies have shown that Yih1 binds directly to Gcn1 without any mediating proteins involved. A reduced amount of cellular actin in an *act1*Δ/*ACT1* heterozygous diploid strain leads to an impaired stress response compared to an isogenic *ACT1*/*ACT1* wild type strain as measured by impaired growth under starvation conditions. This slow growth was exacerbated by overexpression of Yih1 compared to the wild type strain also overexpressing Yih1 [110]. When *YIH1* was deleted in the *act1*Δ/*ACT1* strain, the impaired growth could at least be partially reverted as measured by an enhanced growth in comparison to the isogenic strain expressing Yih1 from a plasmid [110]. These findings raised the possibility that the inhibition of Gcn2 by Yih1 might be regulated by actin. However no physical evidence has been provided so far with regards to the temporal or spatial occurrence of this Yih1 mediated regulation of Gcn2.

The region of Yih1 necessary for the Yih1-actin interaction *in vivo* has recently been assigned to AA 68 - 258 by interaction assays using fragments of Yih1 [108].

Taken together these findings lead to the following model for Yih1 mediated Gcn2 regulation (see figure 1.6). Upon AA starvation, indicated by deacylated tRNAs, Gcn2 is activated by binding to its effector complex Gcn1-Gcn20, the ribosome and uncharged tRNA. The interaction with the latter triggers a conformational change in the kinase domain of Gcn2 allowing the phosphorylation of eIF2α. Subsequently, phosphorylation of eIF2α results in the down regulation of general protein synthesis and up regulation of spe-

cific stress related genes (figure 1.6, panel A). Yih1 resides in the cell in an inactive Yih1-G-actin complex (figure 1.6, B). When Yih1 is released from actin it competes with Gcn2 for Gcn1 binding leading to the inhibition of Gcn2 kinase activity and subsequent stress response.

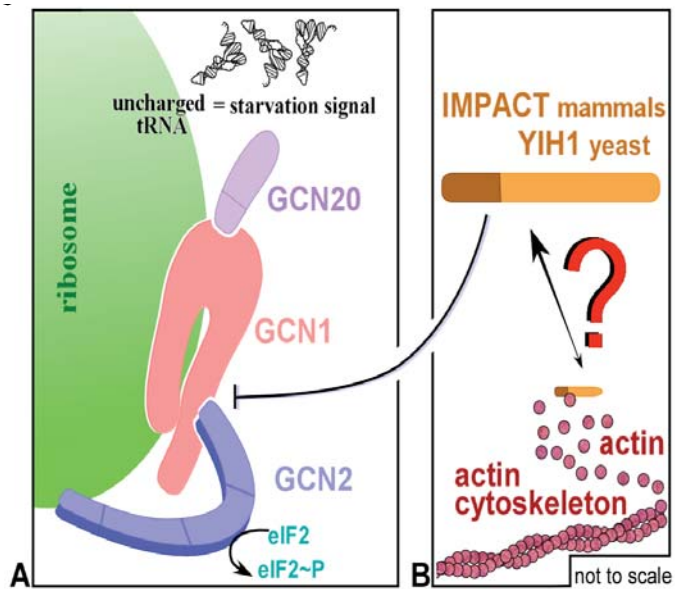

Figure 1.6: Model for Yih1 mediated Gcn2 regulation. Upon amino acid starvation indicated by deacylated tRNAs Gcn2 is activated by binding to its effector complex Gcn1-Gcn20, the ribosome and uncharged tRNA. The interaction with the latter triggers a conformational change in the kinase domain of Gcn2 allowing the phosphorylation of eIF2α resulting in the down regulation of general protein synthesis and up regulation of specific stress related genes (figure 1.6, A). Yih1 resides in the cell in an inactive Yih1-G-actin complex (figure 1.6, B). When Yih1 is released from actin it competes with Gcn2 for Gcn1 binding leading to the inhibition Gcn2 kinase activity and subsequent stress response (E. Sattlegger, unpublished schematic)

1.6 The Yih1 interaction partner actin

The known Yih1 interaction partner, monomeric G-actin is a globular 375 residue polypeptide, which folds into two large domains. Each domain consists of two subdomains numbered I-IV [57]. In its tertiary structure the two large domains form a hinged molecule with a deep cleft in between. Situated

within this cleft are actin's two essential co-factors an adenine nucleotide and a divalent metal ion (see figure 1.7) [57]. By extensive contact with the surrounding protein molecule, these co-factors are believed to stabilize the molecular structure of the monomeric actin molecule [4].

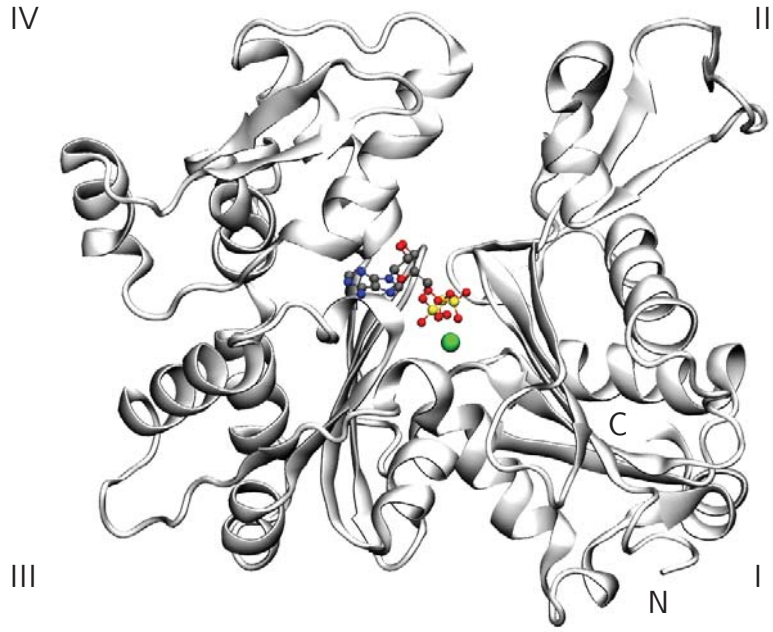

Figure 1.7: The atomic structure of *S. cerevisiae* G-actin was modeled in this study using the published coordinates of actin (PDB code 1ATN, [57]) and the VMD software [54]. Subdomains I - IV and the N/ C-terminus of actin are labelled accordingly. The adenine nucleotide in the cleft between the subdomains is depicted as a simple stick model and the divalent cation as a van-der-Waal's sphere.

In the cell, actin can also be found in its polymerized form called filamentous actin (F-actin). An actin filament consists of non-covalently associated actin monomers, which assemble in a double helical manner [50].

G-actin and F-actin exist in a dynamic equilibrium. F-actin undergoes a constant addition and loss of monomeric actin subunits at its ends with a turnover time of about 60 s [4]. The assembly occurs in a head-to-tail manner. The two ends of the filament are called barbed and pointed end, referring to the arrowhead pattern observed upon decoration with the S1 fragment of the actin binding protein myosin (see figure 1.8) [101]. In order

to assemble an actin filament an initial nucleation step is necessary, which is very slow due to the instability of the initiating actin dimers and trimers. In contrast, once assembled filaments are very stable and undergo a rapid polarized growth. Actin monomer subunits carrying ATP in their nucleotide-binding cleft are added preferentially to the barbed end versus the pointed end (see figure 1.8) [98]. Upon addition of an actin-ATP monomer subunit to the barbed end of a filament, hydrolysis of the bound ATP to ADP and P_i is elicited [100]. The bound P_i is released in a subsequent step producing an actin-ADP dimer [100]. Thus, filaments contain a gradient of enriched ATP-bound subunits near the barbed end, ADP- P_i actin in the middle segment and ADP-actin at the pointed end [80]. The latter dissociate from the filament's pointed end and undergo a nucleotide exchange from ADP $\rightarrow$ ATP. This interchange is necessary for the actin monomer to be able to be added to the actin filament again. The property of addition and dissociation of actin subunits to the filament in a steady-state manner is called treadmilling and is depicted in figure 1.8 [88].

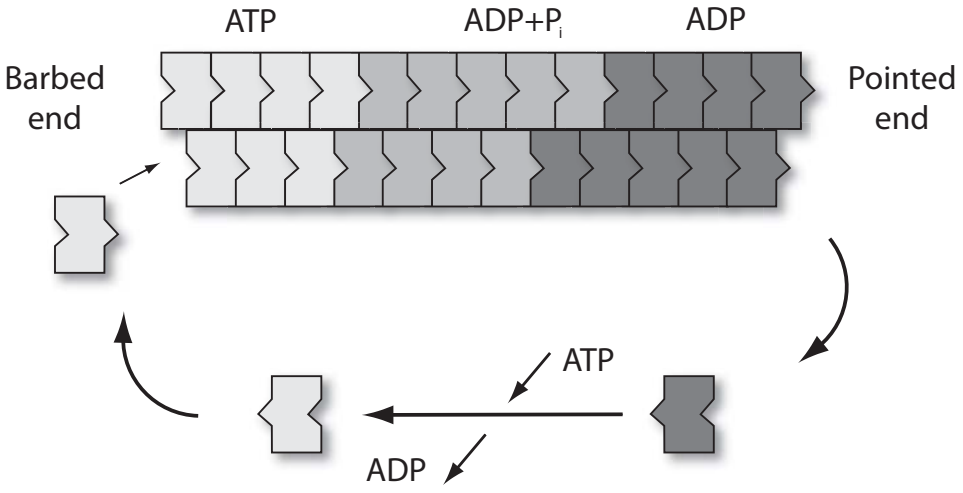

Figure 1.8: Schematic representation of actin filament treadmilling. Actin filaments posses a fast-growing barbed end and a slow-growing pointed end. ATP-bound actin monomers (light grey) preferably bind to the barbed end of the polymer. After ATP hydrolysis, ADP and P_i remain bound to actin (medium grey). P_i is released from the filament to yield an ADP bound actin monomer (dark grey). Subsequently, ADP-actin dissociates from the filament and is recycled into ATP-actin to be able to associate with the filament again. This figure is adapted from [88].

Actin's function in the cell is very versatile. F-actin for example is a major component of the cellular cytoskeleton. Thus F-actin determines the size, shape and mechanical properties of the cell [62]. With the treadmilling ability of actin filaments, the cytoskeleton is a highly dynamic structure and can react quickly to newly arising internal and external cellular needs. By being physically associated with the nucleus, organelles, vesicles and various types of macromolecules like proteins and DNA, the cytoskeleton is involved in a myriad of cellular and molecular processes like the transfer of mitochondria [45] and vacuoles [12] from mother to daughter cells during cell growth, endocytosis [25] and bud formation [1, 60]. Recent studies even suggest a direct involvement of actin in transcription [96, 95] and translation [59, 36, 37].

The actin cytoskeleton itself is regulated by a plethora of highly conserved actin-binding proteins [80, 99] governing filament assembly, organization and turnover. Some of these proteins have been well characterized. For example, fimbrin which cross-links individual actin filaments [1, 11] or tropomyosin which stabilizes filaments [80, 103]. However, the biological significance and the role within the cell of various other identified actin-binding proteins like Yih1 remains unknown [110, 108]. In addition, how these different actin-binding protein function together *in vivo* is uncertain.

S. cerevisiae expresses a single actin encoded by the essential *ACT1* gene [29, 87]. The amino acid sequence of yeast actin is 88% identical to mammalian muscle or cytoplasmic actin [87, 30]. In addition, actins from different species are more than 70% identical [130] thus indicating that actin is a highly conserved protein. A large collection of yeast actin mutations has been created over the years [114, 132, 134] to study interactions of actin with other cellular structures and to identify putative roles of actin in the cell.

1.7 Scope of this study

Gcn2 is an important protein in the cell as it is involved in key cellular functions such as AA homeostasis [6, 105, 117]. Therefore Gcn2 is essential for any organism from yeast to mammal to survive AA starvation. For example, recent studies have shown that *GCN2*$^{-/-}$ mice are viable under non-

starvation conditions. However, when amino acid deprivation occurs, a high morbidity rate was measured [3].

The phosphorylation of eIF2α - the substrate of Gcn2 - has also been shown to have biomedical implications in humans. For example lack of eIF2α phosphorylation results in a disease called Wolcott-Rallison syndrome. This syndrome is characterized by infancy-onset diabetes accompanied by skeletal defects and growth retardation [49].

In addition, Gcn2 has been demonstrated to be involved in highly evolved mechanisms in higher eukaryotes such as long-time memory formation [17] and feeding behavior [35, 42, 77]. In contrast to wild type mice, *GCN2*$^{-/-}$ mice do not reject food with an AA imbalance indicating the involvement of Gcn2 in feeding behavior [22].

Being involved in such diverse processes, Gcn2 has to be precisely regulated to ensure its correct function, in the correct organ, at the right time. However, the exact regulatory mechanism of Gcn2 is not yet completely understood. Whereas several studies have succeeded in deciphering the activation of Gcn2 [24, 105, 137, 76, 125, 31, 109], very little is known about its deactivation.

As Gcn1, Gcn2 and Yih1 are highly conserved throughout the eukaryotic kingdom, findings from the model organism *S. cerevisiae* constitute an excellent starting point for further investigations in higher eukaryotes. To date, Yih1 is the best characterized inhibitor of Gcn2 in yeast [110, 108]. However, it has been shown that Yih1 is not a general inhibitor of Gcn2. It has been proposed that Yih1 only impedes Gcn2 activity upon release from the cytoskeleton compound actin [110, 108]. Actin is a pivotal protein in the cell as it is involved in a myriad of processes from transcription [95] to translation [84], from endocytosis [130] to bud formation [80], and often these processes are intricately interconnected. The knowledge regarding the affect of actin on Gcn2 signaling is limited and the circumstances under which Yih1 is released from actin are unknown. In addition, besides the inhibitory effect of Yih1 on Gcn2 and its interaction with actin and Gcn1, little is known about Yih1 itself.

In order to close these gaps in knowledge and to shed light on the link between the actin cytoskeleton and stress response, the aims of the present study were:

1. to identify mutations in actin affecting the GAAC.
2. to characterize the Yih1-actin interaction *in vitro*.
3. to characterize the Yih1-actin interaction via a yeast-2-hybrid approach. This lead to the discovery of the cyclin dependent kinase 28 as a novel interaction partner of Yih1.

2

Materials and Methods

2.1 Biological materials

The plasmids and yeast strains used in this study are listed in table 2.1 and table 2.2.

Table 2.1: Plasmids used in this study

plasmid	gene	selectable marker	vector	source
Bacterial gene fusions				
pES189-D1A	His_6-YIH1	Kan^R	pET-28a	[110]
Yeast gene fusions, all Amp^R				
pUG6	loxP-KanMX-loxP cassette	Kan^R	pFA6-kanMX4	[38]
p180	*GCN4-lacZ* (uORF 1-4)	URA3	Ycp50	[47]
p238	$GCN4^C$	URA3	Ycp50	[81]
pES245-6	GST-YIH1(2-132)	URA3	pES128-9	[108]
pES246-7	GST-YIH1(2-171)	URA3	pES128-9	[108]
pES247-8	GST-YIH1(68-258)	URA3	pES128-9	[108]
pES248-9	GST-YIH1(68-171)	URA3	pES128-9	[108]
pES249-10	GST-YIH1(133-258)	URA3	pES128-9	[108]
pES187-B1	GST-YIH1(2-258)	URA3	pES128-9	[110]
pES128-9	GST	URA3	pEG(KT)	[109]
p703	URA3 marker	URA3, CEN6/ARSH4	pBLUESCRIPT	[115]
pACTII	yeast-2-hybrid plasmid containing GAL4 activation domain	LEU2, 2μ	pACTI	S. Elledge
pMD_02a	yeast-2-hybrid Yih1 fragment IV (AA 68-171)	LEU2, 2μ	pACTII	M. Dautel
pMD_03a	yeast-2-hybrid Yih1 fragment III (AA 68-258)	LEU2, 2μ	pACTII	M. Dautel
pMD_06a	yeast-2-hybrid Yih1 fragment II (AA 2-171)	LEU2, 2μ	pACTII	M. Dautel
YCplac33	vector control for pMJS1	URA3, ARS1/CEN4	pUC19	[33]
pMJS1	*ACT1*	URA3, ARS1/CEN4	YCplac33	[110]

Table 2.2: Yeast strains used in this study

name	genotype	source
H1511	Mat a leu2-3 leu2-112 trp-Δ 63 ura3-52 GAL2	[28]
H2556	Mat a *gcn1*Δ leu2-3 leu2-112 trp-Δ 63 ura3-52 GAL2	Vazquez de Aldana & Hinnebusch unpublished
H2557	Mat a *gcn2*Δ leu2-3 leu2-112 trp-Δ 63 ura3-52 GAL2	Vazquez de Aldana & Hinnebusch unpublished
H2558	Mat a *gcn20*Δ leu2-3 leu2-112 trp-Δ 63 ura3-52 GAL2	[125]
BY4741	Mat a *his3*Δ1 *leu2*Δ0 *met15*Δ ura3Δ0	Research Genetics
5780	same as BY4741 with *yih1*::Kan^R	Research Genetics
TKY 460	Mat α ACT1 bar1::LYS2 ura3-52 his3-Δ200 lys2-801 leu2-3,112 ade2	[134]
TKY 461	Mat α act1-102::HIS3 (E359A,E361A) bar1::LYS2 ura3-52 his3-Δ200 lys2-801 leu2-3,112 ade2	[134]
TKY 462	Mat α act1-4::HIS3 (E259V) bar1::LYS2 ura3-52 his3-Δ200 lys2-801 leu2-3,112 ade2	[134]
TKY 463	Mat α act1-7::HIS3 (K61N) bar1::LYS2 ura3-52 his3-Δ200 lys2-801 leu2-3,112 ade2	[134]
TKY 465	Mat α act1-123::HIS3 (R68A, E72A) bar1::LYS2 ura3-52 his3-Δ200 lys2-801 leu2-3,112 ade2	[134]
TKY 466	Mat α act1-115::HIS3 (E195A, R196A) bar1::LYS2 ura3-52 his3-Δ200 lys2-801 leu2-3,112 ade2	[134]
TKY 467	Mat α act1-111::HIS3 (D222A, D224A, D226A) bar1::LYS2 ura3-52 his3-Δ200 lys2-801 leu2-3,112 ade2	[134]
TKY 468	Mat α act1-113::HIS3 (R210A, D211A) bar1::LYS2 ura3-52 his3-Δ200 lys2-801 leu2-3,112 ade2	[134]
TKY 469	Mat α act1-116::HIS3 (D187A, K191A) bar1::LYS2 ura3-52 his3-Δ200 lys2-801 leu2-3,112 ade2	[134]
TKY 470	Mat α act1-104::HIS3 (K315A, E316A) bar1::LYS2 ura3-52 his3-Δ200 lys2-801 leu2-3,112 ade2	[134]
TKY 471	Mat α act1-135::HIS3 (E4A) bar1::LYS2 ura3-52 his3-Δ200 lys2-801 leu2-3,112 ade2	[134]
TKY 472	Mat α act1-117::HIS3 (R183A, D184A) bar1::LYS2 ura3-52 his3-Δ200 lys2-801 leu2-3,112 ade2	[134]
TKY 473	Mat α act1-133::HIS3 (D24A, D25A) bar1::LYS2 ura3-52 his3-Δ200 lys2-801 leu2-3,112 ade2	[134]
TKY 474	Mat α act1-10::HIS3 (T89I) bar1::LYS2 ura3-52 his3-Δ200 lys2-801 leu2-3,112 ade2	[134]
TKY 475	Mat α act1-9::HIS3 (D56A) bar1::LYS2 ura3-52 his3-Δ200 lys2-801 leu2-3,112 ade2	[134]
TKY 476	Mat α act1-3::HIS3 (P32L) bar1::LYS2 ura3-52 his3-Δ200 lys2-801 leu2-3,112 ade2	[134]
TKY 477	Mat α act1-20::HIS3 (G48V) bar1::LYS2 ura3-52 his3-Δ200 lys2-801 leu2-3,112 ade2	[134]
TKY 478	Mat α act1-8::HIS3 (H88Y) bar1::LYS2 ura3-52 his3-Δ200 lys2-801 leu2-3,112 ade2	[134]
TKY 479	Mat α act1-129::HIS3 (R177A, D179A) bar1::LYS2 ura3-52 his3-Δ200 lys2-801 leu2-3,112 ade2	[134]
TKY 480	Mat α act1-125::HIS3 (K50A, D51A) bar1::LYS2 ura3-52 his3-Δ200 lys2-801 leu2-3,112 ade2	[134]
TKY 481	Mat α act1-122::HIS3 (D80A, D81A) bar1::LYS2 ura3-52 his3-Δ200 lys2-801a leu2-3,112 ade2	[134]
TKY 482	Mat α act1-124::HIS3 (D56A, E57A) bar1::LYS2 ura3-52 his3-Δ200 lys2-801 leu2-3,112 ade2	[134]
TKY 483	Mat α act1-120::HIS3 (E99A, E100A) bar1::LYS2 ura3-52 his3-Δ200 lys2-801 leu2-3,112 ade2	[134]
TKY 484	Mat α act1-119::HIS3 (R116A, E117A, K118A) bar1::LYS2 ura3-52 his3-Δ200 lys2-801 leu2-3,112 ade2	[134]
TKY 486	Mat α act1-101::HIS3 (D363A, D364A) bar1::LYS2 ura3-52 his3-Δ200 lys2-801 leu2-3,112 ade2	[134]
ESY10447	same as TKY 460 with *yih1*::loxP-KanMX-loxP	Sattlegger, unpublished
MDY 157	same as TKY 462 with *yih1*::loxP-KanMX-loxP	this study
MDY 156	same as TKY 467 with *yih1*::loxP-KanMX-loxP	this study
MDY 146	same as TKY 475 with *yih1*::loxP-KanMX-loxP	this study
MDY 154	same as TKY 476 with *yih1*::loxP-KanMX-loxP	this study
MDY 147	same as TKY 477 with *yih1*::loxP-KanMX-loxP	this study
MDY 148	same as TKY 478 with *yih1*::loxP-KanMX-loxP	this study
MDY 149	same as TKY 479 with *yih1*::loxP-KanMX-loxP	this study
MDY 153	same as TKY 484 with *yih1*::loxP-KanMX-loxP	this study

2.2 Plasmid construction

pMD_06a, Yih1 fragment II

A 510 base pair fragment of *YIH1* (nucleotide 4-513) encoding Yih1 fragment II ranging from amino acid 2-171, was amplified from plasmid p187B1-A using primers ES2036 and ES400-49. This PCR product was purified and then digested with restriction enzyme *Bam*H1 and *Sal*1. The plasmid pACTII was digested with restriction enzymes *Bam*H1 and *Xho*1. Subsequently, the digested PCR product was inserted into the digested plasmid pACTII and the successful insertion was verified by sequencing using primers ES2036 and ES400-49 (see Appendix H for verification results).

pMD_03a, Yih1 fragment III

A 820 base pair fragment of *YIH1* (nucleotide 202-1021) encoding Yih1 fragment III ranging from amino acid 68-258, was amplified from plasmid p187B1-A using primers ES2001 and ES400-2. The PCR product was purified and then digested with restriction enzyme *Bam*H1 and *Sal*1. The plasmid pACTII was digested with restriction enzymes *Bam*H1 and *Xho*1. Subsequently, the digested PCR product was inserted into plasmid pACTII and the successful insertion was verified by sequencing using primers ES 2001, ES 400-2 and ES 400-49 (see Appendix H for verification results).

pMD_02a, Yih1 fragment IV

A 312 base pair fragment of *YIH1* (nucleotide 202-513) encoding Yih1 fragment IV ranging from amino acid 68-171, was amplified from plasmid pES247-8-1b using primers ES2001 and ES400-49. The PCR product was purified and then digested with restriction enzyme *Bam*H1 and *Sal*1. The plasmid pACTII was digested with restriction enzymes *Bam*H1 and *Xho*1. Subsequently, the digested PCR product was inserted into pACTII and the successful insertion was verified by sequencing using primers ES2001 and ES 400-49 (see Appendix H for verification results).

2.3 Deletion of *YIH1* in the chromosome

YIH1 was deleted by homologous recombination using a loxP/Cre gene disruption cassette published by Gueldener *et al*. [39]. In this procedure *YIH1* was replaced by a KanMX cassette flanked by two loxP sequences. The *YIH1* specific disruption cassette was generated by PCR using plasmid pUG6 as a template and primers ES400-34B and ES400-35B, which contain 81/80 nucleotides upstream/downstream of *YIH1* (depicted in red in figure 2.1). The resulting PCR product was transformed into the yeast strain and putative *yih1*Δ strains were selected by growth on plates containing G418. The deletion of *YIH1* was verified both by PCR (primer pairs ES400-30/ ES400-41 and ES400-33/ ES400-42, amplification only if *YIH1* has been substituted by the KanMX cassette in the genome, see figure 2.1) and Western blot analysis using antibodies against Yih1 (see Appendix D for verification results).

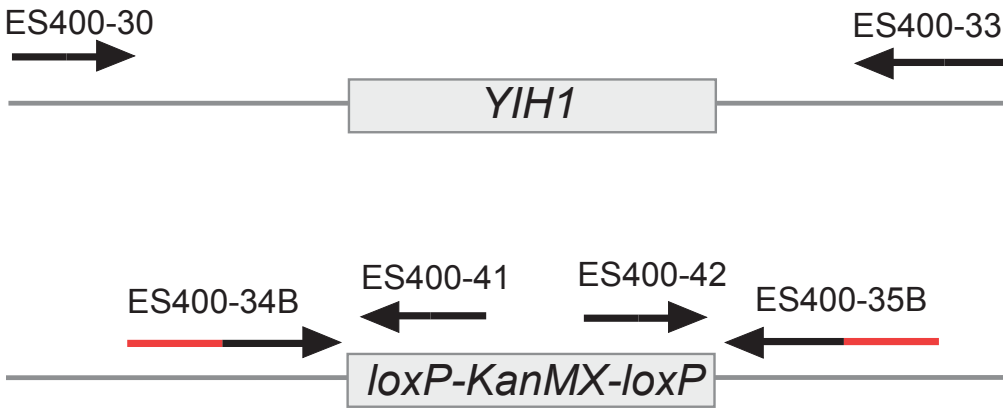

Figure 2.1: Schematic representation of location of primers used to delete *YIH1* in the chromosome. Primers ES400-34B and ES400-35B were used to amplify the loxP-KanMX-loxP cassette from plasmid pUG6. Both primers contain *YIH1* specific sequences which are depicted in red. Primer pairs ES400-30/ ES400-41 and ES400-33/ ES400-42 were used to verify the insertion of the deletion cassette into the genome. Using these primer pairs an amplification only occurs if *YIH1* is substituted by the loxP-KanMX-loxP cassette.

2.4 Media

Media for yeast and bacterial cultures were prepared using deionised Milli-Q® water and sterilized by autoclaving at 121 ℃, 15 psi for 20 minutes or filtered through 0.22 µm Millipore express® membrane filters. Carbon sources were sterilized separately from the media and added prior to use.

Liquid media were cooled to room temperature before the addition of supplements and were stored at room temperature unless mentioned otherwise.

Solid medium was prepared by adding agar to the media to a final concentration of 2% (w/v). Solid medium was cooled to 55 ℃ before supplements were added and poured into petri dishes. The plates were stored at 4 ℃.

All general chemicals and salts were analytical grade, unless specified, and purchased from Ajax Finechem, Sigma-Aldrich, Formedium, BDH, BioRad, Oxoid, Gibco, Thermo Fisher, Univar APS Australia or otherwise stated.

2.4.1 Bacterial media

Luria-Bertani (LB) medium
1% (w/v) Tryptone
0.5% (w/v) NaCl
0.5% (w/v) Yeast Extract
pH = 7

2.4.2 Yeast media

Yeast extract peptone dextrose media (YPD)	Yeast extract peptone glycerol media (YPG)
1% (w/v) Yeast extract	1% (w/v) Yeast extract
2% (w/v) Bactopeptone	2% (w/v) Bactopeptone
2% (w/v) Glucose	3% (w/v) Glycerol

Synthetic dropout media (SD)
0.145% (w/v) Yeast nitrogen base without amino acids (BDH)
or 0.19% (w/v) Yeast nitrogen base without amino acids (Formedium)
0.5% (w/v) Ammonium sulfate
2% (w/v) Glucose
or 2% or 10% (w/v) Galactose
or 2% (w/v) Raffinose

2.4.3 Media supplements

Table 2.3: Antibiotics, drugs and constituents used in this study

	solvent	final concentration
antibiotics		
Kanamycin	water	50 µg/ml
Ampicillin	water	100 µg/ml
G418	-	200 µg/ ml
drugs		
Sulfometuron methyl (SM)	DMSO	0.25 - 6 µg/ml
3-Aminotriazole (3AT)	water	10 - 50 mM
Isopropyl-β-D-thiogalactopyranosid (IPTG)	water	10 mM
constituents		
Adenine	water	0.15 mM
Histidine	water	0.3 mM
Isoleucine	water	0.5 mM
Leucine	water	2.0 mM or 40 mM (imbalance experiment)
Tryptophan	water	0.4 mM
Uracil	water	0.2 mM
Valine	water	0.5 mM

All constituent stock solutions (see table 2.3) were stored at room temperature except for tryptophan which was stored at 4℃ in a brown bottle. Histidine was stored in a brown bottle as well.

2.5 Growth conditions

2.5.1 Bacterial growth conditions

All *Escherichia coli* cultures were grown at 37℃ in LB broth or on LB agar plates supplemented with the appropriate supplements (see table 2.3). When grown in liquid media, the cultures were shaken at 180 rpm. Solid cultures were maintained at 4℃.

2.5.2 Yeast growth conditions

All *Saccharomyces cerevisiae* cultures were grown at the default temperature of 30℃ or the semi-permissive temperatures of 14℃, 20℃, 24℃, 34℃ and 37℃. Cultures were grown in/on SD media supplemented with the appropriate supplements (see table 2.3) or on/in YPD media or on YPG media. If grown in liquid media, cultures were shaken at 120-180 rpm. Solid cultures were maintained at 4℃.

2.6 Permanent storage of yeast/bacterial strains

Bacterial cultures were stored permanently at -80℃ in 66% (v/v) glycerol. Yeast cultures were stored permanently at -80℃ in 30% (v/v) glycerol.

2.7 DNA isolation and purification

2.7.1 Plasmid DNA isolation

A commercial available plasmid isolation kit (Invitrogen) was used to isolate plasmid DNA. The plasmid was extracted according to the manufacturer's specifications.

2.7.2 Genomic DNA extraction

Genomic DNA was extracted by resuspending a small amount of yeast cells in 50 µl 0.2% SDS solution. The cells were lysed by vortexing for 15 s and subsequent boiling at 90℃ for 4 min. The lysate was clarified by centrifugation at 16200 g, 4℃ for 1 min. 1 µl of the supernatant was used for subsequent PCR reactions of 50 µl volume.

0.2% SDS solution
0.2% (w/v) SDS
100 ml water
UV treated for 15 min

2.8 DNA quantification

The quantity of DNA was measured either using the Act Gene Asp 3700 nanodrop or by agarose gel electrophoresis. Here the brightness of the band to be quantitated was compared with the brightness of bands of known concentration.

2.9 Agarose gel electrophoresis

Agarose gels of concentrations between 0.8% and 1% (w/v) were made up in 1x TAE buffer containing 1 µl/ ml ethidium bromide (Sigma). Prior to separation in the gel, the samples were mixed with DNA loading dye. A constant voltage of 100 V was applied using the BioRad PowerPac 3000 (BioRad laboratories, Inc. USA) and the gel was run according to the sample size expected. The DNA was visualized on an UV transilluminator and images of the gel were taken using a Gel Doc imager (Bio Rad laboratories, Inc., USA).

Tris-Acetate-EDTA (TAE) buffer (50x)
2 M Tris
1 M Acetate
100 mM EDTA
pH = 8.1

DNA loading dye
0.25% Bromphenol blue
0.25% Xylene cyanol
50% glycerol

2.10 Restriction endonuclease digestion

For cloning, PCR products and plasmid DNA were digested with restriction enzymes using the buffer conditions and temperature recommended by the manufacturer. 1 µl/50 µl reaction mix CIP (Roche) was used to prevent self-ligation of the digested products. The reaction mix was subjected to agarose gel electrophoresis to check for complete digestion.

2.11 Polymerase chain reaction

DNA fragments were amplified from plasmid or genomic DNA using primers annealing to specific DNA sequences as required. A PCR reaction was typically carried out in a 50 µl reaction volume containing 1x PCR reaction buffer, 1.5 mM Magnesium chloride, 200 µM dNTPs, 40 pmol of primers (forward and reverse), 0.5 U Taq polymerase (Roche) or 1.25 U of proofreading Pfu polymerase (Fermentas) and 10-50 ng template DNA. The conditions used for a standard PCR were: 1.) Initial denaturing: 94℃ for 5 min for one cycle 2.) Denaturation: 94℃ for 30 s 3.) Annealing of primers: T = (T_m of primers - 5℃) for 30-45 s 4.) Elongation: 72℃ for X min (1 min per kb of template to be amplified), Step 2.) - 4.) were repeated for 30-40 cycles 5.) Final elongation: 72℃ for 10 min for one 1 cycle The PCR was performed in an iCycler (Bio Rad Laboratories, Inc. USA).

2.11.1 Primers

The lyophilized primers were resuspended in sterile Milli-Q® water to a stock concentration of 200 pmol/ µl. The stock solution was further diluted to 20 pmol/ µl. This solution was used as a working solution for PCR reactions and sequencing reactions. The primers were stored at -80℃. They were

manufactured by Invitrogen or Sigma. All oligonucleotides used in this study are summarized in table 2.4

Table 2.4: Primers used in this study

name	sequence (5' → 3')	purpose
ES400-2	CGA AAG CTT GTC GAC AGA ACT TGA AAT CGG ATT TCA TT	reverse primer for amplification of *YIH1*
ES400-30	GTA CCC GAC CGG GTT CTG	forward primer for verification of *YIH1* deletion
ES400-33	ACA CGC TGA CCC TAT TCC C	reverse primer for verification of *YIH1* deletion
ES400-34B	TAT ATA TAT ATA TAG ATA TAT ATA CAT ATA TAT AGG AAT ATG TAA CAA GAA AAA AAA AAG AGA GAG GAA AGA AAA GCT CAC AGC TGA AGC TTC GTA CGC	forward primer for amplification of *YIH1* specific KanMX cassette
ES400-35B	AAA TTT TTC CAA AAA ATT TCA AAA AGA ACT CCC GTC GCA TGT GAT CAA GGT TAC AGG TGC TTG ACA TAA TCA TAA TGA GCA TAG GCC ACT AGT GGA TCT G	reverse primer for amplification of *YIH1* specific KanMX cassette
ES400-41	CAT TTA GCC CAT ACA TCC	reverse primer in KanMX cassette
ES400-42	CCT CGA CAT CAT CTG CCC	forward primer in KanMX cassette
ES400-49	CGA AAG CTT GTC GAC TAA TGA TTA GTC GGT CTT CAG TCG GTC TA	reverse primer for amplification of *YIH1* fragment
ES2001	GCG CGC GGA TCC ATG GTG GTG GTA CTT CTT TGG CTA AGC GCG A	forward primer for amplification of Yih1 fragment
ES2036	GCG CGC GGA TCC ATG GTG GTG GTA TGG ATG ACG ATC ACG AAC AG	forward primer for amplification of *YIH1*
ES2125	TGC TGC TTT GGT TAT TGA TAAC	forward primer for amplification of *ACT1* fragment & sequencing
ES2126	AGC AGT GGT GGA GAA AGA GT	reverse primer for amplification of *ACT1* fragment

2.12 DNA purification

PCR products and plasmid DNA were purified using the QiAquick purification kit according to the manufacturer's specifications.

2.13 DNA ligation

2.13.1 Dephosphorylation

To avoid self ligation of the digested plasmid, it was dephosphorylated with 1 U of calf intestinal alkaline phosphatase (CIP) (New England Biolabs Inc., USA) during the restriction digestion. CIP was added directly to the digestion mix and subjected to digestion conditions as recommended by the manufacturer.

2.13.2 Ligation

The digested, purified PCR product and vector were ligated using molar ratios of 1:3 and 1:6 (vector to insert) in a total reaction volume of 10 µl. The ligation mix containing 1x DNA ligase buffer and 1U T4 DNA ligase was subjected to incubation for 20 s at 30℃ and 20 s at 10℃ overnight. 5 µl of this ligation mix was used for subsequent transformation into *E.coli*.

2.14 Transformation of *Escherichia coli*

The protocol used for *E.coli* transformations is adapted from Sambrook *et al*. [107] and is described in the following.

2.14.1 Preparation of calcium chloride competent *E.coli* cells

A saturated overnight culture of a single DH5α colony was used to inoculate 40 ml of LB broth. This culture was subsequently grown to an OD_{600nm} = 1.5. The cells were then harvested by centrifugation at 2791 g for 10 min at 4℃.

The pellet was resuspended in 20 ml of cold calcium chloride solution and incubated on ice for 30 min. The cells were once again spun at 2791 g for 10 min at 4℃ and the pellet was then resuspended in 4 ml of cold glycerol-calcium chloride solution. The chemical competent cells were aliquoted and stored at -80℃.

Calcium chloride solution
50 mM $CaCl_2$
Filter sterilized

Glycerol-calcium chloride solution
15% (v/v) Glycerol
50 mM $CaCl_2$
Filter sterilized

2.14.2 Transformation of *E.coli* using the heat shock method

The competent *E.coli* cells were carefully thawn on ice. 1 µl of plasmid DNA or 5 µl of ligation mix was added to 50 µl of chemical competent cells and incubated on ice for 40 min. The cells were heat shocked at 42℃ for 3 min and immediately incubated on ice for another 10 min. 1 ml of LB media was added and the mix incubated at 37℃ shaking at 180 rpm for one hour. The cells were platted on LB media containing the appropriate antibiotics and incubated at 37℃ overnight.

2.15 DNA sequencing

For sequencing by the Alan Wilson Centre Genome Service 3.2 pmol primer and 300 ng plasmid DNA or 10 ng PCR product were submitted in a total volume of 15 µl.

2.16 Yeast transformation

The protocol used for transforming yeast is adapted from Gietz *et al*. [34] and outlined in the following.

2.16.1 Preparation of competent *Saccharomyces cerevisiae* cells

An overnight culture of *S. cerevisiae* was prepared and incubated at 30℃. 50 ml of YPD media was inoculated with 1 ml of this overnight culture and incubated shaking at 160 rpm until the OD_{600nm} had doubled. Then the cells were spun at 2791 g, 4℃ for 3 min and washed in 5 ml 0.1 M Lithium acetate (LiOAc). The cells were pelleted again at 2791 g, 4℃ for 3 min and resuspended in 500 µl 0.1 M LiOAc. Afterwards the cells were incubated at 30℃ for 30 min and then either used immediately or stored at 4℃ for use within the next 24 hrs.

Lithium acetate (LiOAc)
0.1 M LiOAC
in TE buffer
Filter sterilized

Tris-EDTA buffer (TE)
10 mM Tris
1 mM EDTA
pH = 7.4 with HCl
Filter sterilized

2.16.2 Standard yeast transformation

100 µl of competent yeast cells, 5 µl of plasmid/PCR product and 5 µl of 10 min boiled single stranded Hering sperm DNA were mixed and incubated at 30℃ for 15 min. 600 µl of Lithium acetate/ Polyethyleneglycol (LiOAc/PEG) solution was added and the mix was incubated for another 30 min at 30℃. 70 µl of Dimethylsulfoxide (DMSO) was added to the cells before heat shocking them for 15 min at 42℃. Afterwards the cells were spun at 2791 g for 3 min and the pellet was resuspended in 50 µl SD media. The cells were plated on SD plates containing the appropriate constituents and incubated at 30℃ until colonies were visible.

Lithium acetate/ Polyethyleneglycol (LiOAc/PEG) solution
0.1 M LiOAc in TE buffer
40% PEG 3350
Filter sterilized

2.16.3 Yeast transformation for deleting *YIH1*

The transformation was performed as outlined above with 2 exceptions. First, the DMSO was omitted before heat shocking the cells. Secondly, the cells were grown overnight at 30℃ in liquid YPD media before platting.

2.17 Preparation of yeast whole cell extract

Cells were grown and harvested as outlined in the individual chapters (see chapters 2.24 and 2.25). For breaking the cells 1 pellet volume of ice cold breaking buffer containing inhibitors and 1 pellet volume of acid washed glass beads was added to the pellet. The general breaking buffer outlined below was used if not otherwise stated. The samples were then vortexed for 30 s followed by incubation in an ice-water mix for 30 s. This procedure was repeated 10 times. The cellular debris and glass beads were pelleted by centrifugation at 13800 g for 10 min at 4℃. The supernatant called the whole cell extract (WCE) was stored at -80℃. The total protein concentration of the yeast WCE was determined by the Bradford method (see chapter 2.18).

General breaking buffer
50 mM Tris-HCl, pH = 7.5
50 mM NaCl
0.1% Triton X-100
0.5 M EDTA
1 mM DTT
1 mM PMSF
10 µg/ ml Pepstatin

Table 2.5: Inhibitors used in this study

inhibitor	diluent	stock concentration
PMSF	isopropanol	100 mM
Pepstatin	methanol	1 mg/ ml
DTT	water	1 M

2.18 Estimation of protein concentration by Bradford method

A protocol established by M. Bradford [10] was used to estimate protein concentrations. The procedure is outlined in the following. For estimating the total protein concentration in a sample 1 µl of the sample and for reference increasing concentrations of Bovine Serum Albumin (BSA) (1 µg, 2 µg, 4 µg, 6 µg, 8 µg, 10 µg) were mixed with 200 µl Bradford solution in duplicates in a 96 well clear microtitre plate. The mixture was incubated for 5 min at room temperature and then the absorbance at 595 nm was measured in a FLUOstar OPTIMA plate reader (BMG Labtech). A standard curve was plotted using the BSA references of known concentrations. The protein concentration of the unknown samples was determined by comparison of its absorbance with the standard curve.

Bradford solution
50 mg Coomassie Blue G250
25 ml 95% Ethanol
50 ml 85% H_3PO_4
25 ml 1 M NaOH
store in a brown bottle

2.19 Sodium dodecyl sulfate polyacrylamide gel electrophoresis

Protein samples were separated using both gradient and straight sodium-dodecylsulfate polyacrylamide gel electrophoresis (SDS-PAGE).

2.19.1 Gradient gel electrophoresis

4% - 17% gradient gels were produced by first sealing the gaps created by spacers between two glass plates with 1% agarose in 1.5 M Tris-HCl (pH = 8.8). The gradient was generated by mixing 20 ml of both 4% and

17% premix with 20 µl N,N,N',N'-TetraMethylEthyleneDiamine (TEMED) and 200 µl of 10% ammoniumpersulfate (APS) in individual mixing chambers. By opening a valve between the chambers, the stocks were mixed and a gradient of acrylamide was poured in the gap between the glass plates. A comb was added to create the wells and the gel was solidified for 15-30 min. The dimensions of the resulting gel are 7 cm (height) x 14.5 cm (width) x 1.8 mm (thickness). Before loading the samples, the wells were rinsed with protein running buffer and then mounted into the gel electrophoresis unit. The gel was covered with sufficient protein running buffer and the protein samples were loaded. Prior to loading, the samples were mixed with Laemmli loading dye and denatured at 85℃ for 10 min. 250 V and 100 mA was applied to run the gel until the dye front had reached the end of the gel.

4% Premix (20ml)
2 ml 29:1 (acrylamide: bis-acrylamide) 40% Acrylamide
5 ml 1.5 M Tris-HCl, pH = 8.8
200 µl 10% SDS (w/v)
13 ml Milli-Q® water

17% Premix (20ml)
8.5 ml 29:1(acrylamide: bis-acrylamide) 40% Acrylamide
5 ml 1.5 M Tris-HCl, pH = 8.8
200 µl 10% SDS (w/v)
6.5 ml Milli-Q® water

Protein running buffer
25 mM Tris base, pH = 8.8
192 mM glycine
1% SDS (w/v)

5X Laemmli loading dye
0.312 M Tris-HCl, pH = 6.8
10% SDS (w/v)
25% β-Mercaptoethanol (v/v)
0.05% Bromphenol blue (w/v)

2.19.2 Straight gel electrophoresis

To cast straight gels the Bio RAD Mini PROTEAN 3 system (Bio Rad Laboratories Inc., USA) was used. The resolving gel was poured straight between the glass plates mounted into the pouring apparatus. 1 ml of Isopropanol was layered on top to create a smooth surface. The gel was left to set until solid and the isopropanol was removed. The stacking gel mix was poured on top and a comb was added to create the wells. The gel was left to set

until solid. Before loading the samples, the wells were rinsed with protein running buffer and then mounted into the gel electrophoresis unit. The gel was covered with sufficient protein running buffer and the protein samples were loaded. Prior to loading, the samples were mixed with Laemmli loading dye and denatured at 85℃ for 10 min. 80 mA was applied to run the gel until the dye front had reached the end of the gel.

10% Resolving gel (10 ml)
2.5 ml 29:1 (acrylamide: bis-acrylamide) 40% Acrylamide
2.5 ml 1.5M Tris-HCl pH = 8.8
100 µl 10% SDS (w/v)
100 µl 10% APS
4 µl TEMED
4 ml Milli-Q® water

0.67% Stacking gel (4 ml)
67 µl 29:1 (acrylamide: bis-acrylamide) 40% Acrylamide
0.5 ml 2 M Tris-HCl pH = 6.8
40 µl 10% SDS (w/v)
40 µl 10% APS
4 µl TEMED
2.7 ml Milli-Q® water

2.20 Staining proteins in polyacrylamide gels

To visualize proteins in polyacrylamide gels the gel was stained with Coomassie brilliant blue overnight and destained with Coomassie brilliant blue destainer until the background staining had destained and the bands were visible.

Coomassie brilliant blue stain
21 ml Acetic acid
60 ml Methanol
209 ml water
0.75 g Coomassie R250

Coomassie brilliant blue destainer
21 ml Acetic acid
60 ml Methanol
209 ml water

2.21 Western blotting

2.21.1 Gel transfer

For western blotting the proteins were transferred from the gel onto Immobilion PVDF membranes (Millipore) with a pore size of 0,45μm. The membrane was soaked in Methanol and equilibrated in transfer buffer before usage. The gel and the membrane was assembled in the transfer unit (Idea Scientific Company, USA) and submerged in transfer buffer. The proteins were transfered for 2.5 hrs at 24 V and 1 A.

Transfer buffer
25 mM Tris base, pH = 8.3
192 M Glycine
20% Methanol (v/v)

2.21.2 Staining proteins on PVDF membranes

To visualize the proteins on the membrane, it was incubated shaking with Ponceau S stain for 10 min. The membrane was destained with 1% acetic acid until protein bands were visible.

Ponceau S
0.1% Ponceau S (w/v)
1% Acetic acid (v/v)

2.21.3 Immunological detection of proteins

To visualize specific proteins on the membrane it was first blocked shaking at room temperature with 5% skim milk for 60 min. Then the membrane was incubated for another 60 min with the appropriate primary antibody (see table 2.6). All antibodies used were diluted in 5% skim milk. Before incubating the membrane with the appropriate secondary antibody (see table 2.7) conjugated with horseradish peroxidase for another 60 min at room temperature,

it was washed for 5 min, 10 min and 10 min with TBS-T shaking at room temperature. Finally the membrane was washed another 5 min, 10 min, 10 min, 15 min with TBS-T shaking at room temperature. Super Signal West Pico Chemiluminescence solution (Pierce) was prepared according to the manufacturers specifications and the membrane was incubated with the solution for 5 min. The chemiluminescence signal emitted by the conjugated antibody linked to the protein of interest was detected with the Luminescent Image Analyzer LAS-4000 (Fujifilm). The intensity of the obtained signals was analyzed using the Image J software (NIH) or the Multi Gauge V3.1 software (Fujifilm).

Tris buffered saline - Tween (TBS-T)
1 M Tris-HCl, pH = 7.4
5 M NaCl
0.1% Tween 20

5% skim milk
5% skim milk (w/v) (Pams)
1x TBS-T

Table 2.6: Primary antibodies used in this study

antibody	dilution	secondary antibody	source	order number
actin	1 in 5000	anti guinea pig	D. Botstein [83]	-
Cdc28	1 in 500	anti goat	Santa Cruz	Sc-6709
GST	1 in 10 000	anti bunny	Santa Cruz	Sc-459
HA	1 in 500	anti bunny	Santa Cruz	Sc-805
Pgk1	1 in 5000	anti mouse	Invitrogen	459250
Yih1	1 in 1000	anti bunny	B. Castilho	-

Table 2.7: Secondary antibodies used in this study

secondary antibody	dilution	source	order number
anti bunny	1 in 100 000	Pierce	31458
anti mouse	1 in 50 000	Pierce	32230
anti guinea pig	1 in 5000	Santa Cruz	Sc-2438
anti goat	1 in 5000	Pierce	31400

2.22 Semi-quantitative growth assay

To investigate the growth ability of yeast strains under specific conditions overnight cultures were grown in 3 ml of the appropriate liquid media at 30℃. Saturated overnight cultures were subjected to 10 fold serial dilution with SD media. 5 µl of each dilution and 5 µl of undiluted culture was transferred to solid media supplemented with the appropriate supplements (see table 2.3). At least one plate for each concentration with two biological replicates was used. Plates were incubated at various temperatures until colonies were visible. To document the growth of the strains, the plates were scanned using a conventional document scanner. In the Gcn4^{c} screen the growth was scored using a 10 point system with 10 indicating that in all dilutions colonies were visible and 0 indicating that no colonies were visible (see figure 2.2, panel A). The rate of reversion of the SM^{S} in the actin mutant strain was calculated as outlined in figure 2.2, panel B. In brief, the growth score of the strain expressing the vector alone was subtracted from growth score of the strain expressing Gcn4. This calculation was done for the wild type strain and the actin mutant strain on both starvation and non-starvation plates. The resulting number of the SD plate was subtracted from the number of the SD+SM plate. This calculation was done both for the wild type strain and the actin mutant strain. The resulting number of the wild type strain was subtracted from the number of the actin mutant strain. The resulting number indicates the strength of reversion of the sensitivity to SM when Gcn4 is constitutively expressed. The higher the number, the stronger the reversion. This scoring system was developed by E. Sattlegger.

Christina Ellert performed the 3AT screen, whereas Vivianne Jochmann carried out part of the Gcn4^{C} screen. The SM^{S} screen using *yih1* deleted actin mutant strains was done by Hee Jun Lee. All students were supervised by M.Dautel.

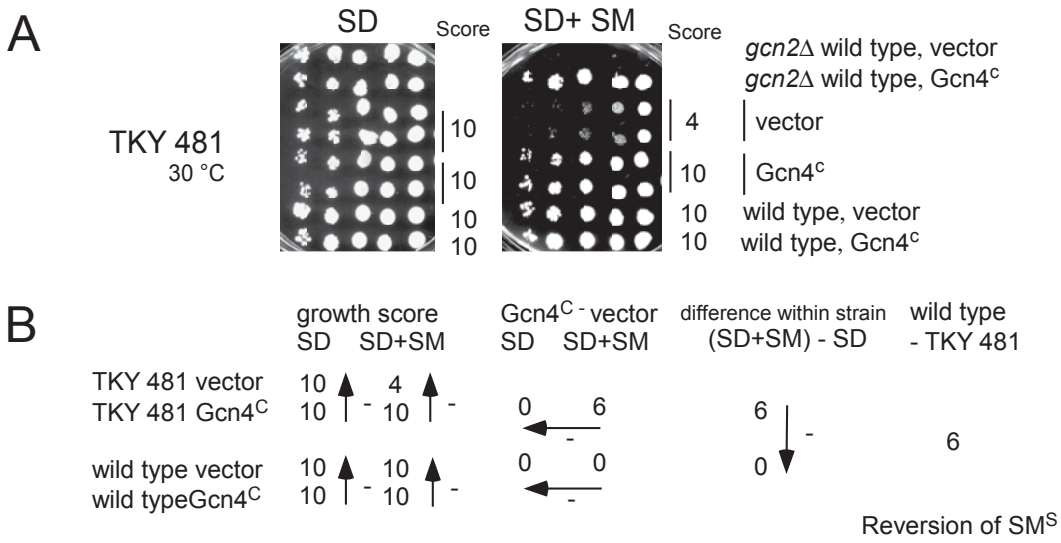

Figure 2.2: Example of the calculation of a SM^S reversion in a semi-quantitative growth assay. A.) Example of scoring the growth B.) Example of the calculation of a SM^S reversion.

2.23 Growth assay to check for petite mutations

To investigate if yeast strains are petite mutants, strains to be investigated, a strain known to be a petite (positive control) and a non-petite strain (negative control) were streaked on YPD and YPG solid media. The plates were incubated at 30℃ until growth was visible. Petite mutant strains are characterized by their lack of growth on YPG in comparison to YPD.

2.24 *lacZ* assay

The protocol used for the Gcn4p-*lacZ* assay is adapted from Miller [79] and is outlined in the following.

2.24.1 Growing of cells

50 ml of non-starvation SD media supplemented with the appropriate constituents and 50 ml of starvation media supplemented with the appropriate constituents were inoculated with saturated overnight cultures to a final OD_{600nm} of 0.4. The cultures were grown at the indicated temperature shaking at 160 rpm. Cells growing in non-starvation media were harvested after 6 hrs. After growing for 2 hrs, cells growing in starvation media were starved with 50 µl of 500 µg/ ml SM for 6 hrs and subsequently harvested. The cell pellets were stored at -80℃.

2.24.2 β-Galactosidase assay

Cells were broken as described earlier (see chapter 2.17) using the *lacZ* breaking buffer, and the total protein concentration was determined using the Bradford method as described earlier (see chapter 2.18). The WCE was mixed with Z-buffer to a total volume of 1 ml and incubate in a water bath at 28℃. The zero time was noted and 200 µl of o-nitrophenyl-β-D-galactosidase (ONPG) solution was added as a substrate to start the reaction. The samples were incubated until a yellow color developped. 500 µl of 1 M Na_2CO_3 was added to stop the reaction and the stop time was noted. The absorption was measured at a wavelength of 420 nm in a FLUOstar OPTIMA plate reader (BMG Labtech). The enzyme activity was calculated as outlined:

$$1 \text{ Miller Unit} = \frac{1.7 \cdot OD_{420nm}}{0.0045 \cdot V \cdot t \cdot c} \cdot 1000 \tag{2.1}$$

where

OD_{420nm}	optical density at 420 nm
V	volume of extract in ml
t	time in min
c	protein concentration in extract in µg/ µl

lacZ breaking buffer
0.2 M Tris-HCl, pH = 8
20% glycerol (v/v)
1 mM PMSF

o-nitrophenyl-β-D-galactosidase (ONPG)
4 mg/ ml OPNG
in Z-buffer

Z-buffer
16.1 g $Na_2HPO_4 \cdot 7\ H_2O$
5.5 g $NaH_2PO_4 \cdot H_2O$
0.75 g KCl
0.246 g $MgSO_4 \cdot 7\ H_2O$
2.7 ml β-Mercaptoethanol
ad 1000 ml
pH = 7

2.25 Glutathione S-Transferase mediated *in vivo* pulldown assay

2.25.1 Growing and breaking of cells

Strains were grown in 300 ml of the appropriate selective SD media supplemented with galactose as the sole carbon source at the indicated temperature until they reached an $OD_{600\,nm}$ of 1. They were harvested by pelleting at 2791 g, for 5 min at 4℃ and transferred with cold water into a 15 ml round bottom tube. The samples were once again spun down at 2791 g for 5 min at 4℃ and processed further or stored at -80℃. For breaking the cell pellet was thawn on ice and 200 µl Glutathione S-Transferase (GST) breaking buffer including inhibitors and one pellet volume of acid washed beads was added. The tubes were vortexed for 30 s with 30 s interruptions on ice. This cycle of vortexing and cooling was repeated 10 times. The resulting whole cell extract was spun at 16200 g, 4℃ for 5 min and the supernatant was transferred to an Eppendorf tube. The total protein concentration in the whole cell extract was determined by using the Bradford method (see chapter 2.18)

2.25.2 Glutathione S-Transferase mediated pulldown

To reduce background binding in the *in vivo* GST pulldown 4,8 mg of whole cell extract was pre-adsorbed with 20 µl [50% (v/v)] washed BioRad Profinity iMac Ni-charged resin for 20 min at 4℃. 200 µl of the pre-adsorbed whole cell extract was subsequently incubated with 45 µl [66% (v/v)] of washed GST beads for 2 hrs at 4℃. The whole cell extract was removed and un-

bound proteins were washed off five times using GST breaking buffer containing inhibitors. The beads were re-suspend in 30 µl Laemmli loading dye and the protein complex still associated to glutathione beads was boiled off the beads at 80℃ for 10 min. The precipitates were resolved by 4% - 17% SDS-PAGE and investigated via immunoblotting using antibodies as indicated. In general 30 µl of sample was loaded. The amount of input control loaded varied and is indicated in the individual results.

GST breaking buffer
30 mM HEPES
50 mM KCl
10% glycerol
1 mM DTT
1 mM PMSF
10 µg/ ml Pepstatin
1 complete tablet with EDTA (Roche) per 25 ml
pH = 7.4

2.26 Purification of His_6-Yih1

For the purification of His_6-Yih1 a protocol established by Sattlegger *et al*. was followed [108]. The purification details are outlined below.

2.26.1 Growing of cells

300 ml of LB media containing kanamycin was inoculated with 4 ml of saturated overnight culture of the bacterial strain pES189-D1A expressing His_6-Yih1. The culture was grow at 30℃ until OD_{600nm} = 0.8. The expression of His_6-Yih1 was induced with 1 mM Isopropyl-beta-D-1-thiogalatopyranosidase (IPTG) before shifting the cultures to 20℃ for 3 hrs. Cells were harvested by pelleting at 2791 g, for 5 min at 4℃ and the resulting pellet was resuspended in 1 ml of breaking buffer with inhibitors. To break the cells 20 µl 10 mg/ ml lysozyme was added and the solution was incubated for 30 min at 4℃. The resulting extract was stored at -80℃. The cell extract was further treated with 1 µl 20 mg/ ml RNase and 16 µl 10 U/ µl DNase (Roche) at

4℃ until liquid and subsequently centrifuged at 16200 g at 4℃ for 10 min. The supernatant containing the soluble protein fraction was used for the subsequent purification of His_6-Yih1 or the *in vitro* binding assay described in chapter 2.28 .

2.26.2 Purification of His_6-Yih1 from bacterial whole cell extract

2.3 ml [50% (v/v)] of BioRad Profinity iMac Ni-charged resin was washed with breaking buffer and immobilized in a column. The supernatant containing His_6-Yih1 was added to the column and incubated on the roller at 4℃ for 60 min. The column was washed with increasing imidazole concentrations (5 mM, 5 mM, 20 mM) and the protein was eluted in three consecutive elution steps with buffer containing 250 mM Imidazole. 20 µl of eluate was mixed with an equal amount of loading dye and 10 µl was separated via SDS-PAGE on a 10% gel. The protein was visualized by staining with Coomassie brilliant blue.

Breaking buffer	Inhibitors per 25 mL buffer
30 mM HEPES	1 complete inhibitor tablet (Roche)
50 mM KCl	1 mM DTT
10% glycerol	1 mM PMSF
pH = 7.4	2 µl β-Mercaptoethanol

2.27 *In vitro* pulldown with F-actin

For the F-actin sedimentation assay a kit (Cytoskeleton) was used and the assay was performed according to the manufacturer's specifications as outlined below.

2.27.1 Protein preparation

His_6-Yih1 preparation 50 µl of 1 mg/ ml purified His_6-Yih1 in 30 mM HEPES, 50 mM KCl, 10% glycerol, 250 mM Imidazole buffer was spun at

150000 g for 60 min at 4℃. The resulting supernatant was used for the consequent assay.

F-actin preparation 250 µg of rabbit muscle actin was resuspended in 250 µl of general actin buffer and incubated on ice for 30 min. Subsequently, 25 µl of actin polymerizing buffer was added to start polymerization. The solution was incubated at room temperature for 60 min.

General actin buffer (Cytoskeleton)
5 mM Tris HCl
0.2 mM $CaCl_2$
pH = 8

Polymerization buffer (Cytoskeleton)
500 mM KCl
20 mM $MgCl_2$
10 mM ATP

2.27.2 *In vitro* F-actin interaction assay

Samples were prepared according to the manufacturer's protocol using 40 µg F-actin, 10 µg His_6-Yih1 and 10 µg α-actinin in a total volume of 50 µl. After incubation at room temperature for 30 min the samples were spun at 150000 g for 60 min at 24℃. The supernatant was taken off and 10 µl of loading dye was added. The pellet was resuspended in 30 µl water and then 30 µl of loading dye was added. 20 µl of supernatant and resuspended pellet was separated by SDS-PAGE on a 4% - 17% gradient gel and the proteins were visualized by Coomassie brilliant blue staining.

2.28 *In vitro* interaction assay of His_6-Yih1 and rabbit G-actin

Whole cell extract containing His_6-Yih1 was generated as described earlier (see chapter 2.26.2). 250 µg of rabbit globular actin was resuspended in 250 µl His_6 pulldown buffer. 30 µl [50% (v/v)] of BioRad Profinity iMac Ni-charged resin was washed with breaking buffer. 100 µl of bacterial whole cell extract containing His_6-Yih1 was added and incubated at 4℃ for 60 min. No whole cell extract was added to the negative control. The beads were

washed with breaking buffer before 20 µg of G-actin was added to His_6-Yih1 coated beads and incubated for 30 min at 4°C. Unbound protein was washed off using His_6 pulldown buffer. The co-precipitates were boiled off the beads in 100 µl loading dye and 20 µl of sample was separated by SDS-PAGE on a 4% - 17% gradient gel. Actin was visualized by Western blot analysis using antibodies against actin. His_6-Yih1 was visualized by Ponceau S staining of the membrane. Modifications of this procedure during the optimization process are indicated in the text.

His_6 pulldown buffer
30 mM HEPES
50 mM KCl
10% glycerol
0.2 mM $CaCl_2$
0.2 mM ATP (Roche)
1 complete inhibitor tablet (Roche) per 25 ml buffer
1 mM DTT
1 mM PMSF
2 µl β-Mercaptoethanol

3

Comprehensive screen of actin mutant strains for an impaired GAAC response

Yih1 is a protein expressed in *S. cerevisiae*. When overexpressed under starvation conditions, Yih1 has been shown to impair the GAAC stress response by inhibiting Gcn2 activation [110, 108]. As outlined in the introduction to this study, several lines of evidence suggest that Yih1 binds to the Gcn2 effector protein Gcn1 and thus hinders Gcn2 function by competing with Gcn2 for Gcn1 binding [110, 108, 69]. However, Yih1 does not seem to be a general inhibitor of Gcn2 as deletion of *YIH1* does not alter the GAAC response [110]. This suggested, that Yih1 itself must be regulated and potential regulators of Yih1 were sought by identifying novel binding partners of Yih1.

Monomeric G-actin has been identified as a binding partner of Yih1 *in vivo* by co-precipitation assays [110] and the Yih1-actin interaction has been

shown to be independent of Gcn1 and vice versa [110, 108]. Recent studies indicate that actin is in fact regulating Yih1 as a reduced level of cellular actin renders the cells unable to respond to AA starvation. This impaired stress response has been shown to be partially dependent of Yih1 [110]. Taken together these findings, lead to the model of Yih1 mediated Gcn2 function, where Yih1 resides in the cell in an inactive Yih1 - actin complex. Upon release of Yih1 from actin it competes with Gcn2 for Gcn1 binding and subsequently inhibits Gcn2 activation (see figure 1.6 in introduction).

However, despite extensive research within the last few years [110, 108] little is known about the Yih1-actin interaction and actin's influence on the GAAC. Considering the fact that actin is an essential protein and leads to lethality of the cell upon deletion, a strategy using actin mutations was employed to increase the knowledge about the Yih1-actin interaction and the affect of actin on the stress response by identify mutations in actin affecting the GAAC. The actin mutant screen focused on affects on the GAAC caused in a Gcn4 expression dependent manner.

The only way to determine the binding of Yih1 to actin in these strains is through Yih1's ability to inhibit Gcn2 upon release from actin, which would result in an impaired GAAC response. Thus, the actin mutant strains were screened for an impaired GAAC response. This approach is based on the assumption that an actin mutation in the Yih1 binding site will trigger a release of Yih1 from monomeric actin. Consequently, the free Yih1 will inhibit Gcn2 activation under starvation conditions which will be indicated by a Gcn^- phenotype caused upstream of Gcn4 expression. As described earlier, the GAAC pathway consists of a cascade of processes beginning with the activation of Gcn2, followed by the phosphorylation of eIF2α and the expression of Gcn4 and its downstream implications. To ensure that an interrupted Yih1-actin interaction is in fact responsible for the impaired GAAC, the affect of the actin mutation on different levels of the pathway were investigated.

For this purpose a set of 24 previously described actin mutant strains was used in this study [134]. This collection of mutants was engineered to be isogenic except at the actin locus, so that differences observed between mutants could be attributed solely to the actin alleles carried [134]. Muta-

tions were systematically targeted to the surface of the protein to guarantee the upmost disruption of actin binding (see figure 3.1).

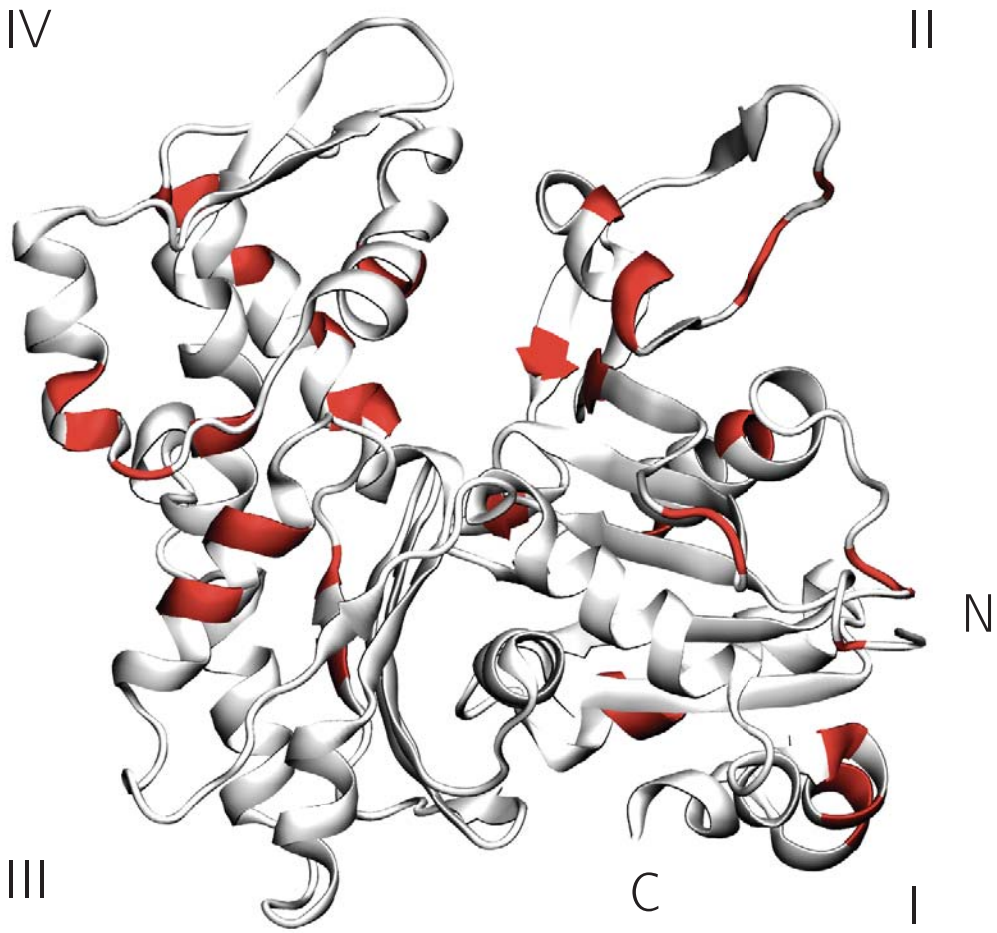

Figure 3.1: Location of actin mutations investigated within the structure of actin. The atomic structure of *S. cerevisiae* G-actin (PDB code 1ATN, [57]) was modeled using the VMD software [54]. Actin point mutations investigated are indicated in red. Subdomains I - IV and the N/ C-terminus of actin are labelled accordingly.

3.1 Screen of actin mutant strains for sensitivity to sulfometuron methyl

The general amino acid response is not triggered by growth in minimal medium as yeast can synthesize all 20 amino acids [48]. Rather the AA biosynthesis must be suppressed by antimetabolites [48] such as sulfometuron methyl (SM). SM inhibits the enzyme acetolactate synthase which is involved in the biosynthesis of Isoleucine, Leucine and Valine [27, 72].

The first step to identify if the actin mutant strains have an impaired GAAC response was to check if the strains are able to respond to AA starvation caused by SM. If a strain is unable to grow when SM is added to the media it is called SM sensitivity (SM^S). This phenotype is a first indication for a dysfunctional stress response in yeast. Therefore the 24 actin mutant yeast strains were subjected to a semi-quantitative growth assay under starvation conditions. Here, the ability of the actin mutant strain to grow under replete conditions was compared to the growth of an isogenic strain containing wild type actin. This particular strain (TKY 460) was used as a wild type reference in this study. A *gcn2*$\triangle$ strain in the H1511 background (H2557) and a *gcn20*$\triangle$ strain in the H1511 background (H2558) which are not able to respond to nutritional stress as *GCN2* and *GCN20* are essential under starvation conditions, were used as negative controls and should not grow under starvation conditions. The wild type strain in the same background (H1511) was used as a positive control. The assay was conducted across a temperature range from semi-permissive to permissive as determined by Wertman *et al*. [132] as it was unknown at which temperature the effect of the actin mutation on the GAAC is detectable. This screen was performed by K. Mann and repeated and analyzed by E. Sattlegger using a 10 point scoring system similar to the one presented in chapter 2.22 (data not shown). The result of the screen is summarized in table 3.1.

Of the 24 strains five actin mutant strains (TKY 461, TKY 465, TKY 466, TKY 469 and TKY 486) showed no reduced growth in the presence of SM. These strains grew as well as the wild type strain TKY 460 under starvation conditions. This suggests, that these particular actin mutations do not af-

Table 3.1: Overview of the screen of actin mutant strains for sensitivity to SM

strain name	actin allele	overall	SM sensitivity						notes
			37°C	34°C	30°C	24°C	20°C	14°C	
TKY 461	*act1-102*	−	0	0	0		0	0	
TKY 462	*act1-4*	+		0.5	1		0	1	
TKY 463	*act1-7*	−/+	3	0	0		0	1	1. screen
TKY 465	*act1-123*	−	0	0	0		0	0	
TKY 466	*act1-115*	−	0	0	0		0	0	
TKY 467	*act1-111*	+			2.5	2	1	2	
TKY 468	*act1-113*	+	0	0	0	0	1	2	
TKY 469	*act1-116*	−	0		0			0	
TKY 470	*act1-104*	−/+	0.5		0		0	1	1. screen
TKY 471	*act1-135*	−/+	0		0		0	1	1. screen
TKY 472	*act1-117*	−/+	0.5		2		0	0	1. screen
TKY 473	*act1-133*	+		3	2.5		1	2	
TKY 474	*act1-10*	−/+	0.5		0		0	0	1. screen
TKY 475	*act1-9*	+	3.5	4	1.5		0	2	
TKY 476	*act1-3*	+	1	1.5	1.5			1	
TKY 477	*act1-20*	+	3	2	2		1	2	
TKY 478	*act1-8*	+	4	2	0.5		1	2	
TKY 479	*act1-129*	+	5	2	1			4.5	
TKY 480	*act1-125*	−/+		1.5	0	2	0.5	0.5	1. screen
TKY 481	*act1-122*	+		0.5	1		2.5	3	
TKY 482	*act1-124*	+		2.5	2		1	2	
TKY 483	*act1-120*	+	0	3.5	3.5			4	
TKY 484	*act1-119*	+	3	3	1			3	
TKY 486	*act1-101*	−			0	0	0	0	

The number indicates the strength of the sensitivity to SM compared to the WT strain. The higher the number, the stronger the sensitivity. The scoring system was developed by E. Sattlegger (see chapter 2.22). The negative and positive control strains grew as expected. The number represents the average sensitivity of two independent screens. − indicates phenotype similar to the wild type strain, + indicates impaired growth compared to the wild type strain, 1. screen indicates that this altered phenotype was only detected in one screen, blank space indicates that this temperature was not included in the screen.

fect the GAAC. The remaining 19 actin mutant strains showed a sensitivity to SM in at least one screen under the conditions investigated. It was concluded, that their specific actin mutation was potentially influencing the AA stress response. To confirm that the observed SM^S phenotype is related to an impaired GAAC, an additional screen was undertaken to determine the influence of AA imbalance on these yeast strains.

3.2 Screen of actin mutant strains for sensitivity to amino acid imbalance

The GAAC pathway enables yeast cells not only to react to AA starvation but also to AA imbalance [89]. Therefore, it was hypothesized that if the GAAC is inhibited in these strains, they should also be unable to respond to this nutritional inequality and not flourish. Thus the 24 actin mutant yeast strains were subjected to a semi-quantitative growth assay under excessive Leucine conditions. The growth of the actin mutant strains was compared to the growth of the wild type strain TKY 460. A *gcn2*Δ strain in the H1511 background (H2557) and a *gcn20*Δ strain in the H1511 background (H2558), which are not able to respond to nutritional stress, were used as negative controls. Wild type strain H1511 was used as a positive control. The assay was conducted at a similar temperature range as the SM^S screen. This screen was performed and analyzed by E. Sattlegger using a 10 point scoring system similar to the one presented in chapter 2.22 (data not shown). The result of the screen is summarized in table 3.2.

The growth of seven yeast strains, namely TKY 461, TKY 463, TKY 465, TKY 466, TKY 469, TKY 474 and TKY 486, was not affected by an excess of Leucine in the media compared to the wild type strain TKY 460. This result suggests, that the GAAC is functional in these mutant strains. This result confirms the result of the previous SM^S screen as the majority of the strains being resistant to AA imbalance is resistant to SM as well. The remaining 17 strains were sensitive to an imbalance of AA as shown by an impaired growth. The reduced growth rate of the mutant strains indicates that their GAAC could be impaired. To ensure that these reduced growth rates are in fact caused by a defective stress response an additional independent screen of the actin mutant strain was performed using the antimetabolite 3-Aminotriazole (3AT).

Table 3.2: Overview of the screen of actin mutant strains for sensitivity to AA imbalance

strain name	actin allele	overall	AA imbalance sensitivity					
			37°C	34°C	30°C	24°C	20°C	14°C
TKY 461	*act1-102*	−	0	0	0		0	0
TKY 462	*act1-4*	+		0	1			0
TKY 463	*act1-7*	−	N/R	N/R	0			0
TKY 465	*act1-123*	−	0	0	0			0
TKY 466	*act1-115*	−	0	0	0			0
TKY 467	*act1-111*	+			0	0	2	0
TKY 468	*act1-113*	+	N/R	N/R	0			1
TKY 469	*act1-116*	−	0		0			0
TKY 470	*act1-104*	+	0		0			1
TKY 471	*act1-135*	+	0		0			1
TKY 472	*act1-117*	+	3		1			3
TKY 473	*act1-133*	+		1	1		1	2
TKY 474	*act1-10*	−	0		0			N/R
TKY 475	*act1-9*	+	2	2	0			2
TKY 476	*act1-3*	+	1	0	0			2
TKY 477	*act1-20*	+	2	1	0			2
TKY 478	*act1-8*	+	3	2	1			2
TKY 479	*act1-129*	+	5	2	1			3
TKY 480	*act1-125*	+		1		0	3	N/R
TKY 481	*act1-122*	+		3	1		2	3
TKY 482	*act1-124*	+		4	2		2	3
TKY 483	*act1-120*	+		3	3			3
TKY 484	*act1-119*	+	2	1	0			2
TKY 486	*act1-101*	−			0			0

The number indicates the strength of the sensitivity to AA imbalance compared to the WT strain. The higher the number, the stronger the sensitivity. The scoring system was developed by E. Sattlegger (see chapter 2.22). The negative and positive control strains grew as expected. The assay was conducted at a similar temperature range as the SM^S screen in chapter 3.1. − indicates phenotype similar to the wild type strain, + indicates impaired growth compared to the wild type strain, N/R indicates that no result was obtained, blank space indicates that this temperature was not included in the screen.

3.3 Screen of actin mutant strains for sensitivity to 3-Aminotriazole

The starvation drug 3AT was used in the following screen. This drug is a competitive inhibitor of the imidazole glycerolphosphate dehydratase, an enzyme involved in histidine biosynthesis [64]. Thus using 3AT consequently leads to histidine starvation in the cell.

Strains which were previously shown to be resistant to SM and/or AA imbalance were omitted from the 3AT assay (TKY 461, TKY 463, TKY 465, TKY 466, TKY 469, TKY 474, TKY 486). In addition, actin mutant strains TKY 470, TKY 471, TKY 472, TKY 474 and TKY 480 were not investigated further due to the fact that their SM^S phenotype could only be detected in one screen. Mutant strain TKY 473 was excluded from the rest of the study as it has been shown to be sensitive to a range of drugs affecting different processes in the cell [59]. Thus, a general drug sensitivity was assumed and the phenotypes observed were not thought to be associated with an impaired GAAC.

To check if the selected actin mutant strains could respond to starvation triggered by 3AT a screen for sensitivity to this drug was conducted using a semi-quantitative growth assay. As the wild type strain TKY 460 is histidine auxotroph and can therefore not be starved for histidine without lethality, the actin mutant strain TKY 465, which is histidine prototroph, was used as a reference for the actin mutant strains in this screen. This strain has been shown previously not to be sensitive to SM (see chapter 3.1) or 3AT (see appendix A). A *gcn2*$\triangle$ (H2557) which is not able to respond to nutritional stress, was used as a negative control. The wild type strain H1511 was used as a positive control. As the actin mutant strains vary in their growth rate, a YPD plate and a SD plate without starvation drugs was added in order to be able to take the individual growth rate into consideration. The growth of the individual strains was scored in comparison to the reference strain on the starvation plates taking the growth on the non starvation plates into consideration, i.e. it was monitored how many dilutions did not grow in comparison to the reference strain. This screen was carried out at the

temperature where a SM^S phenotype was detected earlier (see chapter 3.1), namely 30℃, or 20℃ in case of TKY 468.

The result of this screen is summarized in figures 3.2 and 3.3 and table 3.3 . All strains investigated (TKY 462, TKY 467, TKY 468, TKY 475, TKY 476, TKY 477, TKY 478, TKY 479, TKY 481, TKY 482, TKY 483, TKY 484) show an impaired growth under 3AT starvation conditions in comparison to the reference strain TKY 465, as indicated by reduced growth. All positive and negative controls grew as expected. This result shows that all actin mutant strains investigated display a sensitivity to 3AT, which means they have potentially an impaired GAAC. This conclusion is supported by the previously discovered SM sensitivity and AA imbalance sensitivity of these actin mutant strains. In order to verify further that the GAAC is indeed inhibited in these yeast strains, it was sought to categorize the cause of the SM^S.

Table 3.3: Overview of the screen of actin mutant strains for sensitivity to 3AT

strain name	*act1* allele	3AT sensitivity	missing dilution compared to reference	temperature
TKY 462	*act1-4*	sensitive	3	30°C
TKY 467	*act1-111*	sensitive	2	30°C
TKY 468	*act1-113*	sensitive	2	20°C
TKY 475	*act1-9*	sensitive	3	30°C
TKY 476	*act1-3*	sensitive	4	30°C
TKY 477	*act1-20*	sensitive	3	30°C
TKY 478	*act1-8*	sensitive	1	30°C
TKY 479	*act1-129*	sensitive	2	30°C
TKY 481	*act1-122*	sensitive	4	30°C
TKY 482	*act1-124*	sensitive	3	30°C
TKY 483	*act1-120*	sensitive	4	30°C
TKY 484	*act1-119*	sensitive	3	30°C

Sensitive indicates that strain showed an impaired growth in comparison to the reference strain. The negative and positive control strains grew as expected.

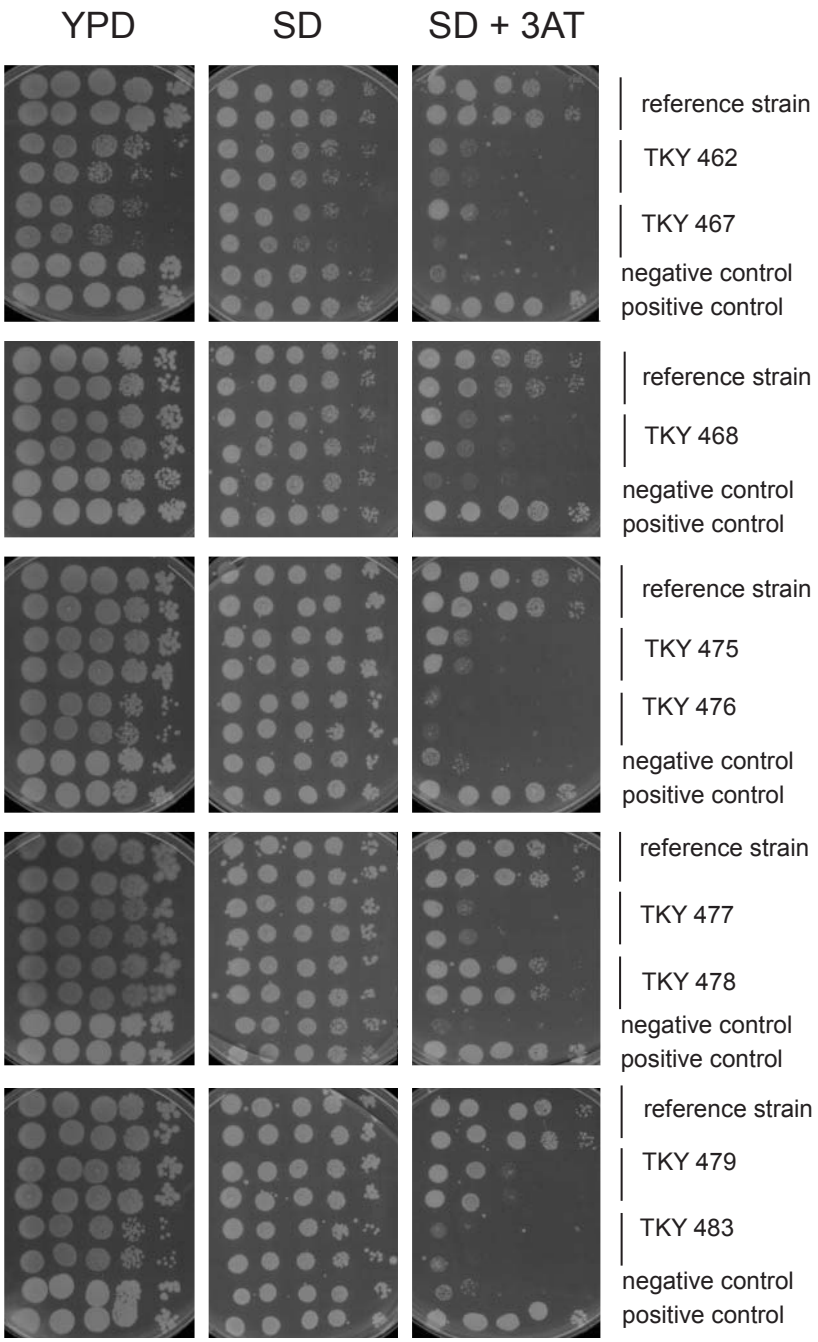

Figure 3.2: Overview of the screen of actin mutant strains for sensitivity to 3AT. Actin mutant strains as indicated, TKY 465 strain (reference strain), H1511 strain (positive control) and H2557 strain (*gcn2*Δ, negative control) were grown to saturation. Saturated overnight cultures were subjected to 10 fold serial dilutions and 5 µl of undiluted culture and 5 µl of each dilution were transferred to solid SD medium containing the AA analogue 3AT (10 mM or 20 mM in case of TKY468), solid SD media not containing any starvation drug and solid YPD media. Plates were incubated at 30°C or 20°C in case of TKY 468 until colonies were visible.

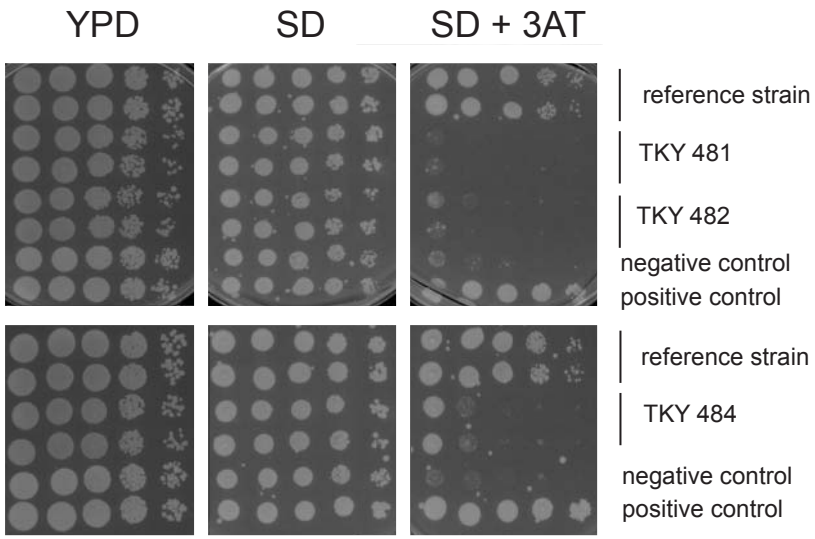

Figure 3.3: Overview of the screen of actin mutant strains for sensitivity to 3AT continued. The assay was performed as outlined in figure 3.2.

3.4 Screen of actin mutant strains for sensitivity to SM when the transcription activator *GCN4* is constitutively expressed

A SM^S phenotype, an AA $imbalance^S$ phenotype or a $3AT^S$ phenotype in a yeast strain is a first indication for an non functional GAAC. However, actin is involved in a myriad of cellular processes like endocytosis, bud formation, transcription and translation as mentioned earlier (see chapter 1.6). Thus mutating this essential protein could lead to secondary effects suppressing cellular growth. To exclude the latter and determine further if the GAAC is indeed inhibited, the cause of the SM^S/ $3AT^S$/AA $imbalance^S$ was categorized in upstream or downstream of the transcription activator Gcn4. Gcn4 is a key component of the GAAC pathway, that is specifically upregulated under starvation conditions. Consequently, the specific stress response is induced while simultaneously the general protein synthesis is downregulated. Therefore, it was hypothesized that if the previously observed growth defects were caused by an impaired GAAC through an altered Gcn4 expression, the growth defect should be reverted by constitutively expressing Gcn4

in the cell. This reversion would be another indication that the growth defect is caused by an impaired GAAC response.

A semi-quantitative growth assay using SM as a starvation drug was performed. In order to increase the amount of Gcn4 in the cell a plasmid constitutively transcribing Gcn4 mRNA ($Gcn4^C$) due to point mutations in the start codons of the four uORFs (p238) was used [81]. As a negative control an empty vector control plasmid (p703) was also included [115]. The 12 mutant strains sensitive to SM, AA imbalance and 3AT and the wild type strain TKY 460 as a reference were used in this screen. The wild type strain TKY 460 was also transformed with both plasmids (p238, p703). As a negative control a *gcn2*Δ strain in the TKY background was used. As *GCN2* is essential under starvation conditions, this strain should not be able to grow under these conditions. The *gcn2*Δ strain containing plasmid p238 was used as another positive control as the lethality of this strain should be rescued by constitutively expressing Gcn4. As a negative control for experimental procedure a *gcn2*Δ strain in the H1511 background (H2557) and a *gcn20*Δ strain in the H1511 background (H2558) were included as both proteins are essential under starvation conditions and these strains should not be able to grow. The positive control for the experimental procedure consisted of the H1511 strain, which should be able to flourish under starvation conditions. The assay was performed at a similar temperature range as the SM^S screen performed in chapter 3.1. The reversion of the SM^S phenotype was scored using a 10 point system taking the growth of the actin mutant strains and the wild type strain TKY 460 under starvation and non-starvation conditions as well as the SM sensitivity of the mutant strain into consideration (see Materials and Methods chapter 2.22). According to this quantification, the higher the reversion number, the higher the reversion of the SM^S sensitivity in the actin mutant strain in comparison to the wild type strain (see table 3.4).

The result of such a semi-quantitative growth assay can be seen in figure 3.4. Under non-starvation conditions the actin mutant strain TKY 484 containing either vector control plasmid p703 or $Gcn4^C$ plasmid p238 and the control strains grew well on solid media. Under these conditions growth is observed for all dilutions. Under starvation conditions, the mutant strain TKY 484 expressing the vector control did not grow as well compared to the

wild type strains indicating a SM^S sensitivity. The TKY 484 mutant strain constitutively expressing Gcn4 grew to the same extent as the vector control strain. All control strains grew as expected. This result indicates, that the SM^S growth defect of TKY 484 has not been rescued by constitutively expressing Gcn4 and there is no reversion.

Under non-starvation conditions the actin mutant strain TKY 481 containing either vector control plasmid p703 or $Gcn4^C$ plasmid p238 and the control strains grew well on solid media. Under these conditions growth is observed for all dilutions. In contrast, under starvation conditions the actin mutant strain TKY 481 expressing the vector control displayed a SM^S compared to the wild type strains. This growth defect is reverted by constitutively expressing Gcn4 as indicated by an enhanced growth. The growth exhibited by mutant strain TKY 481 constitutively expressing Gcn4 is similar to the growth of the wild type strains. The growth of the control strains is as expected. This result indicates, that the growth of TKY 481 has been reverted by expression of Gcn4.

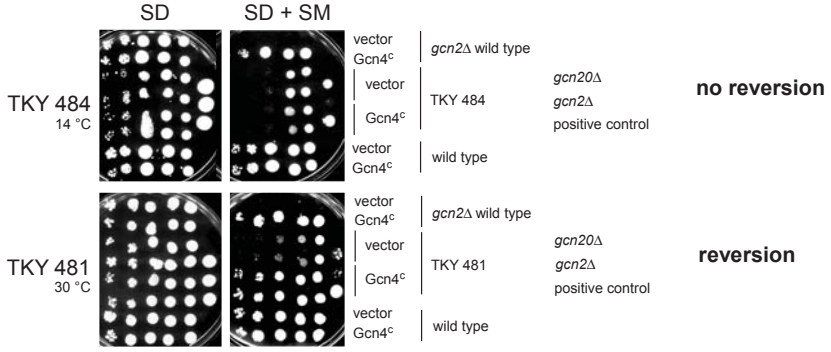

Figure 3.4: Example for a $Gcn4^C$ semi-quantitative growth assay. Actin mutant strains as indicated, wild type strain TKY 460, *gcn2*Δ wild type strain TKY 460 all harboring a plasmid constitutively expressing Gcn4 (p238) and a vector control plasmid (p703), H1511 strain (positive control) and the negative controls strains H2558 (*gcn20*Δ) and H2557 (*gcn2*Δ) were grown to saturation. Saturated overnight cultures were subjected to 10 fold serial dilutions and 5 µl of undiluted culture and 5 µl of each dilution were transferred to solid SD medium containing 4 µg/ ml of the AA analogue SM and solid SD media not containing any starvation drug. 5 µl of undiluted culture of the positive control strain (H1511) and the negative controls strains (H2558, *gcn20*Δ; H2557, *gcn2*Δ) were transferred to the same plates. Plates were incubated at the indicated temperature until colonies were visible.

The result of the Gcn4 expression screen is summarized in table 3.4 and the original data is presented in appendix B. Out of the 12 actin mutant strains investigated, only one yeast strain namely TKY 468 failed to revert the growth defect elicited by SM upon constitutive expression of Gcn4. This lack of reversion indicates that the SM^S in this particular mutant is caused by a Gcn4 independent mechanism. In the other actin mutant strains (TKY 462, TKY 467, TKY 475, TKY 476, TKY 477, TKY 478, TKY 479, TKY 481, TKY 482, TKY 483, TKY 484) the SM^S could be reverted by increasing the amount of Gcn4 in the cell, which is an indication that this phenotype is caused upstream of Gcn4 and is potentially due to an altered Gcn4 expression. The strength of the SM^S reversion varied. It ranged from a slight reversion indicated by a 1 at 34℃ to a stronger reversion as indicated by a 2 at 30℃ and 14℃ as displayed by mutant strain TKY 476. Or the range could be broader ranging from a mild reversion (1 at 30℃) to a severe reversion indicated by a 7 at 20℃ as shown by actin mutant strain TKY 467.

3.5 *In vivo* interaction assay with GST-Yih1 fragment III and actin

All previously described screens investigated whether the actin mutation affects the GAAC pathway and if this affect takes place upstream of Gcn4. Actin mutations were identified which cause a sensitivity to SM, excess AA and 3AT, and in addition seem to have an effect upstream of the transcription activator Gcn4 as indicated by a reversion of the SM^S when Gcn4 is constitutively expressed. Collectively these data indicate that the GAAC could in fact be impaired in these actin mutant strains upstream of Gcn4 expression.

A factor regulating GAAC upstream of Gcn4 is Yih1. Thus one possible reason for this impairment could be the release of Yih1 from actin due to the mutation in actin and the subsequent inhibition of Gcn2. To test this hypothesis, an *in vivo* binding assay with mutated actin and GST-Yih1 was performed. It was reasoned that if the Yih1-actin binding site was mutated, this mutation would alter the interaction capability of actin with Yih1. In an

Table 3.4: Summary of the screen of actin mutant strains constitutively expressing the transcription activator Gcn4 for sensitivity to SM

strain name	actin allele	overall	SM sensitivity				
		result	34°C	30°C	24°C	20°C	14°C
TKY 462	*act1-4*	+		0			2
TKY 467	*act1-111*	+		1	4	7	6
TKY 468	*act1-113*	−				0	0
TKY 475	*act1-9*	+	2	6			N/R
TKY 476	*act1-3*	+	1	2			2
TKY 477	*act1-20*	+	2	1			1
TKY 478	*act1-8*	+	1	4		2	1
TKY 479	*act1-129*	+	1	4			1
TKY 481	*act1-122*	+	0	6		2	0
TKY 482	*act1-124*	+	6	1		1	1
TKY 483	*act1-120*	+	0	2			1
TKY 484	*act1-119*	+	3	2			0

The number indicates the strength of reversion of the sensitivity to SM compared to the WT strain when Gcn4 is constitutively expressed. The higher the number, the stronger the reversion. The scoring system was developed by E. Sattlegger (see chapter 2.22). The negative and positive control strains grew as expected. − indicates no reversion of the sensitivity to SM, + indicates reversion of the sensitivity to SM, N/R indicates no result could be obtained. blank space indicates that this temperature was not included in the screen.

in vivo binding assay such a change in Yih1-actin interaction would result in less or no mutated actin being pulled down in comparison to the wild type strain containing native actin.

All 11 actin mutant strains showing a SM^S, an AA $imbalance^S$ and a $3AT^S$ phenotype where the SM^S could be reverted by constitutively expressing Gcn4 were screened for their interaction with Yih1 in comparison to the wild type strain. The yeast strains were transformed with a plasmid which overexpressed a N-terminally GST-tagged Yih1 fragment III (see figures 5.2 and 5.6) under a galactose inducible promoter (pES247-8) [108] and plasmid overexpressing GST alone under a galactose inducible promoter (pES128-9) [109]. This particular Yih1 fragment was used as it has been previously shown to bind actin the strongest [108]. Two independent colonies of the yeast strains were grown in minimal media with galactose as the sole car-

bon source at 30℃ to an OD_{600nm} = 1 and the yeast WCE was prepared as described in chapter 2.17. Aliquots of equal amounts of total protein as determined by Bradford estimation method were incubated with equal amounts of GST beads for 2 hrs. After extensive washing, the precipitated complexes were boiled off the beads for 10 min in 2x protein loading dye and separated by SDS-PAGE on a 4%-17% gradient gel. The amount of protein in each sample was determined by western blot analysis probing for actin and GST. The amount of precipitated protein was quantitated using either the Western blot or the Ponceau S stained membrane using the Multi Gauge V3.1 software (Fujifilm) or the Image J software (NIH) and the actin/GST ratio was calculated. The relative amount of precipitated actin isolated from the actin mutant strain was first compared to the GST alone control of the same strain to check for specific binding. Then it was compared to the relative amount of actin precipitated in the wild type strain TKY 460.

An example of such an interaction assay is shown in figure 3.5. The results of all other interaction assays can be found in appendix C. In figure 3.5, the actin and GST signals visualized by western blot analysis (A) were quantified and the actin/ GST signal ratio was calculated. The ratio of two biological replicates was averaged and the standard error was calculated (B). In both the wild type strain TKY 460 and the actin mutant strain TKY 478 the actin signal from the GST alone sample is very faint as indicated by a ratio of < 1. In contrast, if GST-Yih1 is overexpressed in these strains the actin signal is stronger as shown by a ratio of about 12. This means that actin is pulled down specifically by GST-Yih1 in both strains. Further, the amount of actin co-precipitated by overexpressed Yih1 from the actin mutant TKY 478 is equal to the amount of actin co-precipitated by the wild type strain TKY 460. The ratio is about 12 in both strains, which indicates that the mutation in actin mutant strain TKY 478 does not alter the binding of Yih1 to actin.

The outcome of all the interaction assays performed is summarized in table 3.5. In all actin mutant strains the amount of actin pulled down was not decreased in comparison to the amount of actin precipitated in the wild type strain. In contrast, it seems that in the majority of the strains the actin

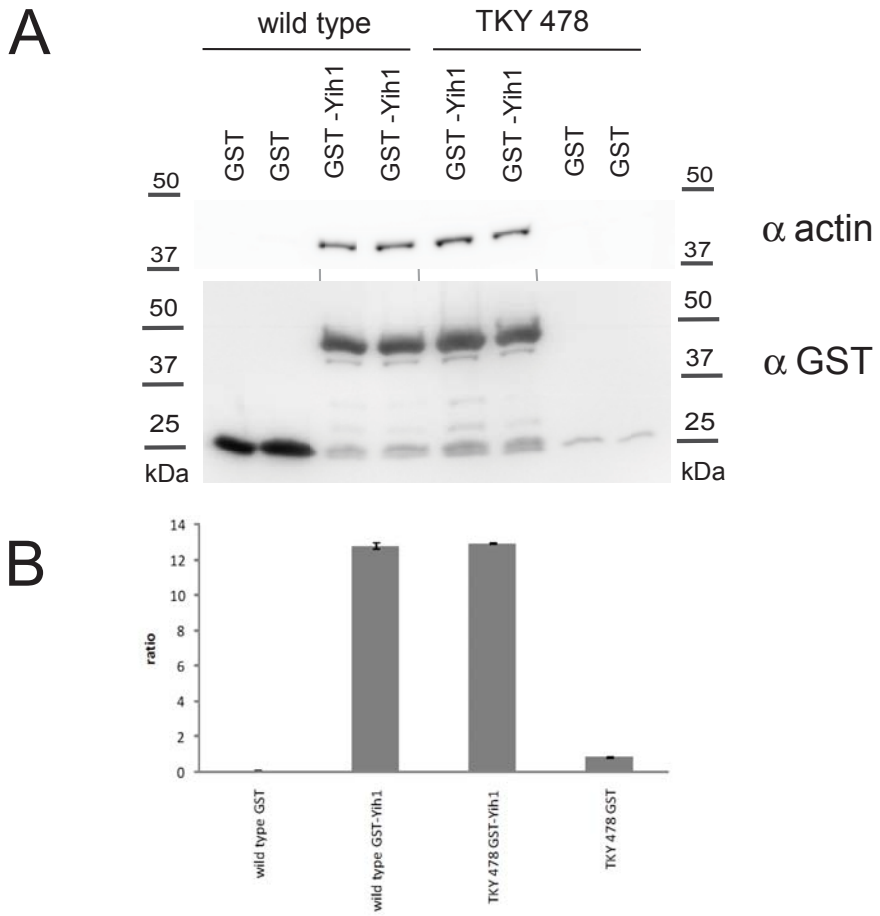

Figure 3.5: Example of an *in vivo* interaction assay with GST-Yih1 fragment III and actin. (A) Two transformants of wild type strain TKY 460 and actin mutant strain TKY 478 containing the galactose inducible genes *GST-YIH1*, nucleotide 202-1021 encoding Yih1 fragment III (on plasmid pES247-8) or *GST* (on plasmid pES128-9) were grown to exponential phase in minimal media containing galactose as carbon source. Whole cell extracts were prepared and aliquots with equal amounts of total protein were subjected to GST pulldown assays using glutathione sepharose beads. The precipitated complexes were separated by SDS-PAGE on a 4%-17% gradient gel and analyzed by western blot analysis using antibodies against actin and GST. (B) The actin and GST signals were quantified using the Multi Gauge V3.1 software (Fujifilm) and the actin/ GST signal ratio was calculated. The ratio of each strain was averaged and the standard error was calculated.

mutations promote the Yih1-actin interaction as the amount of actin interacting with Yih1 is increased compared to the wild type strain. Thus the results obtained argue the converse to the initial assumption as none of the actin mutant strains investigated showed a Yih1-actin interaction reduction.

Table 3.5: Overview of the *in vivo* interaction assays with GST-Yih1 fragment III and actin from actin mutant strains

strain name	*act1* allele	*in vivo* interaction of GST-Yih1 and actin	fold increase in interaction	notes
TKY 462	*act1-4*	↑	4	
TKY 467	*act1-111*	↑	3	*one colony
TKY 475	*act1-9*	↑	2.5	
TKY 476	*act1-3*	↑↑	40	
TKY 477	*act1-20*	↑↑	28	
TKY 478	*act1-8*	↔	1	
TKY 479	*act1-129*	↑	2	
TKY 481	*act1-122*	↔↑		
TKY 482	*act1-124*	↑↑	15	
TKY 483	*act1-120*	N/R		
TKY 484	*act1-119*	↑	5	

The average fold increase in interaction of two biological replicates is presented. ↑ indicates an increased interaction in comparison to the wild type strain, ↑↑ indicates an at least 15 fold increased interaction in comparison to the wild type strain, ↔ indicates a similar interaction to the wild type strain, N/R indicates that no result could be obtained, *one colony indicates that a result of only one colony could be obtained.

An explanation for the observed results could be that by overexpressing GST-Yih1 in the actin mutant strains the interaction is driven towards binding resulting in a misrepresentation of interaction. Therefore with this experimental setup a decreased interaction between GST-Yih1 and actin might not be detectable. A solution to this problem could be to use GST-Yih1 expressed at native levels. However, as the concentration of the Yih1 protein in the cell is low (∼3030 copies/cell [32]) not enough GST-Yih1 can be pulled down *in vivo* to be detectable by western blot analysis (M. Bolech, unpublished data). Therefore an alternative approach namely a growth assay was used. Here, *yih1*Δ actin mutant strains were assessed for their

growth when Yih1 was not present in the organism to investigate if Yih1 is responsible for the impaired stress response in these actin mutants.

3.6 Screen of *yih1*△ actin mutant strains for sensitivity to SM

Out of the 24 actin mutants, 11 had been shown to be sensitive to SM, AA imbalance and 3AT as indicated by impaired growth on media containing these supplements. Furthermore, the SM^S could be reverted in these strains by $Gcn4^C$ expression indicating that the GAAC is potentially impaired in these yeast strains. As the *in vivo* interaction assays were unable to answer the question of whether a release of Yih1 from actin due to the mutations was responsible for these sensitivities, a growth assay experiment with *yih1*△ actin mutant strains was performed. It was hypothesized that if Yih1 is causing these slow growth phenotypes, deletion of *YIH1* should lead to a reversion of these sensitivities.

A semi-quantitative growth assay under SM starvation conditions was performed with actin mutant strains both *yih1*△ and containing native Yih1. Wild type strain TKY 460 was used as a positive control and a *gcn2*△ strain in the TKY background (ESY 10447) was used as a negative control. YPD solid media and SD solid media were added to the assay to be able to quantitate the growth under replete conditions. The screen was carried out at 30℃. Reversion of the growth defect in the *yih1*△ strain was quantified by comparison to the growth of the *YIH1*$^+$ actin mutant strain taking the growth under non- starvation conditions into consideration. This means it was monitored how many dilutions of the wild type Yih1 actin mutant strain did not grow in comparison to the *yih1*△ strain.

YIH1 was deleted by homologous recombination as described in Material and Methods chapter 2.3. Deletion of *YIH1* was verified by PCR and western blot analysis using antibodies against Yih1 (see appendix D for verification results). In three actin mutant strains namely TKY 481, TKY 482 and TKY 483, *YIH1* could not be deleted as the knock-out was not obtainable.

The outcome of these experiments is summarized in table 3.6. The individual results of the growth assays are located in appendix E. In none of the actin mutant strains, that grew, was the growth defect altered when *YIH1* was deleted. All *yih1*Δ were indistinguishable from their isogenic counterpart, that was not deleted for *YIH1*, in their sensitivity to SM. This result is in agreement with experiments conducted by Sattlegger *et al*. [110] where no difference in growth could be detected under SM and 3AT starvation conditions between isogenic strains deleted and not deleted for *YIH1*.

Two interpretations of these results were considered. 1.) Yih1 is not responsible for the impaired stress response. 2.) The concentration of Yih1 is very low in the cell and a deletion of *YIH1* might actually not lead to a distinct phenotype under the conditions investigated. Therefore the next step was to check if the deletion of *YIH1* has an effect on the stress response on a molecular level. In order to investigate this the expression of the transcription activator Gcn4 as one of the key components of the stress response was studied.

Table 3.6: Summary of the screen of *yih1*Δ actin mutant strains for sensitivity to SM

strain name	background strain	*act1* allele	growth compared to undeleted actin mutant	temperature
MDY 157	TKY 462	*act1-4*	same	30°C
MDY 156	TKY 467	*act1-111*	same	30°C
MDY 146	TKY 475	*act1-9*	same	30°C
MDY 154	TKY 476	*act1-3*	same	30°C
MDY 147	TKY 477	*act1-20*	same	30°C
MDY 148	TKY 478	*act1-8*	same	30°C
MDY 149	TKY 479	*act1-129*	same	30°C
	TKY 481	*act1-122*	N/R	
	TKY 482	*act1-124*	N/R	
	TKY 483	*act1-120*	N/R	
MDY 153	TKY 484	*act1-119*	same	30°C

Same indicates that the growth of the *yih1*Δ actin mutant strain was similar to that of the isogenic mutant strain not deleted for *Yih1*. The positive and negative control strains grew as expected. N/R indicates that no *yih1*Δ actin mutant strain was obtainable.

3.7 Screen of actin mutant strains and *yih1*Δ actin mutant strains for expression of the transcription activator Gcn4

The transcription activator Gcn4 is a pivotal element in the GAAC pathway by inducing the AA stress response upon activation of Gcn2 and phosphorylation of eIF2α. Therefore investigating the Gcn4 expression level is required if the influence of Yih1 on the stress response at a molecular level is to be investigated. It was argued, that a release of Yih1 from actin in an actin mutant strain would lead to an impaired Gcn2 function and subsequently to a reduced level of Gcn4 expression. This decrease in Gcn4 expression should be reverted in a *yih1*Δ actin mutant strain. Therefore the level of Gcn4 expression was measured in the actin mutant strains and the isogenic *yih1*Δ actin mutant strains. Only the actin mutants which showed a reverted SM^S in the Gcn^C screen were used in this assay.

To measure the level of Gcn4 expression in the yeast strains a reporter plasmid harboring the *lacZ* gene under the control of the Gcn4 promoter (p180) [47] was transformed into the strains. This means, that the translation of Gcn4 can be quantified in these strains by assaying β-Galactosidase activity. The β-Galactosidase activity was measured under starvation and non-starvation conditions. As the absolute values were inconclusive, the fold expression of the starved to unstarved samples was calculated. The relative activity in the actin mutant strains was compared to that of the wild type strain TKY 460. A *gcn2*Δ strain was used as a negative control as *GCN2* is essential for *GCN4* expression under starvation conditions. The temperature where the reversion of the SM^S was the greatest in the $Gcn4^C$ screen was used. It was expected, that if Yih1 would be released from actin due to the actin mutation and inhibit Gcn2 activation, the β-Galactosidase activity would be decreased in the actin mutant strains compared to the wild type.

All actin mutant strains were investigated in at least two independent experiments. To be able to combine the individual experiments the relative activity of the individual strains (two biological replicates) in each experiment

was averaged and normalized against the wild type. The normalized values of the individual experiments were then averaged and analyzed. As the resulting sample size was very small (n $\leq$ 3) no further statistical analysis was possible.

An example of a *lacZ* assay is presented in figure 3.6. Each individual result is located in appendix F. As expected, the β-Galactosidase activity in the *gcn2*Δ strain is lower than in the wild type strain. This indicates that the experimental procedure worked and the wild type cells were starved. In comparison to the wild type strain approximately half the β-Galactosidase activity was measured in actin mutant strain TKY 475. This indicates, that that the GAAC pathway is impaired in this actin mutant strain. The reduction in β-Galactosidase activity exhibited by TKY 475 can also be observed in the isogenic *yih1*Δ mutant strain. Thus, the reduction in *GCN4* expression cannot be contributed to Yih1 using this experimental approach.

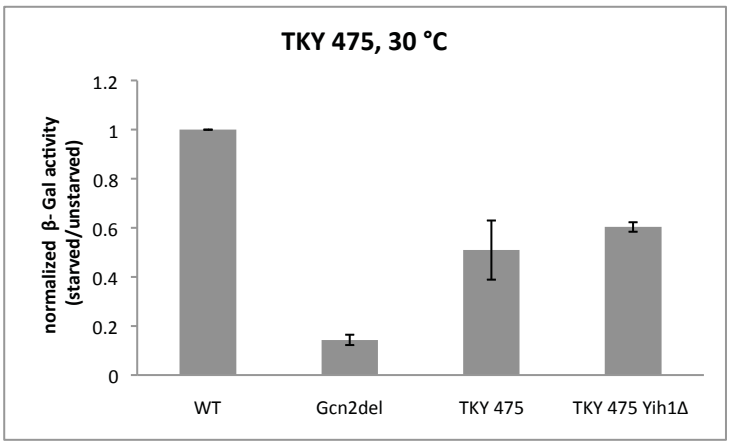

Figure 3.6: Example of a *lacZ* assay with actin mutant strain TKY 475, *yih1*Δ TKY475, wild type strain TKY 460 and *gcn2*Δ TKY 460 strain. The ratio of the β-Galactosidase activity (starved versus unstarved conditions) of each strain (2 biological replicates) was averaged and normalized to the activity of the wild type strain. The values of two independent experiments were averaged. The standard error is indicated.

The overall result of this screen is summarized in table 3.7. When considering the *GCN4* expression levels in the 11 actin mutant strains, the outcome of this set of experiments can be divided into three categories. First,

there are five strains (TKY 467, TKY 475, TKY 479, TKY 481, TKY 483) which show a lower level of *GCN4* expression compared to the wild type strain. This result suggests that the GAAC is impaired in these actin mutant strains due to an inhibited Gcn4 expression. These strains exhibit a Gcn$^-$ phenotype. Second, there are five strains (TKY 462, TKY 477, TKY 478, TKY 482, TKY 484) where the same or possibly a higher level of *GCN4* expression was measured in comparison to the wild type strain. As the impaired stress response is not caused by an impeded Gcn4 expression, these strains were excluded from the rest of the study. Third, for strain TKY 476 no statement can be made about its *GCN4* expression level in comparison to the wild type as the error is too large in these experiments and this strain was consequently excluded from the rest of the study as well.

Table 3.7: Overview of the *lacZ* assays using actin mutant strains and *yih1*Δ actin mutant strains

strain name	*act1* allele	β-Galactosidase activity [MU]				temperature
		actin mutant strain*		*yih1*Δ actin mutant strain**		
		overall	value	overall	value	
TKY 462	*act1-4*	slightly ↑	1.2 ± 0.01	↓	0.8 ± 0.04	14°C
TKY 467	*act1-111*	slightly ↓	0.9 ± 0.04	↔	1.2 ± 0.2	20°C
TKY 475	*act1-9*	↓	0.5 ± 0.1	↔	0.6 ± 0.02	30°C
TKY 476	*act1-3*	inconclusive	1.1 ± 0.3	↔ as WT	0.9 ± 0.03	30°C
TKY 477	*act1-20*	↔	1.0 ± 0.05	↔	0.9 ± 0.05	34°C
TKY 478	*act1-8*	↔	1.0 ± 0.1	↔	1.3 ± 0.2	30°C
TKY 479	*act1-129*	↓	0.7 ± 0.09	↔	0.8 ± 0.1	30°C
TKY 481	*act1-122*	↓	0.6 ± 0.02	-	-	30°C
TKY 482	*act1-124*	↔ or ↑	0.9 ± 0.4	-	-	34°C
TKY 483	*act1-120*	↓	0.6 ± 0.08	-	-	30°C
TKY 484	*act1-119*	↔ or ↑	1.4 ± 0.4	↔	1.3 ± 0.5	34°C

*The level of β-Galactosidase activity in the mutant strains is compared to the activity of the wild type strain TKY 460. **The level of β-Galactosidase activity in the *yih1*Δ mutant strain is compared to the activity of the isogenic undeleted mutant strain.The standard error is indicated. ↑ indicates an increased β-Galactosidase activity, ↓ indicates a decreased β- Galactosidase activity, ↔ indicates a similar β-Galactosidase activity, ↓ indicates a decreased β-Galactosidase activity, - indicates that no result is available.

When considering the results of *yih1*Δ actin mutant strains it can be observed that none of the investigated strains showed a reversion of the *GCN4* expression level in comparison to the mutant strain containing endogenous Yih1. In each strain the expression is the same, or in case of TKY 467 even slightly lower, than the undeleted actin mutant strains. Thus, on a molecular

level the influence of Yih1 on the GAAC in these yeast strains is negligible. This result is in agreement with the semi- quantitative growth assay using *yih1*Δ actin mutant strains where no reversion of the SM^S phenotype was detectable when *YIH1* was deleted (see chapter 3.6). As described earlier, the low copy number of Yih1 in the cell could be a possible reason for this. Thus another approach was sought where the amount of Yih1 was increased by overexpressing the protein and the growth of these strains was investigated under starvation conditions.

3.8 Screen of actin mutant strains overexpressing Yih1 for sensitivity to SM

As the deletion of *YIH1* did not revert the growth defect of the actin mutant strains under starvation conditions or the level of *GCN4* expression, the question was posed whether the overexpression of Yih1 might help to show a relation between an impaired GAAC and Yih1 in the actin mutant strains. By increasing concentration of Yih1 in the cell, an exacerbation of the SM^S is expected if Yih1 is responsible for the inhibited stress response.

To test this hypothesis, a semi-quantitative growth assay was performed using the five actin mutant strains which have an inhibited GAAC as indicated by a decreased level of *GCN4* expression (see table 3.7). Full length GST-Yih1 (pES187-B1) [110] and GST alone (pES128-9) [109] were expressed from a galactose inducible plasmid in the actin mutant strains and the wild type strain TKY 460. A *gcn2*Δ strain in the TKY background was used as a negative control. *GCN2* is essential under starvation conditions and thus the latter strain should not be viable in the presence of SM. Wild type strain TKY 460 was used as a positive control for experimental procedure and was expected to grow under the investigated conditions. Solid minimal media containing 10% galactose and 2% raffinose was used for inducing the overexpression and solid media supplemented with 2% glucose was used as a control for the growth behavior of the strains. Raffinose was used in this assay as an additional carbon source to galactose to allow the cells an easier access to an energy source. The amount of SM used is indi-

cated. This screen was carried out at 30℃. The growth of the actin mutant strains overexpressing GST-Yih1 was first compared to the isogenic strain expressing GST alone, i.e. it was monitored how many dilutions did fail to grow. This growth difference was then compared to the growth difference exhibited between the wild type strain expressing GST and GST-Yih1. An exacerbation of the SM^S is indicated if the growth difference in the actin mutant is greater than in the wild type strain.

The summary of the growth assays can be seen in table 3.8 and figure 3.7. It was observed that not all dilutions grew in the strains overexpressing Yih1 in comparison to the isogenic strain expressing GST alone under starvation conditions. This difference in growth means that the overexpression of Yih1 impairs the growth under starvation conditions in general not only in the actin mutant strains but also in the wild type strain. The same phenomena has been observed by Sattlegger *et al*. [108] when overexpressing full length GST-Yih1 under SM starvation conditions or by Sattlegger *et al*. [110] when overexpressing FLAG-Yih1 under 3AT starvation conditions.

All actin mutant strains show a SM^S phenotype indicated by an impaired growth of the strains expressing GST alone under starvation conditions in comparison to unstarved conditions. Taking the impaired growth of the wild type into account as explained above only one strain - TKY 475 - shows an exacerbated SM^S when Yih1 is overexpressed. Here, the growth difference between TKY 475 expressing GST-Yih1 and GST alone is at least three dilutions whereas the difference between the two wild type strains is only one dilution. This particular strain shows the phenotype expected from an actin mutant strain, where Yih1 is the cause for the impaired GAAC.

Actin mutant strains TKY 467 and TKY 479 show the same ratio of growth reduction as the wild type when Yih1 is overexpressed. In both cases, the same amount of dilutions did not grow in the mutant strains as in the wild type strain. This indicates, that Yih1 is not involved in the impeded stress response.

Actin mutant strains TKY 481 and TKY 483 did not grow as expected. On solid media containing glucose all dilutions of all strains colonies are visible. However, under non-starvation conditions where GST and GST-Yih1 are overexpressed the growth of the strains is seriously impaired as indi-

cated by only two dilutions growing. Therefore no conclusion can be drawn from this experiment about actin mutant strains TKY 481 and TKY 483. One possible reason for the lack of growth was that these two strains were petite mutants with a defect in their respiratory chain. This idea can be investigated by a lack of growth on a non-fermentable carbon source like YPG. However, these strains could grow on YPG (see figure 3.8), meaning that these strains do not have a defect in respiration. As both strains expressing GST alone and GST-Yih1 had difficulties flourishing, another explanation could be that the GST tag has an negative influence on these particular actin mutant strains and inhibits their growth when overexpressed.

Table 3.8: Overview of the screen of actin mutant strains overexpressing Yih1 for sensitivity to SM

strain name	*act1* allele	SM sensitivity	missing dilution in GST-Yih1 strain vs. GST strain	
			wild type	actin mutant
TKY 467	*act1-111*	$\leftrightarrow$	2	2
TKY 475	*act1-9*	$\uparrow$	1	3
TKY 479	*act1-129*	$\leftrightarrow$	1	1
TKY 481	*act1-122*	N/R		
TKY 483	*act1-120*	N/R		

$\uparrow$ indicates an exacerbation of the SM^S phenotype in comparison to the wild type strain, $\leftrightarrow$ indicates that the SM^S phenotype is the same as in wild type strain, N/R indicates that no result could be obtained. The negative and positive control strains grew as expected.

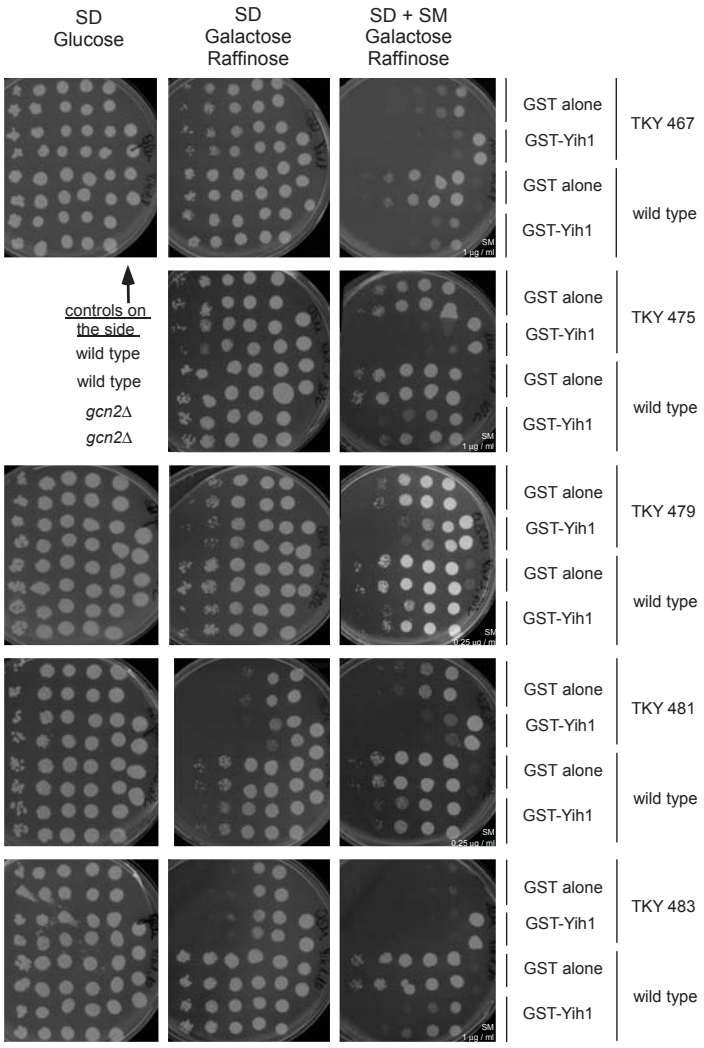

Figure 3.7: Summary of the screen of actin mutant strains overexpressing Yih1 for sensitivity to SM. Actin mutant strains as indicated and wild type strain TKY 460 harboring a plasmid overexpressing GST-YIH1 (pES187-B1) and a plasmid overexpressing GST alone (pES128-9) under a galactose inducible promoter, wild type strain TKY 460 (positive control) and the *gcn2*Δ TKY 460 strain (negative control) were grown to saturation. Saturated overnight cultures of the strain overexpressing GST-Yih1 or GST were subjected to 10 fold serial dilutions and 5 µl of undiluted culture and 5 µl of each dilution was transferred to both solid SD medium containing the amino acid analogue SM as indicated, 10% Galactose and 2%Raffinose and solid SD media not containing any starvation drug but 2% Glucose. 5 µl of undiluted cultures of wild type strain TKY 460 (positive control) and the *gcn2*Δ TKY 460 strain (negative control) were transferred to the same plate. Plates were incubated at 30°C until colonies were visible.

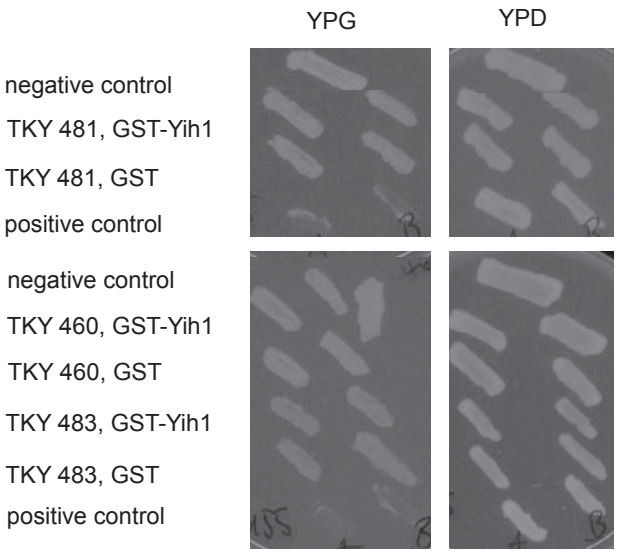

Figure 3.8: Test of yeast strains overexpressing GST-Yih1 and GST alone for petite mutations. Actin mutant strains as indicated, a negative and positive control were streaked out on YPD and YPG solid media. Growth was compared after 2 days of incubation at 30°C.

3.9 Actin complementation assay of actin mutant strains

The GAAC is impaired in actin mutant strains TKY 467, TKY 475, TKY 479, TKY 481 and TKY 483 as indicated by SM^S, sensitivity to AA imbalance, $3AT^S$, reversion of SM^S by $Gcn4^C$ and a decreased *GCN4* expression. The overexpression of GST-Yih1 exacerbates the SM^S phenotype in TKY 475 providing evidence that Yih1 is responsible for this impairment. In order to verify that the hindered stress response is in fact due to the mutation in actin, an actin complementation assay was carried out with these five yeast strains. It was reasoned that if the actin mutation caused the SM^S phenotype in these strain, expressing native actin from a plasmid would revert the slow growth defect in these mutants. Therefore, a semi-quantitative growth assay under SM starvation conditions was performed using actin mutant strains, wild type strain TKY 460 and a *gcn2*$\triangle$ TKY 460 strain (negative control) all harboring a single copy plasmid containing *ACT1* (pMJS1) [110] or a vector control plasmid (YCplac33) [33]. The screen was carried out at 30°C. The

growth on SM of the actin mutant strain expressing the vector only control was compared to the wild type strain containing the same plasmid to check if the strain exhibited a SM^S phenotype. Then the growth of the actin mutant strain expressing *ACT1* was compared to the isogenic vector only control to see if the growth defect was reverted.

An example of such a complementation growth assay can be seen in figure 3.9. All strains grow well under non-starvation conditions. Under starvation conditions, both wild type strains also grow well. In contrast, actin mutant strain TKY 475 expressing the vector control shows a SM^S phenotype as previously observed (see chapter 3.1). In the mutant strain expressing native actin this slow growth phenotype is reverted and this strain grows as well as the wild type. This shows that the actin mutation in this strain is indeed the cause for the SM^S phenotype. The *gcn2*Δ negative control does not grow under starvation conditions as expected.

An overview of this complementation assay is compiled in table 3.9 and the individual results are located in appendix G. In all actin mutant strains investigated the SM^S phenotype could be reverted by expressing *ACT1*. This result demonstrates that in these strains the actin mutation is indeed responsible for the impaired GAAC.

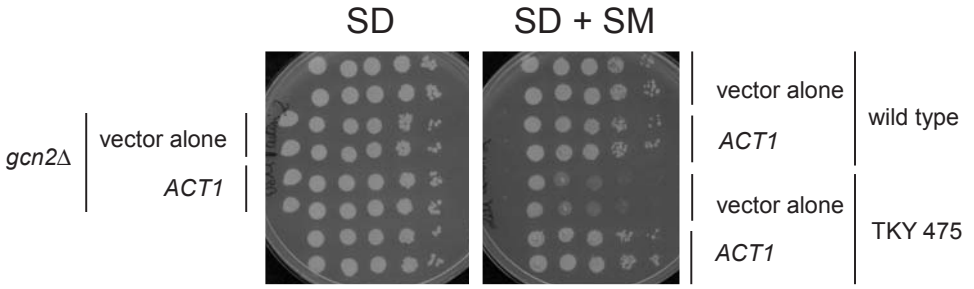

Figure 3.9: Example of the *ACT1* complementation assay of actin mutant strain TKY 475. Actin mutant strain TKY 475, wild type strain TKY 460 and *gcn2*Δ TKY 460 strain (negative control) harboring a plasmid expressing native actin (pMJS1) and a vector control (YCplac33) were grown to saturation. Saturated overnight cultures were subjected to 10 fold serial dilutions and 5 µl of undiluted culture and 5 µl of each dilution was transferred to both solid SD medium containing 2 µg/ ml of the AA analogue SM and solid SD media not containing any starvation drug. 5 µl of undiluted culture of the *gcn2*Δ TKY 460 strains (negative control) were transferred onto the same plates at the side. Plates were incubated at 30°C until colonies were visible.

Table 3.9: Overview of the *ACT1* complementation assay of actin mutant strains exhibiting a decreased *GCN4* expression

strain name	*act1* allele	SM^S phenotype when *ACT1* expressed
TKY 467	*act1-111*	reversion
TKY 475	*act1-9*	reversion
TKY 479	*act1-129*	reversion
TKY 481	*act1-122*	reversion
TKY 483	*act1-120*	reversion

The growth of the actin mutant strain expressing *ACT1* is compared to the growth of the actin mutant strain expressing vector alone. The negative and positive control strains grew as expected.

3.10 Verification of the actin mutation in actin mutant strain TKY 475

In this study it has been shown that actin mutant strain TKY 475 has an impaired GAAC as indicated by a sensitivity to SM, AA imbalance and 3AT. Further the SM^S can be reverted by constitutively expressing the transcription activator Gcn4. The fact that this particular strain possesses a decreased level of *GCN4* expression supported the idea of an impaired starvation response. Due to the fact that an overexpression of Yih1 exacerbates the SM^S phenotype, this growth defect could potentially be attributed to a release of Yih1 from actin due to the actin mutation. To verify that this strain in fact contains a mutation in amino acid 56 in actin, the genomic DNA of TKY 475 encoding the region containing this mutation was sequenced.

As can be seen in figure 3.10, the change from D $\rightarrow$ A at position 56 in the actin gene from the actin mutant strain TKY 475 is confirmed and verified by sequencing.

```
CLUSTAL 2.1 multiple sequence alignment


YFL039C         MDSEVAALVIDNGSGMCKAGFAGDDAPRAVFPSIVGRPRHQGIMVGMGQKDSYVGDEAQS 60
sequencing      ------------------------------SIVGRPRHQGIMVGMGQKDSYVGAEAQS 28
                                               ********************* ****


YFL039C         KRGILTLRYPIEHGIVTNWDDMEKIWHHTFYNELRVAPEEHPVLLTEAPMNPKSNREKMT 120
sequencing      KRGILTLRYPIEHGIVTNWDDMEKIWHHTFYNELRVAPEEHPVLLTEAPMNPKSNREKMT 88
                ************************************************************


YFL039C         QIMFETFNVPAFYVSIQAVLSLYSSGRTTGIVLDSGDGVTHVVPIYAGFSLPHAILRIDL 180
sequencing      QIMFETFNVPAFYVSIQAVLSLYSSGRTTGIVLDSGDGVTHVVPIYAGFSLPHAILRIDL 148
                ************************************************************


YFL039C         AGRDLTDYLMKILSERGYSFSTTAEREIVRDIKEKLCYVALDFEQEMQTAAQSSSIEKSY 240
sequencing      AGRDLTDYLMKILSERGYSFS------------------------------------- 169
                *********************


YFL039C         ELPDGQVITIGNERFRAPEALFHPSVLGLESAGIDQTTYNSIMKCDVDVRKELYGNIVMS 300
sequencing      ------------------------------------------------------------


YFL039C         GGTTMFPGIAERMQKEITALAPSSMKVKIIAPPERKYSVWIGGSILASLTTFQQMWISKQ 360
sequencing      ------------------------------------------------------------


YFL039C         EYDESGPSIVHHKCF 375
sequencing      ---------------
```

Figure 3.10: Multiple sequence alignment of the wild type actin protein sequence (YFL039C) and a fragment of the actin protein sequence of actin mutant strain TKY 475 containing the actin mutation (sequencing). The actin mutation of mutant strain TKY 475 at position 56 is highlighted in red.

3.11 Summary and discussion

In this study actin mutant strains have been investigated for their GAAC stress response and the results of this screen are summarized in table 3.10.

A set of 24 actin mutant strains were screened for sensitivity to SM - a drug that causes starvation for branched amino acids. Sensitivity to this drug is a first indication of a non functional GAAC stress response. Out of the 24 actin mutant strains screened, five strains (TKY 461, TKY 465, TKY 466, TKY 469 and TKY 486) were resistant to the antimetabolite. They did not display a growth defect and grew like the wild type strain in the presence of SM. Thus these mutant strains were considered not to be impaired in their GAAC stress response. Considering the fact that the GAAC is not only triggered by AA starvation but also by an imbalance of AA, the effect of the latter on the 24 mutant strains was investigated as well. All actin mutant strains, except strains TKY 461, TKY 463, TKY 465, TKY 466, TKY 469, TKY 474 and TKY 486, displayed an AA imbalance phenotype which

Table 3.10: Overview of the comprehensive screen of actin mutant strains for an impaired GAAC

strain name	actin allele	mutation	Sensitivity to				*in vivo* interaction with Yih1	reversion of SM^S by deleting *YIH1*	β-Galactosidase activity		Sensitivity to SM when Yih1 overexpressed	*ACT1* complement-ation test
			SM	amino acid imbalance	3AT	SM reverted by $Gcn4^C$			mutant strain	*yih1*Δ mutant strain		
TKY 461	*act1-102*	E359A, E361A	–	–								
TKY 462	*act1-4*	E259V	+	+	+	+	↑	–	slightly ↑	↓		
TKY 463	*act1-7*	K61N	–/+	–								
TKY 465	*act1-123*	R68A, E72A	–	–								
TKY 466	*act1-115*	E195A, R196A	–	–								
TKY 467	*act1-111*	D222A, E224A, E226A	+	+	+	+	↑	–	slightly ↓	↔	↔	+
TKY 468	*act1-113*	R210A, D211A	+	+	+	–						
TKY 469	*act1-116*	D187A, K191A	–	–								
TKY 470	*act1-104*	K315A, E316A	–/+	+								
TKY 471	*act1-135*	E4A	–/+	+								
TKY 472	*act1-117*	R183A, D184A	–/+	+								
TKY 473	*act1-133*	D24A, D25A	+	+								
TKY 474	*act1-10*	T89I	–/+	–								
TKY 475	*act1-9*	D56A	+	+	+	+	↑	–	↓	↔	↑	+
TKY 476	*act1-3*	P32L	+	+	+	+	↑↑	–	N/R	↔ as WT		
TKY 477	*act1-20*	G48V	+	+	+	+	↑↑	–	↔	↔		
TKY 478	*act1-8*	H88Y	+	+	+	+	↔	–	↔	↔		
TKY 479	*act1-129*	R177A, D179A	+	+	+	+	↑	–	↓	↔	↔	+
TKY 480	*act1-125*	K50A, D51A	–/+	+								
TKY 481	*act1-122*	D80A, D81A	+	+	+	+	↔↑	N/R	↓		N/R	+
TKY 482	*act1-124*	D56A, E57A	+	+	+	+	↑↑	N/R	↔ or ↑			
TKY 483	*act1-120*	E99A, E100A	+	+	+	+	N/R	N/R	↓		N/R	+
TKY 484	*act1-119*	R116A, E117A, K118A	+	+	+	+	↑	–	↔ or ↑	↔		
TKY 486	*act1-101*	D363A, E364A	–	–								

– indicates phenotype similar to the wild type strain, + indicates impaired growth compared to the wild type strain
in $Gcn4^C$ assay: – indicates no reversion of the sensitivity to SM,+ indicates reversion of the sensitivity to SM
blank space indicates that this strain was not included in the respective study
in complementation test: + indicates complementation
↑ indicates an increase, ↑↑ indicates an at least 15 fold increase,↔ indicates no increase, ↓ indicates a decrease
N/R indicates no result is available
The level of β-Galactosidase activity is indicated in comparison to the wild type strain and the actin mutant strain not deleted for *YIH1* respectively.

supported the hypothesis that the GAAC is impaired in these strains. Interestingly, all strains that were unaffected by SM were also resistant to an amino acid imbalance confirming an intact GAAC stress response in these particular strains. Given these results it was concluded that, the mutations present in these particular mutant strains do not affect the GAAC.

If yeast cannot respond to nutritional stress due to an impaired stress response then they should also be sensitive to 3AT a drug causing starvation for Histidine. Therefore a test for sensitivity to 3AT was performed. Only strains that exhibited SM^S and AA $imbalance^S$ were included in the following screen. TKY 473 was excluded as a general drug sensitivity was assumed due to a previous study [59].

In agreement with the initial assumption, all actin mutant strains investigated were unable to respond to starvation elicited by 3AT. In conclusion, three independent lines of evidence have shown that actin mutant strains TKY 462, TKY 467, TKY 468, TKY 475, TKY 476, TKY 477, TKY 478, TKY 479, TKY 481, TKY 482, TKY 483 and TKY 484 potentially have an inhibited GAAC stress response as they cannot respond to either AA starvation (branched amino acids, Histidine) or AA imbalance.

As one might expect the sensitivity phenotypes observed may not necessarily result from an impaired GAAC response. Actin is a pivotal protein in the cell with a myriad of functions and interactions [80, 130, 84, 95]. Thus it is possible that the actin mutations influence cellular processes independent of the stress response impairing proliferation. Hence to confirm an impairment of the GAAC, the actin mutant strains were subsequently tested to identify if the SM sensitivity was caused upstream or downstream of the transcriptional activator Gcn4, a key component of the stress response pathway. It was reasoned that if the SM^S growth deficit was caused upstream of Gcn4 than this would be a further evidence for the potential impaired GAAC in those strains. Thus, a screen to identify a reversion of the SM^S phenotype when *GCN4* was constitutively expressed in the mutant strains was carried out. In all strains the SM^S was rescued except TKY 468.

The growth defect phenotypes in all mutant strains except TKY 468 seem to be caused upstream of Gcn4, as the SM^S growth defect was rescued by $Gcn4^C$. This discovery is another indication that the GAAC is possibly im-

paired in these strains and that the defect is upstream of Gcn4. As Yih1 regulates the GAAC upstream of Gcn4, it was speculated that this impairment could potentially result from a release of Yih1 from actin due to the actin mutation, e.g. the Yih1-actin binding site may be altered by the AA modification. As Yih1 is a negative regulator of the GAAC this would lead to an inhibition of Gcn2 activation and an impaired growth under starvation conditions. This growth defect would be reverted by constitutively expressing Gcn4. The growth defects in TKY 468 are caused downstream of Gcn4. As the emphasis of this study lies on affects on the stress response upstream of Gcn4, this strain was consequently excluded from the rest of the study.

To test if Yih1 is able to interact with the mutated actin an *in vivo* interaction assay was undertaken. It was reasoned that there should be a decrease in interaction detectable in comparison to wild type actin if Yih1 could not bind to the mutated actin. Yih1 fragment III (see figures 5.2 and 5.6) was used in this assay as it has been previously shown to bind actin the strongest compared to full length Yih1 or the other Yih1 fragments available [108]. The results obtained argue the converse as no decreased interaction between Yih1 and mutated actin could be detected. In fact Yih1-actin binding was increased in these strains. One possible explanation for this phenomenon is that the actin mutant strains compensate for the defects installed by the mutation in actin by overexpressing the protein. This would lead to a higher level of cellular actin. Consequently, a weakened Yih1-actin interaction would be overcome. However, to date no information about the level of cellular actin in these mutant strains is available. Another explanation for the lack of decreased interaction could be that using overexpressed Yih1 enhances binding by mass action and no true representation of the events in the cell are obtainable. One solution for this problem would be to either use Yih1 expressed at low levels from a single or low copy plasmid or to tag Yih1 in the genome. However, as the native level of Yih1 is low ($\sim$3030 molecules/cell, [32]) the amount of protein interacting in such an assay is below the detection limit (Bolech and Sattlegger, unpublished data) and thus, this approach will not answer the above question. Fluorescence microscopy is a more sensitive technology to validate protein interactions

and could be used alternatively. By using for example a method called Bimolecular fluorescence complementation (BiFC) the Yih1-actin interaction could be investigated *in vivo* at native levels. Here, complementary fragments of a fluorescent reporter protein are fused to proteins postulated to interact. Interaction of these proteins brings the fluorescent fragments within proximity, allowing the reporter protein to form and emit its fluorescent signal.

Considering the outcome of the *in vivo* interaction assays, another approach to test the potential involvement of Yih1 in these growth phenotypes was to delete it. It was reasoned that if Yih1 is involved in causing the growth defects in the mutant strains, removing it from the cell should lead to a reversion of the growth defects in comparison to the mutant strain containing Yih1. However, unexpectedly the growth assays did not show such a reversion in any strain investigated.

A possible explanation is that deleting *YIH1* does not result in a gross phenotypic change and the effect has to be sought on a molecular level. This idea was followed up by measuring the level of *GCN4* expression with a *lacZ* assay. Gcn4 is a key component of the GAAC pathway. Activation of Gcn2 leads to phosphorylation of eIF2 resulting in an increased translation of Gcn4 [48]. Thus the level of *GCN4* expression is directly correlated to the degree of Gcn2 activation and a decreased Gcn4 expression is a strong indication for an impaired GAAC. Thus, if Yih1 is responsible for the inhibited stress response deletion of *YIH1* should result in an increase of *GCN4* expression.

Interestingly, in three actin mutant strains (TKY 481, TKY 482, TKY 483) the deletion of *YIH1* could not be obtained. Considering the fact that actin is involved in a myriad of processes in the cell (see chapter 1.6 in introduction), it is likely that the actin mutations alter processes necessary for a successful deletion via homologous recombination. For example, the uptake of DNA into the cell might be impaired. To confirm this idea, an internalization study with these actin strains would have to be carried out.

The level of *GCN4* expression was measured in the actin mutant strains as well as in the isogenic *yih1*Δ actin mutant strains upon starvation. In actin mutant strains TKY 467, TKY 475, TKY 479, TKY 481 and TKY 483 a

lower Gcn4 expression in comparison to the wild type was detected. Thus, it can be concluded that in these five actin mutant strains the GAAC is indeed impaired and this impairment results from a cause upstream of Gcn4 expression. Their growth defect can be called a Gcn$^-$ phenotype. In contrast, in mutant strains TKY 462, TKY 477, TKY 478, TKY 482 and TKY 484 the level of *GCN4* expression was not decreased. In these strains the impaired stress response is not caused by a decreased Gcn4 expression. No conclusion can be drawn about TKY 476, as the error associated with these experiments make an interpretation impossible.

In contrast to the expectations, deletion of *YIH1* in the actin mutant strains investigated did not result in a reversion of the decreased Gcn4 level. In fact, the deletion did not affect the expression of *GCN4* in comparison to the undeleted strain. Actin mutant strain TKY 462 has to be considered an exception as the level of *GCN4* was slightly decreased. Sattlegger *et al.* suggested a localized Yih1 mediated Gcn2 inhibition restricted to the site of bud emergence, where an optimal translation is required for a rapid bud growth [110]. This model could explain why no reversion of the decreased Gcn4 level could be detected in the investigated total cytoplasmic pool of *yih1*Δ strains. The amount of cytoplasm from the bud where Gcn4 expression is decreased is too little in comparison to the cytoplasm from the mother cell to detect an alteration in Gcn4 expression.

In conclusion, five actin mutant strains (TKY 467, TKY 475, TKY 479, TKY 481, TKY 483) have been confirmed to be impaired in their GAAC stress response and the cause for this impairment is located upstream of Gcn4 expression. As one of the aims of this study was to investigate the influence of actin on the GAAC with a focus on affects upstream of Gcn4, these strains were used in the continuation of this study. So far any involvement of Yih1 in the Gcn$^-$ phenotype could not be shown by interaction assays or an *YIH1* deletion approach. Therefore an alternative technique using overexpressed Yih1 was applied to further pursue the identification of Yih1 as a possible cause for this growth defect. It was argued that overexpression of Yih1 should render the strain more sensitive to SM if Yih1 is causing the growth defect. According to the working model of Yih1 mediated Gcn2 regulation by increasing the amount of free Yih1 by overexpression

while the amount of actin remains constant, more Yih1 should bind to Gcn1. Consequently, this would result to an enhanced inhibition of Gcn2 function leading to a more severe growth defect. In actin mutant strain TKY 475 this assumption has shown to be true suggesting that Yih1 is indeed responsible for the impaired GAAC. In contrast, strains TKY 467 and TKY 476 do not show an exacerbation of their SM^S indicating that Yih1 is not involved in their impeded stress response.

Unfortunately, no result could be obtained for TKY 481 and TKY 483 in this assay as they displayed a serious growth defect when both GST and GST-Yih1 was overexpressed under non-starvation conditions. As these strains were not petite mutants, this result suggests that overexpression of the GST tag affects their growth negatively. This growth impairment was not detected in the GST *in vivo* interaction experiments probably due to the lower concentration of galactose used, leading to a lower concentration of GST/GST-Yih1 expression. By repeating this assay with a lower concentration of galactose or by using a different tag on Yih1 an answer for the involvement of Yih1 in the Gcn^- phenotype may be obtainable.

In order to verify that the phenotypes displayed by the actin mutant strains were specifically due to the mutations in actin and not caused by additional mutations in the genome, an *ACT1* complementation assay was carried out using all strains displaying a Gcn^- phenotype. It was predicted that the growth defect should be reverted by expressing native actin if the actin mutation causes the growth impairment. Given the results that all strains showed a reversion of the growth impairment, it has been confirmed that in all actin mutant strains the actin mutation is responsible for the growth deficit. As the Gcn^- phenotype in TKY 475 has potentially been linked to Yih1 the actin mutation in this strain was verified by sequencing.

From the results presented in this chapter it can be concluded that AA mutations in actin do affect the function of the GAAC. Out of 24 strains investigated, five strains have been confirmed to be impaired in their stress response elicited by nutritional limitation (see 3.11 for location of mutations in the actin molecule). This Gcn^- phenotype was indicated by sensitivity to SM, AA imbalance and 3AT, reversion of the SM^S by $Gcn4^C$ and a decreased level of Gcn4 translation. In one strain -TKY 475 - the Gcn^- phenotype can

potentially be attributed to the inhibitory affect of Yih1 on Gcn2 as overexpression of Yih1 exacerbates the SM^S. Taking the current working model of Yih1 mediated Gcn2 regulation into consideration where Yih1 impedes Gcn2 function upon release from monomeric actin [110, 108] this suggests that the amount of free Yih1 in TKY 475 is increased. On one hand, it is tempting to speculate that the increased concentration of free Yih1 is resulting from an interruption of the Yih1-actin binding due to the mutation in actin. This would suggest that amino acid 56 (see figure 3.11 for location of this mutation in the actin molecule) in yeast actin is the binding site of Yih1 in actin *per se*. If this was true a decrease in Yih1-actin interaction should be detectable in an *in vivo* binding assay. However, this was not the case and an increased Yih1-actin interaction was detected. As explained earlier, there are two potential explanation for this phenomena: 1.) an compensation of the actin mutant strains for the actin mutation by overexpressing the protein. This increased cellular level of the cytoskeleton protein would consequently lead to a higher level of co-precipitated actin. 2.) the overexpression of Yih1 in this experiment, which could enhance binding due to mass force. Therefore as mentioned earlier methods using Yih1 expressed at a lower level would be an alternative to investigate the binding of Yih1 to actin *in vivo*. In addition to these *in vivo* interaction experiments *in vitro* experiments like a co-sedimentation assay with purified Yih1 and purified mutated actin would be necessary to verify this arspatic acid in actin as the Yih1-actin binding site.

On the other hand the possibility that Yih1 is released from actin due to altered actin dynamics caused by the actin mutation has to be considered. This idea is based on the fact that actin mutant strain TKY 475 has been reported to display an unusual F-actin morphogenisis *in vitro*. As shown by Honts *et al.* actin filaments from TKY 475 were observed to undergo self-aggregation in the absence of the actin bundling protein fimbrin [52]. In the presence of fimbrin, the bundles appear more similar to wild type.

By visual inspection of the microscopic images presented by Honts *et al*. [52] there appears to be more F-actin present in comparison to wild type actin. These results suggest, that the mutated actin affects F-actin polymer-

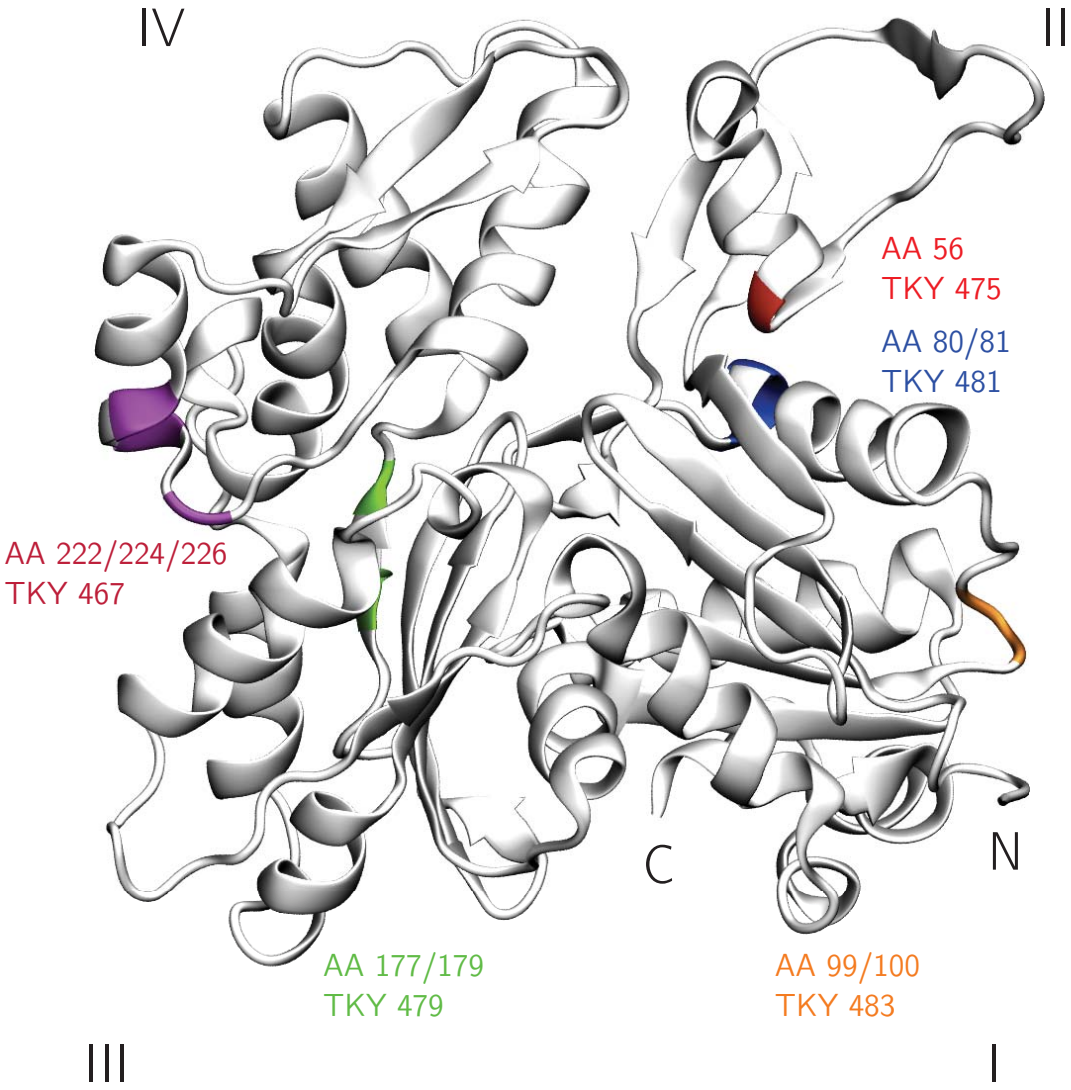

Figure 3.11: Location of actin mutations affecting GAAC. The atomic structure of *S. cerevisiae* G-actin (PDB code 1ATN, [57]) was modeled using the VMD software [54]. Actin point mutations affecting the GAAC are highlighted as follows: AA 56 red, AA 80/81 blue, AA 99/100 orange, AA 177/179 green, AA 222/224/226 purple. Subdomains I - IV and the N/ C-terminus of actin are labelled accordingly.

ization. If this also occurs *in vivo* then due to the fact that there is a constant turn-over from G-actin to F-actin while the total amount of actin remains constant [80], more F-actin in the cell would lead to a decrease of the G-actin pool. Taking the proposed model of Yih1 function into consideration (see figure 1.6 in introduction) this would lead to a decreased pool of inactive G-actin-Yih1 dimer and an increased amount of free Yih1. The released Yih1 consequently functions as an inhibitor of the protein kinase Gcn2 leading to an impaired stress response under starvation conditions as indicated in this study. The cause for the altered F-actin polymerization elicited by this actin mutation has not been investigated. However, as this experiment was performed under *in vitro* conditions with purified protein, it can be excluded that an interruption of the intricate system of actin regulating proteins is responsible for the increased in polymerization. It is more likely that a change in the actin molecule caused by the mutation is altering the polymerization process. The AA modification could for example alter the ionic strength on the surface of actin. Altered ionic strength by modifications in the AA sequence of actin has previously been proposed to alter the binding affinity of actin binding proteins like the actin binding protein tropomyosin [65, 8]. Korman *et al.* have shown that the *in vitro* binding affinity of tropomyosin and actin is increased when two acidic acids on the surface were changed to Alanine. The authors attributed this enhanced affinity to a change of ionic forces on the actin surface. If the affinity of actin binding proteins to actin can be altered by mutations, it can be assumed that the affinity of actin monomers to actin monomers can be altered as well. Thus it is possible that the actin mutation in TKY 475 increases the affinity between actin monomers leading to more interaction which consequently results in an enhanced F-actin polymerization.

Amino acid 56 has not been described previously as being part of the F-actin contact sides. However, as nearby AA (AA 41-50, [50, 44], AA 61-62, [133, 132, 44]) have been implied in being part of the actin-actin contact surface in F-actin, a mutation in the vicinity of these AA is likely to influence the actin-actin interaction [120].

The rate limiting step in actin polymerization is the formation of the unstable initiating dimers and trimers [80]. Assuming an increased affinity be-

tween actin monomers due to the mutation in amino acid 56 helps to overcome this instability, this could lead to an increased filament formation in TKY 475. Taking all this together it is tempting to speculate that the Yih1-G-actin interaction might be indirectly regulated by F-actin polymerization (see figure 3.12). If this is true, a strain defective in its actin polymerization leading to more filamentous actin should display a Gcn$^-$ phenotype. Actin mutant strain act1-159 (not included in this screen) has been previously reported to possess more actin cables *in vivo* [5] and will therefore provide an excellent starting point for investigating this idea further.

Actin is involved in a myriad of processes from transcription [95] to translation [84], from endocytosis [130] to bud formation [80] and often these processes are intricately interconnected. Therefore pinpointing a reason for the Yih1 independent Gcn$^-$ phenotypes caused by the actin mutations is challenging.

In general, a decreased *GCN4* expression leading to a Gcn$^-$ phenotype can result from an inability of Gcn2 to phosphorylate eIF2. As no interaction with actin and Gcn2 or eIF2 has been reported to date, it is highly unlikely that actin is directly involved in the regulation of these proteins.

Interestingly, it has been proposed that the mutation in actin mutant strain TKY 483 abolishes the interaction between actin and the eukaryotic translation elongation factor 1A (eEF1A) [85]. This concept is based on the fact that this strain has been shown to be particularly sensitive to the overexpression of eEF1A [85] while the general protein synthesis and translation fidelity has been shown to be unchanged [59]. In addition, a negatively charged AA is substituted which could potentially interact with the basic eEF1A.

The canonical function of eEF1A is the delivery of aminoacyl-tRNA to the elongating ribosome. Recently eEF1A has also been identified as an inhibitor of Gcn2 activity under non-starvation conditions as 1.) the Gcn2-eEF1A interaction was diminished in AA starved cells, 2.) the Gcn2-eEF1A interaction was disrupted by uncharged t-RNA *in vitro* and 3.) purified eEF1A reduced the ability of Gcn2 to phosphorylate its substrate eIF2α *in vitro* [127]. In accordance with the current working model for eEF1A-Gcn2 inhibition, uncharged tRNA accumulating under starvation conditions dissociate eEF1A from Gcn2 thus allowing Gcn2 activation [127]. Taking these find-

ings together, it can be theorized that by having more eEF1A associating with Gcn2 due to the release of the elongation factor from actin, uncharged tRNAs are unable to dissociate eEF1A from Gcn2. This would result in an inhibition of Gcn2 activation under AA limiting conditions leading to a decrease in eIF2α phosphorylation and a subsequent decrease in *GCN4* translation under starvation conditions as exhibited by TKY 483 in this study (see figure 3.12). A first step to test this hypothesis would be to investigate if actin from TKY 483 is impaired in its interaction with eEF1A in comparison to non mutated actin using *in vivo* or *in vitro* binding assays.

An alternative explanation for the regulation of the GAAC via a non-Yih1 related mechanism arises from the fact that Gcn4 is regulated on a translational level. Studies have suggested a role of actin in translation especially in translation fidelity [59] and it can be theorized that this could cause a Gcn$^-$ phenotype in actin mutant strains. This idea is supported by data presented by Kandl *et al*. [59], who used a set of actin mutant strains to elucidate the function of actin in translation. Here, mutant strain TKY 481 has been shown to be significantly reduced in its translation fidelity as assayed by nonsense suppression and sensitivity to paromomycin a drug which affects translational fidelity [92, 116]. This impaired translation fidelity displayed by TKY 481 could lead to a specific decrease in Gcn4 translation. Considering the sophisticated mechanism of Gcn4 expression including the pre-requiste of a perfectly orchestrated expression of the four uORFs, a defective translation fidelity could cause a decreased expression of Gcn4 (see figure 3.12). It cannot be excluded that the defective translation fidelity does not cause a decreased expression of Gcn2 and/or eIF2 in these mutant strains leading to a growth deficit (see figure 3.12). To investigate this possibility assays measuring the Gcn2 or eIF2 translation levels via western blot analysis would have to be carried out.

The protein synthesis in mutant strain TKY 479 was investigated in the above mentioned study by Kandl *et al*. [59] and was shown to be unchanged as indicated by resistance to drugs inhibiting translation and suppressed expression of nonsense codons. This indicates that an impaired translation fidelity is unlikely the cause for the growth defect in this particular strain. In contrast, yeast strain TKY 467 was not included in this screen and no

information is available about the translation in this particular actin mutation strain.

Actin has been recently proposed to be an important factor in transcription at different steps of the process, e.g. as a component of several transcriptional co-activator complexes [95, 91]. Unfortunately, there is no information available about the level of transcription in TKY 479 or TKY 467. However, if the actin mutation in these actin mutant strains interferes with any of these regulatory steps of gene expression, a decreased level of mRNA would be expected including *GCN4*, *GCN2* or *sui2* (encoding eIF2) mRNA (see figure 3.12). This would lead to a decreased translation of these proteins in comparison to the wild type strain and a Gcn$^-$ phenotype as there might not be enough protein to respond to the stress. Of course, this transcription defect would not only affect proteins involved in GAAC but proteins in general. Consequently these strains would be expected not only impaired in their GAAC but also for example in their general growth. As shown by Whitacre *et al.* TKY 479 and TKY 467 are retarded in their growth as indicated by a longer doubling time in comparison to the wild type strain (wild type strain 2,75 hrs, TKY 467 6,5 hrs, TKY 479 3,05 hrs) [134]. A general growth defect is by no means a direct measurement of transcription and a variety of factors can contribute towards a slow growth in actin mutant strains, e.g. disruption of actin binding proteins like the actin bundling protein fimbrin resulting in an aberrant endocytosis [134]. However, an impeded transcription as the cause of the Gcn$^-$ phenotype cannot be excluded and further experiments checking the transcription of *GCN4*, and/or *GCN2* and/or *sui2* (encoding eIF2) mRNA, e.g. by RT- PCR and a subsequent quantitative PCR, would be necessary to verify this idea.

It has been proposed in this study that Yih1 is responsible for the impaired stress response in actin mutant strain TKY 475. The AA alteration in this strain (D56A, see figure 3.11) is also present in another mutant strain investigated in this screen, namely TKY 482 (D56A, D57A). Considering the fact that both strains possess a common protein sequence modification it was expected that both strains display a Yih1 related Gcn$^-$ phenotype. Surprisingly, this was not the case as in TKY 482 the level of *GCN4* expression was not decreased as in TKY 475.

Taking the proposed model of Yih1 mediated Gcn2 inhibition in TKY 475 into consideration it seems likely that the additional mutation in TKY 482 is responsible for the inconsistency. The release of Yih1 from actin was proposed not to be necessarily caused by a direct interruption of the Yih1-actin interaction but rather by an altered F-actin polymerization leading to a decrease of free G-actin. The change in actin dynamics was attributed to a change in ionic forces on the protein surface due to the AA modification. Considering the fact that TKY 482 has an additional mutation in actin this could lead to different ionic forces on the actin surface of TKY 482 in comparison TKY 475. Thus the effect of an alteration in AA 56 (see figure 3.11) on the actin dynamics could be compensated for with a mutation in location 57 leading to an unaltered actin dynamic. Consequently, this strain would not display a Yih1-related impaired stress response as observed in this study.

To summarize, in this study 24 actin mutant strains have been investigated for their general amino acid response. It has been shown that five out of the 24 strains exhibited a Gcn^- phenotype. In one strain (TKY 475) this growth defect can potentially be attributed to the Gcn2 inhibitor Yih1, which is in agreement with the previously published idea that actin influences the GAAC control via Yih1 [110, 108]. In the remaining strains the Gcn^- phenotype has been shown to be independent of Yih1 (TKY 467, TKY 479) or the relation could not be determined (TKY 481, TKY 483). It was speculated that a disrupted actin-eEF1A interaction leading to an impaired dissociation of eEF1A and Gcn2, an impaired translation fidelity or an affected transcription due to the actin mutation present in these strains could cause the observed growth defects. This lead to the model outlined in figure 3.12. Taking all the results presented in this chapter together illustrates that actin affects the GAAC in more ways than previously assumed. The involvement of actin in the stress response pathway seems to be more profound and complicated than anticipated.

Although a model exists [110, 108], thus far the exact regulation of the Gcn2 inhibitor protein Yih1 is unknown. Based on the findings in this study it was speculated that the Yih1-G-actin interaction might be regulated by F-actin polymerization as assumed previously by Sattlegger *et al.* [110,

108]. Hence, another fundamental biological process in the cell besides translation can now potentially be linked to the GAAC (see figure 3.12).

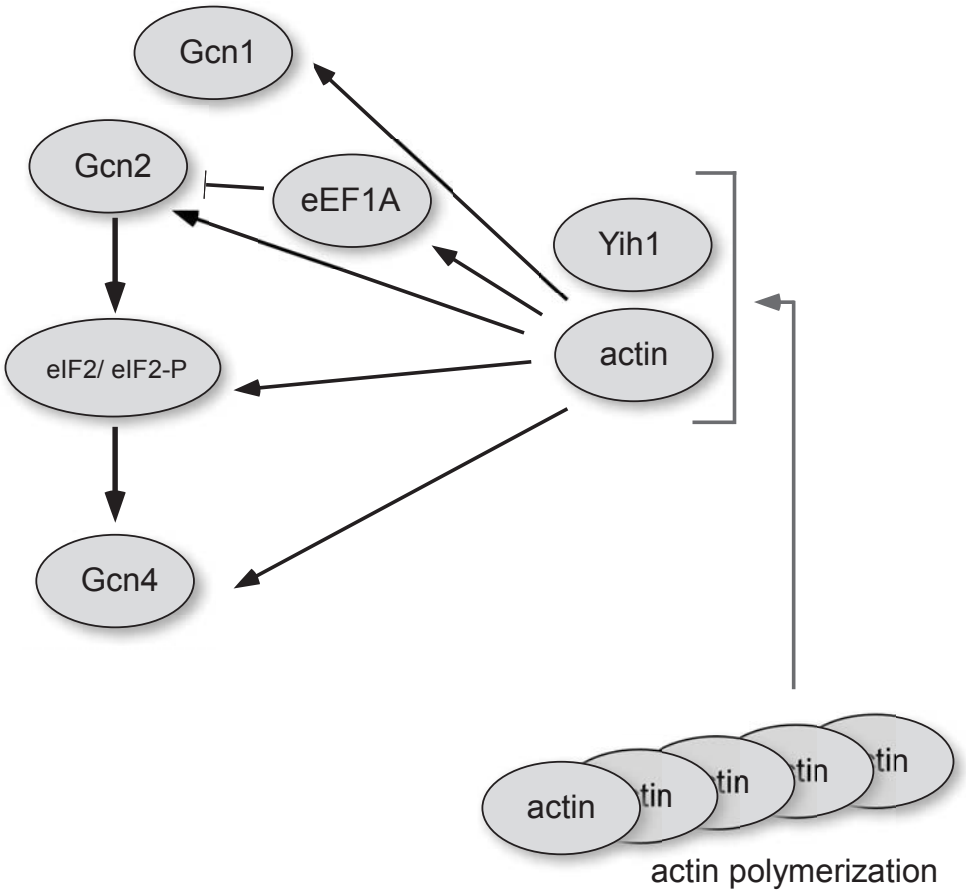

Figure 3.12: Model of the crosstalk between actin and the GAAC and Yih1's involvement in F-actin polymerization as proposed in this study. Actin affects the GAAC pathway on various levels, e.g. by affecting transcription and/or translation of key components of the pathway like Gcn1, Gcn2, eIF2 or Gcn4. In addition, actin affects the interaction between Gcn2 and eEF1A leading to an inhibition of Gcn2 activity. The Yih1-G-actin interaction has been linked to F-actin polymerization. The affect of actin on the general translation and transcription in the cell is not depicted in this model.

4

In vitro binding studies with His_6-Yih1 and actin

The interaction of Yih1 and monomeric actin *in vivo* has been extensively investigated in recent years [110, 108]. However, the *in vitro* verification of the Yih1-actin interaction has not been undertaken. In addition, it is unclear if Yih1 exclusively binds to monomeric actin, as proposed in the current working model of Yih1 mediated Gcn2 inhibition, or also to filamentous actin [110, 108]. To address this gap in knowledge, *in vitro* studies have been performed to increase the understanding of the interaction of Yih1 and actin.

4.1 *In vitro* binding assay of yeast His_6-Yih1 and rabbit muscle filamentous actin

It is unknown if Yih1 binds only to globular actin (G-actin) or also to filamentous actin (F- actin). To investigate this an *in vitro* sedimentation assay using

purified yeast His_6-Yih1 (see figure 4.1, see Material and Methods chapter 2.26 for purification details) and rabbit muscle F-actin was performed.

This assay is based on the principle that Yih1 remains in the soluble fraction upon ultracentrifugation. In contrast, F-actin sediments at 150 000 g. Therefore, if Yih1 binds F-actin it should move from the soluble to the insoluble fraction. α-actinin, a protein known to bind F-actin but not G-actin, was used as a positive control.

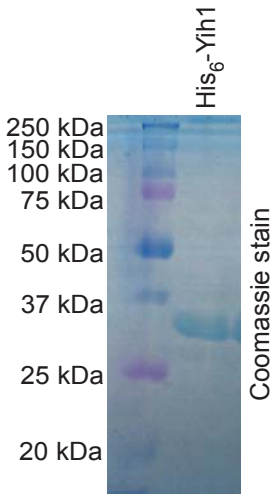

Figure 4.1: Coomassie stain of purified His_6-Yih1. Yih1 fused to a His_6 tag was overexpressed in *E. coli* and coupled to BioRad Profinity iMac Ni-charged resin. Bacterial proteins were removed and His_6-Yih1 was eluted using buffer containing imidazole. The eluate was subjected to SDS-PAGE and the protein was visualized by Coomassie blue staining.

Commercially sourced G-actin (Actin binding protein biochem kit, Cytoskeleton) was polymerized according to the manufacturer's specifications to form F-actin and subsequently incubated with His_6-Yih1 ($\sim$30 kDa) or α-actinin ($\sim$110 kDa). Samples were then subjected to an ultracentrifuge spin at 150 000 g. The supernatant was removed and together with the pellet was investigated via SDS-PAGE for proteins as visualized by Coomassie blue staining.

Under these conditions, filamentous actin ($\sim$45 kDa) is pelleted as can be seen in lanes 1 and 2, 5 and 6, 9 and 10 in figure 4.2 as expected. The

majority of F-actin is present in the pellet fraction and not in the supernatant fraction as expected. Very little α-actinin or His_6-Yih1 is present in the pellet fraction when F-actin is absent (compare lanes 3 & 4 and 7 & 8, figure 4.2). They reside in the supernatant fraction.

As explained earlier, F-actin binding proteins will co-sediment with actin filaments and will be present in the pellet sample. This is observed when F-actin is added to α-actinin (compare lanes 5 and 6, figure 4.2). The α-actinin signal detected at approximately 110 kDa shifts to the pellet fraction as expected for a F-actin interacting protein. The amount of protein of α-actinin and F-actin present in the pellet or supernatant fractions is in agreement with previously reported results [55].

When His_6-Yih1 is incubated with F-actin under these conditions, no more His_6-Yih1 can be detected in the pellet fraction than in the His_6-Yih1 alone pellet sample. In contrast, F-actin is mainly present in the pellet fraction. Taken together with the control samples this experiment shows, that under the conditions investigated, yeast His_6-Yih1 does not bind to rabbit muscle F-actin.

4.2 *In vitro* binding assay of yeast His_6-Yih1 and monomeric rabbit muscle actin

It has been shown previously that Yih1 and actin interact *in vivo* [110, 108]. However, this result has not been verified *in vitro*. For this purpose an *in vitro* interaction assay using rabbit G-actin and yeast Yih1 was carried out. Here, bacterial WCE containing yeast His_6-tagged Yih1 [110] was incubated with BioRad Profinity iMac Ni-charged beads (see Materials and Methods chapter 2.26.2 and 2.28). The bacterial extract was removed and the Yih1 coated beads were washed extensively before commercially sourced rabbit G-actin was added and incubated. The beads were washed and the co-precipitates were boiled off the beads in loading dye. Samples were then separated by SDS-PAGE and immunoblotted using antibodies against actin. His_6-Yih1 was visualized on the membrane with a Ponceau S stain. A sam-

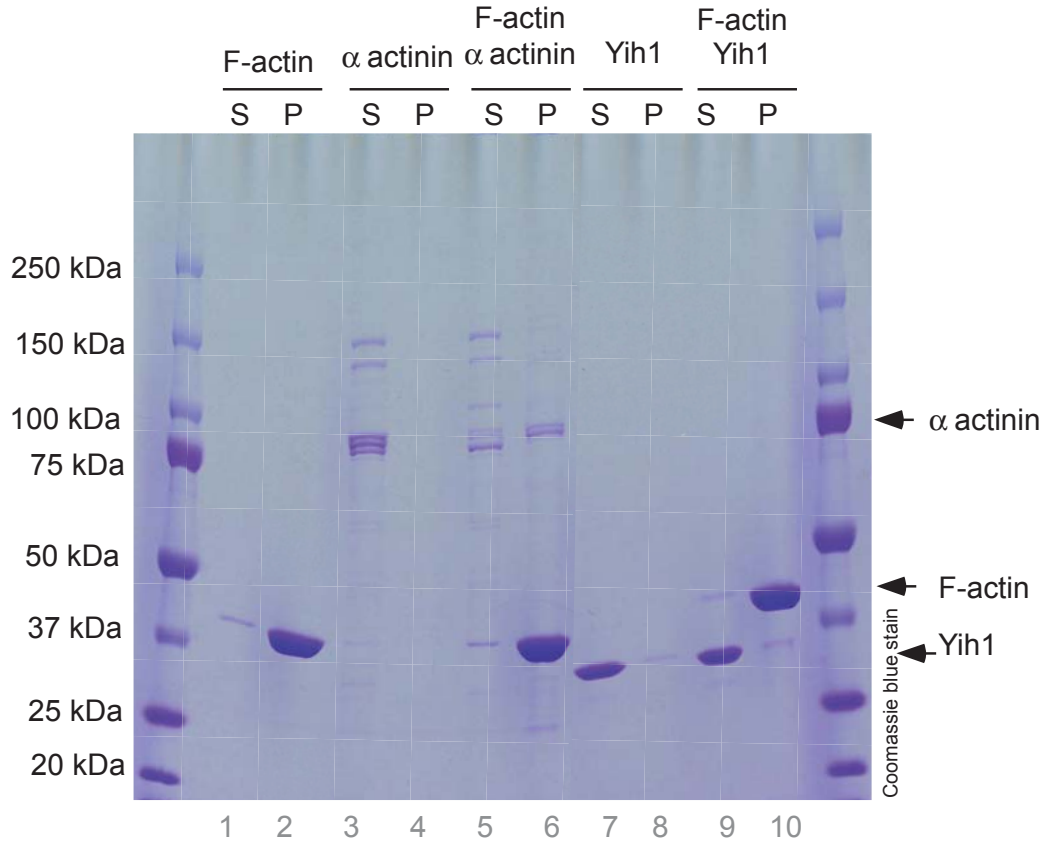

Figure 4.2: *In vitro* sedimentation assay of yeast His_6-Yih1 with rabbit muscle F-actin. F-actin (40 µg) was incubated with purified yeast His_6-Yih1 (10 µg) and α-actinin (10 µg) as a positive control. The sedimentation characteristics of F-actin, α-actinin and His_6-Yih1 were also investigated. Samples were subjected to an ultracentrifuge spin at 150000 g for 60 min. The pellets and the supernatants were investigated by SDS-PAGE on a 4% - 17% gel and the proteins were visualized by Coomassie blue staining. For gel separation 33,33% of samples were loaded, S = supernatant, P = pellet.

ple not containing His_6-Yih1 was used as a negative control for actin binding in the assay. If Yih1 is co-precipitating rabbit G-actin, more actin should be detectable in the samples containing His_6-Yih1 than in the negative control samples.

As observed in figure 4.3 distinct actin bands are visible in the immunoblot (lanes 1, 3-6). However, in contrast to the initial assumption the intensity of the signal is lower in the samples containing His_6-Yih1 than in the negative control samples that do not containing His_6-Yih1, indicating that less actin is co-precipitating in the former conditions (compare lanes 3 & 4 and 5 & 6). This result suggests that the detected interaction is not specific to His_6-Yih1. In other words, actin binds non-specifically to the surface of the Ni-charged beads. This hypothesis is supported by the fact that in the negative control no protein extract is added to the beads. Therefore the binding sites are not pre-bound by protein resulting in binding of actin. In order to reduce the background binding in parallel to the His_6-Yih1 binding step, one sample of beads used as a negative control was incubated with bacterial WCE that did not contain any His_6-tagged protein in the subsequent assay.

When the beads of the negative control were incubated with bacterial whole cell extract, the actin signal intensity was decreased in comparison to the untreated negative control (see figure 4.4, lane 8 and 9). Thus indicating that the non-specific binding of actin to the beads is reduced. However when comparing the signal intensity of the negative control in lane 9 to the samples containing His_6-Yih1 (lane 5 and 6) no difference is detectable suggesting that the binding of actin is still not specific to His_6-Yih1.

In order to reduce non-specific binding in interaction assays a common method is to incorporate a pre-adsorption step before protein incubation. Therefore in the next experiment actin was pre-adsorbed with iMac beads to reduce the non-specific binding of actin.

Despite the pre-adsorption step the actin signal intensity in all samples were similar indicating that the same amount of actin was co-precipitated in the samples containing His_6-Yih1 and the negative controls (compare lanes 5 & 6 with lanes 7 & 8 in figure 4.5). This result suggests that actin is not

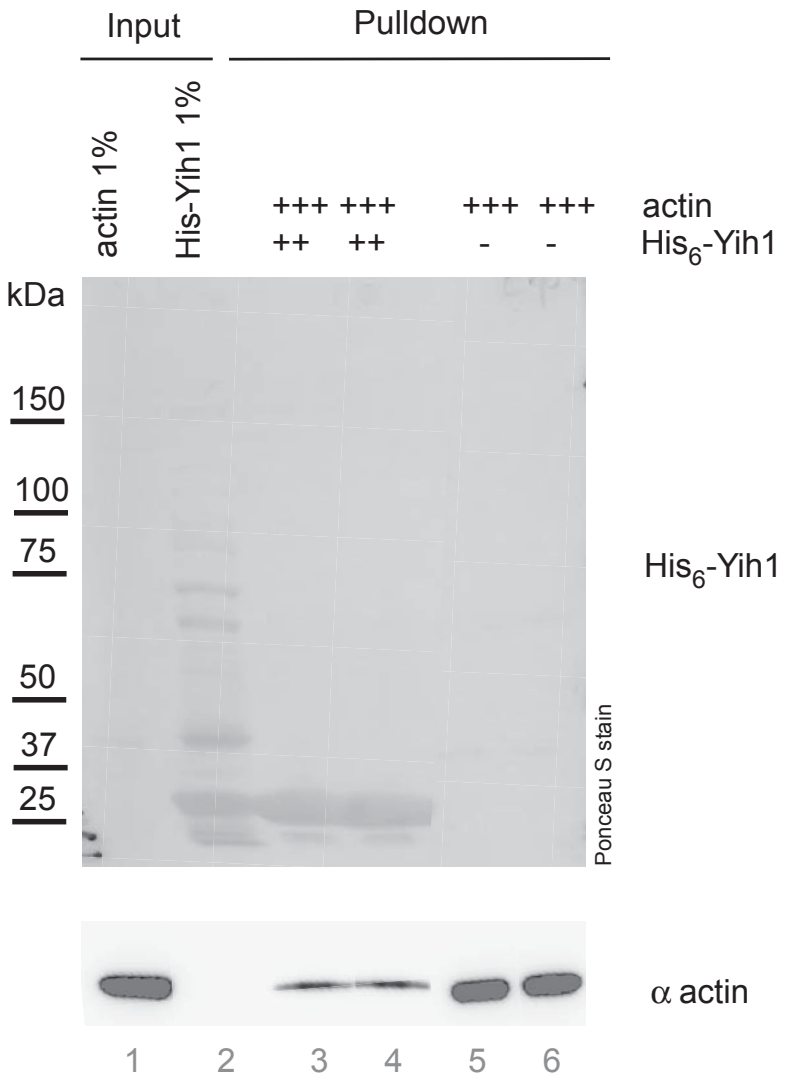

Figure 4.3: *In vitro* binding assay with rabbit muscle G-actin and yeast His_6-Yih1. 100 µl bacterial whole cell extract containing yeast His_6-tagged Yih1 was incubated with BioRad Profinity iMac Ni-charged beads. Bacterial extract was removed and the beads were washed before rabbit G-actin (20 µg) was added and incubated with the His_6-Yih1 coated beads. The beads were washed again and the co-precipitates were boiled off the beads in loading dye. The samples were investigated via SDS-PAGE followed by immunoblot analysis using antibodies against actin. His_6-Yih1 was visualized on the membrane with a Ponceau S stain. A sample not containing His_6-Yih1 was used as a negative control for actin binding in the assay. 33,33% of the samples and 1% of input controls of actin and bacterial whole cell extract containing His_6-Yih1 were loaded. + indicates the indicated protein is added to the sample, - indicates the indicated protein is not added to the sample.

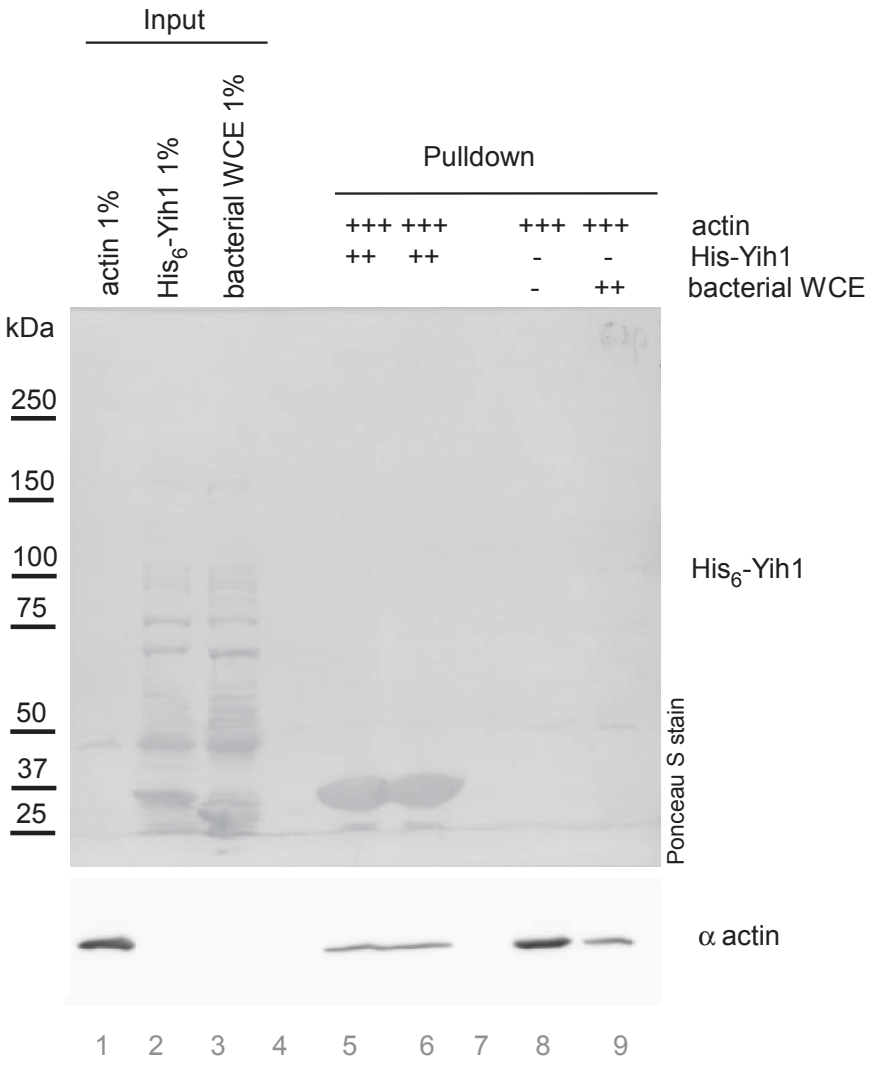

Figure 4.4: *In vitro* binding assay with rabbit muscle G-actin and yeast His_6-Yih1. The interaction assay and western blot analysis was performed as outlined in figure 4.3 with the alteration that the Ni-charged iMAc beads used in one negative control sample were incubated with bacterial WCE (100 µl) not containing any His_6-tagged protein.

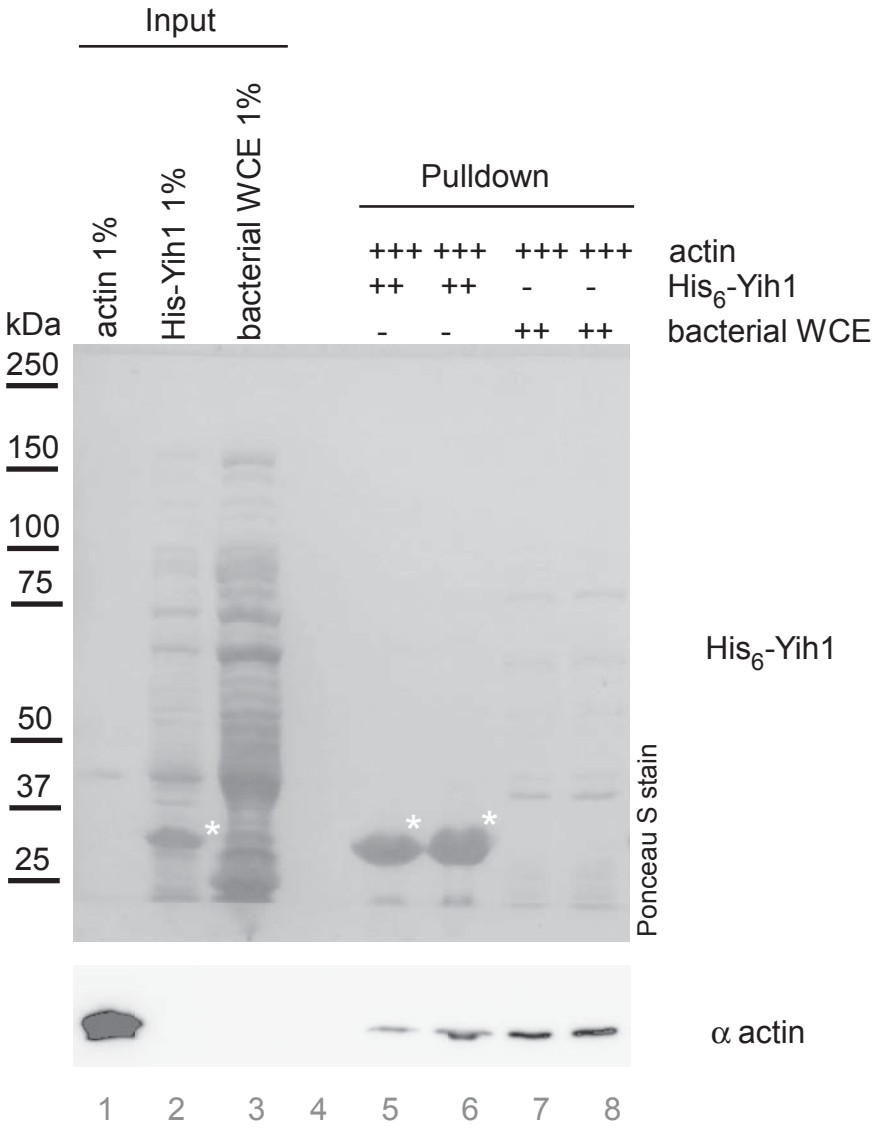

Figure 4.5: *In vitro* binding assay with rabbit muscle G-actin and yeast His_6-Yih1. The interaction assay and western blot analysis was performed as outlined in figure 4.4 with the alteration that the actin solution was pre-adsorbed on iMac beads for 20 min prior to the interaction assay. * indicates the location of His_6-Yih1 on the membrane.

specifically interacting with His_6-Yih1 in this *in vitro* interaction assay.

In conclusion, even with optimizing the *in vitro* interaction assay with regards to non-specific binding of actin, a specific interaction of His_6-Yih1 and actin could not be detected.

4.3 Discussion

In this study it has been shown that yeast His_6-Yih1 does not co-precipitate with rabbit F-actin in an *in vitro* sedimentation assay under the conditions investigated. This observation could be explained in three non-exclusive ways. 1.) Yih1 does not interact with F-actin *per se*. 2.) Yih1 does not interact with F-actin stably enough to withstand sedimentation by ultra centrifugation. 3.) The lack of interaction could be due to species incomparability between rabbit actin and yeast Yih1. Considering the latter, previous studies have suggested, that the yeast actin filament is more open and flexible than its muscle actin counterpart [131]. This difference between mammalian and yeast actin might explain the lack of interaction. However, yeast actin is 88% identical at the AA level to rabbit muscle actin [30, 87] and it is biochemically similar to it [86, 68, 16]. In addition, the mammalian homologue of Yih1, called IMPACT, has been shown to interact with yeast actin *in vivo* [128] highlighting the evolutionary conservation of this interaction. Thus, the latter explanation seems unlikely. To determine if Yih1 is a F-actin binding protein further experiments like *in vivo* co-localization using fluorescence tagged proteins and fluorescence microscopy will be necessary.

Yih1 has been previously reported to interact with actin *in vivo* [110, 108]. To verify this interaction *in vitro*, interaction studies using purified Yih1 and commercially available rabbit actin were performed. Despite optimizing the assay to increase the specific binding of actin to Yih1 an interaction between Yih1 and actin could not be detected.

As indicated above, the different origins of the purified proteins is unlikely to be responsible for the lack of interaction. To test this assumption, an *in vitro* interaction assay would have to be performed using purified yeast Yih1 and yeast actin. Another possible explanation for this unexpected result would be that the Yih1- actin interaction is mediated by an additional

protein not present under the conditions investigated. Thus far, Yih1-actin binding has solely been investigated under physiological conditions where an involvement of additional proteins in the interaction cannot be excluded.

In addition, it is possible that the His_6 tag interferes with the folding of Yih1 and/or with its binding to actin. Also, a post-translational modification in Yih1, which is not occurring in bacteria used to express the protein, might be required for the Yih1-actin interaction. However, the latter two explanations seem highly unlikely considering the fact that Sattlegger *et al.* has shown that His_6-Yih1 interacts with the minimal Gcn1 fragment sufficient for Yih1 binding *in vitro* [108, 110].

Published evidence suggests that G-actin assumes different conformations depending on the kind of molecule bound in the actin binding cleft, e.g. Mg^{2+} or Ca^{2+}, ATP or ADP [119, 82, 61]. Therefore it is possible, that under the standard conditions investigated (0.2 mM $CaCl_2$, 0.2 mM ATP) the three dimensional structure of actin is unfavorable for Yih1 binding and the conditions need to be optimized with regards to the nature of molecules used in the assay. This knowledge may allow us to elucidate the function of Yih1 in the cell. For example, ATP-G-actin is preferably added to the barbed end of the F-actin filament thus indicating a potential involvement of Yih1 at the initiation of a filament as proposed earlier. In contrast, ADP-G-actin is mainly located at the pointed end of the filament and in this formation G-actin is released from the polymer. Hence, the interaction of Yih1 with ADP-G-actin would hint at a role of the Gcn2 inhibitor protein in the depolymerization of filamentous actin.

In summary, in this chapter no interaction of Yih1 with either F-actin or G-actin could be detected under the *in vitro* conditions investigated.

5

Yih1 interacts with the cyclin dependent kinase Cdc28 *in vivo*

In *S. cerevisiae* Yih1 has been shown to interact with monomeric G-actin *in vivo* and with Gcn1 *in vivo* and *in vitro* [110, 108, 70]. These interactions are well established and a lot of effort is being put into identifying and characterizing more binding partners to elucidate the so far unknown regulatory pathway governing Yih1. In recent years large scale high throughput screens have identified additional potential binding partners of Yih1 [18, 67, 124, 94, 118], although these interactions still need to be verified.

In this study, independent approaches namely a yeast-2-hybrid screen and *in vivo* binding assays, were used to identify and confirm the cyclin dependent kinase Cdc28 as a novel binding partner of Yih1.

5.1 Yeast-2-hybrid screen with Yih1 fragments

As already mentioned in the previous chapters, the knowledge about the Yih1-actin interaction is limited. One step towards understanding the Yih1-actin interaction would be to pinpoint the Yih1 binding site in actin. It was reasoned that if a binding site could be determined then comparison with characterized actin binding proteins would provide additional information about Yih1 and associated biological processes or regulator pathways.

In the quest to identify the Yih1 binding site in actin a yeast-2-hybrid screen was undertaken in collaboration with Prof. Dr. David Amberg from Upstate Medical University, New York, who possesses a large yeast-2-hybrid library consisting of 35 actin mutants.

The yeast-2-hybrid technique takes advantage of the possibility to separate the Gal4 transcriptional activator into its DNA-binding domain and activation domain. Thus, the two domains can each be fused to individual proteins. If these two proteins interact they can reconstitute the Gal4 activity *in vivo*. Interactions can therefore be assessed by measuring the activation of a reporter gene under a Gal4 responsive promoter in the living cell (see figure 5.1). In Prof. Dr. Amberg's library protein interactions are scored by the ability of the cells to express the *HIS* gene under the control of a Gal4-responsive promoter. This confers resistance to 3 AT [2].

The approach using actin mutants to identify the Yih1-actin binding site is based on the assumption that a mutation in the Yih1 binding site of actin will abolish the interaction between Yih1 and actin. This would be indicated by an absence of interaction compared to wild type actin. Thus, first an interaction between Yih1 and actin has to be established before investigating the mutated actins.

Full length Yih1 was previously screened using this yeast-2-hybrid approach. However, no interaction between full length Yih1 and actin could be detected (E. Sattlegger, unpublished data). As protein fragments frequently interact more consistently than full length proteins in yeast-2-hybrid screens (Prof. D. Amberg, personal communication), three Yih1 fragments (fragment II, III and IV, see figure 5.2) were selected in this study. These fragments were chosen as they interacted with actin the most compared to full length

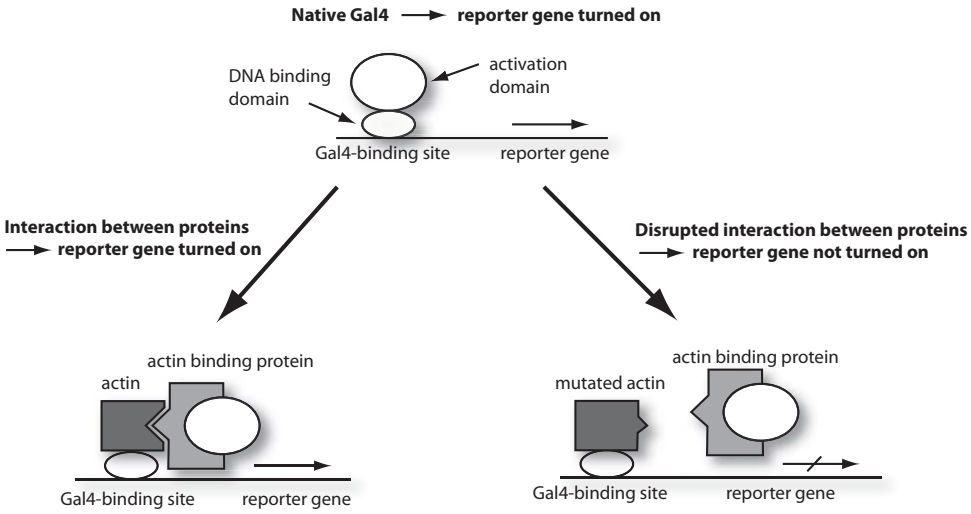

Figure 5.1: Schematic representation of the yeast-2-hybrid system. In this system the Gal4 transcriptional activator is separated into its DNA-binding domain and activation domain. Each domain is then fused to individual proteins investigated. Upon interaction of the two proteins Gal4 is activated and the protein-protein interaction can be assessed by measuring the expression of a reporter gene under a Gal4 responsive promoter.

Yih1 [108]. By using Yih1 fragments that interacted the strongest with actin it was expected that an interaction in the yeast-2-hybrid screen could be detected compared to full length Yih1. In the three plasmids the appropriate Yih1 sequence was fused to the Gal4 activation domain sequence followed by a HA tag sequence (see chapter 2.2). The resulting plasmids were verified by sequencing (see appendix H for sequencing result). The expression of the recombinant protein was confirmed by transforming the plasmids into yeast strain H1511 and performing an SDS-PAGE on the prepared yeast WCE followed by immunoblotting probing for the HA tag and Pgk1. Pgk1 was used as reference for equal loading (see figure 5.4 and 5.3).

The yeast-2-hybrid assay was performed in the Amberg lab using the three recombinant Yih1 fragments. In spite of the fact that the fragments investigated have been shown previously to interact strongly with actin [108], the Yih1-actin interaction was too weak to be scored via a yeast-2-hybrid

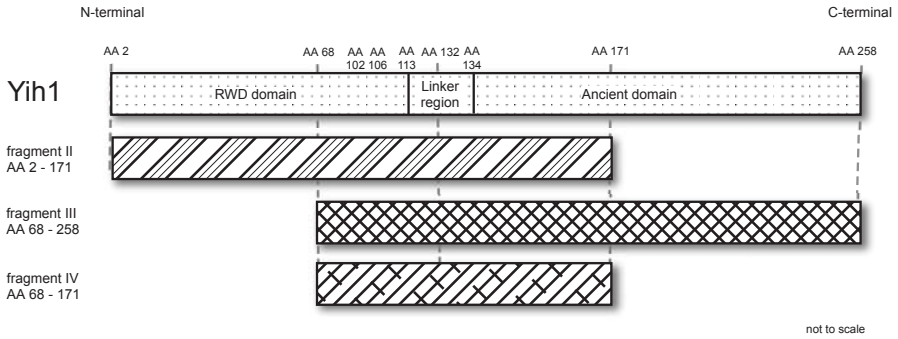

Figure 5.2: Schematic representation of full length Yih1 and Yih1 fragments used in the yeast-2-hybrid screen, drawing is not to scale.

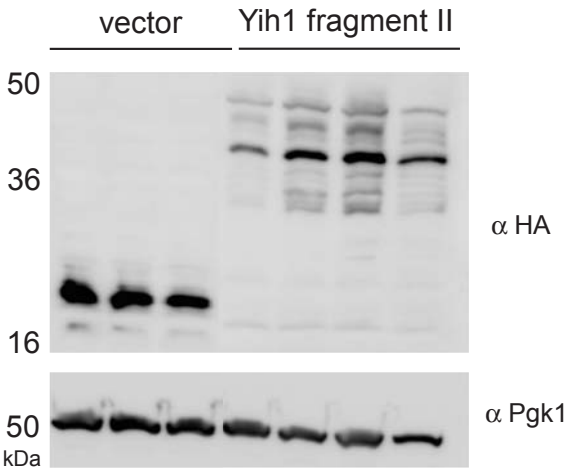

Figure 5.3: Verification of the expression of Yih1 fragment II fused to the Gal4 activation domain. Yeast strains expressing the vector control (pACTII) and Yih1 fragment II (pMD06a) were grown to exponential phase. Yeast WCE were prepared and 40 µg of total protein as determined by Bradford method were then subjected to SDS-PAGE on a 4%-17% gradient gel and to a subsequent western blot analysis probing for HA and Pgk1. Pgk1 was used as reference for equal loading.

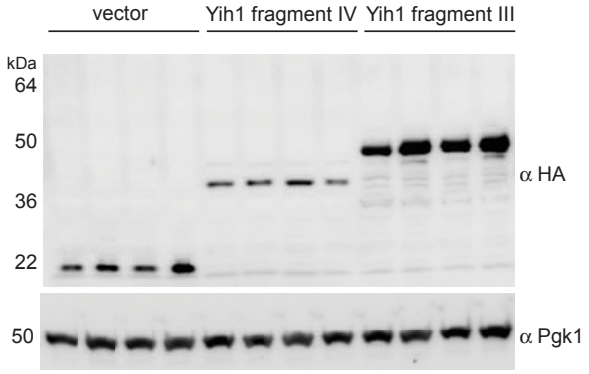

Figure 5.4: Verification of the expression of Yih1 fragments IV and III fused to the Gal4 activation domain. Yeast strains expressing the vector control (pACTII), Yih1 fragment IV (pMD02a) and Yih1 fragment III (pMD03a) were grown to exponential phase. Yeast WCE were prepared and 40 µg of total protein as determined by Bradford method were then subjected to SDS-PAGE on a 4%-17% gradient gel and to a subsequent western blot analysis probing for HA and Pgk1. Pgk1 was used as reference for equal loading.

assay in the Amberg lab (data not shown). Hence it was not possible to study the interaction between Yih1 and mutated actin. However, surprisingly the Amberg lab found that all three fragments tested interacted with the human cyclin dependent kinase 2 (Cdk2), which was used as a negative control for unspecific binding in the screen. As all fragments investigated displayed the interaction with Cdk2, it was decided to investigate the Yih1-Cdk2 interaction further and an *in vivo* interaction assay was carried out.

5.2 *In vivo* interaction assay with GST-Yih1 fragment III

In order to verify whether Yih1 interacts with the cyclin kinase Cdc28 (yeast homolog of Cdk2) an *in vivo* interaction assay using the GST-tagged Yih1 fragment III (see figure 5.6) was carried out. Plasmids expressing the GST-tagged Yih1 fragment or GST (both under the control of a galactose inducible promoter) were transformed into the yeast wild type strain TKY 460. Transformants were grown to exponential phase in medium containing galactose as the sole carbon source. Yeast WCE was prepared as de-

scribed previously (see chapter 2.17) and equal amounts of WCE were then subjected to a GST pulldown assay. The precipitates were investigated via SDS-PAGE and western blot analysis using antibodies against Cdc28 and GST. The intensity of the western blot signals was determined using the Multi Gauge V3.1 software (Fujifilm). The amount of Cdc28 pulled down was normalized against the amount of precipitated GST-Yih1 or GST alone, respectively.

As can be seen in figure 5.5 there is only a Cdc28 signal visible in the GST-Yih1 samples, but not in the GST control samples (compare lane 6 and 7 with 9 and 10 and quantification of GST pulldown). This suggests, that Cdc28 specifically interacts with Yih1 fragment III. The lack of Cdc28 signal in the GST alone samples does not result from a lack of Cdc28 in the sample as the input controls show that there were equal amounts of cell extract used in all samples (see figure 5.5, input samples lane 1-4).

This data supports the idea that Yih1 forms a complex with the cyclin dependent kinase Cdc28 *in vivo*. Interestingly, this complex is not only formed between yeast Yih1 and the human cyclin dependent kinase Cdk2 but also with its fungal homolog Cdc28.

5.3 Mapping the Cdc28 binding site in Yih1

In the previous sections it was established that Yih1 fragment III interacts with human Cdk2 as well as its fungal counterpart Cdc28.

However, given the fact that all three Yih1 fragments screened interacted with Cdk2 in the yeast-2-hybrid assay the question was raised if full length Yih1 also interacts with Cdc28. Secondly, it was asked if this interaction is dependent on the GAAC effector protein Gcn1. Thirdly, a characterization of this interaction by mapping the Cdc28 binding site in Yih1 was sought. If the domain of Yih1 interacting with Cdc28 was identified, it could be compared to the binding site of other Yih1-binding proteins and conclusions about the interplay of these proteins could be drawn.

To answer these questions yeast strains overexpressing five different Yih1 fragments along with full length Yih1 or GST alone under a galactose-

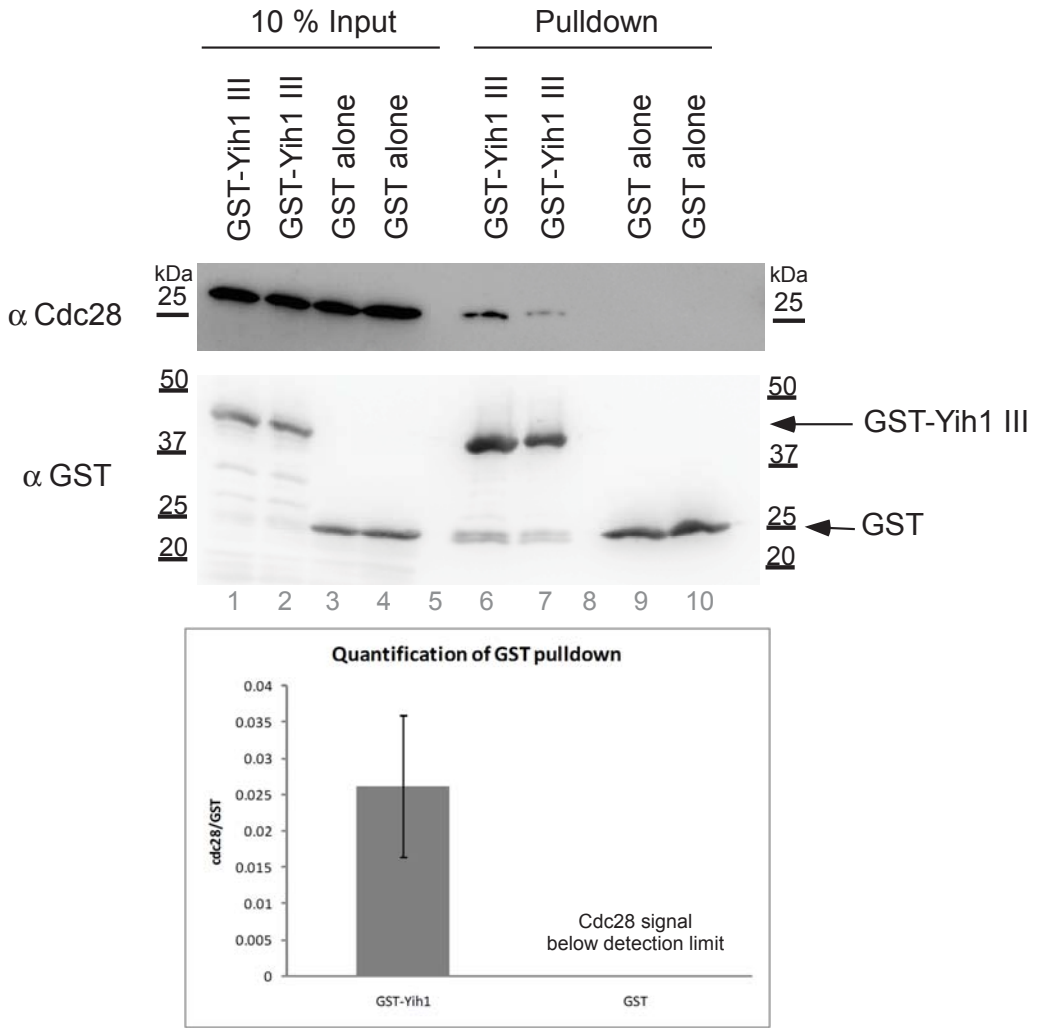

Figure 5.5: *In vivo* binding assay with GST-Yih1 fragment III in yeast wild type strain TKY 460. Equal amounts of total protein from whole cell extracts of TKY 460 yeast strains expressing the GST-Yih1 fragment III and GST alone were incubated with glutathione-linked affinity resin. The precipitates and aliquots of the whole cell extracts were subjected to SDS-PAGE on a gradient gel (4% - 17%) and immunoblotting using antibodies against Cdc28 and GST. The signal intensity of the bands were determined using the Multi Gauge V3.1 software (Fujifilm). The amount of Cdc28 interacting was normalized against the amount of GST-Yih1 or GST alone respectively. The standard error is indicated.

inducible promoter in a *gcn1*△ H2556 strain were used in an *in vivo* interaction assay (see figure 5.6) [108]. These strains were grown to exponential phase in medium containing galactose as the only carbon source. Yeast WCE were prepared and equal amounts of WCE measured by the Bradford method were then subjected to a GST pulldown assay. The precipitates were subjected to SDS-PAGE and subsequently western blotted probing for Cdc28 and GST. As the GST signals were out of the linear range, only the Cdc28 signal was quantified by determining the signal intensity using the Fujifilm Multi Gauge software. To be able to compare individual experiments the Cdc28 signals in the GST-Yih1 fragment samples were normalized to the Cdc28 signal in the GST alone control. An example of an interaction assay including an example of a Cdc28 quantification is depicted in figure 5.7 (panels A and B). Panel C in figure 5.7 displays the overall Cdc28 quantification of all experiments performed. The individual results are available in appendix I.

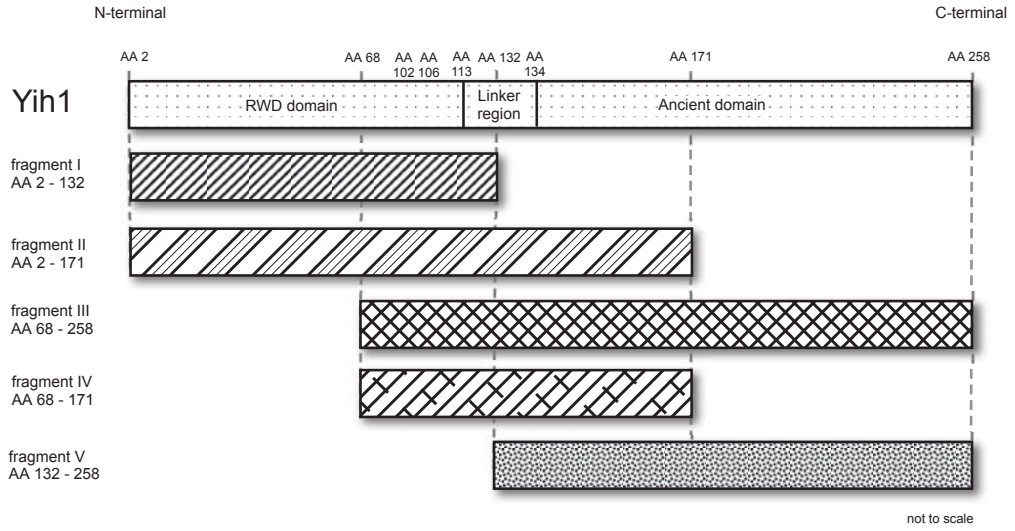

Figure 5.6: Schematic representation of full length Yih1 and Yih1 fragments used for mapping the Cdc28 binding site in Yih1, drawing is not to scale.

In the interaction assay performed previously in chapter 5.2 an interaction between Cdc28 and Yih1 could be detected *in vivo*. As a wild type yeast strain containing endogenous Gcn1 was used in this particular assay,

there was a possibility that the Cdc28-Yih1 interaction was bridged by Gcn1. To rule out this possibility a *gcn1*Δ background was used in this interaction experiment. It was expected that if the binding of Cdc28 to Yih1 was dependent on Gcn1, no interaction between Yih1 and Cdc28 should be detected in this strain background.

Yih1 and Cdc28 co-precipitate even if Gcn1 is not present (see figure 5.7, A, B example experiment, C all experiments). This suggests that the Yih1-Cdc28 interaction is independent of Gcn1. In addition, it was confirmed that full length Yih1 is interacting with Cdc28, indicating that this interaction could occur in the cell and might be biological significant.

Mapping the binding site using different GST-Yih1 fragments was problematic as the expression levels of these proteins varied substantially, e.g. compare GST input controls in figure 5.7. To be able to detect Cdc28 in all Yih1 co-sedimentation assays, a high amount of total protein (2, 4 mg in 200 µl) had to be used in the experiment. However, these measures lead to a GST signal in the immunoblot which was out of the linear range and not quantifiable. However, the precipitated amount of the different GST-Yih1 fragments correlated with their previously published expression levels (see figure 5.8) indicating that the GST-Yih1 fragments bound to the beads with similar efficiencies [108]. Thus, the quantified relative Cdc28 signals obtained in this study were normalized by comparison to the published expression levels of the GST-Yih1 fragments. Sattlegger *et al*. quantified the GST-Yih1 fragments relative to the endogenous Yih1 by measuring their signal intensity on immunoblots using the program NIH Image J [108].

In addition to full length Yih1, fragment I, III and V could be identified as interaction partners of Cdc28 as the Cdc28 signals in these samples are well above the signal of that found for the GST alone control (see figure 5.7 C and individual result in appendix I). Unfortunately, due to the variation in the binding of fragments II and IV no conclusion can be drawn about the interaction between Cdc28 and these regions of Yih1 (see panel C, figure 5.7). These fragments II and IV are expressed the least (see GST input controls in figure 5.7) thus likely resulting in a low amount of Cdc28-GST-Yih1 precipitates. One way to correct for the unequal expression would be

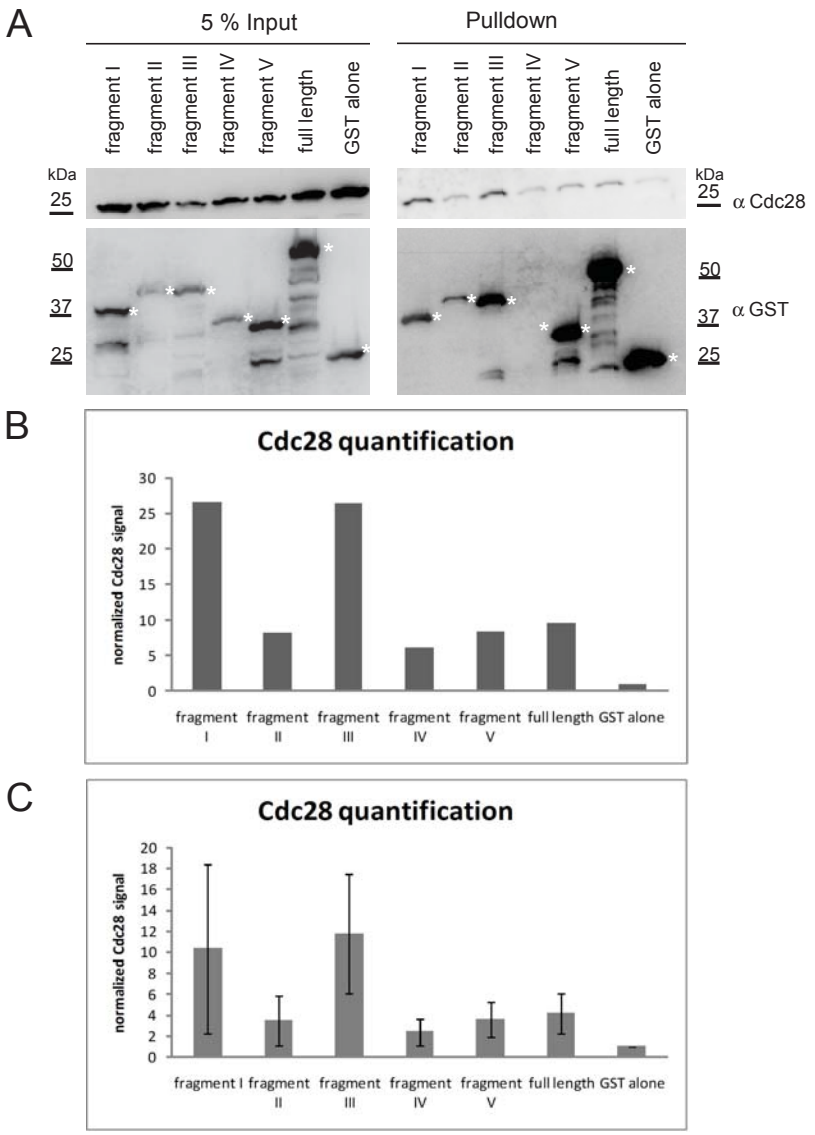

Figure 5.7: Example of mapping the Cdc28 binding site in Yih1, A.) *gcn1*Δ yeast strains overexpressing five different GST-Yih1 fragments, full length GST-Yih1 or GST alone under a galactose-inducible promoter were grown to exponential phase in medium containing galactose as the only carbon source. Yeast WCE were prepared and equal amounts of total protein as determined by Bradford method were subjected to a GST pulldown assay. The precipitates and aliquots of the WCE (input) were subjected to SDS-PAGE on a 4%-17% gradient gel and to a subsequent Western blot analysis probing for Cdc28 and GST. The location of the GST-tagged proteins are indicated with an asterisk. As the GST signals were out of the linear range, only the signal intensity of the Cdc28 blots were determined using the Fujifilm Multi Gauge software. B.) Quantification of the Cdc28 signal in A, normalized to the Cdc28 signal in the GST alone sample. C.) Overall quantification of Cdc28 signals from at least two experiments. The standard error is indicated.

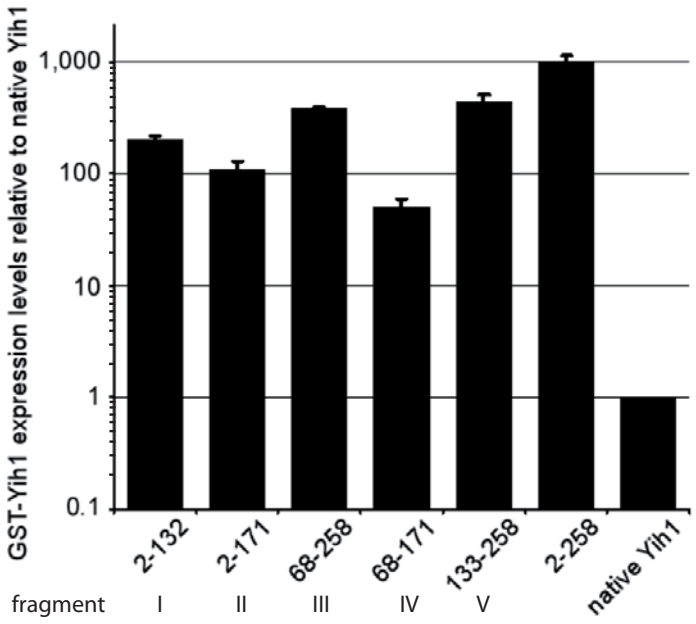

Figure 5.8: Expression levels of GST-Yih1 and GST-Yih1 fragments I - V relative to native Yih1, adapted from Sattlegger *et al.* [108].

to adjust the amount of WCE used in the pulldown to the expression levels of the fragments, i.e. use about 20 times more WCE of fragment IV than of full length Yih1 as the latter is expressed 20 times more than the fragment (see figure 5.8).

As summarized in figure 5.9, GST-Yih1 fragment I, III and V co-precipitated with Cdc28 to some extent as investigated by *in vivo* interaction assay. GST-Yih1 fragment I appears to bind less Cdc28 in comparison to fragment III (see figure 5.7, panel C). However, taking into consideration that fragment I is overexpressed less strongly than fragment III (see figure 5.8), these fragments seem to bind Cdc28 to a similar extent. GST-Yih1 fragment V expression is equivalent to that of GST-Yih1 fragment III (see figure 5.8), but GST-Yih1 fragment V binds Cdc28 the least (see figure 5.7, panel C). This indicates that the binding of this fragment to Cdc28 is not as strong as fragments I and III. Thus, taking their expression levels into consideration it can be concluded that fragments I and III bind Cdc28 the strongest followed by fragment V in these *in vivo* binding assays.

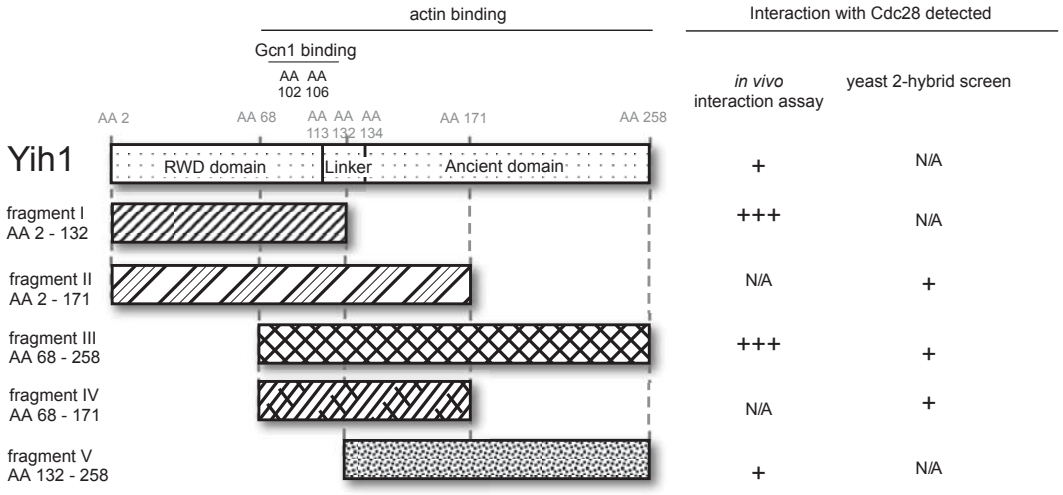

Figure 5.9: Result of mapping the Cdc28 binding site in Yih1, + indicates interaction detected, +++ indicates strong interaction detected, N/A indicates no result available, drawing is not to scale

5.4 Discussion

In a yeast-2-hybrid assay three Yih1 fragments (fragment II, III, IV) were found by the Amberg lab to interact with the human cyclin dependent kinase Cdk2. To verify that such an interaction occurs in yeast cells an *in vivo* interaction assay with Yih1 fragment III and Cdc28, the yeast homolog of Cdk2, was performed. This particular fragment co-precipitated with Cdc28 raising the question if the biological occurring full length Yih1 also interacts with the cyclin dependent kinase. The interaction with full length Yih1 was confirmed in subsequent *in vivo* binding assays. Further, the Yih1 region binding to Cdc28 was determined using five fragments of Yih1 (fragment I, II, III, IV, V) in an *in vivo* binding assay. Taken together with the yeast-2-hybrid screen, it has been proposed that all fragments bind to Cdc28 to some extent. This interaction has been shown to be independent of the Gcn2 regulator protein Gcn1 as the interaction with fragment III has been shown in both a *gcn1*Δ strain and a strain containing endogenous Gcn1.

In eukaryotic cells, the cell cycle is controlled by Cdks. Ccd28 also known as Cdk1 is one of six conserved cyclin dependent kinases in *S. cerevisiae*. Cdc28 is necessary and sufficient to drive the cell cycle in *S.*

cerevisiae [26]. About 300 potential Cdc28 targets have been identified *in vivo* [51] that control critical cell cycle events such as DNA replication and segregation, transcriptional programs and cell morphogenesis like bud formation and bud site selection [26]. Cdc28 is a proline-directed kinase that preferentially phosphorylates the consensus sequence S/T-P-x-K/R (x is any amino acid), although it also phosphorylates the minimal consensus sequence S/T-P [90]. Cdc28 interacts with nine different cyclins throughout the cell cycle [26]. The interaction with cyclins is important for activation of its kinase activity and also for recruitment and selection of substrates. However, in addition to cyclin binding full activation of Cdks requires a stimulatory phosphorylation carried out by cyclin dependent kinase activating kinases (CAK). The yeast CAK is called Cak1 and phosphorylates Cdc28 on T169 [58, 121, 106].

When mapping the Yih1-Cdc28 binding site in Yih1 it was surprising that fragments, which do not overlap but constitute the entire Yih1 protein (fragment I, V) have been shown to interact with Cdc28 *in vivo*. This result suggests that Yih1 does not bind Cdc28 via a single binding site but rather via several binding sites, which are distributed all over the Yih1 surface. Protein-protein interactions being mediated by more than one AA is not unusual, e.g. the Yih1-Gcn1 interaction has been shown to depend on two amino acids in Yih1 *in vivo* (AA 102 & 106, see figure 5.9) [108]. When considering the binding affinity as judged by the amount of Cdc28 co-precipitating versus the amount of GST-Yih1 expressed, Yih1 fragments I and III bind the strongest to Cdc28 in comparison to full length Yih1 suggesting that the main binding determinants are located in a region contained in both fragments. The region common to both of these fragments spans from AA 68 - 132. This is particularly striking as AA 102 and 106 in this region have been identified as the Gcn1 binding site in Yih1 as mentioned earlier (see figure 5.9) [108]. Overlapping binding sites together with the size of Gcn1 (296 kDa) would suggest Cdc28 and Gcn1 are not able to reside on Yih1 at the same time and thus Gcn1 is not bridging the Yih1-Cdc28 interaction. The latter idea was supported by the fact that Cdc28 co-precipitates with Yih1 in the absence of Gcn1 as shown in this study. The region of Yih1 necessary for the Yih1-actin interaction has been recently pinpointed to a region ranging from

amino acid 68 - 258 (see figure 5.9) [108] indicating that the binding sites of Cdc28 and actin in Yih1 potentially overlap. However, as Yih1 has been found in a heterodimeric 1:1 complex with monomeric actin [110], it seems unlikely that actin and Cdc28 reside on Yih1 at the same time.

Yih1 has not been characterized as a Cdc28 binding protein previously, therefore the biological significance of this interaction has not been investigated. Yih1 is most likely not a substrate for Cdc28 as its protein sequence lacks the consensus sequence S/T-P. Supporting this idea, Yih1 has not been identified as a substrate of Cdc28 thus far [122, 75, 51].

Deletion of several Cdc28 binding proteins, e.g. cyclin Bs or CAK, results in lethality [40, 112, 121]. In contrast, a yeast strain deleted for *YIH1* does not exhibit a growth defect in comparison to a strain containing endogenous Yih1, as judged by comparison of the growth rate in a semi-quantitative growth assay. Thus, it seems highly unlikely that Yih1 plays an essential role in the cell cycle via Cdc28. It is more likely that Yih1 has a rather subtle influence on Cdc28.

One possibility is that this Yih1-Cdc28 interaction is involved in bud emergence. Sattlegger *et al.* suggested a localized Yih1 mediated Gcn2 inhibition restricted to the site of bud emergence. This would allow an optimal translation and rapid bud growth [110]. Cdc28 is crucial for bud formation as no buds are formed in cells lacking three G1 cylins [26, 73]. However, Cdc28 is not directly involved in bud emergence but rather promotes bud formation indirectly by stimulating the activity of several important proteins involved in bud growth, e.g. Cdk42 [26]. Taking all this into consideration it is tempting to speculate that Yih1 might act as a stimulator to Cdc28 in the formation of the bud. Yih1 may enable a rapid bud growth first by increasing global translation by impairing the GAAC and secondly by stimulating the involvement of Cdc28 in the formation of the bud. Considering the fact that Yih1's role in this model is of a promoting nature deletion of *YIH1* would not lead to a disruption of budding or growth, as seen in this study. Overexpressing Yih1 should consequently lead to an enhanced bud formation, which might be visualized by microscopic techniques.

Despite the identification of Cdc28 as a novel interaction partner of Yih1, the outcome of the yeast-2-hybrid screen with regards to the actin-Yih1 inter-

action was surprising. Fragments which have been shown to bind strongly to actin were used [108]. Thus an interaction between actin and Yih1 was expected to be detectable. However, this was not the case. One explanation could be that due to the physiological conditions in the nucleus where the interaction in a yeast-2-hybrid assay takes place, Yih1 folding is altered. This altered conformation could interfere with the Yih1-actin interaction leading to a lack of *GAL4* activation. Another limitation of the yeast-2-hybrid technique results from the fact that the *GAL4* activation domain fused to Yih1 could interfere with the Yih1-actin interaction. To circumvent this issue, Yih1 could instead be fused to the DNA binding domain. However, as actin is recombined with the binding domain in the pre-existing yeast-2-hybrid library, this alternative was not an option for this study.

The number of verified and characterized interaction partners with Yih1 are limited to actin and Gcn1. In this study a previously unknown Yih1 binding protein has been identified and verified - namely Cdc28. Cyclins and cdks are well conserved between yeast and mammals as human Cdk2 can substitute for Cdc28 in *S. cerevisiae* [135]. Interestingly, the Yih1-Cdc28 interaction is also conserved between humans and yeast as Yih1 fragment III interacts with both Cdc28 and its human homolog Cdk2 as shown in this study. This suggests the evolutionary conservation of this interaction and indicates an importance of this interaction for the organism.

6
Conclusion

In order to shed light on the link between the actin cytoskeleton and stress response, a comprehensive screen of actin mutant strains for their impaired GAAC was performed in this study. In addition, *in vivo* and *in vitro* interaction assays with the Gcn2 inhibitor protein Yih1 and actin have been carried out to further the understanding of the Yih1-actin interaction. Interestingly, it has been shown in this study that actin mutations affect the function of the GAACl in *S. cerevisiae*. Out of 24 mutant strains five exhibited an impaired stress response as indicated by a Gcn^- phenotype.

The proposed molecular basis for this phenotype is diverse and reflects the myriad of processes actin is involved in within the cell. Results obtained in this study and previously published data suggest that several mechanisms could be the cause for the observed growth defect including 1.) a disrupted actin-eEF1A interaction, which could lead to an impaired dissociation of eEF1A and Gcn2 thus inhibiting Gcn2 activation, 2.) an impaired translation fidelity or 3.) an affected transcription in the actin mutant strains.

Actin has been previously shown to regulate the GAAC via the Gcn2

inhibitor protein Yih1 [110, 108]. However, the results in this study indicate that the regulatory influence of actin on the GAAC goes beyond Yih1. Actin's involvement is more profound than previously assumed as the cytoskeleton protein seems to regulate the GAAC on different levels. This result emphasizes the complex nature of the crosstalk that exist between cellular pathways in the cell and this study has the potential to function as an excellent starting point to further investigate this intricate and interconnected crosstalk between the cytoskeleton protein actin and the GAAC.

Intriguingly, one actin mutation included in this screen has been proposed to affect the GAAC via Yih1 as indicated by an exacerbated Gcn^- phenotype upon overexpression of Yih1(see figure 3.10 in chapter 3). Based on the findings in this study and prior work it was suggested that the Yih1-G-actin interaction may be regulated by F-actin polymerization. In addition, in this study the cyclin dependent kinase Cdc28 has been identified as a novel interaction partner of Yih1 using *in vivo* interaction assays. Based on this finding, it has been speculated that a possible link between Yih1 and bud emergence in the cell may exist. Together these findings not only support the previously reported connection between the GAAC and Yih1 [110, 108], but also link Yih1 to previously unrelated biological processes in the cell as depicted in figure 6.1. Further experiments need to be carried out to verify these proposed additional functions of Yih1.

With findings from this study and previous work a link between Yih1, bud formation, actin polymerization and GAAC was proposed (see figure 6.1 and [110]). It remains unclear whether these links form a four-way connection. Supporting this idea, many physiological stresses (e.g. changing nutrient level, temperature, osmolarity or ethanol concentration) are associated with a transient depolarization of the actin cytoskeleton [53, 14, 74, 71, 123], leading to a delayed bud formation [53]. Yih1 might be the mediator between actin polymerization and bud emergence, GAAC and actin polymerization and GAAC and bud formation. Further experiments need to be carried out to investigate the potential existence of such an intricate network.

Although Yih1 is a yeast specific protein, homologous proteins in higher eukaryotes also exist. The existence of these proteins allows speculation on

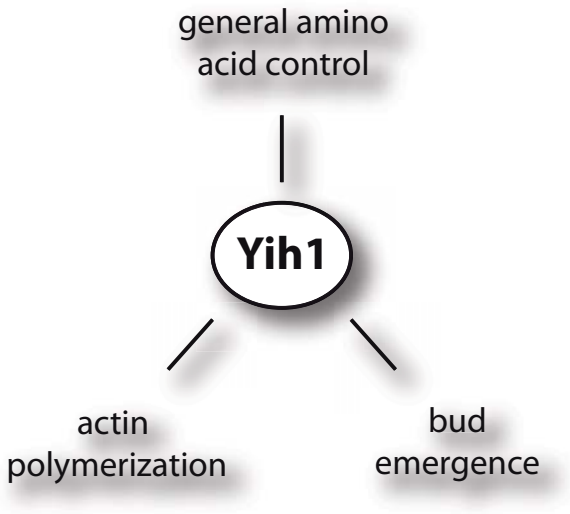

Figure 6.1: Proposed model of Yih1 function in *Saccharomyces cerevisiae* based on findings in this study.

the role of Gcn2 inhibition in higher eukaryotes. Yih1 has been proposed to function in the bud in *S. cerevisiae*, which composes the location of maximal growth in a yeast cell [102]. In mammalian cells such an area of enforced growth is located in the growth cone of neuronal cells. Interestingly, IMPACT, the mammalian homologue of Yih1, is mainly expressed in neuronal cells [97, 9, 41] and Gcn2 has been implicated in long term potentiation and memory in mice [17]. Thus it has been proposed that IMPACT may be involved in brain related functions as well [97]. Taking this and the evolutionary conservation of the GAAC proteins Gcn2, Gcn1 and Yih1 and in particular the Yih1-actin and Yih1-Cdc28 interactions into consideration, it becomes apparent that findings on Yih1 in the model organism *S. cerevisiae* constitute an excellent starting point for further investigations on IMPACT and Gcn2 in higher eukaryotes as discussed by Sattlegger *et al*. [110, 108].

Future research should be directed towards key questions that still remain unanswered, e.g. how does the cell sense that an inhibitory effect of Yih1 on Gcn2 is no longer required? How does the cell sense that a Yih1- Cdc28 interaction is no longer needed? Why is there such an intricate crosstalk between the cytoskeleton and the GAAC?

The aim of this study was to shed light on the link between the actin cytoskeleton and stress response in *S. cerevisiae*. From 24 actin mutant strains investigated, five were unable to activate the GAAC. Interestingly, the proposed molecular basis for this impairment is diverse, ranging from a Yih1 and eEF1A dependent Gcn2 inhibition to an altered transcription and/or translation. These findings strongly suggest, that actin modulates the GAAC at multiple levels, indicating that actin plays a crucial role in the GAAC stress response. Further studies are necessary to fully uncover the biological significance of this intricate interplay. In addition, *in vitro* binding assays suggested that the Yih1-actin interaction is more complex than anticipated. Unexpectedly, the cyclin dependent kinase Cdc28 has been identified as a novel interaction partner of Yih1. Cdc28 has a myriad of functions in the cell including the control of the cell cycle and bud emergence. Thus, raising the possibility that a link between the cell cycle and GAAC regulation might exist. Considering the fact that the GAAC pathway is conserved throughout the eukaryotic kingdom from yeast to mammals, findings from this study constitute an excellent starting point to unravel Gcn2 associated processes in higher eukaryotes such as long-term memory formation or feeding behavior.

A

Result of the semi-quantitative growth assay of actin mutant strain TKY 465

The result of the semi-quantitative growth assay testing actin mutant strain TKY 465 for sensitivity to 3AT is summarized in this appendix.

Actin mutant strain TKY 465, H1511 strain (positive control) and H2557 strain (*gcn2*△, negative control) were grown to saturation. Saturated overnight cultures were subjected to 10 fold serial dilutions and 5 µl of undiluted culture and 5 µl of each dilution were transferred to solid SD medium containing 10 mM- 50 mM 3-Aminotriazole, solid SD media not containing any starvation drug and solid YPD media. Plates were incubated at 30℃ until colonies were visible.

Actin mutant strain TKY 465 does not exhibit a sensitivity to 3AT compared to the positive control H1511.

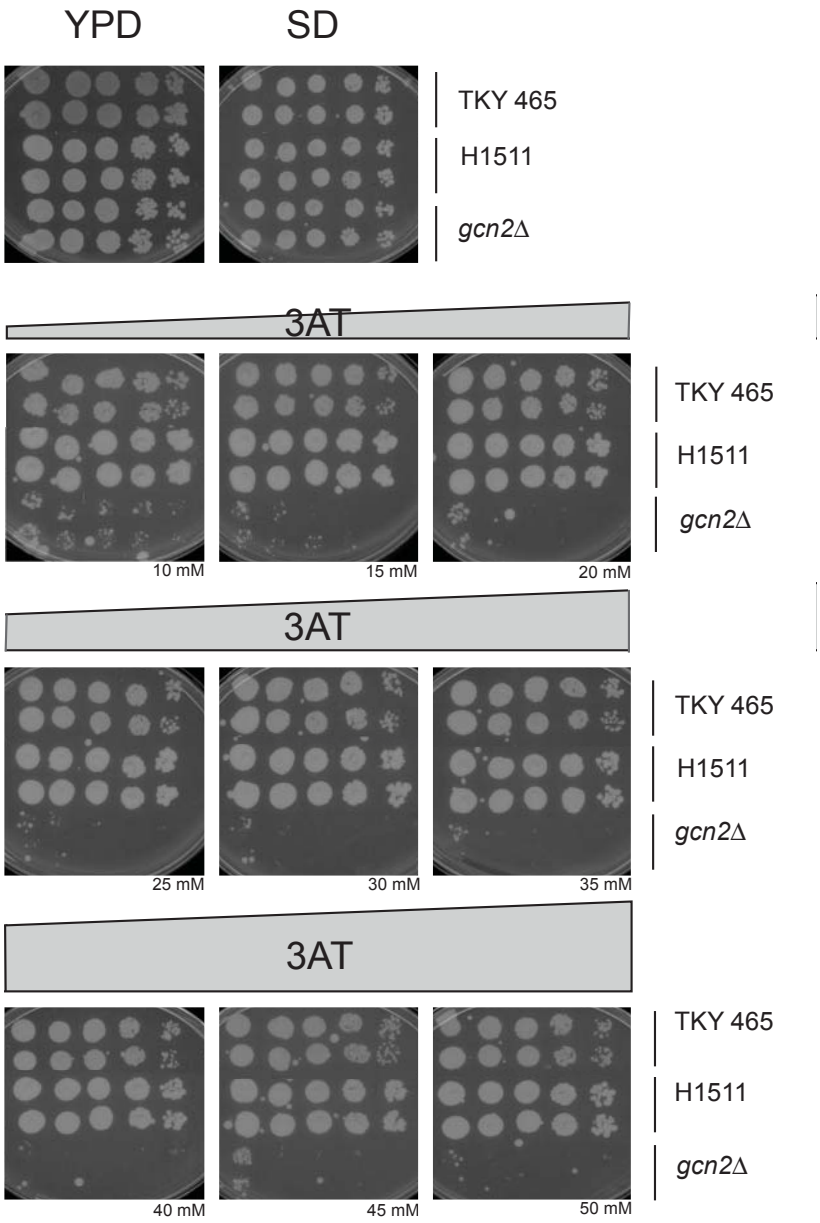

Figure A.1: Overview of the screen of actin mutant strain TKY 465 for sensitivity to 3AT. The growth assay was performed as outlined in the introduction to this appendix.

B

Results of the Gcn4^{c} semi-quantitative growth assays

All results of the screen of actin mutant strains for sensitivity to SM when the transcription activator Gcn4 is constitutively expressed are summarized in this appendix.

Actin mutant strains as indicated, wild type strain TKY 460, *gcn2*△ wild type strain TKY 460 all harboring a plasmid constitutively expressing Gcn4 (p238) and a vector control plasmid (p703), H1511 strain (positive control) and the negative controls strains H2558 (*gcn20*△) and H2557 (*gcn2*△) were grown to saturation. The overnight cultures were subjected to 10 fold serial dilutions and 5 µl of undiluted culture and 5 µl of each dilution were transferred to solid SD medium containing the amino acid analogue SM as indicated and solid SD media not containing any SM. 5 µl of undiluted culture of the positive control strain (H1511) and the negative controls strains (H2558, *gcn20*△; H2557, *gcn2*△) were transferred to the same plates. Plates were incubated at the indicated temperature until colonies were visible

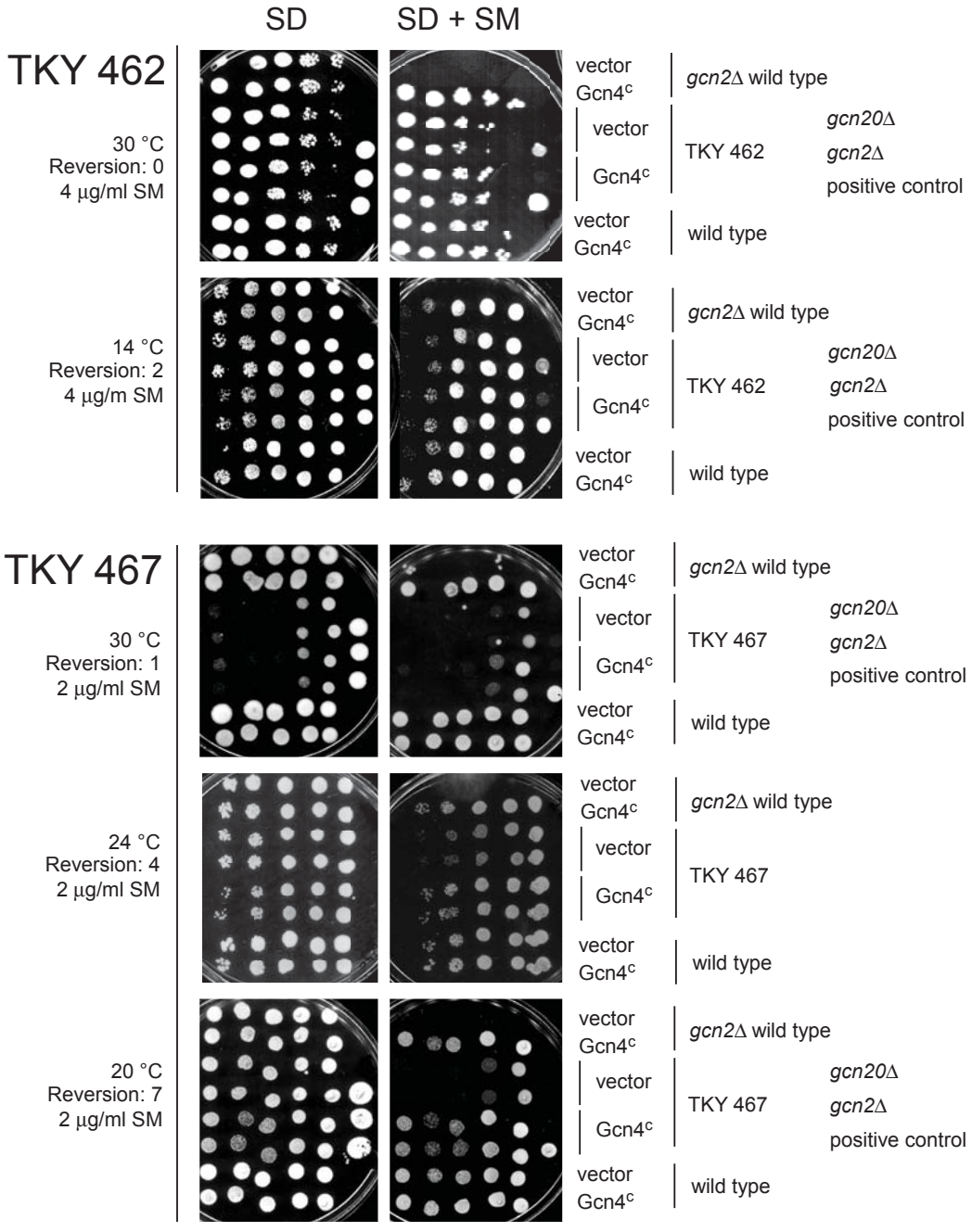

Figure B.1: Screen of actin mutant strains for sensitivity to SM when the transcription activator Gcn4 is constitutively expressed. The semi-quantitative growth assay was performed as described in the introduction to this appendix.

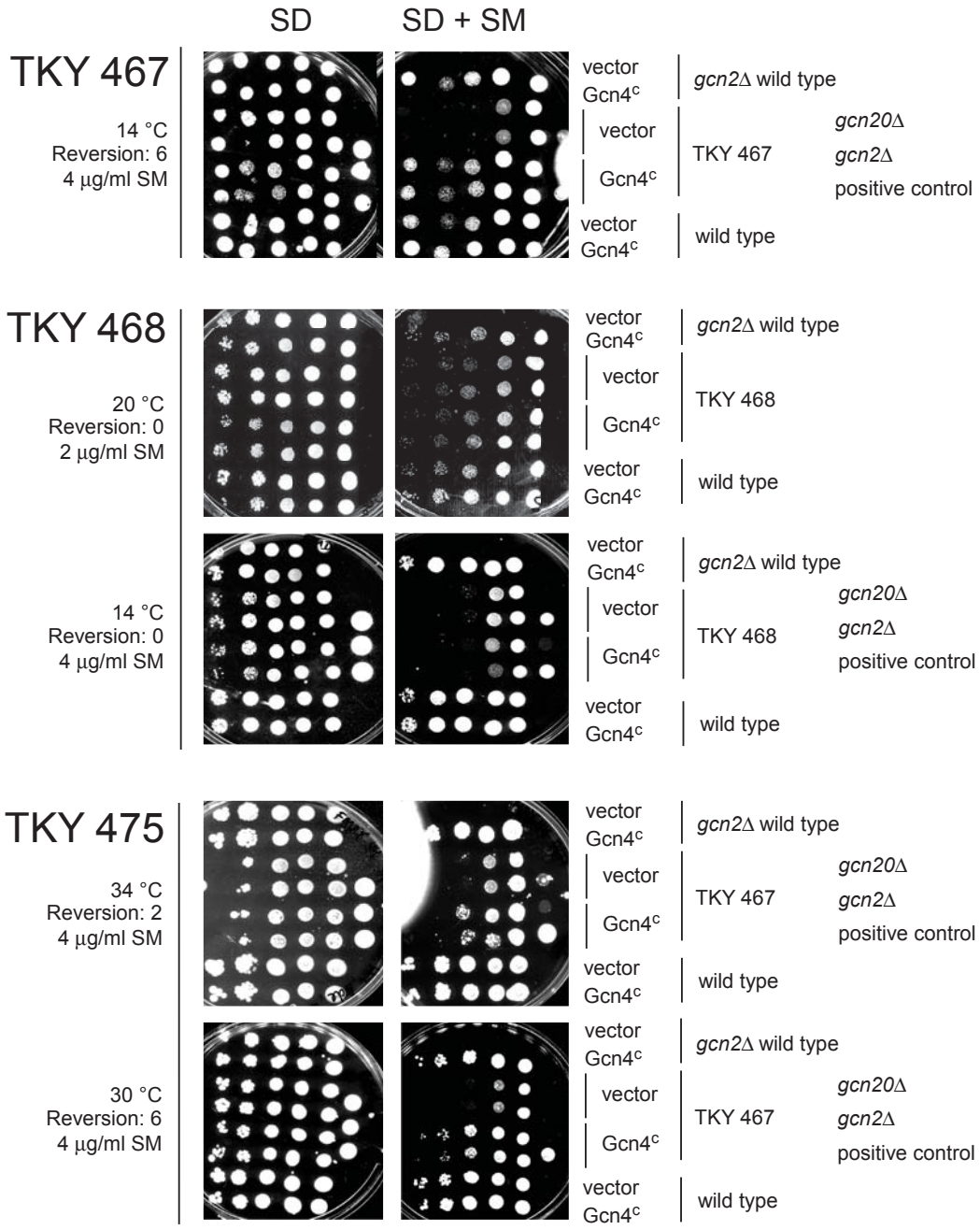

Figure B.2: Screen of actin mutant strains for sensitivity to SM when the transcription activator Gcn4 is constitutively expressed continued. The semi-quantitative growth assay was performed as described in the introduction to this appendix.

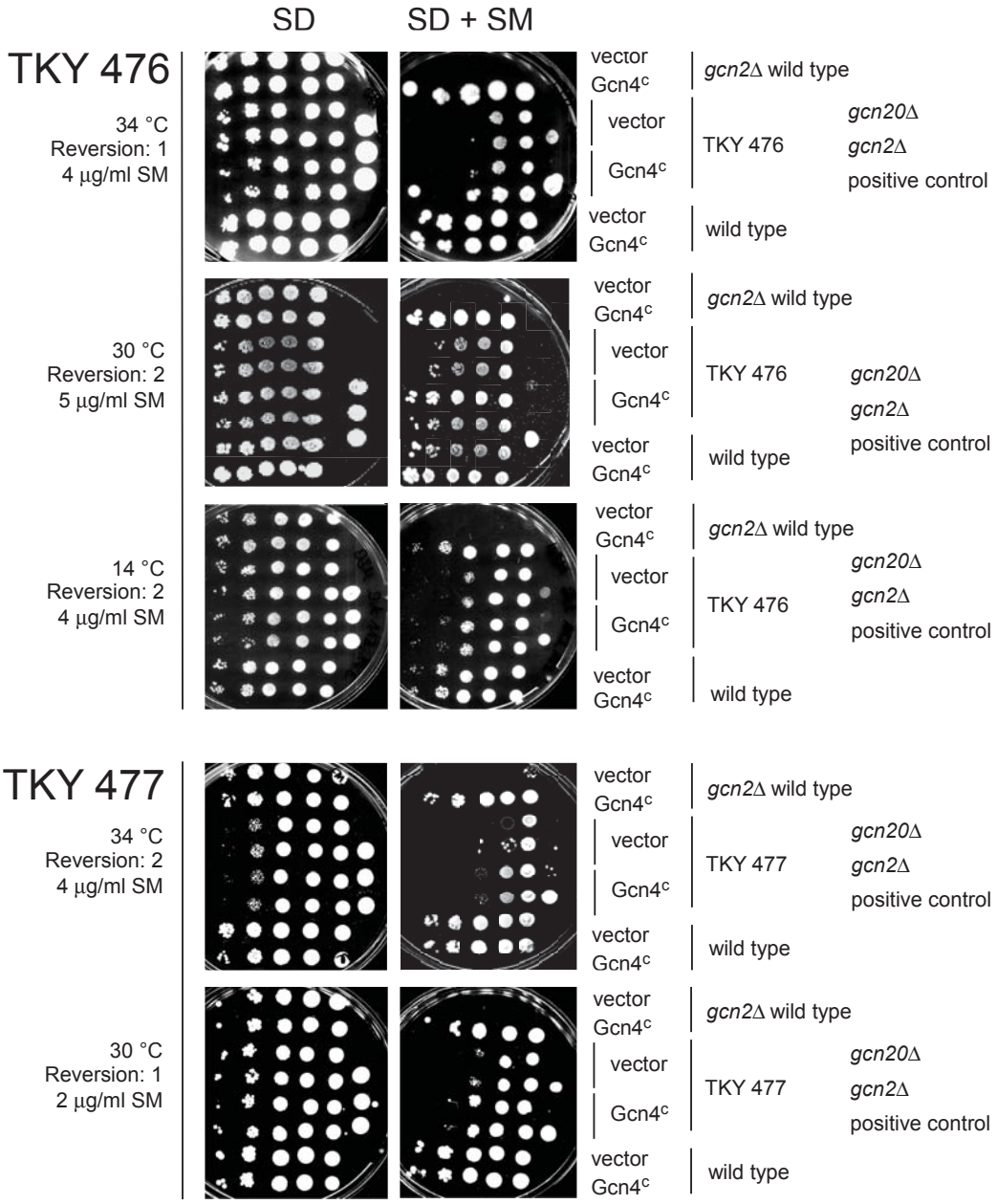

Figure B.3: Screen of actin mutant strains for sensitivity to SM when the transcription activator Gcn4 is constitutively expressed continued. The semi-quantitative growth assay was performed as described in the introduction to this appendix.

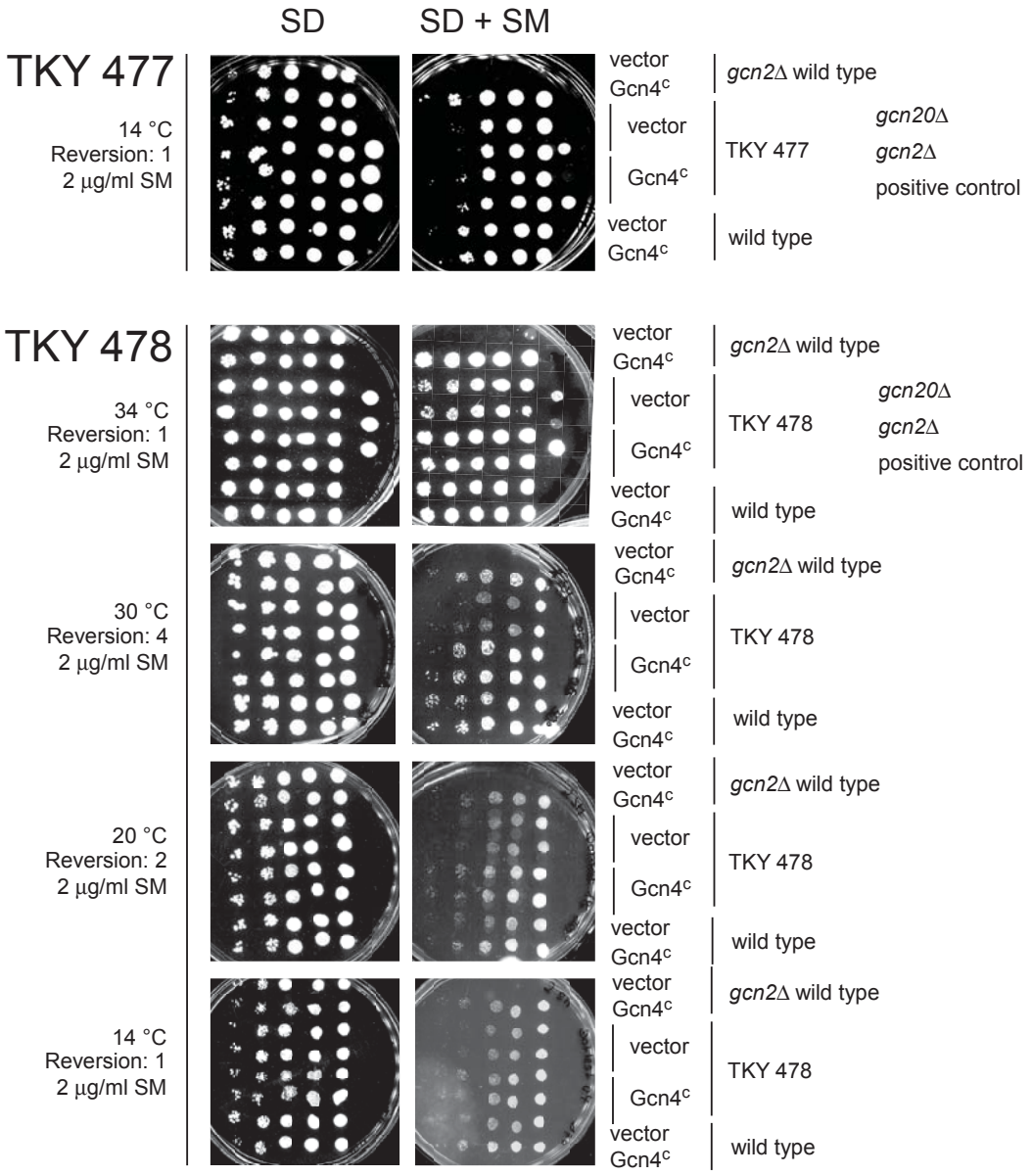

Figure B.4: Screen of actin mutant strains for sensitivity to SM when the transcription activator Gcn4 is constitutively expressed continued. The semi-quantitative growth assay was performed as described in the introduction to this appendix.

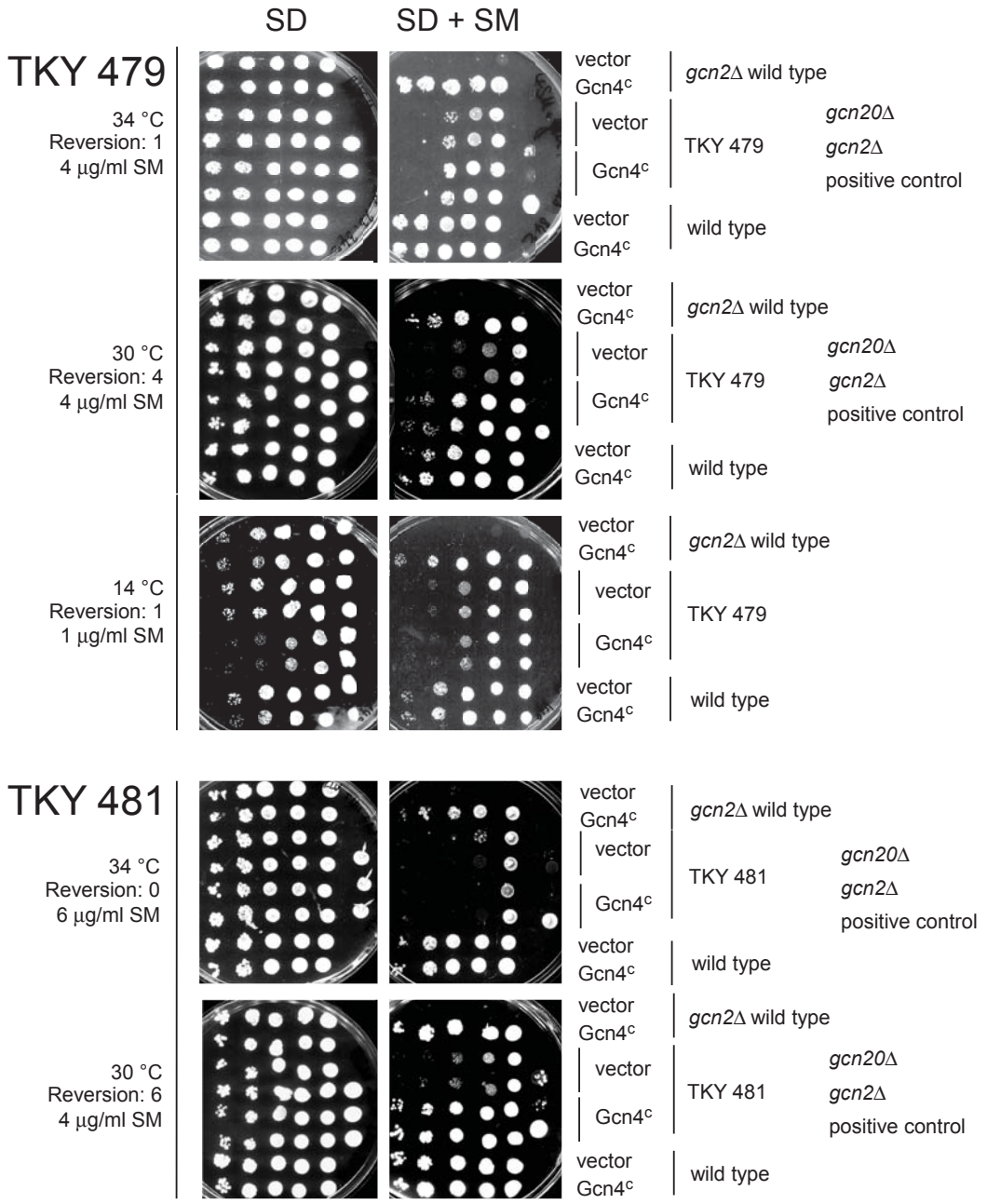

Figure B.5: Screen of actin mutant strains for sensitivity to SM when the transcription activator Gcn4 is constitutively expressed continued. The semi-quantitative growth assay was performed as described in the introduction to this appendix.

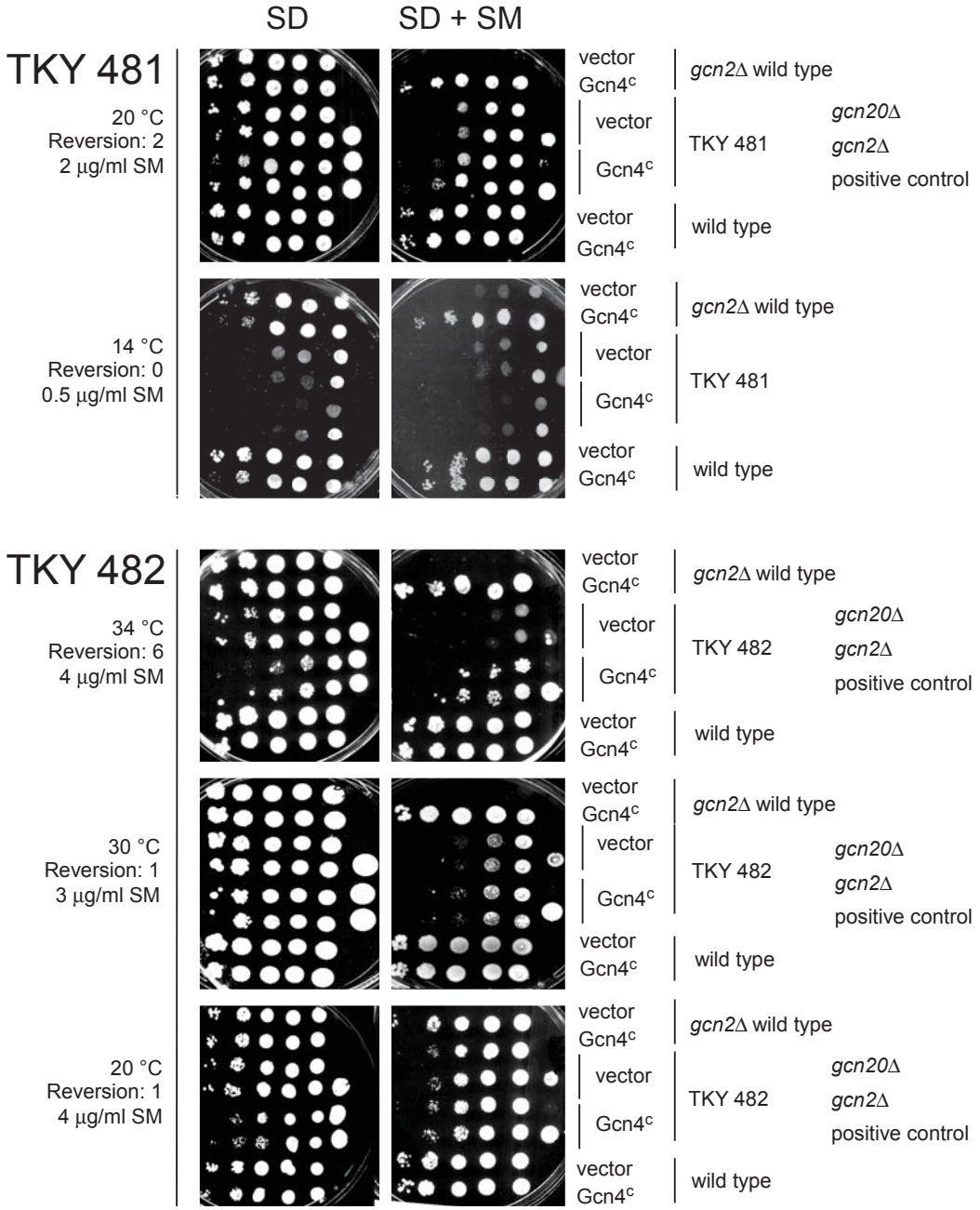

Figure B.6: Screen of actin mutant strains for sensitivity to SM when the transcription activator Gcn4 is constitutively expressed continued. The semi-quantitative growth assay was performed as described in the introduction to this appendix.

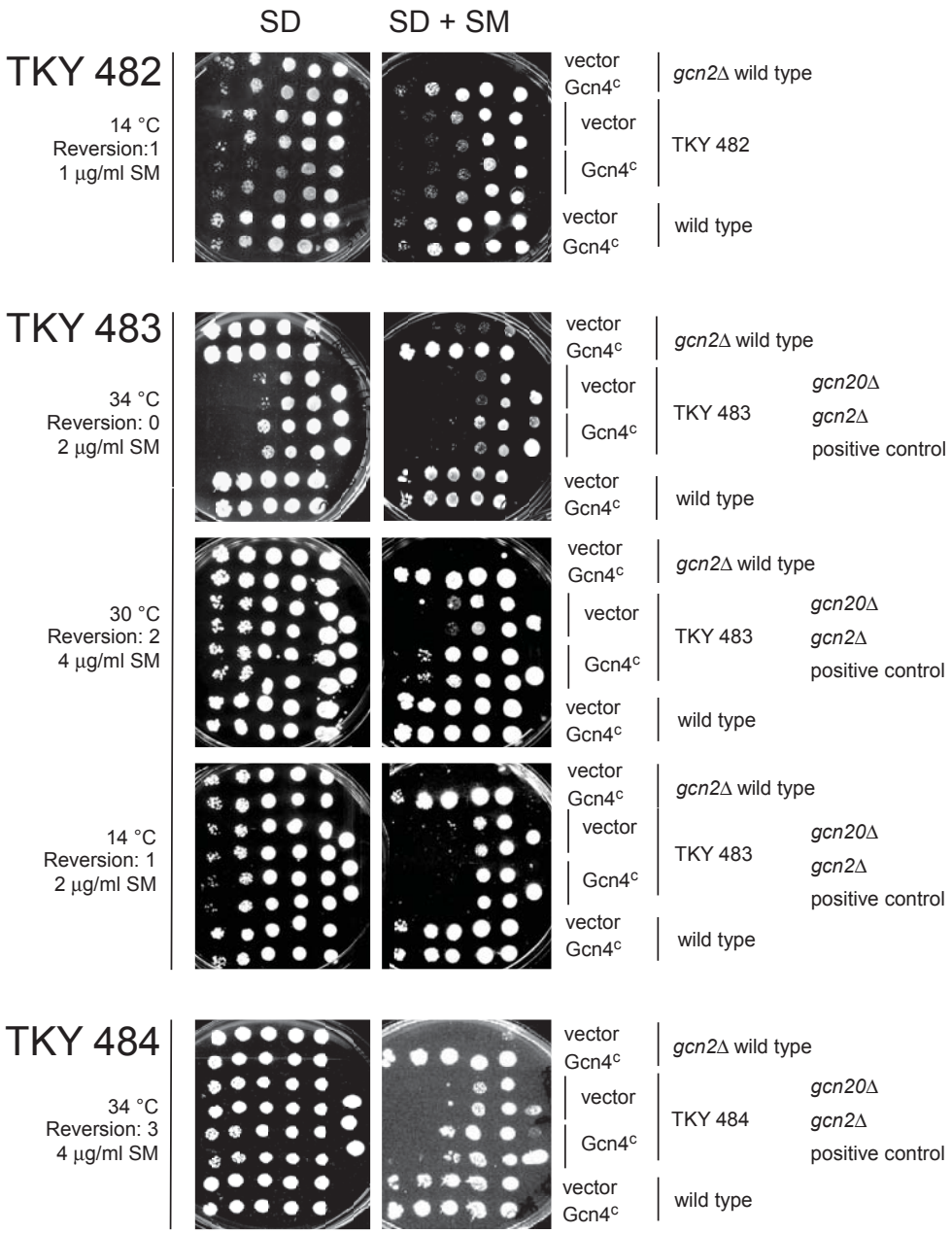

Figure B.7: Screen of actin mutant strains for sensitivity to SM when the transcription activator Gcn4 is constitutively expressed continued. The semi-quantitative growth assay was performed as described in the introduction to this appendix.

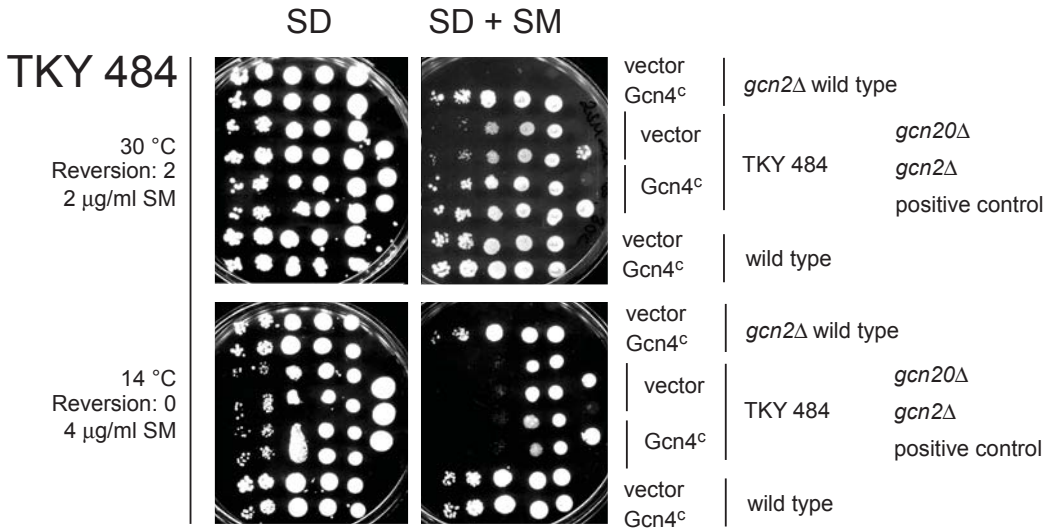

Figure B.8: Screen of actin mutant strains for sensitivity to SM when the transcription activator Gcn4 is constitutively expressed continued. The semi-quantitative growth assay was performed as described in the introduction to this appendix.

C

Results of the *in vivo* interaction assays

The results of all *in vivo* interaction assays with GST-Yih1 fragment III and actin from actin mutant strains are summarized in this appendix.

The individual results are structured as follows: (A) Transformants of wild type strain TKY 460 and actin mutant strains containing the galactose inducible genes *GST-YIH1*, nucleotide 202-1021 encoding Yih1 fragment III (on plasmid pES247-8) and *GST* (on plasmid pES128-9) were grown to exponential phase in minimal media containing galactose as carbon source. Whole cell extracts were prepared and aliquots with equal amounts of total protein were subjected to GST pulldown assays using glutathione sepharose beads. The precipitated complexes were separated by SDS-PAGE on a 4%-17% gradient gel and analyzed by Western blot analysis using antibodies against actin and GST. (B) The actin and GST signals were quantitated using the Multi Gauge V3.1 software (Fujifilm) or ImageJ (NIH) and the actin / GST signal ratio was calculated. The actin / GST ratio

of two independent colonies of each strain was averaged and the standard error was calculated.

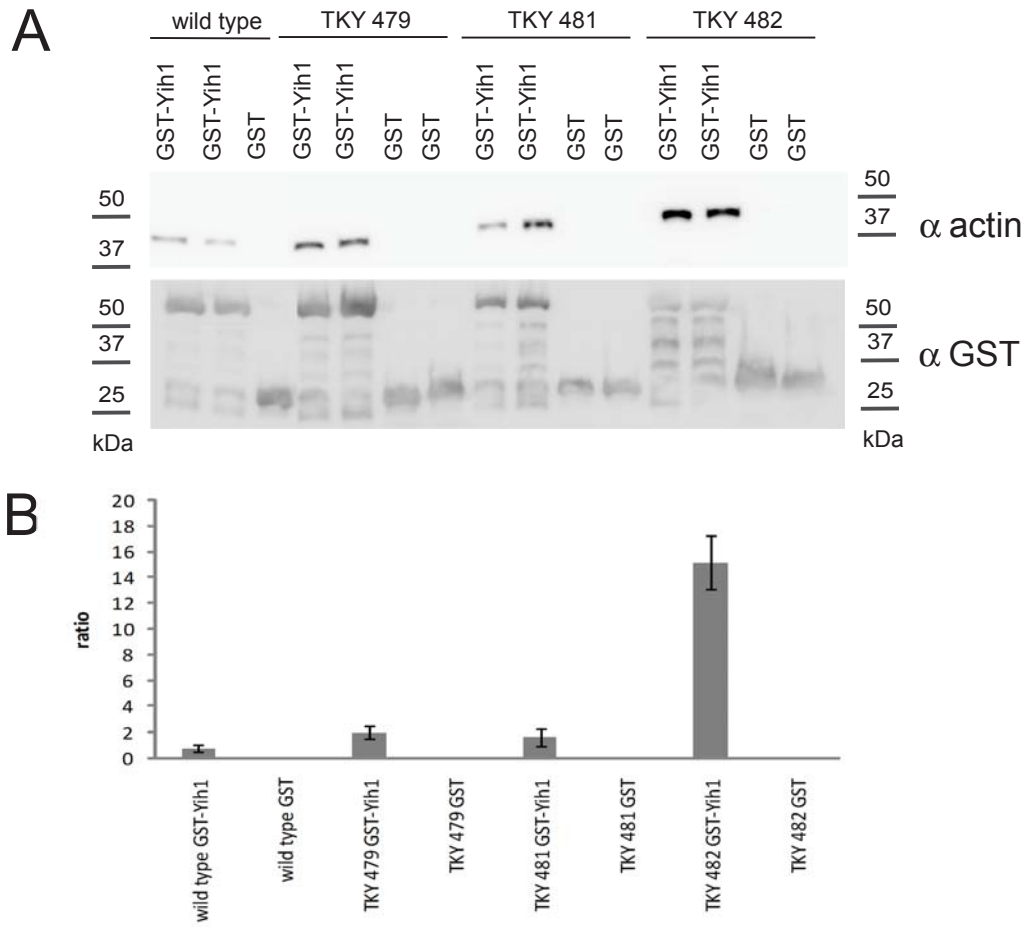

Figure C.1: *In vivo* interaction assay with GST-Yih1 fragment III and actin from actin mutant strains. The interaction assay and the analysis was performed as described in the introduction to this appendix.

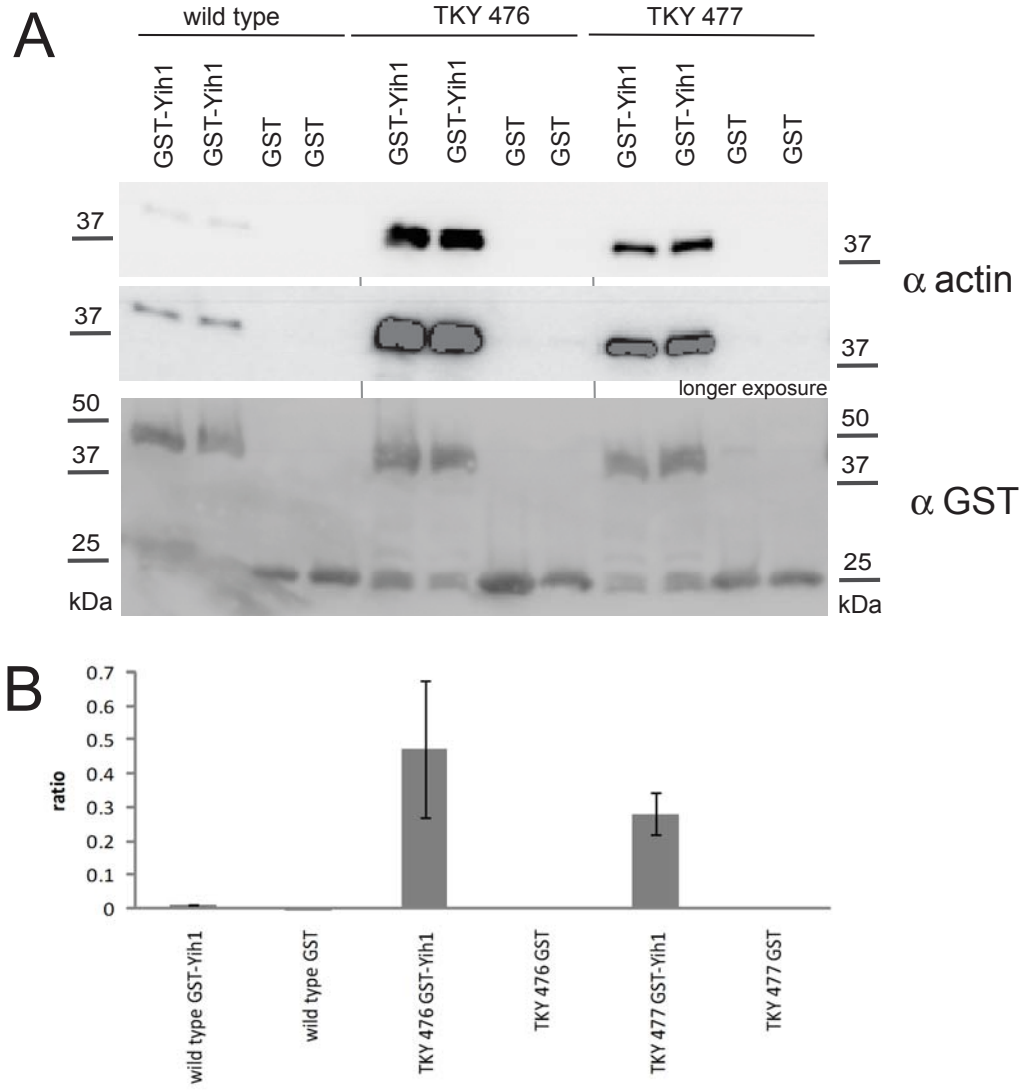

Figure C.2: *In vivo* interaction assay with GST-Yih1 fragment III and actin from actin mutant strains. The interaction assay and the analysis was performed as described in the introduction to this appendix.

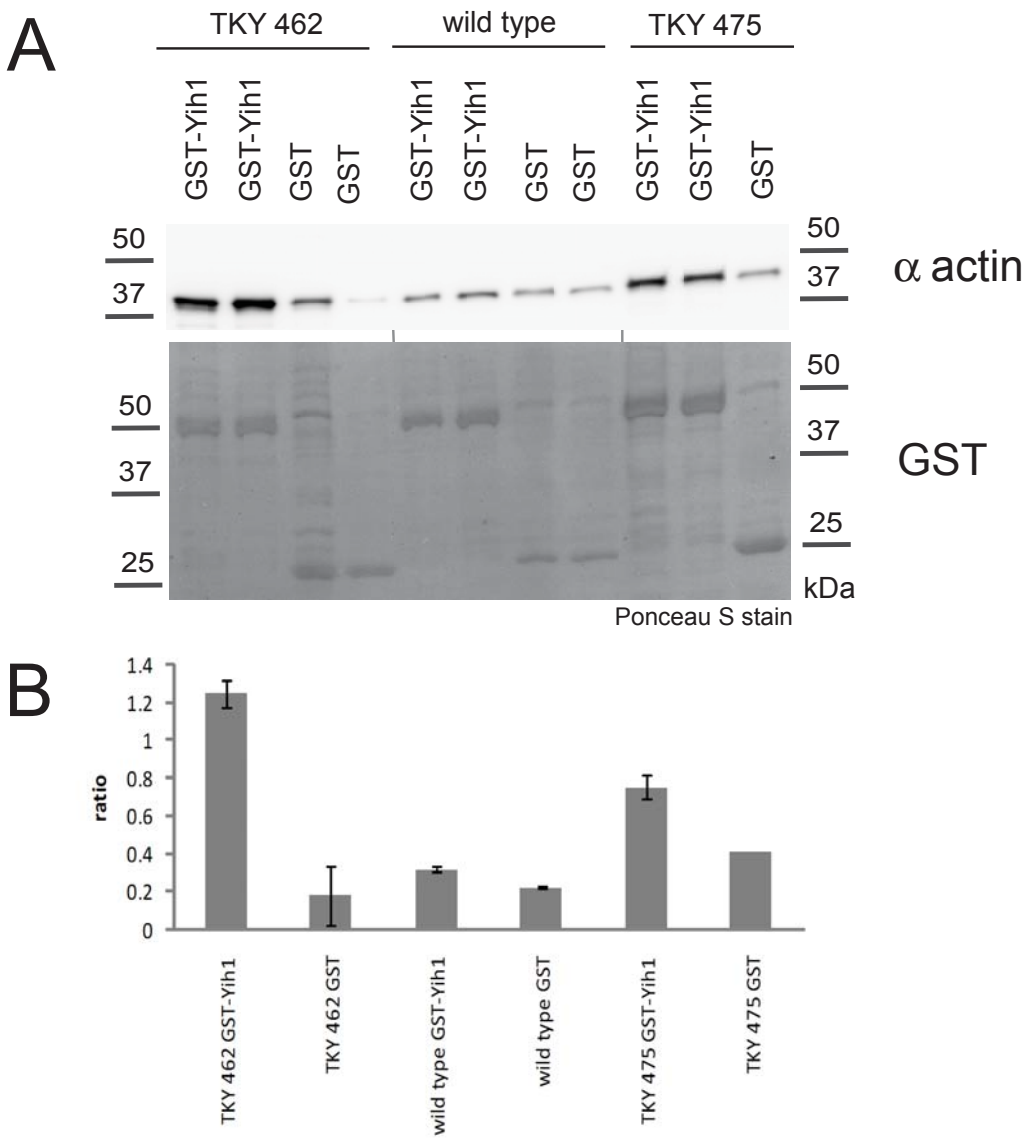

Figure C.3: *In vivo* interaction assay with GST-Yih1 fragment III and actin from actin mutant strains. The interaction assay and the analysis was performed as described in the introduction to this appendix.

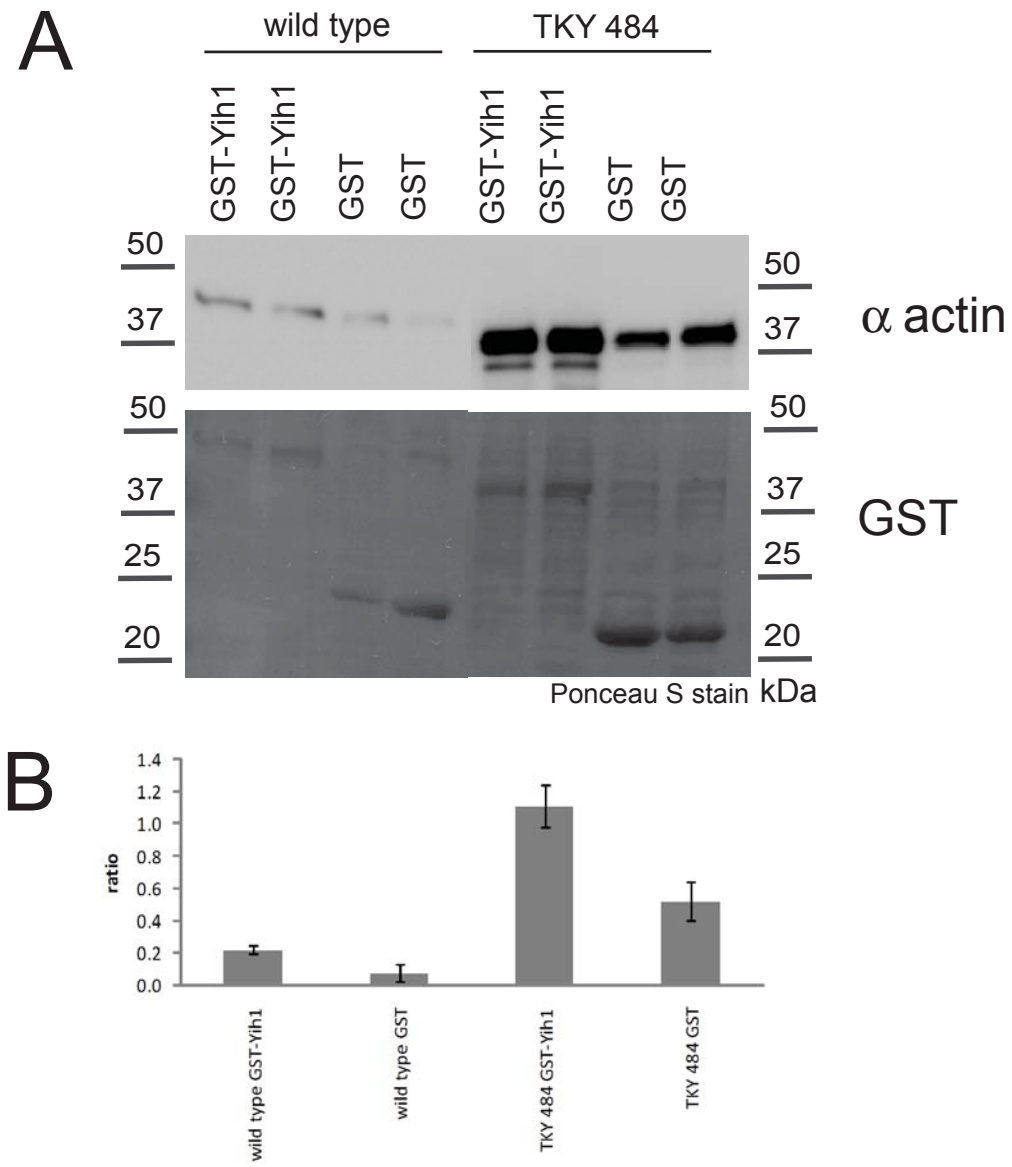

Figure C.4: *In vivo* interaction assay with GST-Yih1 fragment III and actin from actin mutant strains. The interaction assay and the analysis was performed as described in the introduction to this appendix.

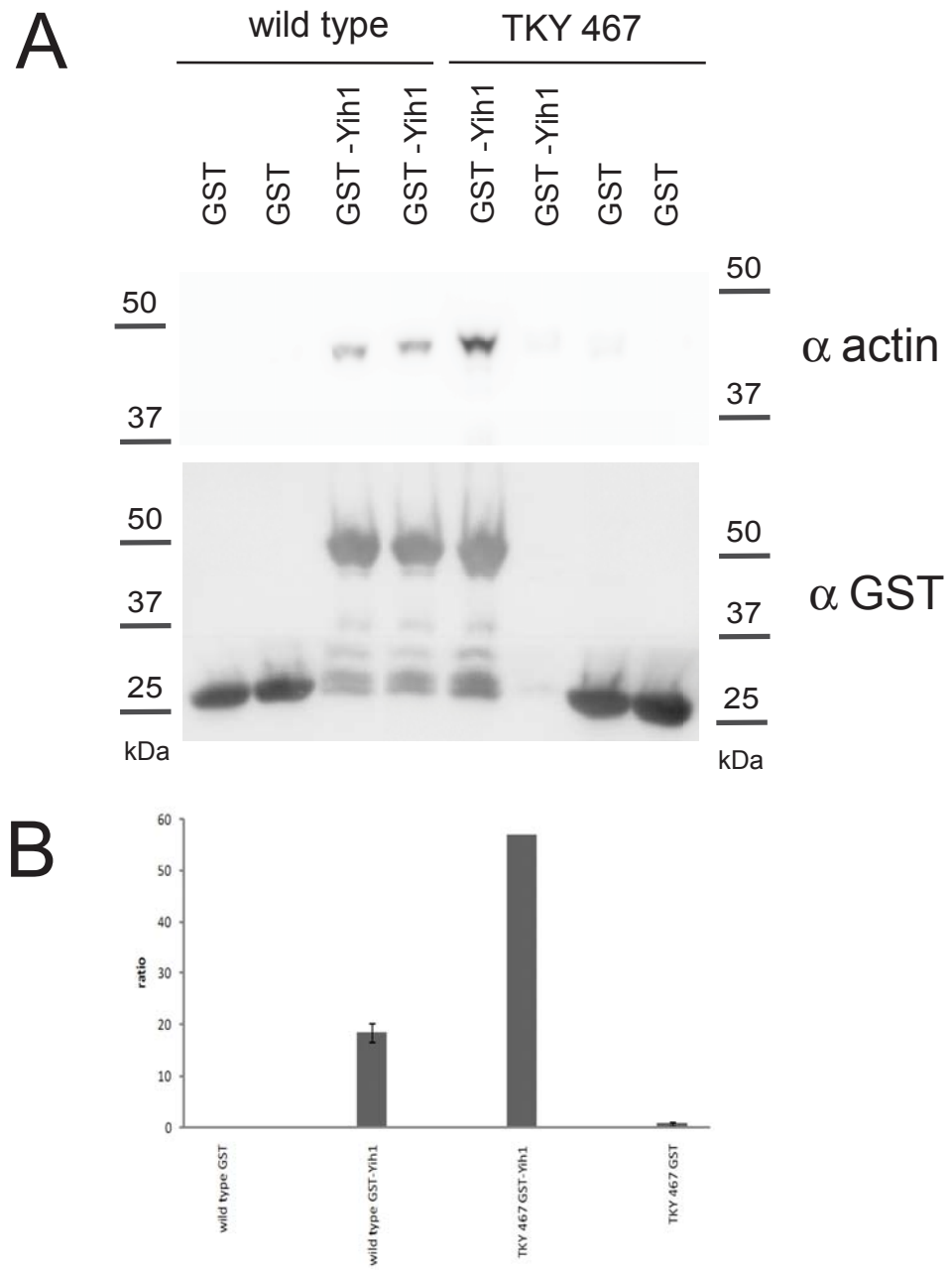

Figure C.5: *In vivo* interaction assay with GST-Yih1 fragment III and actin from actin mutant strains. The interaction assay and the analysis was performed as described in the introduction to this appendix.

D

Verification of the deletion of *YIH1*

The deletion of *YIH1* in actin mutant strains was verified both by PCR and Western blot analysis probing for Yih1.

PCR verification of the KanMX cassette insertion at the *YIH1* locus was performed using primer pairs ES 400-33 & ES 400-42 (see panel A. in figure D.1) and ES 400-30 & ES 400-41 (see panel B. in figure D.1). As a negative control, a sample not containing any DNA was used. 5 µl of the resulting PCR products (550 bp) were resolved on a 1% agarose gel, stained with EtBr and visualized in a transilluminator. 5 µl of a λ HindIII DNA marker or a 100 bp DNA marker were used as indicated.

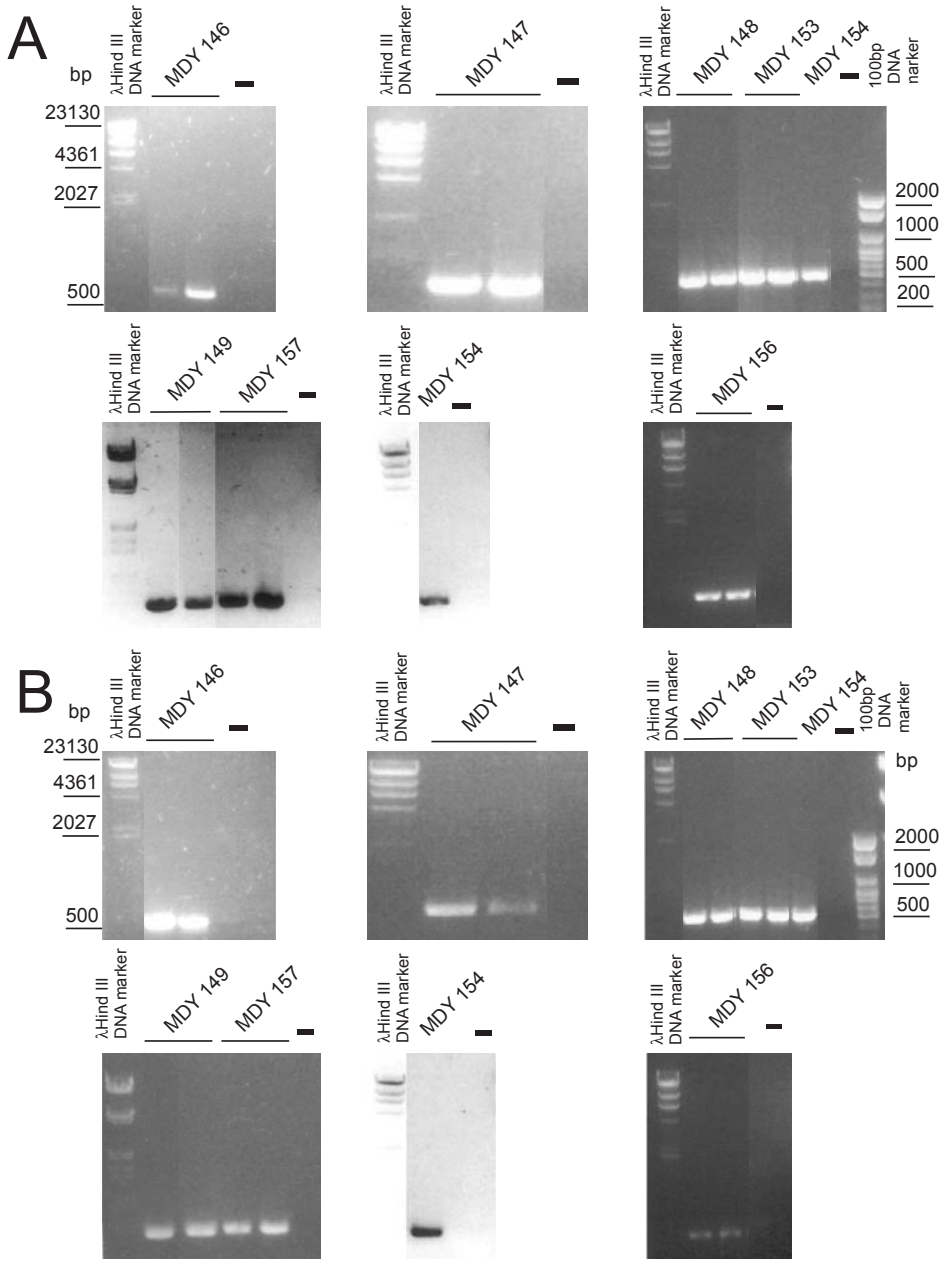

Figure D.1: Verification of the deletion of *YIH1* in actin mutant strains by PCR. The PCR was performed as described in the introduction to this appendix. - indicates the negative control.

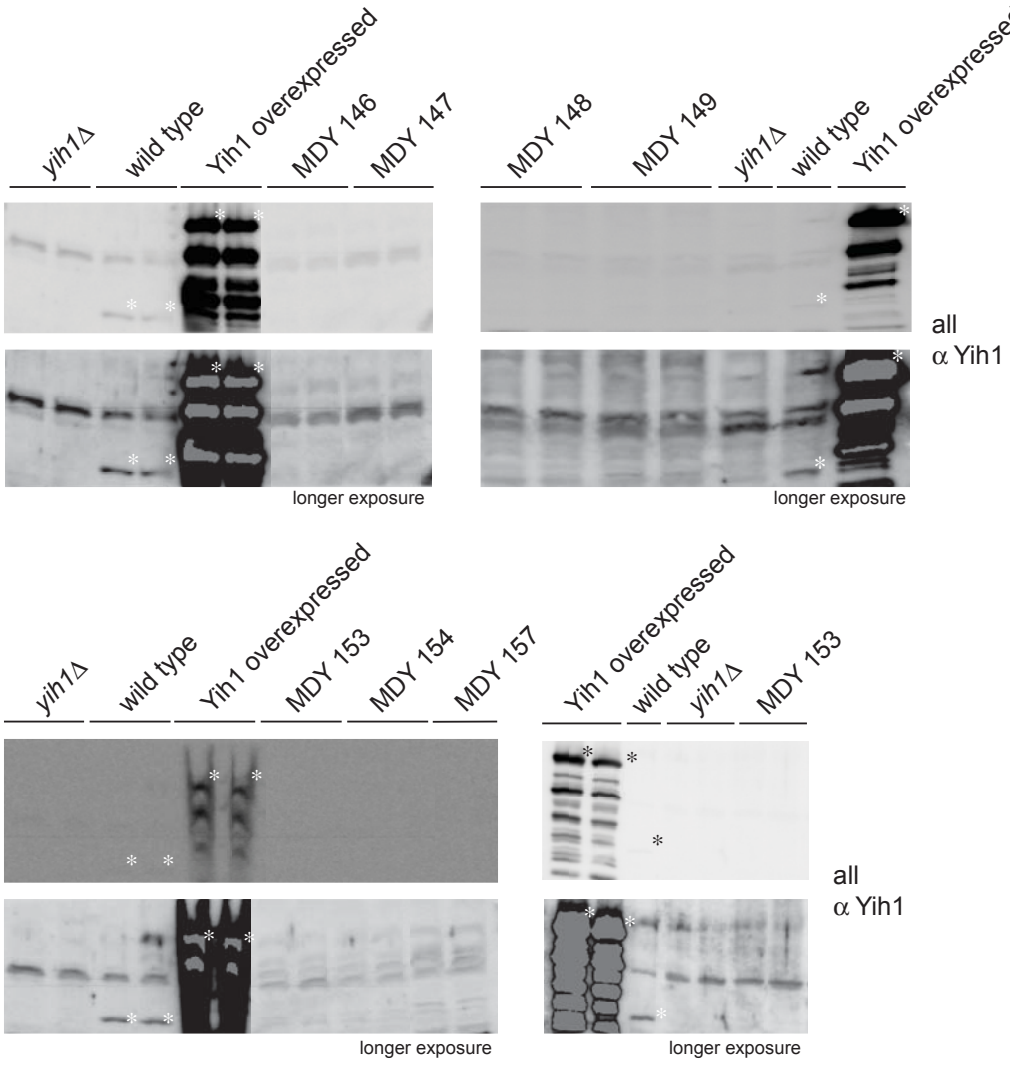

Figure D.2: Verification of the deletion of *YIH1* in actin mutant strains by Western blot analysis using antibodies against Yih1. Yeast strains MDY 146 (TKY 475 *yih1*Δ) , MDY 147 (TKY 477 *yih1*Δ), MDY 148 (TKY 478 *yih1*Δ), MDY 149 (TKY 479 *yih1*Δ), MDY 153 (TKY 484 *yih1*Δ), MDY 154 (TKY 476 *yih1*Δ), MDY 156 (TKY 467 *yih1*Δ), MDY 157 (TKY 462 *yih1*Δ), wild type strain (B4741, Research genetics background) and a strain overexpressing GST-Yih1 (ESY 10579, H2556 background) as a positive control and a *yih1*Δ strain (5780, research genetic background) as a negative control were grown to exponential phase in the appropriate media. Yeast whole cell extracts were prepared. 10 µg (GST-Yih1 overexpression strain) or 50 µg (all other strains) of total protein as determined by Bradford method were resolved in SDS-PAGE on a 4%-17% gradient gel and subjected to immunoblotting using antibodies against Yih1. The location of GST-Yih1 and Yih1 is indicated by an asterisk.

E

Results of the semi-quantitative growth assays of *yih1*△ actin mutant strains

The results of all semi-quantitative growth assays investigating *yih1*△ actin mutant strains for their sensitivity to sulfometuron methyl are summarized in this appendix.

The screen was carried out as described in the following. *yih1*△ actin mutant strains, undeleted actin mutant strains, wild type strain TKY 460 (positive control) and a *gcn2*△ strain in the TKY background (ESY 10447, negative control) were grown to saturation. Saturated overnight cultures were subjected to 10 fold serial dilutions and 5 µl of undiluted culture and 5 µl of each dilution was transferred to solid SD media, solid SD media containing the amino acid analogue sulfometuron methyl as indicated and solid YPD media. Plates were incubated at 30℃ until colonies were visible.

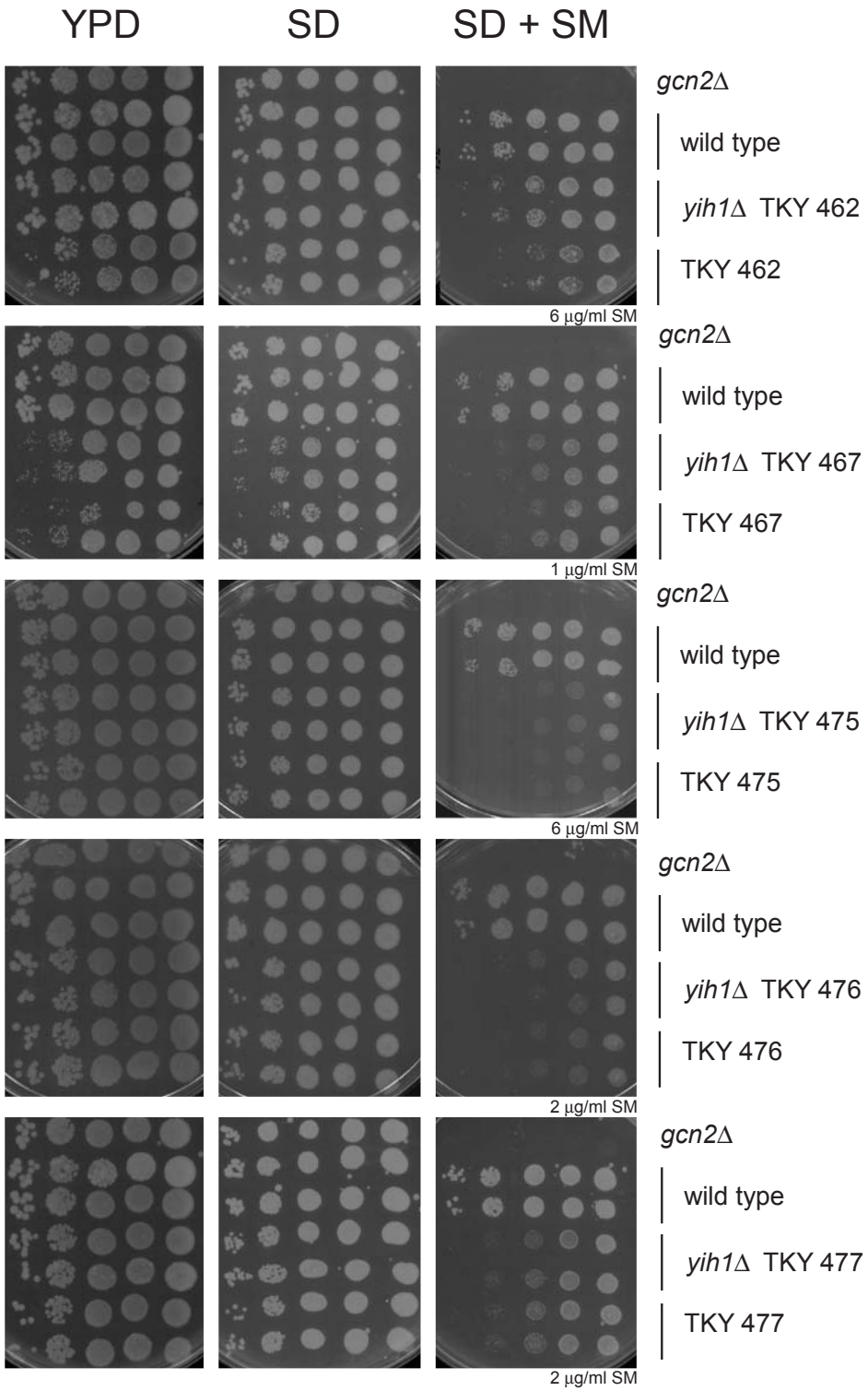

Figure E.1: Semi-quantitative growth assay of *yih1*Δ actin mutant strains under SM starvation conditions. The assay was performed as described in the introduction to this appendix.

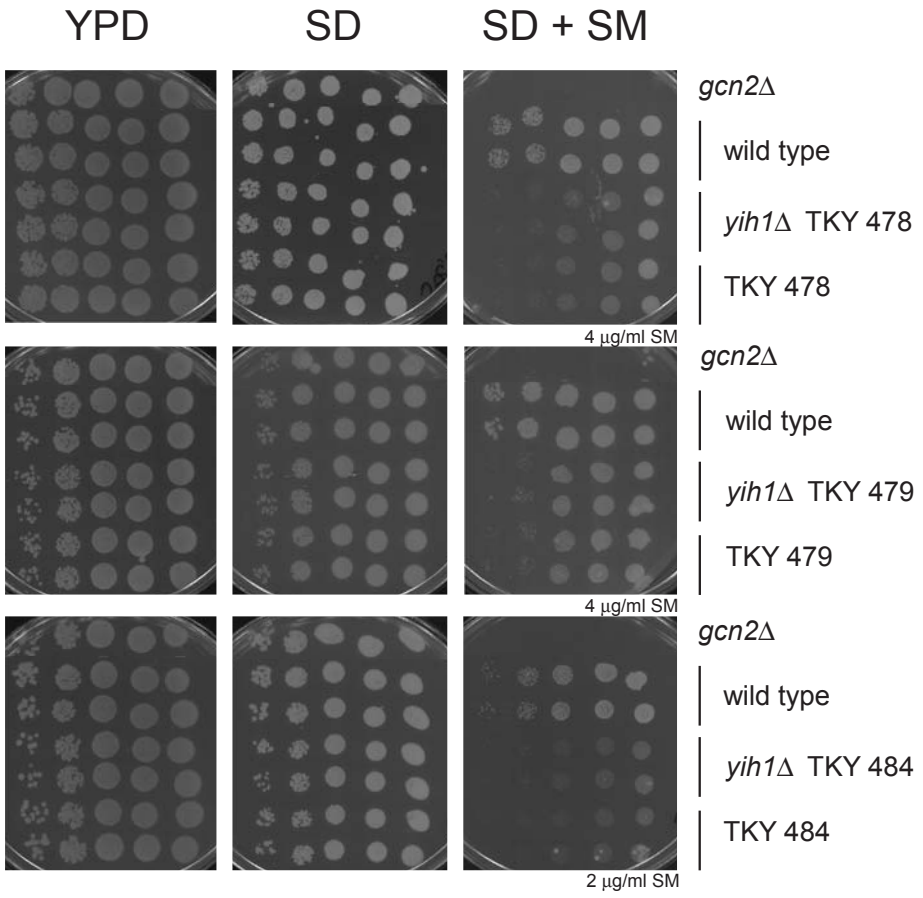

Figure E.2: Semi-quantitative growth assay of *yih1*Δ actin mutant strains under SM starvation conditions continued. The assay was performed as described in the introduction to this appendix.

F

Results of the *lacZ* assays

The results of all *lacZ* assays investigating actin mutant strains and isogenic *yih1*Δ actin mutant strains for the expression of the transcription activator Gcn4 are summarized in this appendix.

The expression of Gcn4 was assayed by monitoring the β-Galactosidase activity in actin mutant strains and isogenic *yih1*Δ actin mutant strains as indicated, wild type strain TKY 460 and a *gcn2*Δ TKY 460 strain. The ratio of the β-Galactosidase activity (starved versus unstarved conditions) was normalized to the activity of the wild type strains and the result of two independent experiments were averaged. The standard error is indicated.

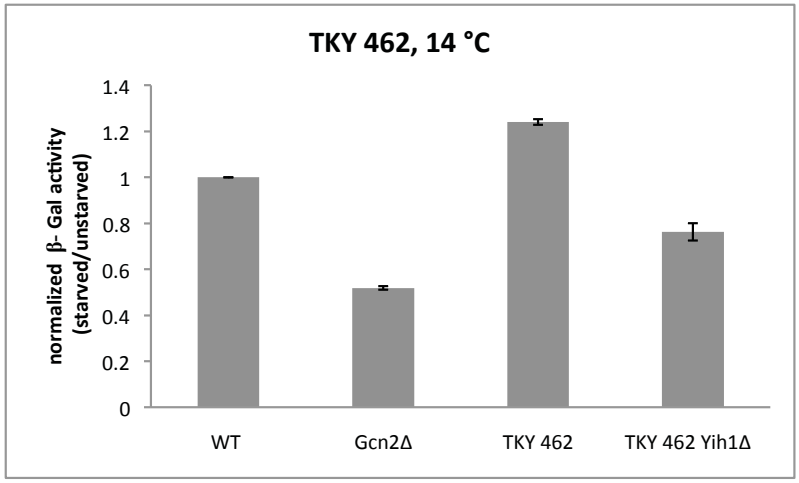

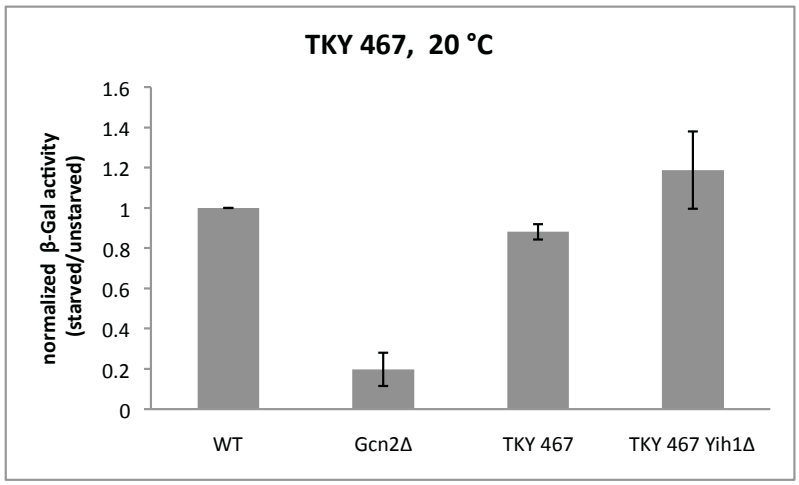

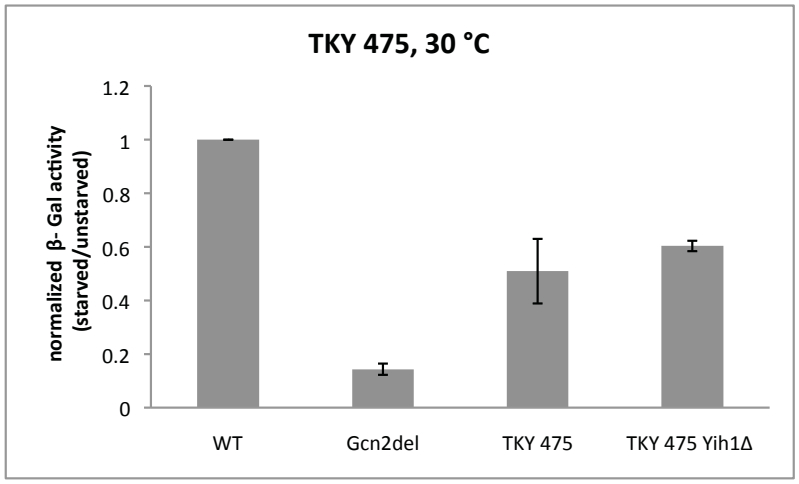

Figure F.1: Results of *lacZ* assays. The assay was performed as outlined in the introduction to this appendix.

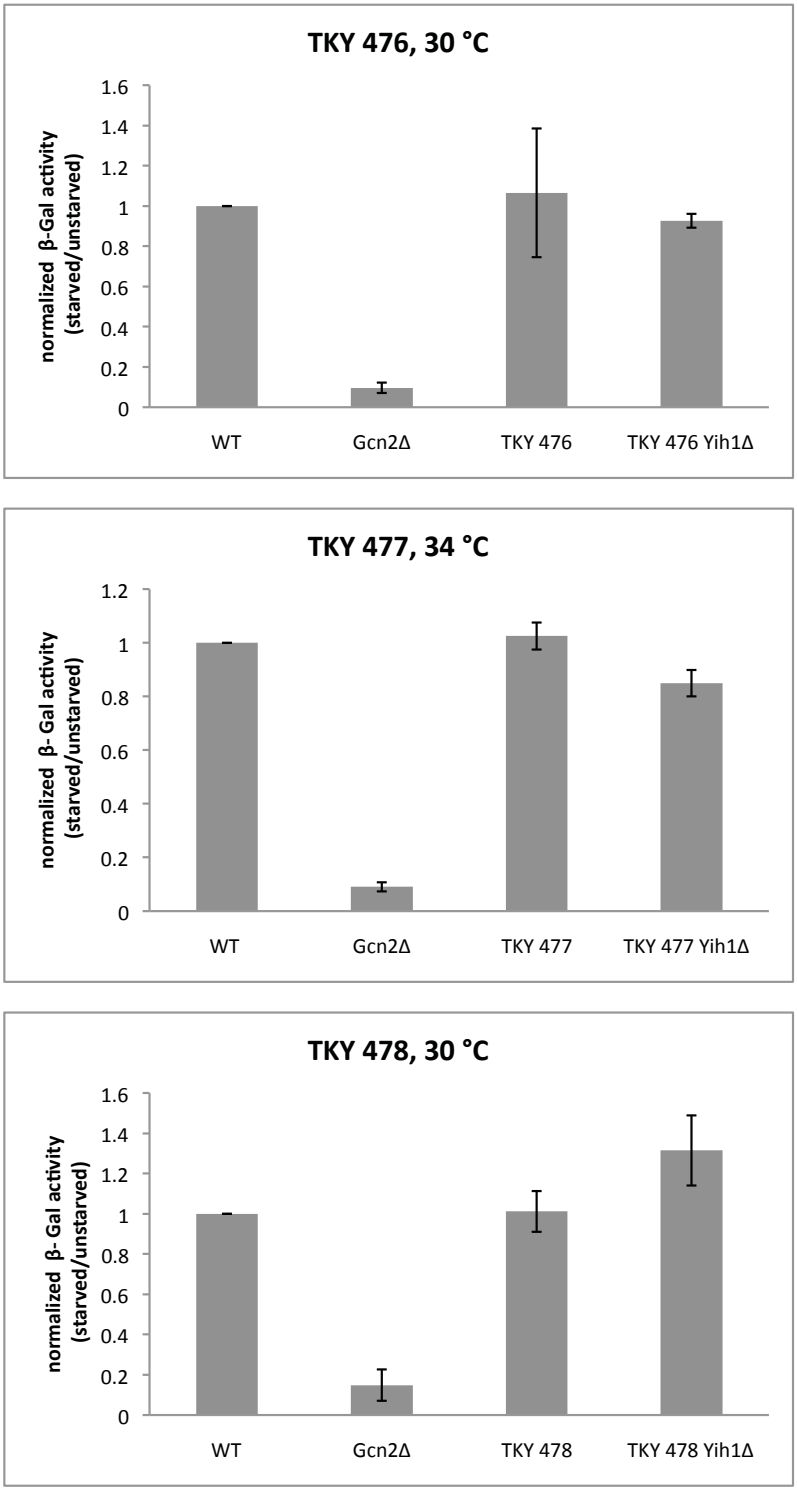

Figure F.2: Results of *lacZ* assays continued. The assay was performed as outlined in the introduction to this appendix.

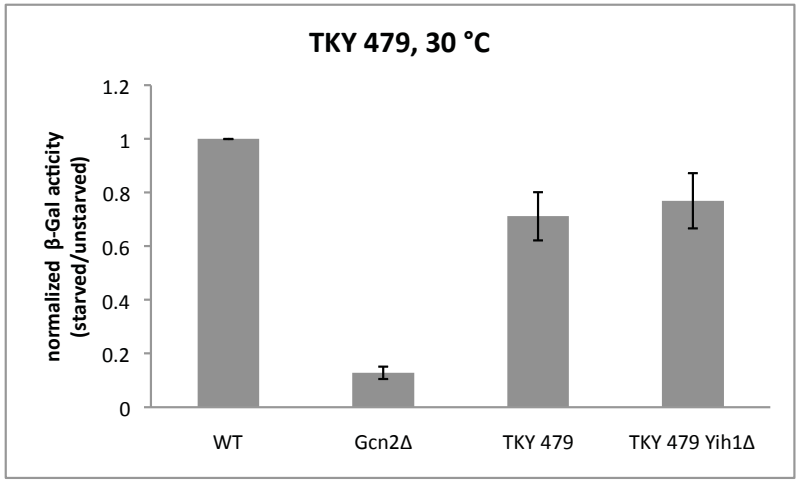

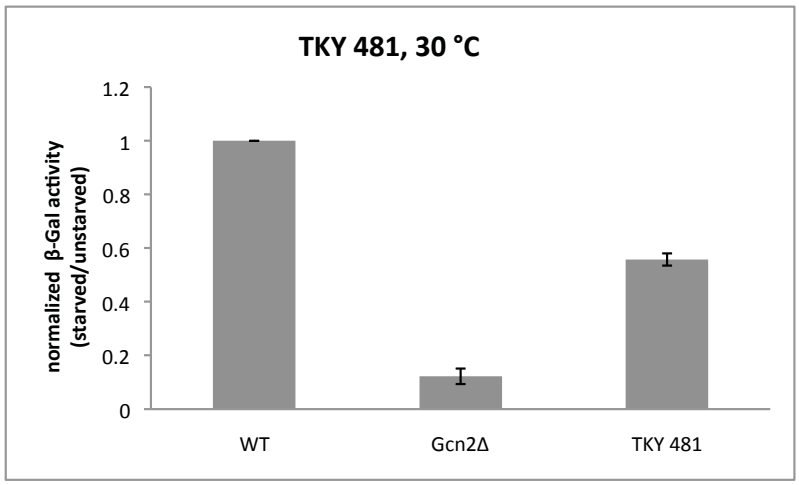

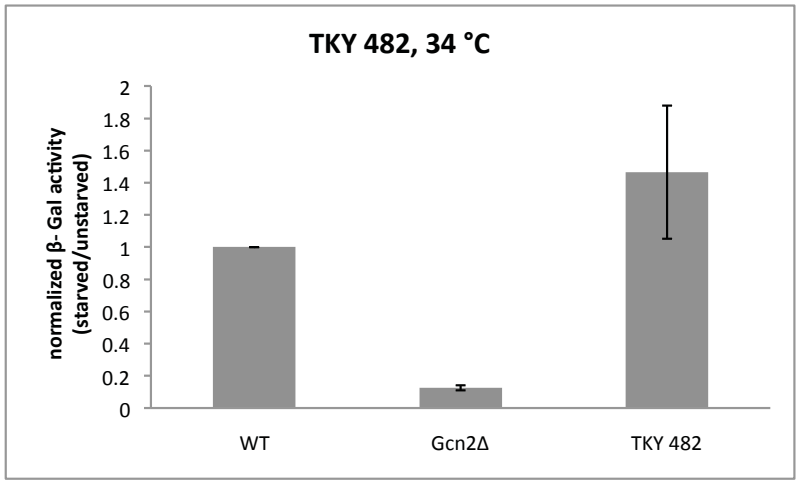

Figure F.3: Results of *lacZ* assays continued. The assay was performed as outlined in the introduction to this appendix.

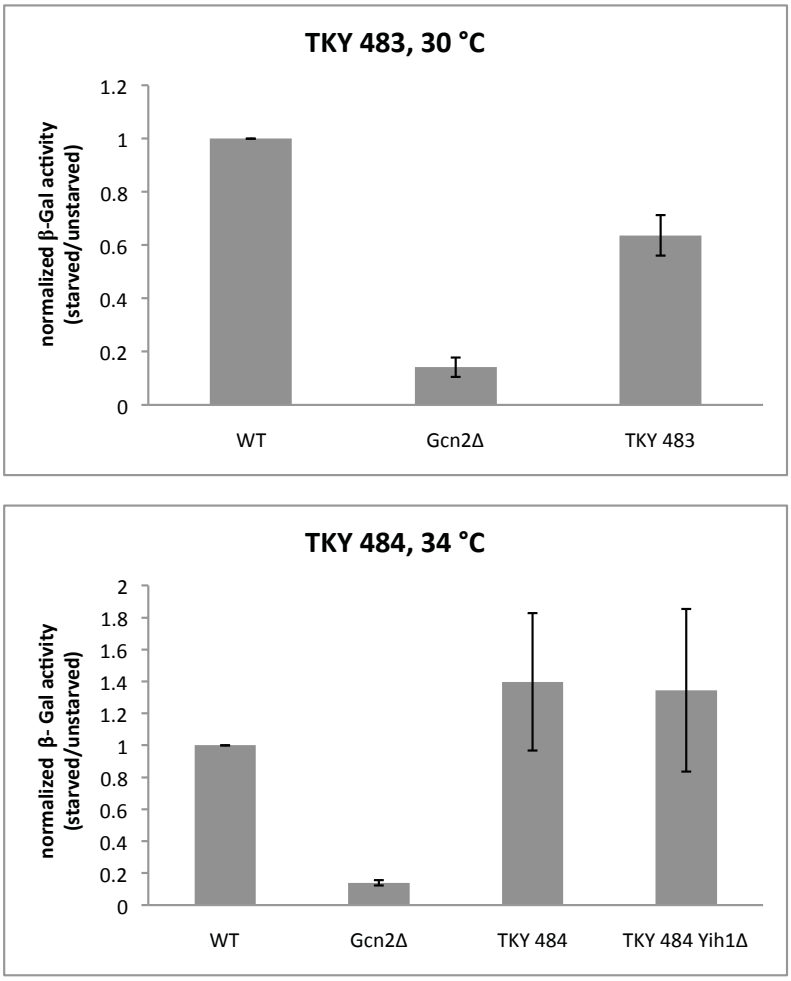

Figure F.4: Results of *lacZ* assays continued. The assay was performed as outlined in the introduction to this appendix.

G

Results of the *ACT1* complementation assays

All results of the *ACT1* complementation assays are summarized in this appendix.

Actin mutant strains as indicated, wild type strain TKY 460 and a *gcn2*△ TKY 460 strain (negative control) harboring a plasmid expressing native actin (pMJS1) and a vector control (YCplac33) were grown to saturation. Saturated overnight cultures were subjected to 10 fold serial dilutions and 5 µl of undiluted culture and 5 µl of each dilution was transfered to both solid SD medium containing the amino acid analogue sulfometuron methyl as indicated and solid SD media not containing any starvation drug. 5 µl of undiluted culture of the *gcn2*△ TKY 460 strains (negative control) were transfered onto the same plates. Plates were incubated at 30℃ until colonies were visible.

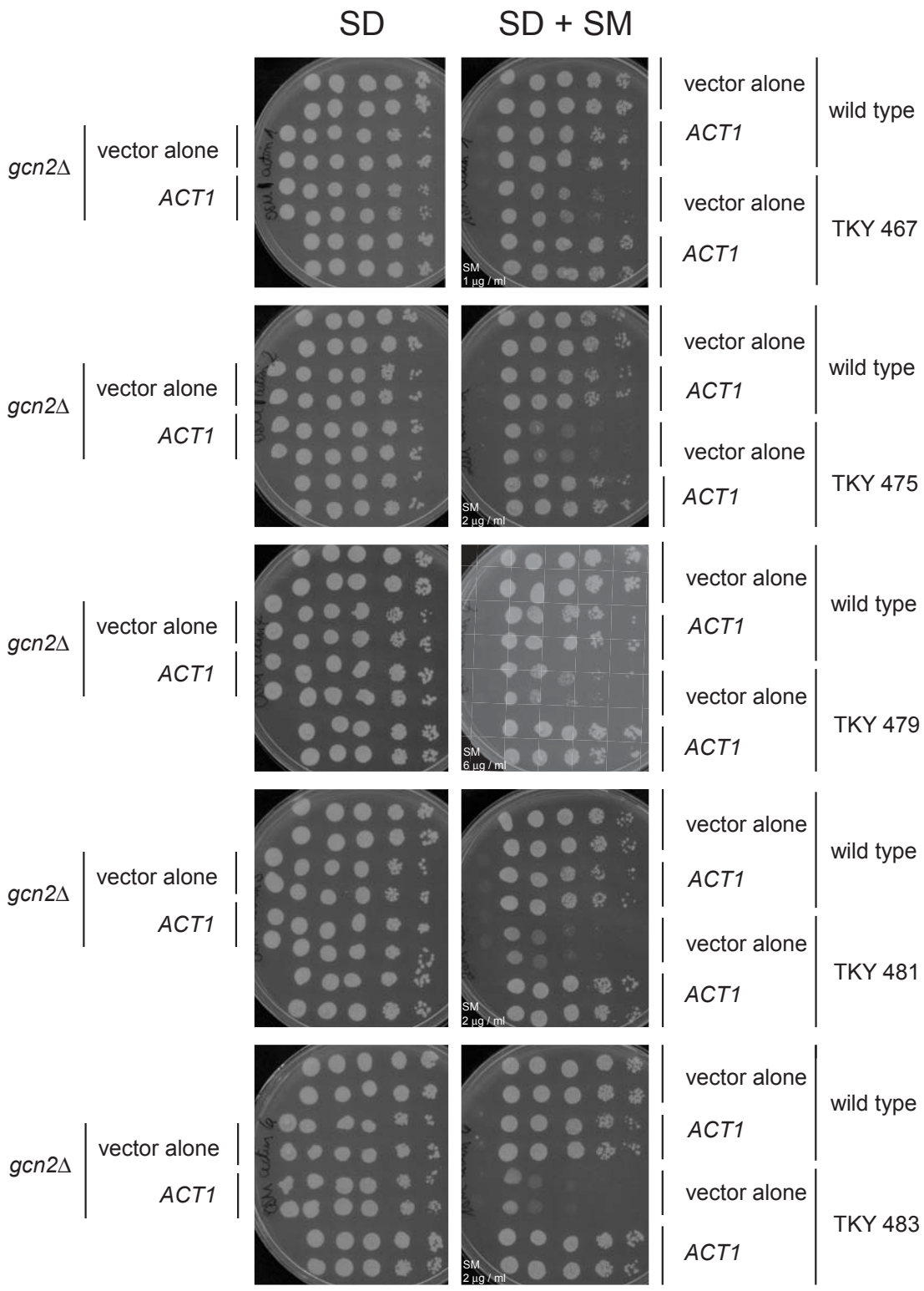

Figure G.1: Summary of the *ACT1* complementation assay. The semi-quantitative growth assays were performed as outlined in the introduction to this appendix.

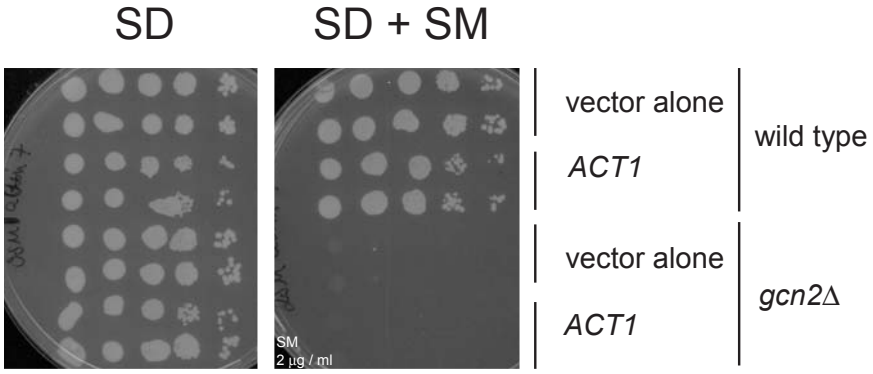

Figure G.2: Summary of the *ACT1* complementation assay continued. The semi-quantitative growth assays were performed as outlined in the introduction to this appendix.

H

Verification of the yeast-2-hybrid plasmids

All three yeast-2-hybrid plasmids constructed in this study were verified by sequencing. The sequencing results are summarized in this appendix.

```
CLUSTAL 2.0.11 multiple sequence alignment

In              CATATGGCCATGGAGGCCCCGGGGATCCACTTCTTTGGCTAAGCGCGATCTCTACGATAC 60
ES2001          ------------------------------------------------------------

In              CAAGTACCTTCAGCATTTGTTCCAGGAAGTGATGGACTCTGTTTTCCACCGCGGATCTGT 120
ES2001          ------------------------------------------------------------

In              CTGTCTATTTGACTTCCTCACAGAACTCGACGGTGTCTTGTACGTTGAACCAGAGGAGGA 180
ES2001          ----------------------------ACGGTGTCTTGTACGTTGAACCAGAGGAGGA 31
                                             ********************************

In              GACAGAACCGGTCCAGCAGAGTGACATTCCCACAGACCCCTTCGAGGGCTGGACCGCGTC 240
ES2001          GACAGAACCGGTCCAGCAGAGTGACATTCCCACAGACCCCTTCGAGGGCTGGACCGCGTC 91
                ************************************************************

In              GGACCCCATTACTGATAGAGGCTCGACTTTCATGGCCTTTGCAGCACATGTTACCTCCGA 300
ES2001          GGACCCCATTACTGATAGAGGCTCGACTTTCATGGCCTTTGCAGCACATGTTACCTCCGA 151
                ************************************************************

In              GGAACAAGCGTTTGCCATGCTAGACCTACTGAAGACCGACTAATCATTAGTCGAGAGATC 360
ES2001          GGAACAAGCGTTTGCCATGCTAGACCTACTGAAGACCGACTAATCATTAGTCGAGAGATC 211
                ************************************************************

CLUSTAL W (1.81) multiple sequence alignment

In              ----------------------------CATATGGCCATGGAGGCCCCGGGGATCCATGGT
rev400-49       GTTCCAGATTACGCTAGCTTGGGTGGTCATATGGCCATGGAGGCCCCGGGGATCCATGGT
                                             ********************************

In              GGTGGTACTTCTTTGGCTAAGCGCGATCTCTACGATACCAAGTACCTTCAGCATTTGTTC
rev400-49       GGTGGTACTTCTTTGGCTAAGCGCGATCTCTACGATACCAAGTACCTTCAGCATTTGTTC
                ************************************************************

In              CAGGAAGTGATGGACTCTGTTTTCCACCGCGGATCTGTCTGTCTATTTGACTTCCTCACA
rev400-49       CAGGAAGTGATGGACTCTGTTTTCCACCGCGGATCTGTCTGTCTATTTGACTTCCTCACA
                ************************************************************

In              GAACTCGACGGTGTCTTGTACGTTGAACCAGAGGAGGAGACAGAACCGGTCCAGCAGAGT
rev400-49       GAACTCGACGGTGTCTTGTACGTTGAACCAGAGGAGGAGACAGAACCGGTCCAGCAGAGT
                ************************************************************

In              GACATTCCCACAGACCCCTTCGAGGGCTGGACCGCGTCGGACCCCATTACTGATAGAGGC
rev400-49       GACATTCCCACAGACCCCTTCGAGGGCTGGACCGCGTCGGACCCCATTACTGATAGAGGC
                ************************************************************

In              TCGACTTTCATGGCCTTTGCAGCACATGTTACCTCCGAGGAACAAGCGTTTGCCATGCTA
rev400-49       TCGACTTTCATGGCCTTTGCAGCACATG------------------------------
                ****************************

In              GACCTACTGAAGACCGACTAATCATTAGTCGAGAGATCT
rev400-49       ---------------------------------------
```

YIH1 fragment

Figure H.1: Verification of plasmid pMD02a by sequencing. The *in situ* sequence encoding Yih1 fragment IV contained in plasmid pMD02a (labeled In and highlighted in grey) is aligned with the sequencing result of plasmid pMD02a using primers ES2001 and ES400-49. The multiple alignment was performed using Clustalw.

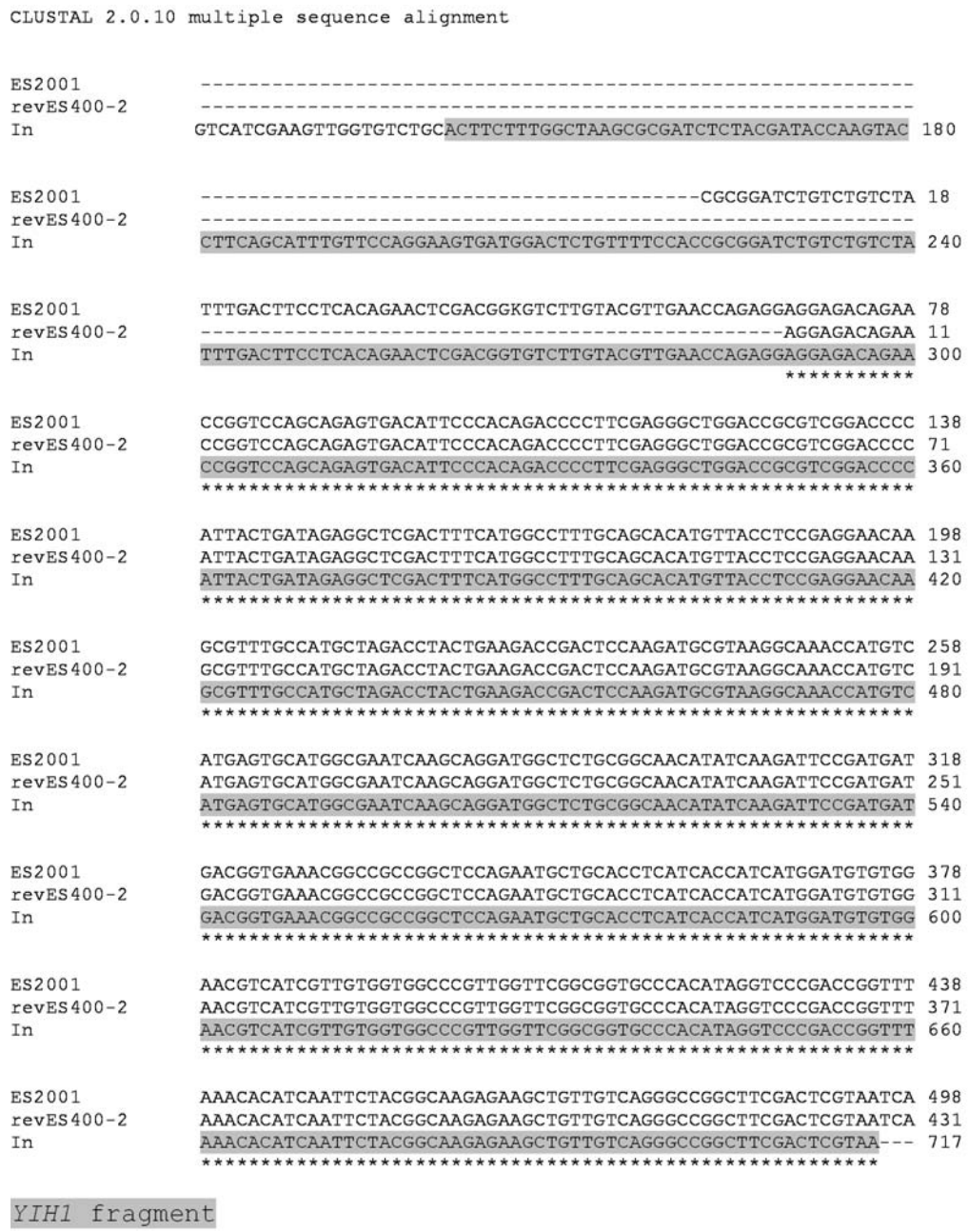

Figure H.2: Verification of plasmid pMD03a by sequencing. The *in situ* sequence encoding Yih1 fragment III contained in plasmid pMD03a (labeled In and highlighted in grey) is aligned with the sequencing result of plasmid pMD03a using primers ES2001 and ES400-2. The multiple alignment was performed using Clustalw.

```
CLUSTAL 2.0.10 multiple sequence alignment

In              GTCATCGAAGTTGGTGTCTGCACTTCTTTGGCTAAGCGCGATCTCTACGATACCAAGTAC 240
revES400-49     ----------------------ACTTCTTTGGCTAAGCGCGATCTCTACGATACCAAGTAC 39
                                       ************************************

In              CTTCAGCATTTGTTCCAGGAAGTGATGGACTCTGTTTTCCACCGCGGATCTGTCTGTCTA 300
revES400-49     CTTCAGCATTTGTTCCAGGAAGTGATGGACTCTGTTTTCCACCGCGGATCTGTCTGTCTA 99
                ************************************************************

In              TTTGACTTCCTCACAGAACTCGACGGTGTCTTGTACGTTGAACCAGAGGAGGAGACAGAA 360
revES400-49     TTTGACTTCCTCACAGAACTCGACGGTGTCTTGTACGTTGAACCAGAGGAGGAGACAGAA 159
                ************************************************************

In              CCGGTCCAGCAGAGTGACATTCCCACAGACCCCTTCGAGGGCTGGACCGCGTCGGACCCC 420
revES400-49     CCGGTCCAGCAGAGTGACATTCCCACAGACCCCTTCGAGGGCTGGACCGCGTCGGACCCC 219
                ************************************************************

In              ATTACTGATAGAGGCTCGACTTTCATGGCCTTTGCAGCACATGTTACCTCCGAGGAACAA 480
revES400-49     ATTACTGATAGAG---------------------------------------------- 232
                *************

In              GCGTTTGCCATGCTAGACCTACTGAAGACCGACTCCAAGATGCGTAAGGCAAACCATGTC 540
revES400-49     ------------------------------------------------------------

YCR059C         ATGAGTGCATGGCGAATCAAGCAGGATGGCTCTGCGGCAACATATCAAGATTCCGATGAT 600
revES400-49     ------------------------------------------------------------

YCR059C         GACGGTGAAACGGCCGCCGGCTCCAGAATGCTGCACCTCATCACCATCATGGATGTGTGG 660
revES400-49     ------------------------------------------------------------

YCR059C         AACGTCATCGTTGTGGTGGCCCGTTGGTTCGGCGGTGCCCACATAGGTCCCGACCGGTTT 720
revES400-49     ------------------------------------------------------------

YCR059C         AAACACATCAATTCTACGGCAAGAGAAGCTGTTGTCAGGGCCGGCTTCGACTCGTAA 777
revES400-49     ------------------------------------------------------------
```

YIH1 fragment

Figure H.3: Verification of plasmid pMD03a by sequencing continued. The *in situ* sequence encoding Yih1 fragment III contained in plasmid pMD03a (labeled In and highlighted in grey) is aligned with the sequencing result of plasmid pMD03a using primer ES400-49. The multiple alignment was performed using Clustalw.

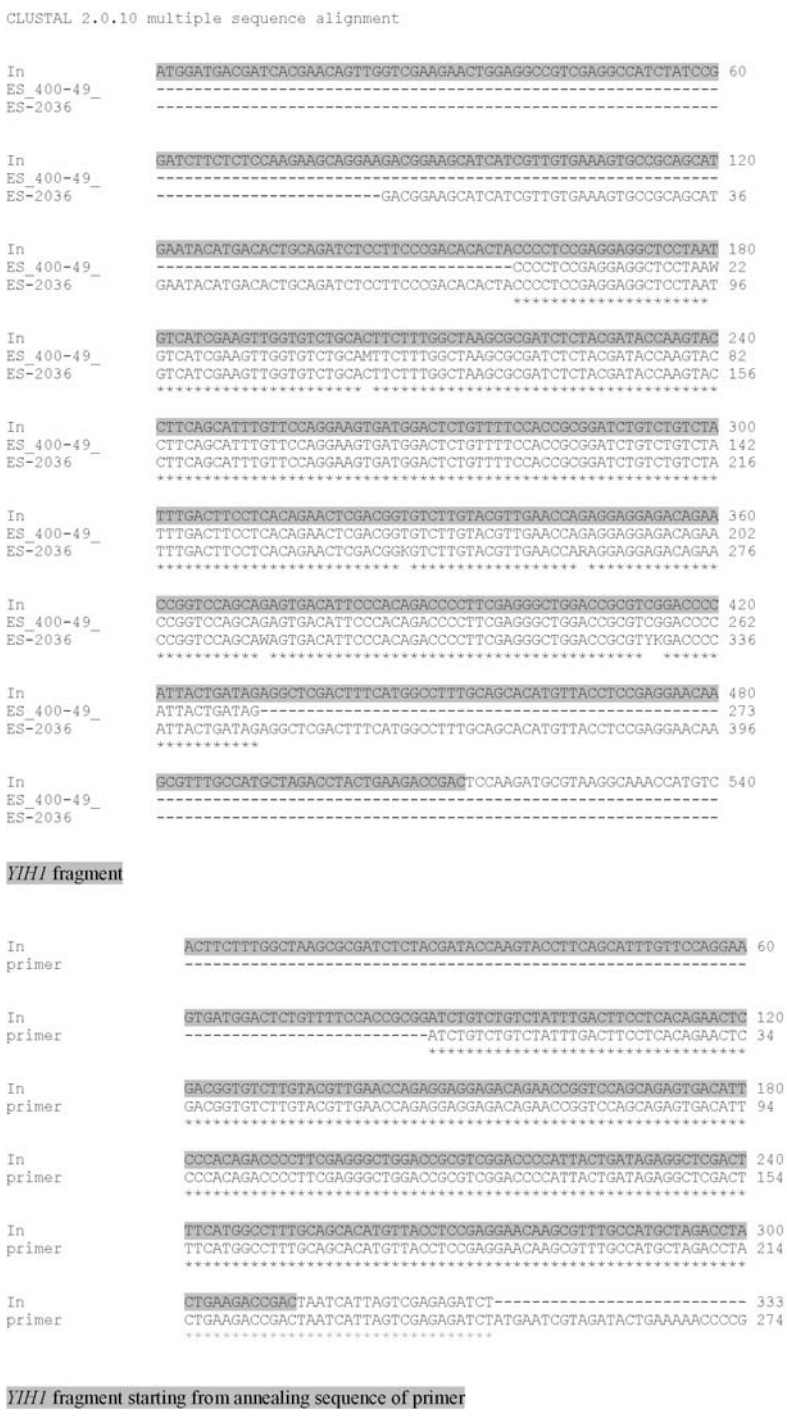

Figure H.4: Verification of plasmid pMD06a by sequencing. The *in situ* sequence encoding Yih1 fragment II contained in plasmid pMD06a (labeled In and highlighted in grey) is aligned with the sequencing result of plasmid pMD06a using primers ES2036 and ES400-49. The multiple alignment was performed using Clustalw.

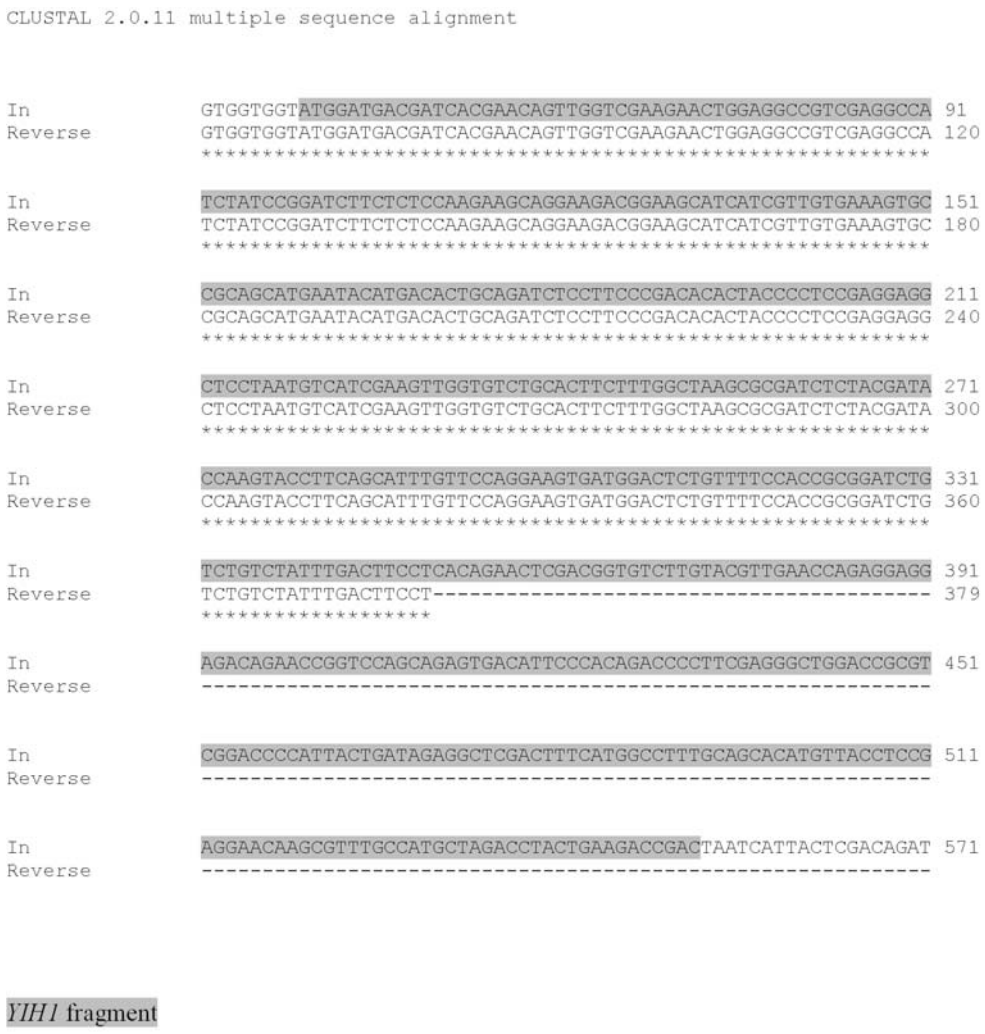

Figure H.5: Verification of plasmid pMD06a by sequencing continued. The *in situ* sequence encoding Yih1 fragment II contained in plasmid pMD06a (labeled In and highlighted in grey) is aligned with the sequencing result of plasmid pMD06a using primers ES2011 and ES400-47. The multiple alignment was performed using Clustalw.

Results of mapping the Cdc28 binding site in Yih1

The individual results of all *in vivo* interaction assays used to map the Cdc28 binding site in Yih1 are summarized in this appendix.

The interaction assay was performed as outlined. *gcn1*Δ yeast strains overexpressing three different Yih1 fragments, full length Yih1 and GST alone under a galactose-inducible promoter were grown to exponential phase in medium containing galactose as the only carbon source. Yeast whole cell extracts were prepared and equal amounts of total protein were then subjected to a GST pulldown assay. The precipitates and aliquots of the whole cell extracts were then subjected to SDS-PAGE and to a subsequent Western blot analysis probing for Cdc28 and GST. The location of the GST-tagged proteins are indicated with an asterisk. The signal intensity of the Cdc28 blots were determined using the Fujifilm Multi Gauge software (panel A). The quantification of the Cdc28 signal is depicted in (B). The Cdc28 signals were normalized to the Cdc28 signal in the GST alone sample.

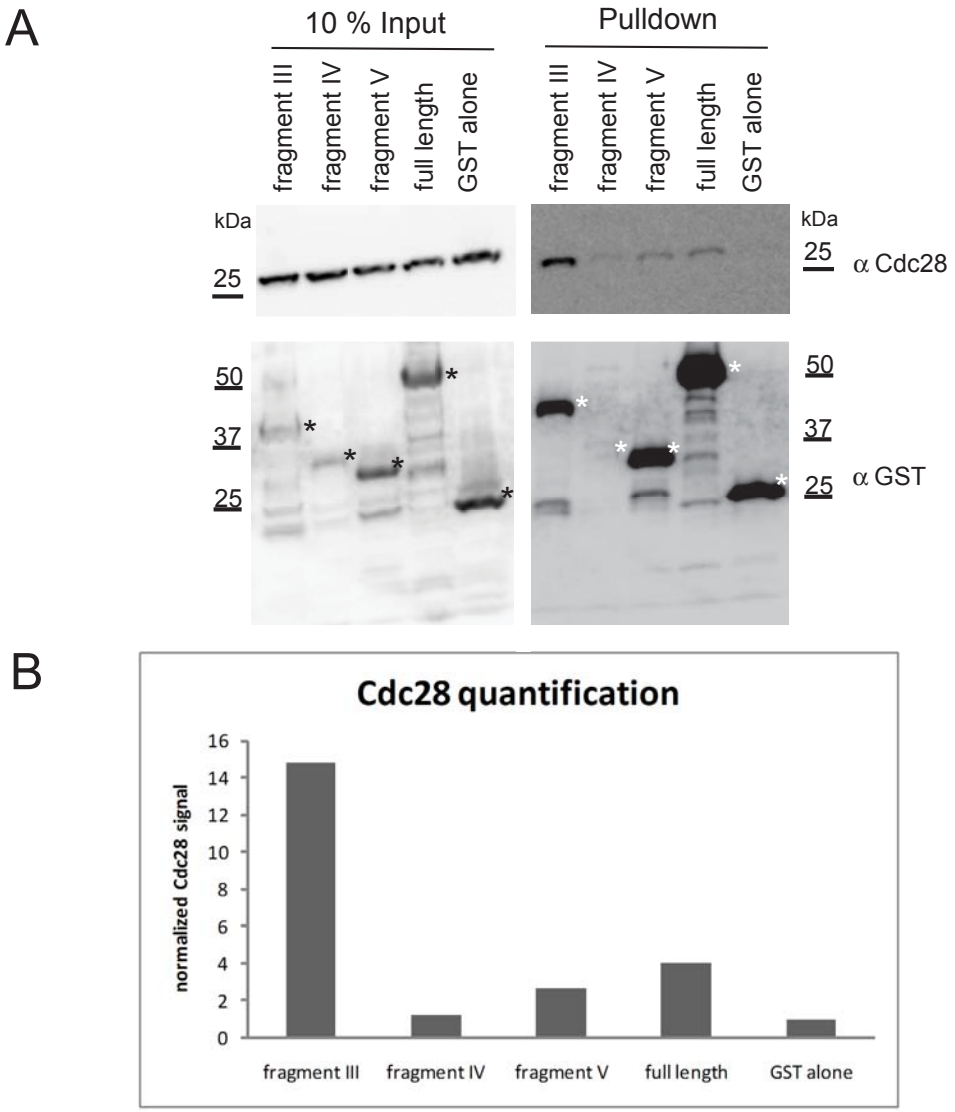

Figure I.1: Mapping of the Cdc28 binding site in Yih1. The GST pulldown assay (A) and the subsequent quantification (B) were performed as outlined in the introduction to this appendix. The location of the GST-tagged proteins are indicated with an asterisk.

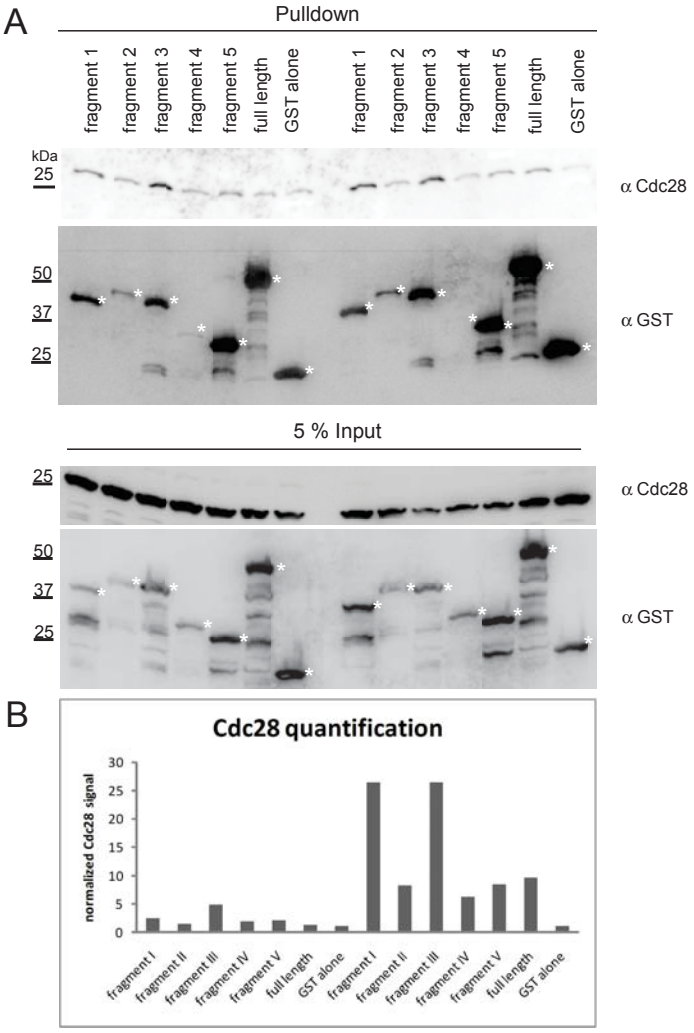

Figure I.2: Mapping of the Cdc28 binding site in Yih1 continued. The GST pulldown assay (A) and the subsequent quantification (B) were performed as outlined in the introduction to this appendix. The location of the GST-tagged proteins are indicated with an asterisk.

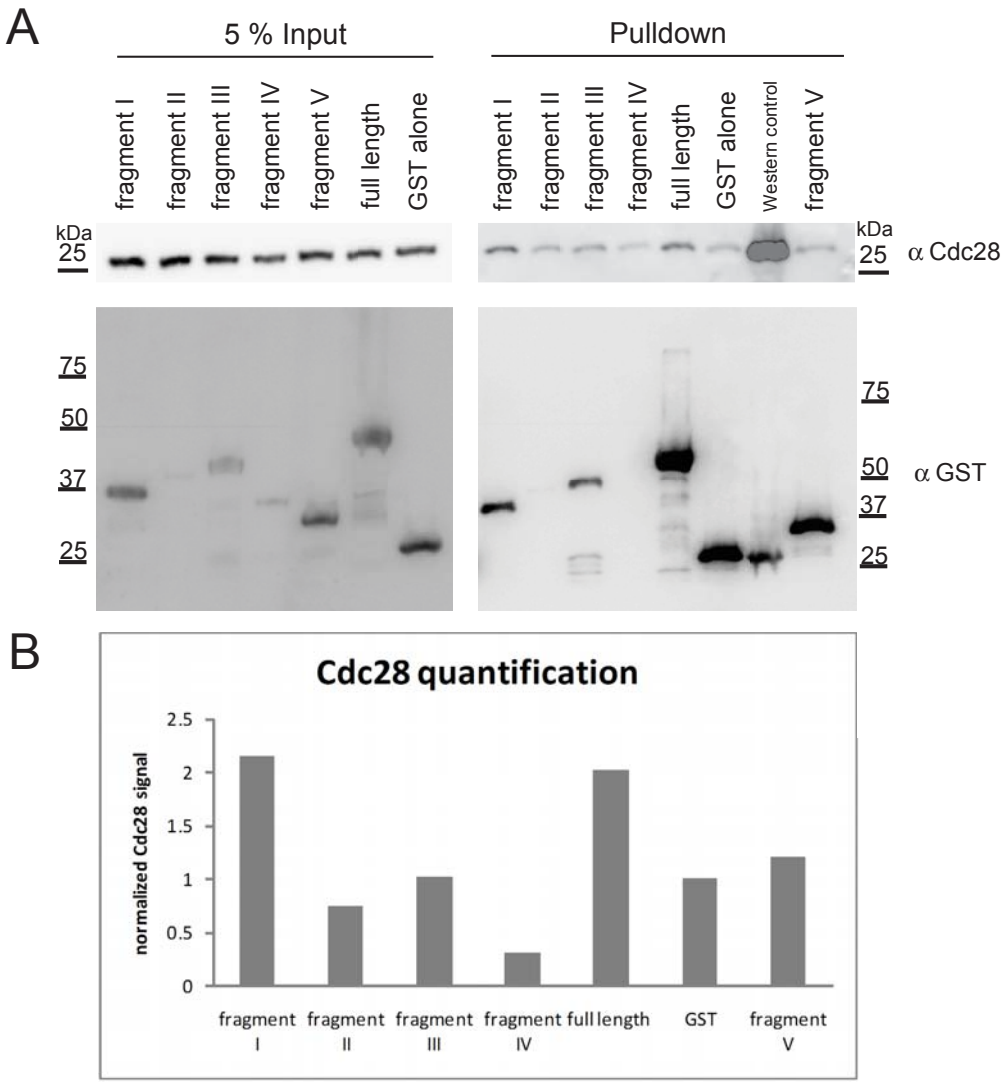

Figure I.3: Mapping of the Cdc28 binding site in Yih1 continued. The GST pulldown assay (A) and the subsequent quantification (B) were performed as outlined in the introduction to this appendix.

J

Nature protocol exchange publication

The following publication was published with contributions of M. Dautel in Nature protocol exchange [126].

PROTOCOL EXCHANGE | COMMUNITY CONTRIBUTED

Generating highly concentrated yeast whole cell extract using low-cost equipment.

Jyothsna Visweswaraiah,

Martina Dautel

& **Evelyn Sattlegger**

Sattlegger Lab

Abstract

This protocol describes a cost effective method for generating highly concentrated yeast whole cell extracts (WCE) at concentrations of 50 µg protein/µl or 0.3 A_{260nm}/µl. Highly concentrated extracts are used for many applications such as protein purification, purification of protein complexes (in particular when interactions are weak), protein-protein interaction studies, and velocity sedimentation studies. Normally highly concentrated extracts are generated with homogenizers or the French press. However, such equipment 1) is expensive, 2) is not available to every researcher, and/or 3) often cannot be used for cells from small culture volumes. The procedure described here can be used for breaking cells originating from cultures as small as 100 ml, although a culture volume of at least 200 ml gives the best result. Furthermore, this method is also effective for breaking formaldehyde crosslinked

cells.

Subject terms: Biochemistry; Microbiology; Isolation, Purification and Separation

Keywords: Saccharomyces cerevisiae; highly concentrated whole cell extract; efficient cell breakage; efficient cell lysis

Reagents

Reagents

• Breaking buffer. The composition depends on the experiment planned after cell breakage. For protein-protein interaction assays we used 30 mM HEPES, pH 7.4, 50 mM KCl, 10 % Glycerol [1]. For velocity sedimentation assays we used 20 mM TrisHCl, pH 7.5, 50 mM KCl, 10 mM $MgCl_2$ [2].
• Breaking buffer with protease inhibitors. Add inhibitors as required for your particular application. For example, we used 1 complete tablet without EDTA (Roche) per 50 ml breaking buffer, 1 mM phenylmethylsylfonyl fluoride, 0.1 mg/ml pepstatin, 1 mM dithiothreitol or 2-mercaptoethanol.
• Yeast cell pellets, obtained from a culture grown to A_{600nm}=1 or less, washed with ice cold water or breaking buffer. Pellet may be fresh or stored at -20°C or -80°C.
• If required, reagents to determine protein concentration (here we used the Bradford method).

Material

• Round base tubes, 13 ml, 16×100mm, polypropylene, (Sarstedt, order No 62.515.006), or round base tubes with similar diameter.
• 1.5 ml microfuge tubes.
• Acid washed and autoclaved glass beads, 0.5 mm diameter.
• Cuvettes for spectrophotometer.

Equipment

• Vortexer, optimally 3000 rpm. If more than 2 samples are being processed preferably use 2 vortexers. It is important that the vortexers have cup heads. Do not use platform heads.
• Microfuge centrifuge.
• Centrifuge that holds the above 13 ml round base tubes (e.g. Heraeus multifuge 1S-R). If not available transfer samples to microfuge tubes and use microfuge centrifuge instead.
• Spectrophotometer to determine protein concentration or to determine A_{260nm}.

Procedure

1. Cell pellets should be in round base tubes, no more than 0.8 g of wet weight cell pellet per tube (equivalent to a 300 ml yeast cell culture grown to A_{600nm}=1).
2. If cell pellet is frozen, thaw in a mixture of ice and water.
3. Dissolve pellet in 200 µl of ice cold breaking buffer with inhibitors.
4. Add 700 µl volume of acid washed glass beads.
5. Vortex sample at maximum speed for 30 sec. Important: See Figure 2 for the exact procedure. Efficient breakage is visible by the sample forming a whitish film and tiny bubbles on the inside wall of the tube (see Figure 1).
6. Place sample in a mixture of ice and water for 30 sec.

7. Repeat steps 5 and 6 seven more times.
Tip: If more than one sample needs to be processed the time spent for cell breakage can be shortened by vortexing 2 samples at a time on 2 vortexers for 30 sec. While these samples rest for 30 sec the next 2 samples can be vortexed.
8. Spin samples at 4°C for 3 min at low g (e.g. 2,500g). If a centrifuge for round base tubes is not available, transfer samples to microfuge tubes and spin in microfuge centrifuge at low speed.
9. Transfer supernatant to fresh microfuge tubes.
10. Spin in microfuge centrifuge at 4°C for 10 min at 10,000 rpm.
11. Transfer supernatants to fresh tubes.
Note: A highly concentrated WCE has an opaque appearance. A yellowish colour is due to pigments and does not necessarily indicate good breakage.
12. Depending on your subsequent application, determine the protein concentration e.g. via the Bradford method, or determine the A_{260nm}, using breaking buffer alone as reference.

Timing

Approximately 1 hour:
Thawing and preparation of cells – 15 min;
Cell breakage – 8 min for 4 samples if using 2 vortexers;
Centrifugations – 20 min.

Troubleshooting

Inefficient breakage:
a) Make sure cells were harvested in exponential phase.
b) Do not use more than 0.8 g of wet weight cell pellet per round base tube.
c) Use round base tubes of the indicated size.
d) Do not use more than 700 µl volume of glass beads of the correct size (0.5 mm diameter).

e) Make sure the tubes are being positioned on the vortexer as described in Figure 2, and the vortexers have cup heads.

Anticipated Results

The anticipated result is highly concentrated yeast whole cell extract. Expected are protein concentrations of 50 µg/µl or ribonucleotide concentrations of 0.3 A_{260nm}/µl.

References

[1] E. Sattlegger, Barbosa, JARG, Moraes, MCS, Martins, RM, Hinnebusch, AG, and Castilho BA, Gcn1 and actin binding to Yih1: Implications for activation of the eIF2 kinase Gcn2. Journal of Biological Chemistry (in press).

[2] E. Sattlegger, and A.G. Hinnebusch, Polyribosome binding by GCN1 is required for full activation of eukaryotic translation initiation factor 2 alpha kinase GCN2 during amino acid starvation. J Biol Chem 280 (2005) 16514-21.

Figures

Figure 1: Photographs of samples before and after cell breakage.

Download Figure 1

Photographs of samples before and after cell breakage.

After efficient cell breakage tiny air bubbles (smaller than the 0.5 mm glass beads) and a thin white layer of cell debris coat the inside wall of the round base tube.

Figure 2.: Illustration of round base tubes rotating on vortex cup heads.

Download Figure 2.

Illustration of round base tubes rotating on vortex cup heads.

A Holding the tube on the cup head very gently allows maximum movement of the tube. This results into maximum movement of the sample and glass beads in the tube (indicated in red). **B** Pressing the tube onto the cup head restricts movement of the tube. This results in the sample and the glass beads racing around only at the bottom of the tube instead of further up in the tube (indicated in red).

Associated Publications

This protocol is related to the following articles:

- **Gcn1 and actin binding to Yih1: Implications for activation of the eIF2 kinase Gcn2**

  See other protocols related to this article

Author information

Affiliations

. **Sattlegger Lab, Institute of Natural Sciences, Massey University, Auckland, New Zealand**

Jyothsna Visweswaraiah, Martina Dautel & Evelyn Sattlegger

Competing financial interests

The authors declare no competing financial interest.

Corresponding author

Correspondence to: Evelyn Sattlegger
(e.sattlegger@massey.ac.nz)

Readers' Comments

Comments on this thread are vetted after posting.

- *Protocol Exchange*
- ISSN 2043-0116

DRC 16

MASSEY UNIVERSITY
GRADUATE RESEARCH SCHOOL

STATEMENT OF CONTRIBUTION
TO DOCTORAL THESIS CONTAINING PUBLICATIONS

(To appear at the end of each thesis chapter/section/appendix submitted as an article/paper or collected as an appendix at the end of the thesis)

We, the candidate and the candidate's Principal Supervisor, certify that all co-authors have consented to their work being included in the thesis and they have accepted the candidate's contribution as indicated below in the *Statement of Originality*.

Name of Candidate: Martina Dautel

Name/Title of Principal Supervisor: Dr. Evelyn Sattlegger

Name of Published Research Output and full reference:

Generating highly concentrated yeast whole cell extract using low-cost equipment. (2011)
Visweswaraiah J, Dautel M, & Sattlegger E.
Nature Protocol Exchange. doi:10.1038/protex.2011.212

In which Chapter is the Published Work: Appendix

Please indicate either:

- The percentage of the Published Work that was contributed by the candidate: 15%

  and / or

- Describe the contribution that the candidate has made to the Published Work:

  Provided biological material
  Taken photographs
  Commented on manuscript

Martina Dautel — Digital unterschrieben von Martina Dautel DN: cn=Martina Dautel, o=Massey University, ou=INS, email=m.dautel@massey.ac.nz, c=NZ Datum: 2012.03.01 16:13:30 +13'00'
Candidate's Signature

01/03/2012
Date

Evelyn Sattlegger — Digitally signed by Evelyn Sattlegger DN: cn=Evelyn Sattlegger, o=Massey University, ou=INS, email=e.sattlegger@massey.ac.nz, c=NZ Date: 2012.03.01 12:22:44 +13'00'
Principal Supervisor's signature

28/2/2012
Date

GRS Version 3– 16 September 2011

Bibliography

[1] A.E. Adams, D. Botstein, and D.G. Drubin. A yeast actin-binding protein is encoded by SAC6, a gene found by suppression of an actin mutation. Science, 243(4888):231–233, 1989.

[2] D. C. Amberg, E. Basart, and D. Botstein. Defining protein interactions with yeast actin *in vivo*. Nature Structural Biology, 2(1):28–35, 1995.

[3] T. G. Anthony, B. J. McDaniel, R. L. Byerley, B. C. McGrath, D. R. Cavener, M. A. McNurlan, and R.C. Wek. Preservation of liver protein synthesis during dietary leucine deprivation occurs at the expense of skeletal muscle mass in mice deleted for eiF2 kinase GCN2. Journal of Biological Chemistry, 279(35):36553–36561, 2004.

[4] K. R. Ayscough, D. G. Drubin, and A. G. Hinnebusch. ACTIN: general principles from studies in yeast. Annual Review of Cell and Developmental Biology, 12:129–60, 1996.

[5] L. D. Belmont and D. G. Drubin. The yeast V159N actin mutant reveals roles for actin dynamics *in vivo*. The Journal of Cell Biology, 142(5):1289–1299, 1998.

[6] J. J. Berlanga, J. Santoyo, and C. de Haro. Characterization of a mammalian homolog of the GCN2 eukaryotic initiation factor 2 kinase. European Journal of Biochemistry, 265(2):754–762, 1999.

[7] J. J. Berlanga, I. Ventoso, H. P Harding, J. Deng, D. Ron, N. Sonenberg, L. Carrasco, and C. de Haro. Antiviral effect of the mammalian translation initiation factor 2[alpha] kinase GCN2 against RNA viruses. EMBO Journal, 25(8):1730–1740, 2006.

[8] W. Bing, A. Razzaq, J. Sparrow, and S. Marston. Tropomyosin and troponin regulation of wild type and E93K mutant actin filaments from *Drosophila* flight muscle. Journal of Biological Chemistry, 273(24):15016–15021, 1998.

[9] S. Bittencourt, C. M. Pereira, M. Avedissian, A. Delamano, L. E. Mello, and B. A. Castilho. Distribution of the protein IMPACT, an inhibitor of GCN2, in the mouse, rat, and marmoset brain. Journal of Comparative Neurology, 507(5):1811–1830, 2008.

[10] M. M. Bradford. A rapid and sensitive method for the quantitation of microgram quantities of protein utilizing the principle of protein-dye binding. Analytical Biochemistry, 72(7):248 – 254, 1976.

[11] A Bretscher. Fimbrin is a cytoskeletal protein that crosslinks F-actin *in vitro*. Proceedings of the National Academy of Sciences, 78(11):6849–6853, 1981.

[12] N. L. Catlett and L. S. Weisman. The terminal tail region of a yeast myosin-V mediates its attachment to vacuole membranes and sites of polarized growth. Proceedings of the National Academy of Sciences, 95(25):14799–14804, 1998.

[13] J. Chen. Heme-regulated eIF2α kinase. Cold Spring Harbor Monograph Archive, 39(0), 2000.

[14] S. Chowdhury, K. W. Smith, and M. C. Gustin. Osmotic stress and the yeast cytoskeleton: phenotype-specific suppression of an actin mutation. The Journal of Cell Biology, 118(3):561–571, 1992.

[15] M. Clemens. Protein kinases that phosphorylate eIF2 and eIF2B, and their role in eukaryotic cell translational control. Cold Spring Harbor Monograph Archive, 30(0), 1996.

[16] R. K. Cook, W. T. Blake, and P. A. Rubenstein. Removal of the amino-terminal acidic residues of yeast actin. Studies *in vitro* and *in vivo*. Journal of Biological Chemistry, 267(13):9430–9436, 1992.

[17] M. Costa-Mattioli, D. Gobert, H. Harding, B. Herdy, M. Azzi, M. Bruno, M. Bidinosti, C. Ben Mamou, E. Marcinkiewicz, M. Yoshida, H. Imataka, A. C. Cuello, N. Seidah, W. Sossin, J. C. Lacaille, D. Ron, K. Nader, and N. Sonenberg. Translational control of hippocampal synaptic plasticity and memory by the eIF2 alpha kinase GCN2. Nature, 436(7054):1166–1170, 2005.

[18] M. Costanzo, A. Baryshnikova, J. Bellay, Y. Kim, E. D. Spear, C. S. Sevier, H. Ding, J. L. Y. Koh, K. Toufighi, S. Mostafavi, J. Prinz, R. P. St. Onge, B. Vandersluis, T. Makhnevych, F. J. Vizeacoumar, S. Alizadeh, S. Bahr, R. L. Brost, Y. Chen, M. Cokol, R. Deshpande, Z. Li, Z. Y. Lin, W. Liang, M. Marback, J. Paw, B. J. S. Luis, E. Shuteriqi, A. H. Y. Tong, N. Van Dyk, I. M. Wallace, J. A. Whitney, M. T. Weirauch, G. Zhong, H. Zhu, W. A. Houry, M. Brudno, S. Ragibizadeh, B. Papp, C. Petrovs, F. P. Roth, G. Giaever, C. Nislow, O. G. Troyanskaya, H. Bussey, G. D. Bader, A. C. Gingras, Q. D. Morris, P. M. Kim, C. A. Kaiser, C. L. Myers, B. J. Andrews, and C. Boone. The genetic landscape of a cell. Science, 327(5964):425–431, 2010.

[19] J. Delforge, F. Messenguy, and J Wiame. The regulation of arginine biosynthesis in *Saccharomyces cerevisiae*. European Journal of Biochemistry, 57(1):231–239, 1975.

[20] J. Deng, H. P. Harding, B. Raught, A. Gingras, J. J. Berlanga, D. Scheuner, R. J. Kaufman, D. Ron, and N. Sonenberg. Activation of GCN2 in UV-irradiated cells inhibits translation. Current Biology, 12(15):1279 – 1286, 2002.

[21] T. E. Dever, L. Feng, R. C. Wek, A. M. Cigan, T. F. Donahue, and A.G. Hinnebusch. Phosphorylation of initiation factor 2α by protein kinase GCN2 mediates gene-specific translational control of *GCN4* in yeast. Cell, 68(3):585 – 596, 1992.

[22] T.E. Dever and A.G Hinnebusch. Gcn2 whets the appetite for amino acids. Molecular Cell, 18(2):141 – 142, 2005.

[23] T. Doerks, R. R. Copley, J. Schultz, C. P. Ponting, and P. Bork. Systematic identification of novel protein domain families associated with nuclear functions. Genome Research, 12(1):47–56, 2002.

[24] J. Dong, H. Qiu, M. Garcia-Barrio, J. Anderson, and A.G. Hinnebusch. Uncharged tRNA activates GCN2 by displacing the protein kinase moiety from a bipartite tRNA-binding domain. Molecular Cell, 6(2):269 – 279, 2000.

[25] A. E.Y. Engqvist-Goldstein and D. G. Drubin. Actin assembly and endocytosis: From yeast to mammals. Annual Review of Cell and Developmental Biology, 19(1):287–332, 2003.

[26] J. Enserink and R. Kolodner. An overview of Cdk1-controlled targets and processes. Cell Division, 5(1):11, 2010.

[27] S. C. Falco and K. S. Dumas. Genetic analysis of mutants of *Saccharomyces cerevisiae* resistant to the herbicide sulfometuron methyl. Genetics, 109(1):21–35, 1985.

[28] M. Foiani, A. M. Cigan, C. J. Paddon, S. Harashima, and A. G. Hinnebusch. GCD2, a translational repressor of the *GCN4* gene, has a general function in the initiation of protein synthesis in *Saccharomyces cerevisiae*. Molecular and Cellular Biology, 11(6):3203–3216, 1991.

[29] D. Gallwitz and R. Seidel. Molecular cloning of the actin gene from yeast *Saccharomyces cerevisiae*. Nucleic Acids Research, 8(5):1043–1059, 1980.

[30] D. Gallwitz and I. Sures. Structure of a split yeast gene: complete nucleotide sequence of the actin gene in *Saccharomyces cerevisiae*. Proceedings of the National Academy of Sciences, 77(5):2546–2550, 1980.

[31] M. Garcia-Barrio, J. S. Dong, S. Ufano, and A. G. Hinnebusch. Association of GCN1-GCN20 regulatory complex with the N-terminus of eIF2 alpha kinase GCN2 is required for GCN2 activation. EMBO Journal, 19(8):1887–1899, 2000.

[32] S. Ghaemmaghami, W. K. Huh, K. Bower, R. W. Howson, A. Belle, N. Dephoure, E. K. O'Shea, and J. S. Weissman. Global analysis of protein expression in yeast. Nature, 425(6959):737–41, 2003.

[33] D.R. Gietz and A. Sugino. New yeast-*Escherichia coli* shuttle vectors constructed with *in vitro* mutagenized yeast genes lacking six-base pair restriction sites. Gene, 74(2):527 – 534, 1988.

[34] R. D. Gietz, R. H. Schiestl, A. R. Willems, and R. A. Woods. Studies on the transformation of intact yeast cells by the LiAc/SS-DNA/PEG procedure. Yeast, 11(4):355–360, 1995.

[35] D. W. Gietzen, C. M. Ross, S. Hao, and J. W. Sharp. Phosphorylation of eIF2alpha is involved in the signaling of indispensable amino acid deficiency in the anterior piriform cortex of the brain in rats. The Journal of Nutrition, 134(4):717–723, 2004.

[36] S. R. Gross and T. G. Kinzy. Translation elongation factor 1A is essential for regulation of the actin cytoskeleton and cell morphology. Nature Structural and Molecular Biology, 12(9):772–8, 2005.

[37] S. R. Gross and T. G. Kinzy. Improper organization of the actin cytoskeleton affects protein synthesis at initiation. Molecular and Cellular Biology, 27(5):1974–89, 2007.

[38] U. Gueldener, S. Heck, T. Fiedler, J. Beinhauer, and J. H. Hegemann. A new efficient gene disruption cassette for repeated use in budding yeast. Nucleic Acids Research, 24(13):2519–2524, 1996.

[39] U. Gueldener, J. Heinisch, G. J. Koehler, D. Voss, and J. H. Hegemann. A second set of loxP marker cassettes for Cre-mediated multiple gene knockouts in budding yeast. Nucleic Acids Research, 30(6):23, 2002.

[40] S. B. Haase and S. I. Reed. Evidence that a free-running oscillator drives G1 events in the budding yeast cell cycle. Nature, 401(6751):394– 397, 1999.

[41] Y. Hagiwara, M. Hirai, K. Nishiyama, I. Kanazawa, T. Ueda, Y. Sakaki, and Takashi Ito. Screening for imprinted genes by allelic message display: Identification of a paternally expressed gene *Impact* on mouse chromosome 18. Proceedings of the National Academy of Sciences, 94(17):9249–9254, 1997.

[42] S. Hao, J. W. Sharp, C. M. Ross-Inta, B. J. McDaniel, T. G. Anthony, R. C. Wek, D. R. Cavener, B. C. McGrath, J. B. Rudell, T. J. Koehnle, and D. W. Gietzen. Uncharged tRNA and sensing of amino acid deficiency in mammalian piriform cortex. Science, 307(5716):1776–1778, 2005.

[43] H. P. Harding, Y. Zhang, and D. Ron. Protein translation and folding are coupled by an endoplasmic-reticulum-resident kinase. Nature, 397(6716):271–274, 1999.

[44] E. S. Hennessey, D. R. Drummond, and J. C. Sparrow. Molecular genetics of actin function. The Biochemical Journal, 282(3):657–671, 1993.

[45] G. J. Hermann and J. M. Shaw. Mitochondrial dynamics in yeast. Annual Review of Cell and Developmental Biology, 14(1):265–303, 1998.

[46] J.W.B. Hershey and W.C. Merrick. Pathway and mechanism of initiation of protein synthesis. In Translational control of gene expression. Cold Spring Harbour Laboratory Press, 2000.

[47] A. G. Hinnebusch. A hierarchy of trans-acting factors modulates translation of an activator of amino-acid biosynthetic genes in *Saccharomyces cerevisiae*. Molecular and Cellular Biology, 5(9):2349–2360, 1985.

[48] A. G. Hinnebusch. Translational regulation of *GCN4* and the general amino acid control of yeast. Annual Review Microbiology, 59:407–50, 2005.

[49] M. Holcik and N. Sonenberg. Translational control in stress and apoptosis. Nature Reviews Molecular Cell Biology, 6(4):44–49, 1990.

[50] K. C. Holmes, D. Popp, W. Gebhard, and W. Kabsch. Atomic model of the actin filament. Nature, 347(4):318–27, 2005.

[51] L. J. Holt, B. B. Tuch, J. Villen, A. D. Johnson, S. P. Gygi, and D. O. Morgan. Global analysis of Cdk1 substrate phosphorylation sites provides insights into evolution. Science, 325(5948):1682–1686, 2009.

[52] J. E. Honts, T. S. Sandrock, S. M. Brower, J. L. Odell, and A. E. M. Adams. Actin mutations that show suppression with fimbrin mutations identify a likely fimbrin-binding site on actin. Journal of Cell Biology, 126(2):413–422, 1994.

[53] A. S. Howell and D. J. Lew. Morphogenesis and the cell cycle. Genetics, 190(1):51–77, 2012.

[54] W. Humphrey, A. Dalke, and K. Schulten. VMD: Visual molecular dynamics. Journal of Molecular Graphics, 14(1):33, 1996.

[55] Cytoskeleton Inc. Actin binding protein biochem kit manual. Manual, Version 8.1.

[56] H. Jiang and R. C. Wek. GCN2 phosphorylation of eIF2alpha activates NF-kappaB in response to UV irradiation. Biochemical Journal, 385(2):371–380, 2005.

[57] W. Kabsch, H. G. Mannherz, D. Suck, E.F. Pai, and K.C. Holmes. Atomic structure of the actin: DNase I complex. Nature, 347:37–44, 1990.

[58] P. Kaldis, A. Sutton, and M.J. Solomon. The Cdk-activating kinase (CAK) from budding yeast. Cell, 86(4):553 – 564, 1996.

[59] K. A. Kandl, R. Munshi, P. A. Ortiz, G. R. Andersen, T. G. Kinzy, and A. E. Adams. Identification of a role for actin in translational fidelity in yeast. Molecular Genetics and Genomics, 268(1):10–8, 2002.

[60] J. V. Kilmartin and A. E. Adams. Structural rearrangements of tubulin and actin during the cell cycle of the yeast *Saccharomyces*. The Journal of Cell Biology, 98(3):922–933, 1984.

[61] E. Kim, M. Motoki, K. Seguro, A. Muhlrad, and E. Reisler. Conformational changes in subdomain 2 of G-actin: fluorescence probing by dansyl ethylenediamine attached to Gln-41. Biophysical Journal, 69(5):2024 – 2032, 1995.

[62] S. Kim and P.A. Coulombe. Emerging role for the cytoskeleton as an organizer and regulator of translation. Nature Reviews Molecular Cell Biology, 11(1):75–81, 2010.

[63] S.R. Kimball. Eukaryotic initiation factor eif2. The International Journal of Biochemistry and Cell Biology, 31(1):25 – 29, 1999.

[64] T. Klopotowski and A. Wiater. Synergism of aminotriazole and phosphate on the inhibition of yeast imidazole glycerol phosphate dehydratase. Archives of Biochemistry and Biophysics, 112("3):562 – 566, 1965.

[65] V. L. Korman, V. Hatch, K. Y. Dixon, R. Craig, W. Lehman, and L. S. Tobacman. An actin subdomain 2 mutation that impairs thin filament regulation by troponin and tropomyosin. Journal of Biological Chemistry, 275(29):22470–22478, 2000.

[66] M Kozak. The scanning model for translation: an update. The Journal of Cell Biology, 108(2):229–241, 1989.

[67] N. J. Krogan, G. Cagney, H. Yu, G. Zhong, X. Guo, A. Ignatchenko, J. Li, S. Pu, N. Datta, A. P. Tikuisis, T. Punna, J. M. Peregrev-Alvarez, M. Shales, X. Zhang, M. Davey, M. D. Robinson, A. Paccanaro, J. E. Bray, A. Sheung, B. Beattie, D. P. Richards, V. Canadien, A. Lalev, F. Mena, P. Wong, A. Starostine, M. M. Canete, J. Vlasblom, S. Wu, C. Orsi, S. R. Collins, S. Chandran, R. Haw, J. J. Rilstone, K. Gandi, N. J. Thompson, G. Musso, P. St Onge, S. Ghanny, M. H. Y. Lam, G. Butland, A. M. Altaf-Ul, S. Kanaya, A. Shilatifard, E. O'Shea, J. S. Weissman, C. J. Ingles, T. R. Hughes, J. Parkinson, M. Gerstein, S. J. Wodak, A. Emili, and J. F. Greenblatt. Global landscape of protein complexes in the yeast *Saccharomyces cerevisiae*. Nature, 440(7084):637–643, 2006.

[68] S. J. Kron, D. G. Drubin, D. Botstein, and J. A. Spudich. Yeast actin-filaments display ATP-dependent sliding movement over surfaces coated with rabbit muscle myosin. Proceedings of the National Academy of Sciences, 89(10):4466–4470, 1992.

[69] H. Kubota, K. Ota, Y. Sakaki, and T. Ito. Budding yeast GCN1 binds the GI domain to activate the eIF2alpha kinase GCN2. Journal of Biological Chemistry, 276(20):17591–6, 2001.

[70] H. Kubota, Y. Sakaki, and T. Ito. GI domain-mediated association of the eukaryotic initiation factor 2 alpha kinase GCN2 with its activator GCN1 is required for general amino acid control in budding yeast. Journal of Biological Chemistry, 275(27):20243–6, 2000.

[71] S. KUBOTA, I. TAKEO, K. KUME, M. KANAI, A. SHITAMUKAI, M. MIZUNUMA, T. MIYAKAWA, H. SHIMOI, H. IEFUJI, and D. HIRATA. Effect of ethanol on cell growth of budding yeast: Genes that are important for cell growth in the presence of ethanol. Bioscience, Biotechnology, and Biochemistry, 68(4):968–972, 2004.

[72] R. A. LaRossa and J. V. Schloss. The sulfonylurea herbicide sulfometuron methyl is an extremely potent and selective inhibitor of acetolactate synthase in *Salmonella typhimurium*. Journal of Biological Chemistry, 259(14):8753–7, 1984.

[73] D. J. Lew and S. I. Reed. Morphogenesis in the yeast cell cycle: regulation by Cdc28 and cyclins. The Journal of Cell Biology, 120(6):1305–1320, 1993.

[74] S. H. Lillie and S. S. Brown. Immunofluorescence localization of the unconventional myosin, Myo2p, and the putative kinesin-related protein, Smy1p, to the same regions of polarized growth in *Saccharomyces cerevisiae*. The Journal of Cell Biology, 125(4):825–842, 1994.

[75] M. Loog and D. O. Morgan. Cyclin specificity in the phosphorylation of cyclin-dependent kinase substrates. Nature, 434(7029):104–108, 2005.

[76] M. J. Marton, D. Crouch, and A. G. Hinnebusch. GCN1, a translational activator of GCN4 in *Saccharomyces cerevisiae*, is required for phosphorylation of eukaryotic translation initiation factor 2 by protein kinase GCN2. Molecular and Cellular Biology, 13(6):3541–3556, 1993.

[77] A. Maurin, C. Jousse, J. Averous, L. Parry, A. Bruhat, Y. Cherasse, H. Zeng, Y. Zhang, H.P. Harding, D. Ron, and P. Fafournoux. The GCN2 kinase biases feeding behavior to maintain amino acid homeostasis in omnivores. Cell Metabolism, 1(4):273 – 277, 2005.

[78] W. C. Merrick. Mechanism and regulation of eukaryotic protein synthesis. Microbiology and Molecular Biology Reviews, 56(2):291–315, 1992.

[79] J.H. Miller. Experiments in molecular genetics. Cold Spring Harbor Laboratory, 1972.

[80] J. B. Moseley and B. L. Goode. The yeast actin cytoskeleton: From cellular function to biochemical mechanism. Microbiology and Molecular Biology Reviews, 70(3):605–645, 2006.

[81] P. P. Mueller and A.G. Hinnebusch. Multiple upstream AUG codons mediate translational control of *GCN4*. Cell, 45(2):201 – 207, 1986.

[82] A. Muhlrad, P. Cheung, B. C. Phan, C. Miller, and E. Reisler. Dynamic properties of actin. structural changes induced by beryllium fluoride. Journal of Biological Chemistry, 269(16):11852–11858, 1994.

[83] J. Mulholland, D. Preuss, A. Moon, A. Wong, D. Drubin, and D. Botstein. Ultrastructure of the yeast actin cytoskeleton and its association with the plasma membrane. Journal of Cell Biology, 125(2):381–91, 1994.

[84] A. L. Munn and E. Sattlegger. Yeast studies reveal new roles for an ancient skeleton. Australian Biochemist, 40(2):9–13, 2009.

[85] R. Munshi, K. A. Kandl, A. Carr-Schmid, J. L. Whitacre, A. E. M. Adams, and T. G. Kinzy. Overexpression of translation elongation factor 1A affects the organization and function of the actin cytoskeleton in yeast. Genetics, 157(4):1425–1436, 2001.

[86] B. Nefsky and A. Bretscher. Yeast actin is relatively well behaved. European Journal of Biochemistry, 206(3):949–955, 1992.

[87] R. Ng and J. Abelson. Isolation and sequence of the gene for actin in *Saccharomyces cerevisiae*. Proceedings of the National Academy of Sciences, 77(7):3912–3916, 1980.

[88] S. Nicholson-Dykstra, H.N. Higgs, and E.S Harris. Actin dynamics: Growth from dendritic branches. Current Biology, 15(9):R346 – R357, 2005.

[89] P. Niederberger, G. Miozzari, and R. Huetter. Biological role of the general control of amino acid biosynthesis in *Saccharomyces cerevisiae*. Molecular and Cellular Biology, 1(7):584–593, 1981.

[90] E. A. Nigg. Cellular substrates of p34(cdc2) and its companion cyclin-dependent kinases. Trends in Cell Biology, 3(9):296 – 301, 1993.

[91] I. A. Olave, S. L. Reck-Peterson, and G. R. Crabtree. Nuclear actin and actin-related proteins in chromatin remodeling. Annual Review of Biochemistry, 71(1):755–781, 2002.

[92] E. Palmer, J. M. Wilhelm, and F. Sherman. Phenotypic suppression of nonsense mutants in yeast by aminoglycoside antibiotics. Nature, 277(5692):148–150, 1997.

[93] G. D. Pavitt, K. V.A. Ramaiah, S. R. Kimball, and A. G. Hinnebusch. eIF2 independently binds two distinct eIF2b subcomplexes that catalyze and regulate guanine-nucleotide exchange. Genes & Development, 12(4):514–526, 1998.

[94] J. Peng, D. Schwartz, J. E. Elias, C. C. Thoreen, D. Cheng, G. Marsischky, J. Roelofs, D. Finley, and S. P Gygi. A proteomics ap-

proach to understanding protein ubiquitination. Nature Biotechnology, 21(8):921–926, 2003.

[95] P. Percipalle. The long journey of actin and actin-associated proteins from genes to polysomes. Cellular and Molecular Life Sciences, 66(13):2151–2165, 2009.

[96] P. Percipalle and N. Visa. Molecular functions of nuclear actin in transcription. J Cell Biol, 172(7):967–71, 2006.

[97] C. M. Pereira, E. Sattlegger, H. Y. Jiang, B. M. Longo, C. B. Jaqueta, A. G. Hinnebusch, R. C. Wek, L. E. Mello, and B. A. Castilho. IMPACT, a protein preferentially expressed in the mouse brain, binds GCN1 and inhibits GCN2 activation. Journal of Biological Chemistry, 280(31):28316–23, 2005.

[98] T. D. Pollard. Rate constants for the reactions of ATP- and ADP-actin with the ends of actin filaments. The Journal of Cell Biology, 103(6):2747–2754, 1986.

[99] T. D. Pollard, S. Almo, S. Quirk, V. Vinson, and E. E. Lattman. Structure of actin binding proteins: Insights about function at atomic resolution. Annual Review of Cell Biology, 10(1):207–249, 1994.

[100] T. D. Pollard, L. Blanchoin, and R. D. Mullins. Molecular mechanisms controlling actin filament dynamics in nonmuscle cells. Annual Review of Biophysics and Biomolecular Structure, 29(1):545–576, 2000.

[101] T.D Pollard and G.G. Borisy. Cellular motility driven by assembly and disassembly of actin filaments. Cell, 112(4):453 – 465, 2003.

[102] J.R. Pringle, J.R. Broach, and E.W. Jones. The molecular and cellular biology of yeast *Saccharomyces*, Volume 3, Cell cycle and cell biology. Cold Spring Harbor Laboratory Press, 1997.

[103] D. Pruyne. Tropomyosin Function in Yeast, volume 644 of Advances in Experimental Medicine and Biology. Springer-Verlag Berlin, Berlin, 2008.

[104] H. Qiu, M. T. Garcia-Barrio, and A. G. Hinnebusch. Dimerization by translation initiation factor 2 kinase GCN2 is mediated by interactions in the C-terminal ribosome-binding region and the protein kinase domain. Molecular and Cellular Biology, 18(5):2697–2711, 1998.

[105] M. Ramirez, R. C. Wek, and A. G. Hinnebusch. Ribosome association of GCN2 protein kinase, a translational activator of the *GCN4* gene of *Saccharomyces cerevisiae*. Molecular and Cellular Biology, 11(6):3027–3036, 1991.

[106] K. E. Ross, P. Kaldis, and M. J. Solomon. Activating phosphorylation of the *Saccharomyces cerevisiae* cyclin-dependent kinase, Cdc28p, precedes cyclin binding. Molecular Biology of the Cell, 11(5):1597–1609, 2000.

[107] J. Sambrook and D. W. Russell. Preparation and transformation of competent *E. coli* using calcium chloride. Cold Spring Harbor Protocols, 2006(1):3932, 2006.

[108] E. Sattlegger, J. A. Barbosa, M. S. Moraes, R. M. Martins, A. G. Hinnebusch, and B. A. Castilho. Gcn1 and actin binding to Yih1. Journal of Biological Chemistry, 286(12):10341–10355, 2011.

[109] E. Sattlegger and A. G. Hinnebusch. Separate domains in GCN1 for binding protein kinase GCN2 and ribosomes are required for GCN2 activation in amino acid-starved cells. EMBO Journal, 19(23):6622–33, 2000.

[110] E. Sattlegger, M. J. Swanson, E. A. Ashcraft, J. L. Jennings, R. A. Fekete, A. J. Link, and A. G. Hinnebusch. YIH1 is an actin-binding protein that inhibits protein kinase GCN2 and impairs general amino acid control when overexpressed. Journal of Biological Chemistry, 279(29):29952–62, 2004.

[111] A. Schuerch, J. Miozzari, and R. Hueter. Regulation of tryptophan biosynthesis in *Saccharomyces cerevisiae*: Mode of action of 5-methyl-tryptophan and 5-methyl-tryptophan-sensitive mutants. Journal of Bacteriology, 117(3):1131–1140, 1974.

[112] E. Schwob, T. Bohm, M. D. Mendenhall, and K. Nasmyth. The B-type cyclin kinase inhibitor p40SIC1 controls the G1 to S transition in *S. cerevisiae*. Cell, 79(2):233 – 244, 1994.

[113] Y. Shi, K. M. Vattem, R. Sood, J. An, J. Liang, L. Stramm, and R. C. Wek. Identification and characterization of pancreatic eukaryotic initiation factor 2α-subunit kinase PEK involved in translational control. Molecular and Cellular Biology, 18(12):7499–7509, 1998.

[114] D. Shortle, P. Novick, and D. Botstein. Construction and genetic-characterization of temperature-sensitive mutant alleles of the yeast actin gene. Proceedings of the National Academy of Sciences, 81(15):4889–4893, 1984.

[115] R. S. Sikorski and P. Hieter. A system of shuttle vectors and yeast host strains designed for efficient manipulation of DNA in *Saccharomyces cerevisiae*. Genetics, 122(1):19–27, 1989.

[116] A. Singh, D. Ursic, and J. Davies. Phenotypic suppression and misreading in *Saccharomyces cerevisiae*. Nature, 277(5692):146–148, 1979.

[117] R. Sood, A. C. Porter, D. Olsen, D. R. Cavener, and R. C. Wek. A mammalian homologue of GCN2 protein kinase important for translational control by phosphorylation of eukaryotic initiation factor2-α. Genetics, 154(2):787–801, 2000.

[118] L. M. Starita, R. S. Lo, J. K. Eng, P. D. von Haller, and S. Fields. Sites of ubiquitin attachment in *Saccharomyces cerevisiae*. Proteomics, 12(2):236–240, 2012.

[119] H. Strzelecka-Golaszewska, J. Moraczewska, S.Y. Khaitlina, and M. Mossakowska. Localization of the tightly bound divalent-cation-dependent and nucleotide-dependent conformation changes in G-actin using limited proteolytic digestion. European Journal of Biochemistry, 211(3):731–742, 1993.

[120] R. L. Tellam, D. J. Morton, and F. M. Clarke. A common theme in the amino acid sequences of actin and many actin-binding proteins? Trends in Biochemical Sciences, 14(4):130 – 133, 1989.

[121] J. Thuret, J. Valay, G. Faye, and C. Mann. Civ1 (CAK *in Vivo*), a novel Cdk-activating kinase. Cell, 86(4):565 – 576, 1996.

[122] J. A. Ubersax, E. L. Woodbury, P. N. Quang, M. Paraz, J. D. Blethrow, K. Shah, K. M. Shokat, and D. O. Morgan. Targets of the cyclin-dependent kinase Cdk1. Nature, 425(6960):859–864, 2003.

[123] Y. Uesono, M. P. Ashe, and A. Toh-e. Simultaneous yet independent regulation of actin cytoskeletal organization and translation initiation by glucose in *Saccharomyces cerevisiae*. Molecular Biology of the Cell, 15(4):1544–1556, 2004.

[124] P. Uetz, L. Giot, G. Cagney, T. A. Mansfield, R. S. Judson, J. R. Knight, D. Lockshon, V. Narayan, M. Srinivasan, P. Pochart, A. Qureshi-Emili, Y. Li, B. Godwin, D. Conover, T. Kalbfleisch, G. Vijayadamodar, M. J. Yang, M. Johnston, S. Fields, and J. M. Rothberg. A comprehensive analysis of protein-protein interactions in *Saccharomyces cerevisiae*. Nature, 403(6770):623–627, 2000.

[125] C.R. Vazquez de Aldana, M.J Marton, and A.G. Hinnebusch. GCN20, a novel ATP binding cassette protein, and GCN1 reside in a complex that mediates activation of the eIF-2 alpha kinase GCN2 in amino acid-starved cells. EMBO Journal, 14(13):3184–3199, 1995.

[126] J. Viswesvaraiah, M. Dautel, and E. Sattlegger. Generating highly concentrated yeast whole cell extract using low-cost equipment. Nature Protocol Exchange, doi:10.1038/protex.2011.212, 2011.

[127] S. Visweswaraiah, J.and Lageix, B. A. Castilho, L. Izotova, T. Kinzy-Goss, A. G. Hinnebusch, and E. Sattlegger. Evidence that eukaryotic translation elongation factor 1A (eEF1A) binds the Gcn2 C-terminus and inhibits Gcn2 activity. Journal of Biological Chemistry, 286(42):36568–36579, 2011.

[128] T. Waller, S. Lee, and E. Sattlegger. Evidence that Yih1 resides in a complex with ribosomes. FEBS Journal, 279(10):1761–1776, 2012.

[129] S. A. Wek, S. Zhu, and R. C. Wek. The histidyl-tRNA synthetase-related sequence in the eIF-2 alpha protein kinase GCN2 interacts with tRNA and is required for activation in response to starvation for different amino acids. Molecular and Cellular Biology, 15(8):4497–506, 1995.

[130] M. D. Welch, D. A. Holtzman, and D. G. Drubin. The yeast actin cytoskeleton. Current Opinion in Cell Biology, 6(1):110–119, 1994.

[131] K Wen and P. A. Rubenstein. Acceleration of yeast actin polymerization by yeast Arp2/3 complex does not require an Arp2/3-activating protein. Journal of Biological Chemistry, 280(25):24168–24174, 2005.

[132] K. F. Wertman, D. G. Drubin, and D. Botstein. Systematic mutational analysis of the yeast *ACT*1 gene. Genetics, 132(2):337–50, 1992.

[133] K.F. Wertman and D.G. Drubin. Actin constitution: guaranteeing the right to assemble. Science, 258(5083):759–760, 1992.

[134] J. Whitacre, D. Davis, K. Toenjes, S. Brower, and A. Adams. Generation of an isogenic collection of yeast actin mutants and identification of three interrelated phenotypes. Genetics, 157(2):533–43, 2001.

[135] C. Wittenberg and S. I. Reed. Conservation of function and regulation within the Cdc28/cdc2 protein kinase family: characterization of the human Cdc2Hs protein kinase in *Saccharomyces cerevisiae*. Molecular and Cellular Biology, 9(9):4064–4068, 1989.

[136] M. Wolfner, D. Yep, F. Messenguy, and G.R Fink. Integration of amino acid biosynthesis into the cell cycle of *Saccharomyces cerevisiae*. Journal of Molecular Biology, 96(2):273 – 290, 1975.

[137] S. Zhu and R. C. Wek. Ribosome-binding domain of eukaryotic initiation factor-2 kinase GCN2 facilitates translation control. Journal of Biological Chemistry, 273(3):1808–1814, 1998.